Overt Selection and Processing of Visual Stimuli

Dissertation
zur Erlangung des Grades
"Ph.D. in Cognitive Science"
im Fachbereich Humanwissenschaften
der Universität Osnabrück

vorgelegt von
José P. Ossandón D.

Osnabrück, im November 2015

Supervisor:

Prof. Dr. Peter König
University of Osnabrück, Osnabrück, Germany

Additional reviewers:

Prof. Dr. Frank Jäkel
University of Osnabrück, Osnabrück, Germany

Dr. rer. nat. Tobias Heed
University of Hamburg, Hamburg, Germany

The human understanding when it has once adopted an opinion ... draws all things else to support and agree with it. And though there be a greater number and weight of instances to be found on the other side, yet these it either neglects and despises, or else by some distinction sets aside and rejects, in order that by this great and pernicious predetermination the authority of its former conclusions may remain inviolate.

Novum Organum
FRANCIS BACON

Going beyond accepted data is not very different from filling gaps, except that interpolations are limited to the next accepted data point; extrapolations, however, have no end point in what is known or assumed, so extrapolations may be infinitely daring, and so may be dramatically wrong.

Perception as hypothesis
RICHARD L. GREGORY

Abstract

To see is to act. Most obviously, we are continuously scanning different regions of the world with the movement of our eyes, head, and body. These overt movements are intrinsically linked to two other, more subtle, actions: (1) the prior process of deciding where to look; and (2) the prediction of the sensory consequences of overt movements. In this thesis I describe a series of experiments that investigate different mechanisms underlying the first process and that evaluate the existence of the second one.

The aiming of eye movements, or spatial visual selection, has traditionally been explained with either goal-oriented or stimulus-driven mechanisms. Our experiments deal with the tension of this dichotomy and present further evidence in favor of two other type of mechanisms, not usually considered: global orienting based on non-visual cues and viewing biases that are independent of stimulus and task.

Firstly, we investigate whether stimulus-driven selection based on low-level features can operate independently of top-down constraints. If this is the case, the inhibition of areas higher in the hierarchy of visual processing and motor control should result in an increased influence of low-level features saliency. The results presented in Chapter 2 show that inhibition of the posterior parietal cortex in humans, by a permanent lesion or by transient inhibition, result in similar effects: an increased selection of locations that are characterized by higher contrast of low-level features. These results thus support a selection system in which stimulus-driven decisions are usually masked by top-down processes but can nevertheless operate independently of them.

Secondly, we investigate how free-viewing selection can be guided by non-visual content. The work in Chapter 3 indicates that touch is not only an effective local spatial cue, but that, during free viewing, it can also be a powerful global orienting signal. This effect occurs always in an external frame of reference, that is, to the side where the stimulation occurred in the external world instead of being anchored to the side of the body that was stimulated.

Thirdly, we investigate whether selection can operate even without reference to any sensory stimulus or goal. Results from our experiments presented in Chapters 2 to 5, demonstrate normal and pathological biases during free-viewing. First, patients with neglect syndrome show a strong bias to explore only the right side of images (ch. 2). In contrast, healthy subjects present a strong leftward bias, but only during the early phase of exploration (ch. 3 & 4). Finally, patients with Parkinson's disease show a subtle overall bias to the right and no initial leftward bias (ch. 5).

The results described so far indicate that visual selection operates based on diverse mechanisms which are not restricted to the evaluation of visual inputs according to top-down constraints. Instead, selection can be solely guided by the stimulus, which can be of a multimodal nature and result in global rather than local orienting, and by strong biases that are also independent of both stimuli and goals.

The second part of this thesis studies the possibility that eye movements result in predictions of the inputs they are about to bring into sight. To investigate this with electroencephalography (EEG) we had to first learn how to deal with the strong electrical artifacts produced by eye movements. In Chapter 6, a taxonomy of such artifacts and the best way of removing them is described. On this basis, we studied trans-saccadic predictions of visual content, presented in Chapter 7. The results were compatible with the production of error signals after a saccade-contingent change of a target stimulus. These errors signals, coding the mismatch between trans-saccadic predictions and sensory inputs, depend on the reliability of pre-saccadic input. The violation of predictions about veridical input (presented outside the blind spot) results in stronger error signals than when the pre-saccadic stimulus is only inferred (presented inside the blind spot). Thus, these

results support the idea of active predictive coding, in which perception consists in the integration of predictions of future input with incoming sensory information.

In conclusion, to see is to act: We actively explore the visual environment. We actively select which area to explore based on various competing factors. And we make predictions about the sensory consequences of our actions.

Contents

Chapter 1

General Introduction

By transducing light to neural activity, the eyes provide extensive information about the reflectance properties of surfaces and their spatial relations, information that is highly useful for multiple tasks like translation, foraging, avoidance of potential threats, and object manipulation. Besides their ecological relevance, eye movements are also the most frequent action performed by animals that is not by default an automatic process, thus arguably representing also the most frequent decision process carried out by the nervous system.Yet the underlying cognitive mechanisms and their perceptual impact are not well understood. Within the framework of this dissertation I will present and discuss a series of experiments that were driven by two main questions: (1) How do we decide where to look? and (2) What are the effects of ocular movements on visual processing?

The first question originates in how visual information is normally sampled in animals with functional eyes. In most mammals, eyes are highly movable with respect to the head, through eye movements, and with respect to the body, through head movements. Humans perform various types of eye movements (see Fig. 1.1a-b), but for the purpose of the research discussed and presented here I will manly focus on *saccades*, which consist of fast ballistic rotations of the eyes and on *fixations*, which comprise the periods between saccades. During fixations, the eyes remain in a relative stable position, even though a fair amount of smaller movements, both passive and active, can still occur. Human saccades are executed via six small muscles within each eye orbit, which allow the re-orientation of the eyes that is necessary for evaluating areas of the surrounding environment not yet in the field of view, and the re-alignment of the area of the retina with the highest resolution, the central fovea, with the locations of the field of view that are important at a given moment. Since the seminal works of G. Buswell (111) and A. Yarbus (949), two of the earliest researchers that were able to measure ocular movements and gaze direction, we known that both the latency and the destination of eye movements are highly variable. As an example of this variability, figure 1.1c-d illustrates the viewing behavior of a large group of human subjects that were asked to look freely at static photographs on a screen. In these examples it is readily apparent what is common knowledge since the beginning of eye movements research, namely that exploration is not homogenous but clustered around regions of interest. Nevertheless there is a high variability among observers while they explore the same image (fig. 1.1c), within single observers in successive views of the same image, and depending on the specific instructions of what to look at (949). This variability arises from many different factors, such as the characteristics of the visual input, the subjects' goals, the spatial and temporal context, the influence of other sensory modalities, and from systematic biases. These different factors have been intensely studied during the last century, and multiple functional mechanisms have been proposed for integrating them in a decision framework for *visual selection*. In the first section of this introduction, I will present a summarized view of some of these mechanisms, focusing specially on the ones that are the motivation of the empirical work presented in Chapters 2 to 5.

The second question that guides this thesis is closely related to the first one, since it focuses on what are the consequences of eye movements on visual processing. Once light is transformed to neuronal activity in the retina, it continues to be processed in different unimodal visual brain areas, starting at the subcortical structures of the visual thalamus and superior colliculus, to then diverge, in successive stages, to a multitude of cortical areas. Although vision has been one of the most studied functional systems of the brain, the understanding of how visual inputs are processed is still far from clear, even at the earlier stages (650, 120). One of the reasons of this was that, for long time, vision was researched almost

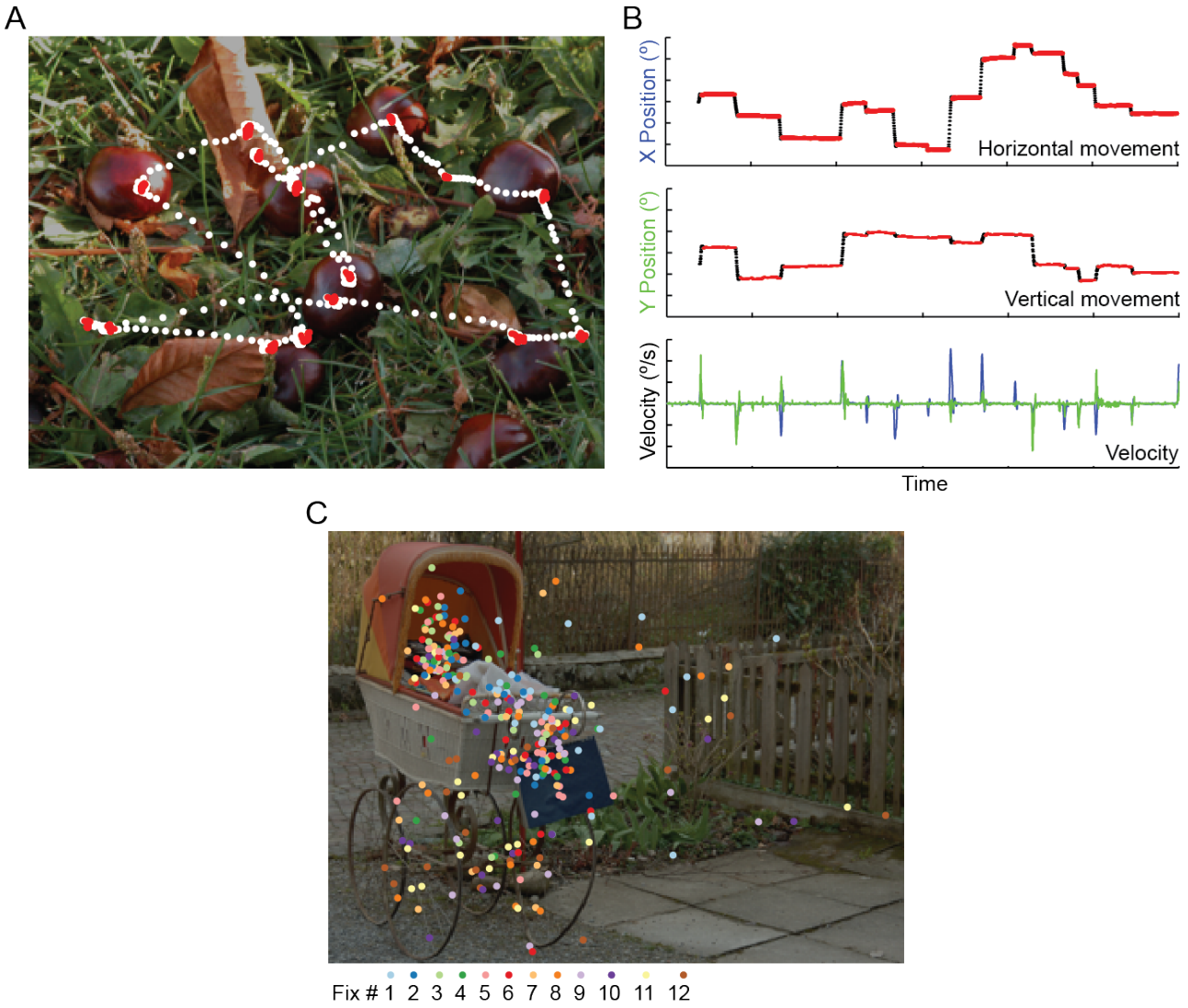

Figure 1.1: Examples eye movement measurements. (A) Six seconds of exploration by one subject over a natural scene. Each dot over the image is one sample of the eye-tracking measurement of gaze position. White samples are parts of saccades and red samples are parts of fixations. In (B) the same data is shown in a different form. The gaze movement is displayed as change in horizontal and vertical position, or as a change in velocity in each dimension (green - vertical, blue - horizontal), which is one of the criteria used to define when the eyes are moving (saccade) or still (fixation). (C) First twelve fixations performed in an image by 53 different subjects. In this image the sample information is gone, each point represent a singular fixation, color coded accordingly to its order in the exploration. Here is evident the variability in how different subjects look at different locations at different moments of their exploration. It is also apparent that there is a strong leftward bias to areas with interesting content.

exclusively in conditions of passive stimulation. Accordingly, the second part of this general introduction will provide a brief description of how eye movements affect visual processing. I will specially focus on the possibility of an active *predictive coding* of visual information, in which the agent's actions involved in sampling sensory information are an intrinsic part of the neural code through the generation of predictions of future content, which serves as the motivation for the empirical work presented in Chapters 6 and 7.

1.1 Visual selection

The first part of this thesis focuses on the study of free *overt* visual selection, or in other words, the study of how we decide where to look by means of eye movements. Of special interest to me was the study of visual exploration under free-viewing conditions, that is, when there are no explicit instructions to perform a defined movement or specific task. To start understanding the functional mechanisms underlying overt visual selection it is helpful to look first into the large body of research about the mechanisms of *covert* selection. Covert selection consists in focusing on, or attending to, a limited region of the visual field, usually in the periphery, without making an eye movement that directs the line of gaze to it. It was with covert selection experiments that H. von Helmholtz started the modern study of attention in the second half of the 19th century. Helmholtz performed a series of experiments to evaluate the everyday experience of being able to attend to something without directly looking at it (898, p.455). The main finding of Helmholtz, which have been extensively confirmed thereafter (e.g., 812, 230, 234, 233, 47, 693), was that humans are able, without moving their head or eyes, to report the visual contents in a selected area better than outside it. The results of covert selection experiments served as a basis to develop the first understanding of the scientific idea of *spatial attention*, the possibility to intentionally privilege a certain part of the sensory input. This operation of focusing on a region of space in detriment of others, was the first evidence that indicated that attention, like eye movements, sometimes works in a serial way; we are continuously selecting the next area of the visual landscape to attend.

However, it is also apparent from everyday experience that some regions of space, seem "to select themselves" due to the characteristics of the sensory input occurring at them, without our will having any part of it. The mechanisms involved in this reflexive operation were since then conceptually distinguished from the ones involved in voluntary selection, as they were thought to occur earlier, in a *pre-attentive* stage (618, 869, 407). In the following sections I will present an overview of the characteristics of these two types of processes, with a focus on the elements indicating that selection can be guided automatically by the low-level features of visual stimuli.

1.1.1 Mechanism based on stimuli local content and goal sets

Cueing tasks

Cueing experiments provide a good example for the inherent rivalry between voluntary and reflexive selection mechanisms. In a typical cueing task, the process of covert visual selection is directed by some kind of cue that points to a certain location in space. In the most common form of the task, as it is schematically illustrated in figure 1.2A, a single target can appear in one of two predefined locations, either without prior notice or preceded by a cue. Cues could be neutral, predicting the soon appearance of the target stimulus but without indicating any region of space, or spatial, associated to a specific location. This spatial cueing can be valid or invalid (matching or not matching the location where the target will appear) and of variable informativeness: completely non-predictive of where the target will appear (i.e. 50% valid trials / 50% invalid trials), predicting the target location with a probability higher than 50%, or giving absolute certainty that the target will appear at the cued location (100% valid trials). To differentiate between reflexive and voluntary mechanisms, two different types of spatial cues are used. In the first kind, named *direct* or *exogenous* cueing, the cue is a visual stimulus that appears at the target location. In the second kind, named *symbolic* or *endogenous* cueing, the cue appears somewhere else, usually in the centre of the display, and only indicates to a region of space by means of some symbolic mapping. This mapping can be either well-known to the subjects, like arrows that point to some location (which, however, are not anymore considered a good choice for symbolic cueing, see 719), or only contingent to the specific experimental setting, for instance, mapping a given color or number to the appearance of a target in a specific region of space.

The results of multiple experiments indicate that both types of cues can result in reaction time or detection benefits when compared to the control conditions where no-cue or a neutral cue is provided (fig. 1.2b) (699, 693). With respect to the temporal profile of cueing benefits, direct cues have been shown to be most effective at short latencies between the

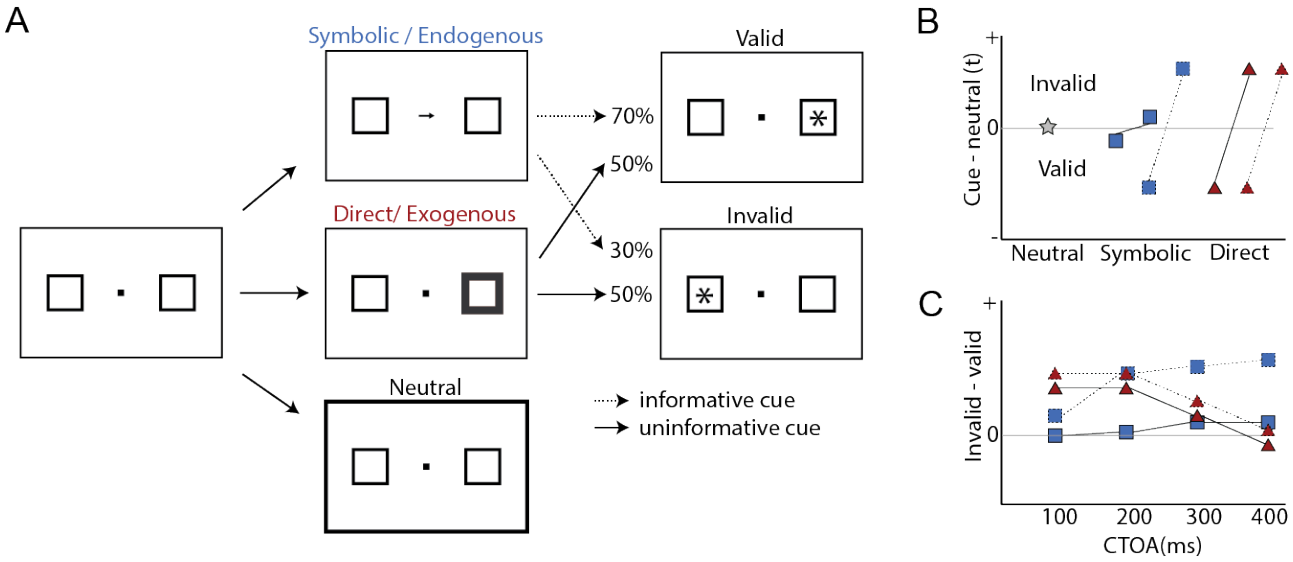

Figure 1.2: Examples of a covert cueing task. (A) An usual task trial starts with subjects fixating at a middle point and with two boxes that indicate where targets can appear. Afterwards different types of cueing can happen: symbolic or direct indicating an area of space, or neutral just indicating that soon a target will appear. Target appearance can be congruent (valid) or incongruent (invalid) with the spatial cueing, and of different predictability and informativeness. (B) Idealized results, whereas direct cueing results in advantages for valid trials both in informative and uninformative trials; the effect of symbolic cueing is more dependent on the cueing being informative. (C) The benefits of valid cueing vary depending on the cue-target onset asynchrony. Direct cues are effective at short latencies between cue and target, whereas symbolic cue become effective at larger intervals.

cue and the target, usually less than 200 ms (693, 695, 694, 594, 612, 775, 131, 596). At longer latencies direct cues sometimes result in reaction times costs instead of benefits (694, 594, 596), a phenomenon named *inhibition of return* (fig. 1.2c) (697, 444). In contrast, symbolic cues start to be effective at longer latencies (>200 ms) and remain effective for longer time windows that can go beyond one second after the cue presentation (fig. 1.2c) (594, 596, 131). For symbolic cues, their informativeness is central to the cueing effect. Informative cues that consistently predict the target location result in a stronger effect than uninformative cues (699, 595). Direct cues, by contrast, are effective both at low- and high-informativeness levels (fig. 1.2b). This observation, together with the described temporal profile led to the idea that direct cues operate as some kind of pre-activation or sensory priming, which for a short time facilitates the processing of an incoming stimulus occurring at the same location (473, 595, 939, 940). The insensitivity to informativeness also suggests that direct cues trigger an automatic process that is beyond control contingent to the task goals. The difference between direct and symbolic cues extend to respective sensitivities to interferences, with only symbolic cueing being affected by an increase of attentional load in dual tasks, or to the instruction to ignore the cue (401), thus supporting the idea that the effect of symbolic cues is mediated by contingent mechanisms that compete for a pool of limited resources.

All together, from these differences between direct and symbolic cueing emerged a picture in which two modes of attention control can be distinguished (940). *Stimulus-driven* control would be the result of direct (exogenous) cues that direct visual selection to the location of space where they appear, but only for a limited period of time and in a way that is insensitive to different goal sets, attention load, and the overall validity or behavioral relevance of the cue. In contrast, *goal-driven* control is the result of symbolic (endogenous) cues that direct visual selection to a location different to the one where they appear. It requires a longer period of time to become effective but also remains beneficial for a longer period of time. It is dependent on the explicit instructions given, the validity of the cue and suffers from interference with higher attention loads. Thus, these distinctions seem to identify stimulus-driven processing with a sensory advantage, that is mostly pre-attentional or in parallel and automatic. In contrast, goal-directed control is effortful, requires time to come in effect and could be influence by multiple factors.

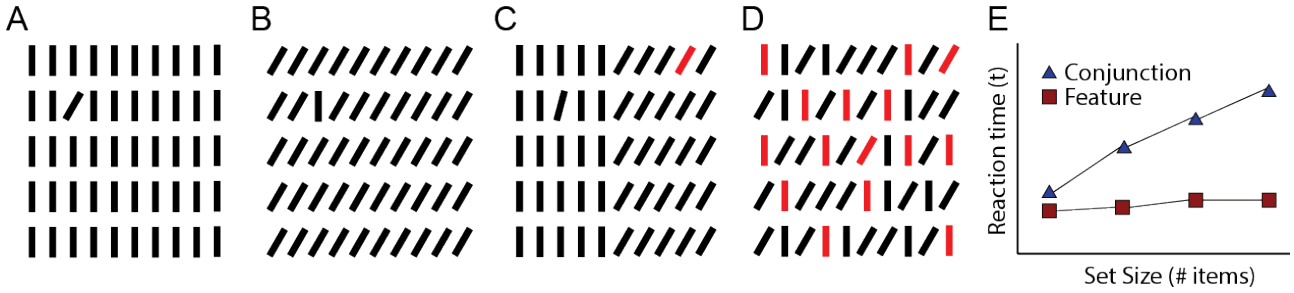

Figure 1.3: (A-C) Examples of feature search task. (A-B) A pair of displays that show asymmetries in feature search. The target odd-element is easier to find in A than in B; to find an oblique element among vertical ones is easier than to find a vertical target among oblique distractors. (C) More than one element can pop-out in a display, depending on the local context. For instance, the oblique item in the left part of the display has the same orientation as all the element in the right side (and in the next panel to the left), but pop-outs due to local contrast. (D) An example of a conjunction search, the target odd-item here is a red oblique bar that shares its features with other distractors. (E) Typical pattern of results for feature and conjunction search, whereas for feature search there is a flat relationship between reaction time and the amount of distractors, for conjunction search there is a monotonically increasing relationship.

Visual search tasks

While cueing tasks are informative about the ways visual selection can be directed trough explicit spatial cues, visual search tasks can help us to understand how visual selection can be directed to a specific goal and also about how difficult or easy it is to find a target dependent on its low-level characteristic (i.e., contrast, orientation, color, etc). Figure 1.3a-d depicts typical examples of displays used for search tasks, which are configured by a set of simple visual elements. Participants are asked to find a target element, sometimes defined specifically (e.g.,"search for an oblique red bar"), and sometimes more generally (e.g., "search for the odd item").

The motivation behind using this simple setting is that, by manipulating the amount of distractor items, it is possible to determine the level of difficulty of a specific search. Easy or efficient tasks are the ones in which targets can be found fast and independently of the amount of distractors. This results in a flat linear relationship between search reaction times and the amount of distractors (fig. 1.3e). In contrast, when a task is hard it takes longer to find the target, proportional to the amount of distractors. Efficient searches are usually the result of the target being different from the distractors in one specific feature dimension. For instance, it is easy to find an oblique bar among vertical ones (fig. 1.3a). An element of this sort is said to being *salient* with regard to one or more low-level visual features and to *pop-out* from its surroundings (869). Basic feature dimensions that have been proposed to result in this kind of efficient *feature search* are color, motion, orientation, line termination, contrast, curvature, and size (933, 936).

The easiness to find a pop-out target, independently of the amount of distractors, led to propose that this kind of efficient search is the result of a mechanism that works in parallel across the entire visual field (755, 869, 450, 188), occurring in a pre-attentive sensory stage of visual processing, similar to the proposed mechanism for the direct cueing effects discussed in the previous section (88, 628). As the pop-out effect occurs even in ignorance of which one is the target feature, it suggests that different features are processed in different channels and that efficient search occurs in parallel across the different feature channels. Each sensory dimension pushes for selection when a feature at one location is distinctively unique with respect to the rest of the visual field.

In contrast to the efficient feature search there is the case of *conjunction search*. Here, a target is characterized by a conjunction of features instead of by a single one, for example, being of a specific color and orientation among distractors that share one of that specific feature with the target but not both (fig. 1.3d). Targets characterized by a conjunction of features usually result in inefficient search, with reaction time increasing linearly with the number of distractors (fig. 1.3e)(e.g., 869, 936), and thus suggesting some kind of processing bottleneck or serial mechanism.

Although this view of pre-attentive/parallel and attentive/serial mechanisms for search tasks is appealing and simple, it has proven to be still incomplete. The distinction between feature and conjunction search is not as clear-cut as it appeared initially (937, 866, 932, 933, 847, 194, 936). There is large variability in the relationship between reaction times and set size, best described by a meta-analysis of hundreds of experiment performed across several years in J. Wolfe's research group.

Their results show that there is no clear-cut division between feature and conjunction search, but a continuum of efficiency (932). This reflects plenty of examples of tasks that failed to accommodate with the feature/conjunction characterization described above. The automaticity and pre-attentive characteristic of feature search has been challenged by experiments that show the disappearance of pop-out effects with additional attentional demands (403, 194). Moreover, for a target to pop out, a minimum distance within the feature dimension is necessary, which is greater than the smaller noticeable difference (609, 265). Pop-out effects are also usually not symmetric (934). This means that when a given feature difference results in a efficient search, it does not necessarily mean that the reversed task, that is, when the characteristics of target and distractors are interchanged, will also result in a pop-out or be as efficient (see fig. 1.3a-b). The parallel attribute that would result in efficient search is also challenged as local instead of global field contrast seems to be most relevant for an element to pop-out (see 1.3c) (406, 407, 585, 625, 626). This will be an important point later for the attempt to generalize the idea of saliency to complex images. With respect to conjunction search, there is also evidence showing that this kind of tasks can also result in efficient search, faster than what would be expected by strictly serial mechanisms (216, 613, 937, 847). Following these discrepancies, it has been proposed that search efficiency resides in a continuum that depends on target-distractor and distractor-distractor similarity as well as on local versus global contrast mechanisms (65, 213, 265, 932).

Besides the effectiveness of feature-based, stimulus-driven mechanisms facilitating search, it is also possible to evaluate other high-level mechanism in relation to learning and memory. The pre-attentive view of feature search emphasizes that even with long practice a conjunction target does not become *unitized* and easier to find (869). However, this is challenged by many experiments showing the influence of learning as for example: the benefit of extensive task training (170, 5, 6, 790); the role of familiarity, as evidenced in differential effects when over-learned elements like letters are used in common or uncommon orientations (913); the ability to learn specific spatial layouts or global contexts (142); and the effect of the mapping consistence of target and distractor elements (170, 143, 510). It has also been proposed that pop-out effects might occur even for complex visual configurations that constitute natural categories, for example, in the case of faces (357, 358, 482). However, whether this interpretation is accurate is still unclear, since the respective findings might likewise reflect an effect of low-level confounds (891, 435).

Although the variability of effects precludes the generation of a simplistic model for visual search, the frequent occurrence of effective feature search indicates that some visual stimuli configurations of high local contrast in one feature dimension are a powerful and fast guide of visual selection. However, since some goal sets can revert the effectiveness, the automaticity of this guidance is still unclear.

Attentional capture

There is an alternative way to study stimulus driven visual selection, by altering the saliency of the distractors during a search task. In contrast to the tasks described in the previous section, in which the saliency of targets is manipulated, in the capture task, one of the distractor items is salient, usually a feature-singleton that pops out. We can recognize such capture effects in our daily lives, for instance, when new objects suddenly appear, or when objects that are already present unexpectedly start to move and thus attract our attention. The extent of how much a salient distractor disrupts a search reflexively is then reflected in an increased latency to find the target.

The most clear and robust feature able to capture attention is a visual onset, specially when it involves a luminance change (947, 402, 857, 946, 844, 386). The onset effect in other feature dimensions like color and texture is less clear (402, 844, 386). However, the degree of capture of a salient singleton distractor, even an onset event, seems to be dependent on different factors such as the feature type, the subject's goals set, and on whether the target is also a feature singleton or not, therefore casting doubts on a purely automatic capture of attention. Specifically, attentional capture seems to be strongly dependent on the similarity between the features that make the distractor and target salient and on how fixed these dimensions are across experimental trials (262, 33, 415, 846, 479, 945, 468, 386). Even when distractors are salient in a different feature dimension than the target, it is possible that reflexive capture is secondary of an implicit goal set that adapts to the fact that in most experiments target and distractors are feature singletons. This could result in that subjects operationalize the task goal

into a "singleton detection mode" instead of a "feature search mode" (33). The underlying idea behind these effects, that challenges pure reflexive capture, is that capture is always *contingent* to the task demands (262).

In contraposition to the idea of contingent capture, other experiments show conflicting evidence of task sets in which top-down selectivity to a specific stimulus dimension might not be possible (842, 843, 478), even when distractors features are completely dissociated from the task goals (271). Part of the controversy seems to be due to differences in the relative salience between targets and distractors among tasks; distractors capture attention only when they are more salient than the target (843). Additional support for "pure" reflexive capture comes from observations that it occurs for features and locations that have pop-out or been targets in previous trials (527, 528, 685). Capture effects are also short lived.

A way to reconcile the opposing views of automatic versus contingent capture is provided by the proposition that capture is overcome only when salient distractor items are excluded from the spatial frame of attention (948, 843). This can be exemplified by the common experience of watching TV, which is actually similar to most lab settings. Within the television display, or spatial frame, sudden event onsets cause reflexively reorientation. However, similar event onsets outside the frame of the television, for instance, someone turning on the lights, or people's movements, do not necessarily attract attention. The framing of the attentional window, usually a subset of the screen in an experiment, would be under attentional control. This allows to exclude the stimulus-driven guidance of visual selection from some areas in space, but not within the attended spatial frame, in which pre-attentive mechanisms are at work and salient items or events are selected reflexively.

The attentional capture task combines the effects of reflexive selection by direct cues with the pop-out effect of feature-singletons seen in visual search tasks, but now guiding visual selection to distractors instead of targets. Altogether, the experiments described in the previous three sections suggest that visual selection can be divided in at least two major components, one of which is related to stimulus characteristics that elicit reflexive *bottom-up* responses, and a second component that is more contingent to the current situation and thus guiding selection from the *top-down*.

Overt visual selection

The above-mentioned effects of spatial cues (693, 776, 131), the capture of attention by salient items (386), and the differences between serial and parallel search (959) are also observed in experiments that allow eye movements.

The link between covert and overt attention becomes more evident when studying shifts of attention that go along with eye movements. Often this is done by probing the detection of briefly presented stimuli presented at, or near, the location of a saccadic target. This type of experiments shows that, briefly before an eye movement is performed, the focus of attention shifts to the next location to be fixated (716, 776, 754, 365, 460, 191, 203, 190, 727, 726). This happens both for saccades elicited by direct (460, 754) and symbolic cues (776, 460, 191). Moreover, this shift of covert attention is automatic and obligatory, thus making it impossible to efficiently direct attention elsewhere immediately prior to an eye movement (776, 365, 191, 203). The relationship between covert attention and eye-movements is different for endogenous and exogenous attention. Stimulus-driven selection is actually dependent on the possibility of planning an eye movement, as demonstrated by the absence of direct cueing benefits in subjects with reduced eye motility (695, 163, 765, 281, 796). In contrast, the inability to perform eye movements does not prevent goal-directed covert selection induced by symbolic cuing (795). Furthermore, the same dissociation between exogenous and endogenous attention can be seen in healthy subjects for cued locations that cannot be accessed by a saccade (163, 796).

Capture effects are also present in eye movements tasks. For instance, in a task where the goal is to look for a target that is embedded in an array of items with one salient distractor, movements that start very early are sometimes erroneously directed to the salient distractor whereas movements with longer latencies are directed to the target (386, 887). This happens even in the case when the distractor is salient in a different feature dimension than the target (889, 888).

In summary, covert and overt attention could be in principle governed by completely different selection mechanisms. However, the evidence so far indicates that visual selection operates in a similar fashion with or without eye movements. This functional similarity and the partial overlap of the neural correlates of overt and covert selection in the primate brain

led to the idea that covert and overt selection mechanisms only differ by the occurrence of an eye movement (753, 721, 30). However, this view is challenged by the above mentioned findings about differences between endogenous and exogenous attention when eye movements are not possible (163, 796). Something similar is observed in dual tasks where the preparation of an eye movement does not result in faster covert stimulus detection, or vice versa (442, 378, 443). Thus, although similar principles govern both covert and overt attention, this does not mean that both processes are driven by exactly the same decision system.

1.1.2 Free viewing selection based on low-level mechanisms

Even in experiments with explicit instructions and controlled environments, one often encounters a disagreement in the results of different research groups, and even within a research group, that are sometimes secondary to only subtle differences in experimental setups. This is of course the way research progress; it is in this subtle differences and replication failures were theories are challenged or refined. However, in the specific case of the study of visual attention, it has had the disadvantage of generating experimental paradigms, which sometimes develop to complete research subfields, that are progressively more and more removed from the activities they seek to ultimately explain. This leads to the methodological risk of providing, as general mechanisms of brain function, theoretical constructs that are only an adjustment of the real mechanisms to artificial tasks. For this reason, complementary research lines have been permanently emerging that attempt to observe and generate hypotheses of cognitive functions in conditions that are closer to the ones in which they are normally exercised. Something like this also occurs in the field of attention, in which the restrictive and tightly controlled experimental paradigms described in previous sections are supplemented with tasks that allow subjects to explore freely, as our usual viewing behavior is done, and over complex stimulus, similar to or the actual visual environments we are confronted in our every day lives.

It is thus not clear whether the stimulus-driven selection effects found with simple stimuli and restricted experimental settings generalize to more natural viewing conditions. Saliency guidance of free-viewing behavior during the observation of complex scenes is only at first sight supported by previous results. The experiments that reveal some kind of bottom-up stimulus-driven guidance are done with simple displays, usually presenting a feature singleton, and with clearly defined task goals. In contrast, in a complex natural scene, multiple low-level features overlap at different spatial scales and there is no clear goal (see an example of a low-level decomposition in fig. 1.4). Although it is possible to find many examples of local feature singletons, most real life scenes are cluttered, with relative fewer instances of strong local feature contrast. Therefore it is necessary to evaluate whether stimulus driven guidance of attention also occurs during free-viewing.

Feature correlation evidence

A first step to test stimulus-driven guidance of attention was by searching for correlations between the physical characteristics of stimuli and where subjects fixate. Multiples free-viewing studies show that, indeed, participants tend to fixate locations where the feature contrast or predicted saliency is higher than at other locations (714, 464, 666, 664, 674, 834, 74, 652). This is illustrated by the correlations between the fixation map and feature maps in the example presented in figure 1.4. However, because there are many different low-level features, which in turn may be spatially correlated within complex scenes, it is not always clear which features drive the observed viewing pattern (fig. 1.4). Attempts to evaluate the independent contributions of different features show that the salience of a location can be explained by a simple additive linear model (231, 652) – an observation that is backed up by studies with simpler stimuli and search tasks (627, 453). As will be discussed next, the relevance of a given feature depends on task goals, but even when there is no explicit goal, not all low-level features are equally predictive of fixations' locations. The importance of different features diminishes after the addition of spatial phase noise, indicating that their effect depends on higher-order image statistics (221). These high-order

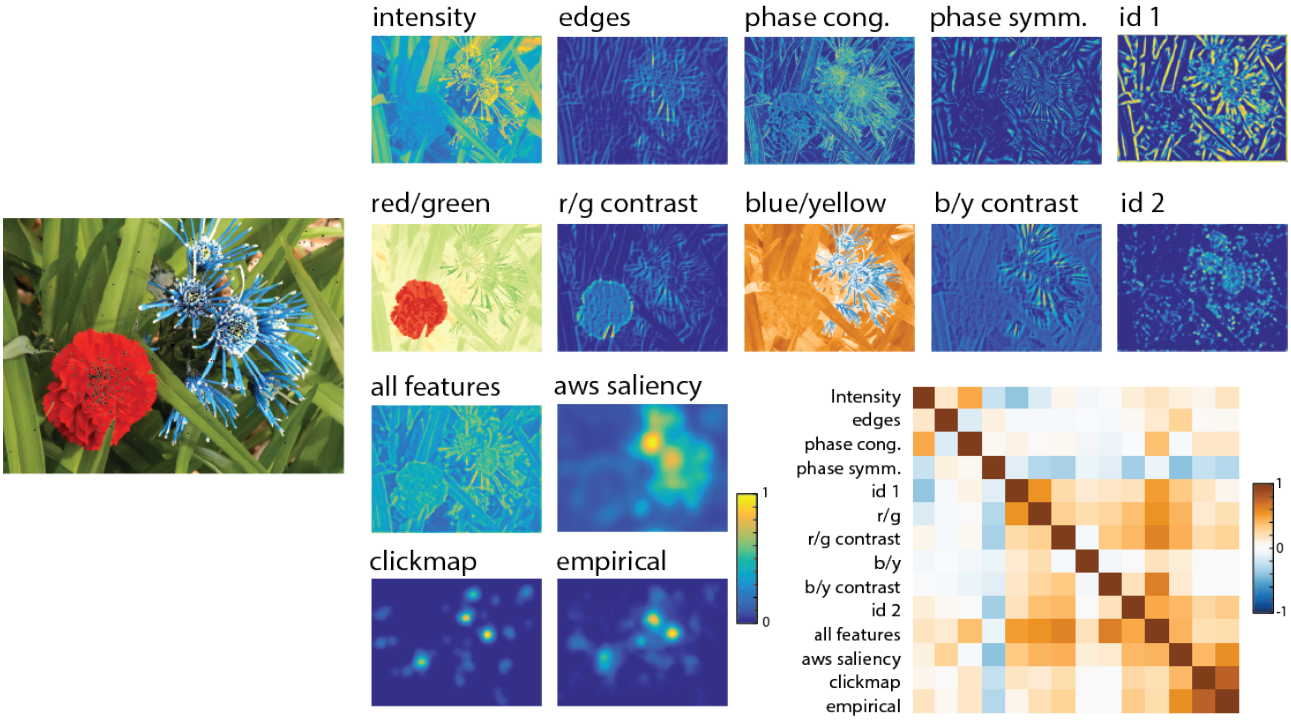

Figure 1.4: The image on the left was broke down into ten different 2D feature maps shown in the top two rows. All maps but the ones that show the color content opponent channels were coded in the same colormap with the most yellow value representing the maximum value of that feature for the image. Color opponent channels were coded in a corresponding intuitive colormap. The four maps in the centre show: (1) an average of the features above; (2) the result of the analysis with one of best available saliency model, the adaptive whitening saliency model (283, 74); (3) a click-map constructed by asking thirty participant to clink in the five most "interesting" part of the image; and an empirical saliency map that show were forty-eight subjects fixated in the image. The box in the bottom-right show the matrix of spatial correlation between all features, saliency, click and empirical saliency map. Note that different low-level features are correlated, and that saliency and click maps are highly spatially correlated with the locations subjects fixated.

statistic usually represent specific spatial configurations and thus their effect can be also seen in the high predictiveness of high-spatial frequency content like edges (37) and their intersections (652).

The causal influence of low-level features on viewing behavior can also be tested by introducing artificial modifications in feature strength and see how this intervention modifies the subjects' exploration patterns. In humans, both local decrements and increments of contrast attract attention (220, 1). This is also the case for gradients of contrast across hemifields, both in healthy subjects (221, 222) and in patients with neglect syndrome where they counteract pathological attentional biases (49).

In summary, the correlation between stimulus features and fixation behavior suggests that during free-viewing the exploration of complex scenes can be driven by low-level features. As mentioned, features might excerpt their influence following a simple additive model, which leads to the discussion of the different ways features are selected and combined in computational models of low-level driven vision.

Saliency models

C. Koch and S. Ullman proposed an influential computational model for covert visual selection in which they introduced the idea of a master saliency map (450). In this model, following the known pattern of distributed and parallel processing of visual features in the brain (see section 1.2.2, p.16), elementary features are represented in explicit topographic maps in which inhibitory connections perform local contrast operations, resulting in the coding of within-feature salience. The global saliency of a location is then integrated in a single topographic map, the saliency map, which combines the information of all features maps. As natural scenes will likely result in a saliency map with peaks at different locations, the dynamic selection of locations is implemented by a winner-take-all mechanism with consecutive decay of

the unit that was maximally active.

This saliency map model was influential in the discussion of the results of search tasks, but it was not until an actual implementation by L. Itti et al (391, 389) that it could also be used to analyze and model viewing behavior of complex naturalistic scenes and thus became a landmark within the field of computational vision. Since then, multiple different implementations of the model have been put forth (73, 925). Most of them nevertheless keep the same basic architecture of elementary feature maps, a saliency map, and a mechanism for dynamic selection (925). The different variations deal with the problem of which features to use, how to combine them and how to process information at different spatial scales. While the initial saliency map proposal was indifferent on how features were combined, new models also attempt to include the effect of top-down influences, as for instance by dynamic feature weighting (873, 127), maximization of image information gathering (97), combining low-level salience computations with statistical knowledge about object features (615, 961), or by using Bayesian spatial priors that incorporate information about the scene context (641, 863, 864).

The efficiency of saliency models to predict where people will look in a scene is fairly good but limited. Although the predictive power is not far from the gold standard, which is to predict a subject's viewing behavior based on the viewing behavior of other subjects, the good performance only holds for the overall distribution of fixations. In contrast, the models are much more limited when it comes to predict the succession of fixations, the gaze *scanpath*, and second-order spatial statistics like fixations pair correlations (228). This, together with the observation that saliency models using different features and integration principles achieve similar performance, cast doubts on saliency maps being the mechanism underneath human visual selection behavior (925).

Is low-level guidance during free viewing a likely mechanism?

The influence of low-level features during free viewing exploration has been challenged by two lines of argumentation. Firstly, high-frequency edges and junctions, the features that correlate strongest with human fixation behavior, are also characteristic for regions that contain objects (224). Therefore it is possible that is not the low-level features but rather their high-level counterpart, as for example object identity, the ones driving viewing behavior. When comparing the independent contributions of locations containing objects on one hand and low-level saliency on the other hand, it appears that high-level factors are stronger involved in guiding visual selection (223, 631, 652, 823). Moreover, a measure of informativeness obtained by asking subjects to rate the "informativeness" or "interestingness" of image patches or regions, is much more predictive than low-level features (351, 652). This is illustrated in figure 1.4b, where the highest correlation with the fixation map is given by the click-interestingness map. When the independent contributions of high- and low-level features are formally tested, low-level features do seem to contribute with an independent, but rather small, component to visual selection in free-viewing conditions (455, 652).

Secondly, many experiments show that the correlation between low-level features and viewing behavior can be overridden by changing the task goal. Just asking subjects to locate a patch with a specified content can completely modify the distribution of feature values at fixated locations (835, 692, 877). Likewise, the strong effect of contrast gradients in free viewing can be easily overcome when the task is to search for a target that can be anywhere on the display (223). Similarly, salient objects that are fixated early during a free-viewing memory task are afterwards neglected when the task is to search for low saliency targets (878).

Given the evidence for stimulus-driven selection from cueing, search and capture tasks, plus the correlational evidence observed in the case of free viewing, it is likely that reflexive low-level guidance is a real mechanism of selection during free-viewing. However, stimulus driven guidance is also contingent to task specifications, the subject's goals and many other factors, which may mask or override low-level control. Therefore, we hypothesized that when top-down guidance is impaired, stimulus driven guidance should become dominant. We tested this in a series of experiments presented in **Chapter 2** where we look into the free-viewing behavior of three different groups of humans participants: healthy subjects, patients with hemineglect syndrome, and subject that underwent a repetitive transcranial magnetic stimulation (rTMS) protocol to inhibit the parietal cortex. In both patients and subjects during rTMS we expected that the top-

down goal-directed control of visual selection would be impaired thus revealing more clearly the function of low-level mechanisms.

1.1.3 Visual selection and multimodal cues

So far, I have described the visual selection process in terms of stimulus- and goal- directed mechanisms that are restricted to the visual domain. However, from our daily experience we know that when exploring the world we orient our head and eyes also to signals that are not visual. The integration of different sensory modalities is most frequently studied in terms of interactions between visual and auditory information, since auditory cues can give away spatial information about events occurring at locations that might not be accessible by vision. Tactile information on the other hand is less informative about events in the surroundings as it is exclusively linked to the body surface and thus to peripersonal space. Still, touch can serve as a powerful cue for visual selection as for example with regard to object manipulation and interpersonal interaction.

Detection tasks

The simplest example for a crossmodal link is when a signal in one modality serves as a non-spatial cue for the occurrence of a signal in another one. Multimodal stimuli are detected faster, even when the target stimulus is defined in only one of the modalities (856, 577, 672, 264, 198, 602). This effect is known as *redundancy gain* and does not require the stimuli to be spatially coincident in order to be effective (856, 355, 588, 577, 295, 900, 264, 198, 602). Although most studies deal with the link between audition and vision, bimodal tactile-visual stimuli have also been shown to elicit faster responses (856, 264, 198). Two main alternative views are proposed to functionally explain crossmodal redundancy gain. In the *race model* the different modalities are always processed in parallel until they reach some activation threshold that trigger the response, thus resulting in statistical facilitation (707). In contrast, the model of *intersensory facilitation* proposes that faster responses are the result of the convergence of signals in a single integrator. Most of the studies that find crossmodal benefits seem to be explained by some kind of multisensory integration rather than by statistical facilitation (577, 295, 264, 198, 602).

Cue tasks

Crossmodal facilitation has also a spatial component (806, 264, 602), similar to the visual cueing effects described earlier. Depending on their spatial alignment, auditory cues can help or be detrimental to orient to a visual target and vice versa (924, 398). More specifically, crossmodal visual-auditory cueing results in faster responses for valid/spatially coincident targets while spatial disparity increases reaction times (806, 582, 914, 884, 552). Moreover, irrelevant tones enhance visual discrimination when both stimuli are spatially congruent (553, 272). Crossmodal spatial cueing is also effective for visuo-tactile stimuli, with tactile stimulation affecting visual localization both locally, when visual and tactile stimulus are close, and globally, by a more general orienting effect to a complete side of the world (809, 428, 429). These effects extend to endogenous orienting, when expecting a stimulus from only one modality to appear at one side, attentional benefits are also seen for a second modality (810).

Importantly, tactile stimuli is first coded in a skin-based somatotopic reference frame and need to suffer some type of coordinate system transformation to be a successful cue for visual selection. This results, in the case of local tactile cueing, in effects that can be observed in two different reference frames depending on the interval between tactile cue and visual stimulus (31). These two different reference frames can be disentangled by positioning the limbs in conflicting locations, for instance, crossing the left-hand to a position in the right visual field. This represents an incongruent crossed-limb condition, in which short cue-target intervals produce a cueing effect directed to the side of the body stimulated (e.g., left side for left-hand) instead of to the external location of the stimulation (e.g., right visual field when the left-hand is

crossed). Thus, in the study of visual selection guided by tactile cues it is always necessary to assess in which reference frame the cueing effect takes place.

Overt attention tasks

In general, saccades are faster and more accurate to visual than auditory (955, 274, 338) or tactile targets (321, 617, 72). The interaction between vision and touch for spatial decisions and eye movements is likely biased to the most informative dimension of vision; visual distractor induce higher error rates for somatosensory guided saccades than the inverse (12). Irrelevant tactile stimuli facilitate saccades to a visual target when presented before the visual stimulus, specially when spatially congruent (12, 199) and bimodal targets are fixated faster than compared to only visual stimulation (321).

However, during free viewing, the evidence for crossmodal influences is scarce. In a previous study, by Onat *et al.* (651), the presentation of auditory cues resulted in an reorientation of exploration towards the hemifield where the sound originated. This led us to the question of whether tactile cues, which can also have a spatial local and global orienting effect in cueing tasks, could also guide visual selection during free viewing. Finding such an effect could be of potential use for developing multi-sensory displays that can give spatially-directed warning signals, for example, while driving (807). For such a purpose, it is of special interest in which reference frame tactile-to-visual effects would occur, as discussed above for the case of local tactile cueing. Previous overt-selection experiments in which a tactile stimulus serves as the goal (local) of a saccade, have shown that early movements might be guided incorrectly in a skin-based reference frame (321, 660). However it is not clear if such will be the case when the tactile stimuli is irrelevant and the possible orienting effect is global. We performed an experiment to understand this possible different guiding effects of tactile stimulation during free-viewing behavior, which is described in **Chapter 3**.

1.1.4 Visual selection and bias

Visual attention is usually discussed in terms of the tension between stimulus-driven and goal-oriented mechanisms. Even though these conceptual distinctions are already relatively broad, actual human behavior does not always seem to fit in one of these categories. There is another set of factors that is often overlooked, namely *spatial biases*, which describe the tendency to explore certain areas of the visual field independently of given instructions and actual image content.

Perceptual and action bias

Biases in overt exploration are hinted by biases in tasks that require perceptual judgements or actions others than eye-movements. Studies employing covert tasks have shown that human subjects have a preference for stimuli within the left visual hemisphere. This perceptual bias is sometimes expressed by a biased motor action, for instance, as shown in the phenomenon of *pseudoneglect*: human subjects, when asked to bisect a line in the middle, usually err slightly towards the left (394). Other examples of perceptual bias were discovered by using chimeric stimuli, for example, when presenting faces composed by two hemifaces with different attributes (e.g., different emotions, identities, or gender). Several studies have shown that subjects presented with chimeric stimuli consistently overreport the attributes presented on the left side (46, 112, 327, 328, 489, 565, 680). These biases are present for brief stimulus presentation (not allowing eye movements) and thus indicate that they reflect a covert selection bias. However, they have also been shown in free-viewing paradigms (112), sometime with even stronger effects (113), suggesting that biased eye movements had also an effect on biased perceptual reports.

Free viewing bias

Overt visual exploration is also biased. For example, human subjects display a center bias expressed in a tendency to explore first and preferentially the center of an image (e.g., 665, 666, 834, 833, 871). A straightforward explanation for such bias

would be that it follows a content bias present in photographic images, in which the most important items are presented in the center or slightly off-center (224). However, usual composition recommendations for photographers suggest, for stronger appeal, to place most important content off-center (*rule of thirds* and *golden triangle rule*, e.g. 411). This is supported by experimental evidence showing that humans do prefer images where the object of interest is located off-center (493, 138, 177). In any case, the centre bias can also be shown to be independent of content or feature bias (833), and is also present during visual exploration in the real world (758) or over wide homogenous fields (417, 416).

Still, the presence of a centre bias does not explain why we observe a perceptual bias along the horizontal dimension. Besides the above mentioned leftward perceptual bias, it was a common anecdotal observation of eye movement researchers that, during free viewing, there is a left bias during early exploration (this can already be seen informally in the examples in fig. 1.1c-d). However, to confirm this, it is necessary to perform an experiment that disentangles any observed horizontal spatial bias from content biases within the presented images. To study the existence and causes of horizontal biases during free viewing behavior we performed a series of experiments, which will be presented in **Chapter 4**.

Pathological biases

Spatial biases are also a hallmark attribute of some neurological conditions. The best known condition that results in a spatial bias is neglect syndrome, which is characterized by an attentional and awareness impairment of, most commonly, the left side of the world. This attentional bias is accompanied by a similar bias to only explore the right side of the world (416, 521), which is also the case for the group of patients that participated in the experiment described in **Chapter 2** (599).

There are clear parallels between normal and pathological biases. As explained above, healthy humans show consistent biases to the left, whereas in the neglect syndrome the attentional bias is to the right, after cortical or subcortical lesions of the right hemisphere. Strokes in homologous areas in the left hemisphere do not usually produce a corresponding bias to the left, or this happens only in the acute phase after brain injury (80). Many theories have been advanced for this functional and pathological asymmetry, which are discussed more extensively in the General Discussion (section 8.1.4, p.136). In general they are formulated in terms of structural and functional cortical asymmetries. However, there is also a large body of evidence showing that the brain circuits responsible for attentional and eye-movement control are composed by a large, bilateral, cortical and subcortical network, in which natural or pathological structural asymmetries of any node can result in indirect disfunction of the complete network (see reviews by 669, 360, 449). The main subcortical structures involved in visual selection are located within the forebrain basal ganglia and the midbrain superior colliculus. It is likely that a substantial part of the pathological bias in neglect syndrome is due to the right lateralization of some of the cortical components of the attentional network (e.g., 44, 157). However, the relevance of post-injury functional asymmetries in subcortical structures, particularly of the basal ganglia and superior colliculus are also supported by extensive evidence. In human and in different animals models, it has been repeatedly shown that attentional and exploratory biases produced by a cortical lesion are reduced by further contralateral lesions in those subcortical structures (814, 912, 901, 917, 734), highlighting the importance of an overall, cortical and subcortical, balance between hemispheres for a normal unbiased deployment of spatial attention (669).

Another case of pathological bias is the one observed in Parkinson's patients. Parkinson's disease is caused by a degeneration of dopamine neurons in the substantia nigra pars compacta, a small bilateral nucleus of the basal ganglia. Patients with Parkinson's show a variety of symptoms, especially the triad of motor symptoms of bradykinesia, tremor and rigidity, but also multiple other cognitive and emotional symptoms. Patients with predominantly left motor disease, which in turns reflects a stronger degeneration of the right basal ganglia, show signs of attentional rightward biases. This can be evidenced in bedside tests like the line-bisection task, but also in the patterns of overt visual exploration of simple and complex stimulus (215, 752). Complementary to this clinical observations, normal asymmetries in dopamine content between the left and right hemisphere have also been related to slight, general exploratory biases in rats (963) and humans (179, 580). This suggests that a part of the normal small biases observed in healthy people might be explained not only by cortical structural asymmetries, but also by subcortical asymmetries in the basal ganglia dopamine system. In the case of patients

with Parkinson, this effect would be exacerbated by stronger asymmetries produced by an asymmetrical progression of the disease.

Together with the already mentioned evidence for a central role of subcortical balance in the case of neglect syndrome, this suggests that pathological biases may be controlled by manipulation of the basal ganglia. One possible method that could be used in this context is deep brain stimulation therapy, in which electrodes are chronically implanted in the brain to electrically stimulate the basal ganglia. Although the exact physiological effect of stimulation is still under debate (555, 583), its benefits as a therapy are undoubted, as it usually leads to substantial improvement of the patient's symptoms and quality of life (182). Following the results of experiments with animal models, and of two human cases, in which unilateral left injury of the basal ganglia or superior colliculus resulted in remission of neglect, we hypothesized that in Parkinson's patients the unilateral stimulation of the basal ganglia should result in the reversion of bias, or alternatively in the induction of a temporary bias in the case when it is not present. We tested this in a experiment described in **Chapter 6**, in which a group of patients with Parkinson's disease participated in a free-viewing task. By evaluating the effects of bilateral and unilateral stimulation of the sub-thalamic nucleus on visual selection, we tested the possibility of using such a therapy for the treatment of symptoms of spatial neglect.

1.2 Visual processing and eye movements

So far, this introduction focused on the decision process of visual selection. But also during and after the execution of an eye movement the processing of visual information in the brain is modified. In the following, I will provide a description of the effects that different stages of an eye movement have on the processing of visual information. First I will describe neural events before and during an ocular movement, with a short detour about the artifacts that eye movements introduce to electrophysiological recordings, which is the main topic of the research presented in **Chapter 6**. Finally, I will give an overview of the processing hierarchy inside the visual system in order to discuss the possible impact of eye movements at different stages within this hierarchy, thus providing the background for the last experiment presented in **Chapter 7**.

1.2.1 Changes in neural activity around eye movements

Pre-movement effects

As described in a previous section, eye movements are preceded by attentional shifts into the region of space targeted by the movement. In general, any kind of attentional benefit has a neural counterpart of change in the activation of the neurons with receptive fields (RF) that spatially coincide with the attended region (110, 586, 591, 418, 86, 282, 800, 802). This is also the case for attentional shifts occurring in the peri-saccadic period (110, 152, 293). Furthermore, some neurons in higher visual areas, for instance in the lateral intraparietal cortex and the frontal eye fields, dynamically change the location of their receptive fields in the moment prior to an eye movement (212, 876, 307, 471, 859, 610, 347). This RF remapping has been related to the control of successive eye movements in absence of visual cues and to the maintenance of visual stability across eye movements (941, 590).

During-movement effects

During the execution of an eye-movement, the retina receives rapidly changing input, equivalent to a movement of the visual field during fixation. However, the processing of these two equivalent inputs is not equal; we do not experiences sudden movement of the visual world during each saccade. This matches psychophysical results showing that the sensibility for visual events during eye-movements, specially for low-spatial frequency luminance changes, is largely reduced (105, 196), whereas a comparable whole field motion, in the absence of an eye movement, is clearly visible (104, 196). The absence of a movement experience is correlated with the suppression (or sometimes enhancement) of neural activity during eye movements (717, 852, 828, 381, 87).

The processing of visual events before and during saccades is also associated with a series of distortions in the perception of space and time (reviewed in 730, 749). For instance, stimuli flashed briefly before a saccade, are usually mislocalized and compressed in the direction of the eye movement (542, 729, 116, 483, 409). Similar peri-saccadic changes in visual perception exist even when eye movements are impeded by experimental muscular paralysis (822, 543, 921), indicating that they are associated to the movement command instead of to the registration of the actual movement.

This kind of results has been mainly interpreted as evidence for an internal, *forward model* of a stable world that gets updated by means of efferent copies of motor signals. Distortions of space and time perception would then be the result of wrong updates due to, for instance, temporal uncertainty of events that occur just before or after a movement, or when the movement fails to be executed (941). However, not all experimental results are easily accommodated by this framework (90), hence casting doubts on explanations in terms of a forward model and favoring alternative mechanisms, for instance, in terms of trans-saccadic memory and object template matching processes (192, 90).

During-movement artifacts

Eye movements can produce large non-brain-related artifacts in electroencephalographic (EEG) recordings. Although EEG experiments that allow eye-movements have been appearing from the beginnings of the usage of EEG (238, 315), ex-

perimental paradigms allowing movement (of any kind) are mostly avoided due to the strong electrical artifacts produced by the movement of the eyes. A large part of these artifact are due to the eyes being equivalent to an electrical dipole that results in electrical potentials at the scalp that are orders of magnitude stronger than the electrical dipoles associated to brain activity. This poses a general methodological problem in the context of EEG experiments and particularly so with regard to studying the neural correlates of processes involved in the execution of eye movements and their effect on visual processing in humans. To overcome this problem and to be able to use EEG under free-viewing conditions we studied the characteristics of ocular artifacts and investigated possible correction methods, work that is described in **Chapter 6**.

Post-movement effects

Finally, measuring EEG during viewing behavior also allows us to investigate changes in neural activity that occur in response to eye movements. These changes are not completely explained by the registering of a new visual input as in passive stimulation. Post-saccadic responses can be demonstrated even in the absence of visual stimuli, during movements in the dark or over an homogenous field (268, 791, 710, 656). On the contrary, it is reasonable to propose that visual processing after eye movements is qualitatively different to visual processing without eye movements, as briefly introduced above in relation to the distortion of spatial and temporal perception for events occurring around the movement event. For a better understanding of these phenomena it is helpful to briefly review the cornerstones of visual processing within the brain.

1.2.2 Overview of visual system organization

The visual system is organized in multiple cortical and subcortical modules

The visual system is organized in multiple subcortical and cortical structures that are separable due to anatomical criteria and by distinguishing whole sections of the cortex that present a complete, or close to complete, topographical representation of the visual field (549, 247, 766, 885). More specifically, in most visual areas the spatial arrangement of neurons directly reflects the spatial structure of the visual input (318). This means that areas of the world that are adjacent, and thus project to adjacent locations on the retina, provide visual inputs that also result in an activation of close-by neurons. However, this topographic retinotopic mapping of the visual world does not result in all locations of the visual field having the same amount of cortex and neurons dedicated to them. Regions of the world that projects to the retina's fovea, the central part which is aligned with the line of gaze, are represented by a larger cortical area than regions of similar spatial extent but at more peripheral regions (173, 862). Note that the cortical magnification of some regions of the world does not always result in the preferred processing of central locations, since some visual field maps show preferred representations of the periphery (492, 526). However, in general, polar visual field maps with preferred processing of the foveal region are prototypical within cortical and subcortical structures, and thus have served as one of the main ways to establish separate visual areas.

Visual areas are organized in a processing hierarchy

From the study of simple gross connectivity, it is possible to postulate that visual areas are organized hierarchically, since most of the projections from the visual thalamus go to the primary visual cortex (V1), and then to other areas via successive cortico-cortico (or via the thalamus) connections. This hierarchical organization derived from anatomical connectivity is not unidirectional, since most areas are reciprocally connected (247). This reciprocal connectivity provides further support for a hierarchical organization because it shows that projections between cortical areas can be divided in two main types depending on the cortical layer in which they start and end. *Feedforward* connections from a functionally lower area to a higher one, results from projections of neurons in superficial and deep layers to layer 4. In contrast, *feedback* projections from a higher to a lower area, which also emerge from both deep and superficial layers terminate in layers other than 4 (724, 247, 534). This hierarchical organization with a feedback component, which is usually even stronger

than the feedforward component (534), is assumed to be essential for perceptual learning and also for inferential neural codes (see below).

Next to physiological aspects there are also functional considerations that support the view of the visual system as being hierarchically organized. Neurons early in the hierarchy respond to simpler stimuli while at higher stages neurons respond to increasingly complex patterns, arguably by building-up on the convergent combination of features computed in lower areas (831, 770). This is also evidenced in the observation that the receptive fields of neurons become increasingly larger as one progresses from lower to higher processing stages (957, 286, 794). Neurons in V1, for instance, can have receptive fields smaller as a fraction of one visual degree for the foveal area (376, 286), while neurons in the ventral temporal cortex might respond to stimuli at almost any location within the visual field (189, 79).

In summary, both structural and functional criteria support the idea of a hierarchical organization of the visual system. This hierarchical organization is nevertheless not restricted to a single stream nor there is a single area of convergence. Instead the distributed characteristic of the visual system allows for functional specialization of the different cortical and subcortical modules (958).

Visual areas are organized in functional streams

The relevance of a sensory stimulus does usually not depend on its absolute intensity but on relative differences across space and time. Thus, sensory systems are not simple devices for the transmission of, for instance, a spatial distribution of light, but they are organized to detect patterns of the world that have some ecological of behavioral relevance for the animal and, therefore, an associated behavioral response (490). Following this logic, neurons in different brain areas respond to different stimulus features, which leads to at least two different ways of functional organization of sensory systems.

Firstly, following the idea of hierarchical processing, functional specialization results in that early stages process simple features, which in turn serve as a basis for the processing of more complex features in latter ones. This was demonstrated as early as in the studies by D. Hubel and T. Wiesel on the visual areas of cats and monkeys, in which the responses of some set of neurons could be explained through combination of other simpler ones (374, 375). For example, neurons in V1 respond to straight lines, edges of different orientations, motion, disparity between eyes, and color contrast (119). In the next level, namely in V2, the neighbor area to V1, we find stronger response for angles and intersection patterns (346, 388). Likewise, it is possible to find specialized areas for multiple other features like global and fast motion processing (area V5, 956), or color constancy and form processing (area V4, 957). Finally in the highest levels of the visual hierarchy, neurons are responsive to complex patterns that correspond to object categories (118, 523), with even complete sections of the cortex dedicated to a specific category like faces (413, 412), human body parts (208) or spatial landmarks (232, 3).

While the view of sensory processing as feature detection has been an immensely fruitful research approach, it should not be interpreted as if neurons within each area are responsive to only one feature dimension (288), nor that the hierarchical organization is composed by a single sequential hierarchy. Specially at early stages, neurons are selective to multiple stimulus dimensions (491, 289) and different areas are organized in several structural and functional parallel streams. This leads to the second way in which functional specialization can be understood, since we can identify the functional specialization of not only single areas but of complete (parallel) streams of processing that seem to be involved in different functional realms.

Two distinct parallel streams can be distinguished in terms of both, their anatomical structure and by the kind of information they convey. The first runs from the occipital pole to temporal and frontal areas that are located more ventrally and laterally. The second one also runs from the occipital pole to parietal and frontal areas that are located dorsally and laterally (880, 522). As initially proposed by L. Ungeleider and M. Mishkin, the dorsal pathway is often referred to as the "Where?" pathway as its respective structures are mainly involved in the processing of spatial information such as object location and movement perception. The ventral stream on the other hand is functionally related to the perception of object features and is thus called the "What?" pathway (880, 578). These distinction were based in anatomical and functional considerations derived from neurophysiological and lesions experiment with monkeys. Dorsal lesions result in stronger

localization deficits but do not impair the identification of objects, whereas lesions in ventral areas have the opposite effect. This gross division evolved to the now more popular view of the ventral and dorsal stream being involved with conscious perception and action respectively. This was suggested by M. Milner and D. Goodale based on the clinical case of a patient that was unable to identify objects but able to manipulate them (305, 304). More recently there has been attempts of a more refined distinction between visual functional streams, which have resulted in further division and specifications of both the dorsal (462) and ventral streams (463) that nevertheless maintain the general idea of large parallel and distributed streams.

In summary, probing neurons or cortical areas with different types of stimuli, reveals that the visual system is composed of multiple pathways and processing modules. As one progresses from one stage to the next, neurons become responsive to increasingly more complex patterns, thus supporting the view that the visual system is organized hierarchically. However, although the respective evidence is vast it is also methodological biased by the reductionistic approach of probing sensory systems passively with simple stimuli that are isolated from any spatial and temporal context. The use of simple parametric stimuli allows to study the activity of visual neurons, and brain areas, as linear systems that combine a unique basis set of processing functions, for instance, optimal filtering function like 2D Gabors (181). Sensory processing is, however, populated by non-linearities. Models of neural processing that also incorporate some basic static non-linearities to implement luminance and gain control so neuronal activity remains bounded, sensitive to weak stimuli, and responsive to relative, rather than to absolute differences, are able to explain a much larger amount of the variance of neural responses in retina and the lateral geniculate nucleus, both for simple and naturalistic stimuli (136, 532). However, even the models with this additional basic non-linearities become increasingly inadequate as we advance in the visual hierarchy. In this context an increasing number of researchers advocate for the use of complex naturalistic stimuli, since sensory systems are likely to be adapted to ecological rather than to synthetic stimuli (789, 650, 249). Corresponding experiments have revealed that the sum of the neural responses to simple synthetic stimuli cannot explain the neural activity observed in response to spatially and temporally complex stimuli (36, 896, 174). These considerations and the highly recurrent organization of the visual system, which is to a large extent unnecessary for a feature detection system in the form of a feedforward hierarchical system, have lead to multiple theoretical, computational and empirical lines of research that try to explain sensory processing in terms of efficient processing and probabilistic inference.

1.2.3 Vision as efficient information processing

A different understanding of the mechanisms of neural sensory processing, not necessarily incompatible with the feature detection view, is that they evolved to efficiently represent the sensory world. This efficiency can be understood in terms of adaptation to the statistics of natural stimuli, or in terms of optimal information transfer in the presence of noise and uncertainty.

The study of sensory processing as the optimization of an information transmission problem followed the development of information theory by C. Shannon (773) and started with the realization that natural sensory inputs are highly redundant (27, 40). In any projection of a natural scene, adjacent locations tend to be very similar over space and time, a regularity that can be easily detected by humans (431). These redundancies could in principle be exploited by an information processing system. Moreover, this could be thought as a design principle, so the system is maximally efficient in terms of transmitting information with the most compact code possible (26).

An efficient redundancy-reduction code would result in multiple benefits such as reducing stimuli dimensionality, which then can be processed by a smaller physical system using less energy. Taking into account the high metabolic rate of firing neurons, with 20% of body oxygen consumption by the brain for only 2% of the total body mass (556), a neural code that both maximize representational capacity and minimizes energy expenditure requires that only a small subset of neurons are active for any given stimulus (495, 485, 28, 488). Moreover, efficient coding has potential benefits in terms of

cognitive processing, since redundancy reduction naturally result in the generation of feature detectors that can be used to recognize frequent stimulus patterns and to learn similar new ones (915, 41, 26).

The field of computational vision has provided multiple forms of evidence that supports the idea of efficient coding. This has been usually in the form of neural network implementations of algorithms like Principal and Independent Component Analysis. When trained with natural stimuli, these algorithms result in outputs that display spatial characteristics similar to the receptive fields of visual neurons (334, 647, 57). One of the most interesting computational principles in this respect is sparse coding, where the individual processing units are not only forced to be uncorrelated but also to fire sparsely. The result is statistical independence between units that is higher than in other types of coding that take in account only the redundancy secondary to linear correlations in the stimulus (648). Inputs are thus represented minimally, as the linear combination of few basis functions, which are chosen from an "over-complete" set (648). At first glance, this appears to oppose the idea of efficiency as redundancy reduction, since an over-complete set of basis functions would be of higher dimensionality than the possible inputs. Nevertheless, this seems to be in agreement with the observed pattern of divergence and expansion of projections from V1 to higher areas (649). More importantly, the efficiency of the code results from neurons having the same probability to respond across all images but with few neurons being active for the representation of a given single input (250). These more selective and statistically independent responses would result in metabolic benefits and allow for easier manipulation at higher processing levels (647, 648, 649).

In summary, the development of these different computational models, together with a deeper understanding of the organizational principles within the visual system, has led to a different perspective on efficient coding. It has shifted from an emphasis in redundancy reduction to a focus on the advantages of a code that exploit the statistical properties of the environment, through "internalizing environmental regularities" (42) for behavior. In other words, what is relevant is the ability to recognize patterns that are frequent in the world rather than compressing redundant information. In this view, redundancy is made explicit rather than eliminated, such that neurons respond with greater specificity to patterns that are likely to be experienced. In theory, this results in an improved signal-to-noise ratio, with feature detectors that are "tuned" to an optimal interpretation of behaviorally relevant features (42). In this way, efficient coding is transformed into an inference process, in which the feature detectors represent general statistics of the world.

1.2.4 Vision as a probabilistic inference

While sensory information is often redundant, it is also more ambiguous than we consciously realize. In the light of this dichotomy between redundancy and uncertainty, it has been proposed that the mechanisms for sensory processing are inherently probabilistic, in which perceptions are equivalent to inferences about inputs' causes instead of just the detection of behaviorally relevant patterns. The idea of the brain as an inference machine was already put forward more than a century ago by von Helmholtz (898) and has been repeatedly proposed as one of the basic mechanisms of neural function ever since (317, 598, 176, 432, 447, 278, 260, 145, 769).

In the last decades, multiple lines of evidence have shown that in many cases behavior is statistically optimal with respect to the sensory information available (447, 769). Most of the respective experimental evidence was acquired in tasks that require the subjects to judge a certain property of an object based on information coming from different sensory sources. The cues then need to be integrated, according to their reliability, with the prior knowledge about the prevalence of different states in the world. This consideration leads directly to the use of a Bayesian statistical framework, to study behavior and to evaluate how optimal subjects responses are with respect to the current and historical information available to them. A bit more formally, the likelihood of an input to occur under the current circumstances is combined with learned priors. These priors in turn correspond to the probability of such an input to occur in general (i.e. under all possible circumstances). Likelihood and prior are then used to make predictions about the next input, and to subsequently update the set of beliefs about the world. Humans and other animals often do behave Bayes optimally (reviewed in 447), although this

is not always the case (85). In the "Bayesian coding hypothesis" (447, 278), however, it is proposed that not only behavior can be analyzed using Bayesian methods but that the brain itself operates as a Bayesian hierarchical generative model of the world. This probabilistic view can be used to understand the evolution of cognitive functions, with animals that are adapted to their environments through the acquisition of statistical knowledge about the natural world. From this perspective neural activity encodes prior and likelihood distributions that in combination with utility fitness functions permits to performs optimally in terms of survival (290). It is important to note though, that in addition to the multiple cases in which subjects do not behave optimally, it is also not clear whether the results showing optimal behavior do necessarily entail that perception and the underlying brain functions employ Bayesian inference. The observed optimum could equally be implemented in multiple other ways (529, 153), for instance via a "table-lookup observer" organization (529).

With respect of the possible brain mechanisms implementing probabilistic inference, D. Mumford was one of the first to propose that the hierarchical recursive organization of the visual system might implicate some kind of probabilistic coding (598). Crucially, he proposed that the relevant cortical computations were mainly operations between, rather than within, areas of the hierarchy, carried out through the pervasive reciprocal connectivity that results in cortico-cortico inference loops. Following this idea, higher areas would encode templates that fit the input coming from lower areas which in turn would compare these templates with their own inputs to compute the corresponding residual. This residual is then sent again to higher areas via the feedforward path. These ideas were later formally conceptualized as a hierarchical Bayesian neural network (487, 279), a model that provides a series of predictions about what kind of activity should be encountered at different cortical areas. By now, some of these predictions have been partially confirmed by diverse neurophysiological experiments (487, 48).

A similar view on the implementation of probabilistic inference by the brain is predictive coding. It was first postulated as such by M. Sirinivasan and colleagues as the mechanism underneath the inhibitory surround structure of the receptive fields of retinal neurons (816), and as a way to increase neural sensitivity. Complementary to the efficient coding hypothesis, the predictive coding scheme was also seen as a way to deal with intrinsic noise, which bounds the smallest resolvable signal. Given the correlational structure of natural stimuli, it is possible to make predictions based on spatial context. These predictions results in a reduced total signal amplitude, which allows to resolve small non-redundant fluctuations over the intrinsic noise, while at the same time permitting a wider response range. Importantly, in this formulation predictions are based on the correlational structure of the average of natural stimuli statistics, and thus they are not an adaptive process to singular inputs. The current modern view of predictive coding is that one set of neurons encodes a probabilistic model of the external world that is used to make predictions of sensory inputs, and another set of error computes the mismatch between prediction and inputs, transmitting only what was not predicted (i.e., the error signal) (711, 279, 815, 372). As in efficient coding, support for probabilistic coding is found in computational models in which both classical and extra-classical receptive field properties of neurons in primary visual cortex can be modeled by the predictive coding scheme (711, 815).

While there is mounting evidence showing the compatibility of animal behavior with a Bayesian inference mechanism, there is relatively little neurophysiological evidence supporting the idea that this is mediated by some kind of predictive coding mechanism. Most of the evidence is limited, however, to highly artificial scenarios of repetitive stimulation that is passively perceived. Following the view of the brain implementing probabilistic inference during sensory processing, it can be further proposed that actions are a way to gather additional information about both the currently perceived input and about parts of the world that are not currently sensed. In the case of vision such sampling actions take the form of eye and head movements. These make it possible to access to more accurate information from peripheral regions of the visual field and from parts of the world that are beyond of what is visible at the moment. In this respect, K. Friston and colleagues formulates the role of action as, if perceptions are hypotheses about the world, then eye movements are experiments to confirm these hypotheses (280). To do so the brain selects prior belief about to where to move the eyes to minimize perceptual uncertainty, which will result in a proprioceptive prediction of the actual movement that will be carried out through a reflex arc, and in predictions of the visual consequences of the movements. The sensory consequence of moving the eyes can also be cast in terms of predictive coding, in which the over-learned sensorimotor

contingencies between eye-movements and the corresponding changes on the visual input are used as a generative model. If the prediction does not match the sensory input that results from a new fixation an error signal is generated. The last experiment of this book, presented in **Chapter 7**, tests this idea by means of a saccadic-contingent change experimental design. More specifically, in some trials we changed the peripheral visual input during an eye movement, which should result in a corresponding error signal after the new fixation. Crucially, we varied the stimulus reliability by presenting it inside (veridical information) and outside the blindspot (inferred information), which, if the idea of predictive coding holds up, should result in a difference in neural activity.

Chapter 2

Unmasking the contribution of low-level features to the guidance of attention

Abstract

The role of low-level stimulus-driven control in the guidance of overt visual attention has been difficult to establish because low- and high-level visual content are spatially correlated within natural visual stimuli. Here we show that impairment of parietal cortical areas, either permanently by a lesion or reversibly by repetitive transcranial magnetic stimulation (rTMS), leads to fixation of locations with higher values of low-level features as compared to control subjects or in a no-rTMS condition. Moreover, this unmasking of stimulus-driven control crucially depends on the intra-hemispheric balance between top-down and bottom-up cortical areas. This result suggests that although in normal behavior high-level features might exert a strong influence, low-level features do contribute to guide visual selection during the exploration of complex natural stimuli.

This chapter was published as a peer reviewed article: **Ossandón JP**, Onat S, Cazzoli D, Nyffeler T, Müri R, König P. Unmasking the contribution of low-level features to the guidance of attention. *Neuropsychologia*, **50**:3478-3487 (2012).

2.1 Introduction

Both low- and high-level features of visual stimuli have been proposed to guide overt visual attention (156, 188, 390). Under appropriate task settings, locations in the visual field that are salient on a single feature dimension are detected effortlessly via pre-attentional mechanisms (188, 869). However, in complex visual stimuli it is still controversial how much independent influence low-level visual features (e.g., luminance and color contrast) exert during visual exploration. In this case, low-level visual information is usually not organized in such a way that locations can be distinguished globally, and high-level visual information, like the identity and structure of objects and scenes, is preeminent. This type of high-level information guides ocular movements in a non-reflexive manner driven by subjects' context and goal sets. During the unconstrained exploration of complex stimuli these contextual factors and goals are internally generated and presumably in continuous change, thus resulting in high within- and between-subjects viewing variability. It has been proposed that low-level features could still guide visual selection of complex stimuli by means of a spatially-organized saliency map that integrates local saliency across multiple feature dimensions (389, 450). Supporting this idea, the unconstrained exploration of complex visual stimuli results in the selection of locations with higher low-level features values than non-fixated locations (1, 220, 464, 665, 714, 834). However, there are two strong arguments that question the causal effect of low-level features. First, explicit differences in task requirements result in substantial changes of low-level content at fixated locations, thus challenging automatic effect (222, 835). Second, low- and high-level visual content are spatially correlated in complex stimuli. Locations may therefore be selected only based on their high-level content (223, 351, 425).

An alternative approach to understanding the role of low and high-level information in visual selection is to look at the effects of a disruption of the integration of high-level information for goal-oriented control. Such disruption occurs in various clinical conditions like visuospatial neglect. Neglect syndrome is characterized by a loss of attention to, awareness of, and exploration of visual stimuli that is located in the contra-lesional hemifield. Although neglect patients can present a striking lack of awareness, they actually do process a substantial amount of high-level information from the neglected stimuli, up to the analysis of object identity (536, 554). Similarly, they are also able to produce some types of goal-directed behavior to the neglected hemifield. For example, they are able to spatially orient to the neglected hemifield when instructed by non-local cues (e.g., 474). In spite of this residual functioning that can be shown experimentally, neglect patients are unable to use high-level information to guide spontaneous behavior. On the other hand, guidance of visual selection based on low-level information seems to be preserved when tested (209). For instance, in visual search tasks, neglect patients' performance in the neglected hemifield is better when the target is distinctive in a single feature dimension compared to when it is defined by a conjunction of visual features. Moreover, similar to healthy subjects, their reaction times for the search of these feature singletons do not change with an increased number of distracters (2, 237, 393). These studies suggest that a "bottom-up" mechanism based in low-level features extraction could have a role in the exploration of scenes independent of "top-down" mechanisms based in high-level visual processing and goal- oriented visual selection.

Here we attempt to clarify the role of stimulus-driven control of attention by systematically studying the influence of low-level features on free-viewing behavior of complex scenes. First, in Experiment 1, we studied the viewing behavior of a group of healthy subjects during exploration of images with similar low- level content but different high-level content. Then, in Experiment 2, we examined a group of neglect subjects to test whether their attentional deficits unmask selection by low-level content during free-viewing of complex visual stimuli. Our hypothesis is that although patients might still be able to process high-level content in the neglected hemifield, this information is not integrated for ocular movement control; therefore, we should observe quantitative differences in the influence of low-level features between neglected and non-neglected hemifields and when compared with control subjects. Finally, in Experiment 3, we studied the behavior of subjects that underwent rTMS to inhibit the posterior parietal cortex (PPC) unilaterally or bilater- ally, aiming to reproduce the effects of a brain lesion and to study inter-hemispheric competition effects.

2.2 Experiment 1: Baseline study

2.2.1 Methods

Subjects: Forty-eight healthy subjects, students at the University of Osnabrück (25 males, mean age: 23.1 years) participated in the study. Written informed consent was obtained from all participants prior to participation. Experimental procedures conformed to the Declaration of Helsinki and national guidelines.

Stimuli: Two categories of visual stimuli were used. The first category (naturals) included 64 images depicting outdoor scenes (Calibrated Colour Image Database, 646) and 64 urban scenes of public spaces around Zürich.The second category included 63 pink noise color images. These images were generated from the images in the first category. Natural images were transformed to the Fourier space and their average power spectra were combined with random phases taken from a uniform distribution to generate the pink noise images. Images were presented in full screen at an 80 cm viewing distance on a 21" CRT monitor (SyncMaster 1100 DF, Samsung Electronics) at a resolution of 1280 x 960. Examples of the different images used are presented in Figure 2.2.

Eye tracking: Eye movements were recorded with a head-mounted video oculographic eye-tracking system using binocular pupil tracking at 500 Hz (Eyelink II, SR Research Ltd., Mississauga, Canada). Calibration was repeated until the average error fell below 0.3°(baseline).

Procedure: In all experiments presented here, subjects performed a free-viewing task. In the first experiment, images were presented for 6 s. Subjects sat in a darkened room in front of the monitor and were instructed to "study the images carefully".

Data analysis: We estimated the influence of low-level features in visual selection by comparing the distribution of feature values taken from fixated locations with a distribution of control values. A summary of the general analysis procedure is presented in Figure 2.1. In brief, we computed, for every image, a compound feature map that included different low-level features (Fig. 2.1a, see Section *Feature maps*) and a fixation probability distribution (fixation-pdf) of the probability to fixate in different regions of each image (see Section *Fixations spatial distribution map*). Additionally, we also created a bias-pdf that includes all fixation locations selected by the subjects; this map represents the overall spatial bias of exploration. With these feature maps, fixational-pdf and bias-pdf, two distributions of feature values could be generated, one with feature values that were actually fixated and an a priori distribution. The a priori distribution consists of the control feature values of the presented image according to the bias-pdf. The a priori distribution is independent of the exact stimuli presented since the feature values were taken for each image from locations selected during the exploration of the other images (see Section *A priori and actual feature distributions*). Finally, the distributions were compared by measuring the Kullback-Leibler divergence (KLD) between the two distributions.

Feature maps: To evaluate the low-level feature content on fixated and non-fixated locations, we used a compound feature map that combined three basic low-level features: luminance contrast, color contrast, and the edge content of the images (389, 834). Luminance contrast maps were calculated taking the standard deviation of the intensity values present in a circular patch (radius = 1°) centered at every pixel in the images. For color analysis, we transformed the images' RGB color content into the DKL color space (187). This space represents the images' color content in three orthogonal axes based on the relative excitation of three channels: red/green opponent axis, blue/yellow opponent axis, and luminance axis. Color contrast maps were then generated with the same method used to calculate luminance contrast, thus generating red/green and blue/yellow contrast feature maps. The edge content map was evaluated by filtering the images with a set of log-gabor filters (251), using six space scales and six orientations. To generate the final compound feature map of the images, each of the four image maps was scaled to values between 0 and 1 and then averaged in a single map.

Fixations spatial distribution map: We generated 2D probability distribution functions to visualize and calculate spatial biases and to calculate the influence of low-level features on visual selection. Two types of pdfs were used in Experiment 1: (1) fixation-pdf, calculated by taking the actual fixations done in each image/trial, and (2) bias-pdfs, which were calculated by taking the average fixation-pdf across all images and subjects, one for natural images and a second one for noise images. These different pdfs were further smoothed by convolution with a circular 2D Gaussian kernel of unit integral and a standard deviation of 0.5°.

R–L index: Exploration biases on the horizontal dimension were measured using the right–left (R–L) index. The index was calculated from the bias-pdfs of each subject, subtracting the overall fixation probability in the left hemifield from the overall fixation probability of the right hemifield:

$$R - L = P_{fix}(\text{right hemifield}) - P_{fix}(\text{left hemifield})$$

The R–L value indicates the proportion of biased fixation to the left or right hemifield. Accordingly, an R–L value of 1 means that exploration in a given experimental condition was only in the right hemifield, an R–L value of –1 indicates that the exploration was only in the left hemifield, and an R–L value of 0 means an unbiased exploration.

A priori and actual feature distributions: The influence on visual selection of a compound low-level feature was evaluated by measuring the Kullback-Leibler Divergence (KLD) between the distribution of feature values at fixated locations and an a priori distribution of the feature values available in the images. For the a priori distribution, we constructed a distribution of images' feature values using the spatial-bias fixation-pdf of the corresponding experimental condition (natural or noise images). This was done in order to take into account the pure spatial biases of each group, either by normal variations or by setup differences, and the general content biases present in the images. This approach is more appropriate than comparing values at fixated locations against all or randomly taken values (666, 834) and is used to avoid the confound that low-level content is not homogeneously distributed in the images. For instance, spatial bias like the central bias (which is independent of both image content and exploration starting point, see 833) can artificially inflate the influence of low-level features (834). Specifically, to generate this a priori feature distribution, we took the sum of the fixation

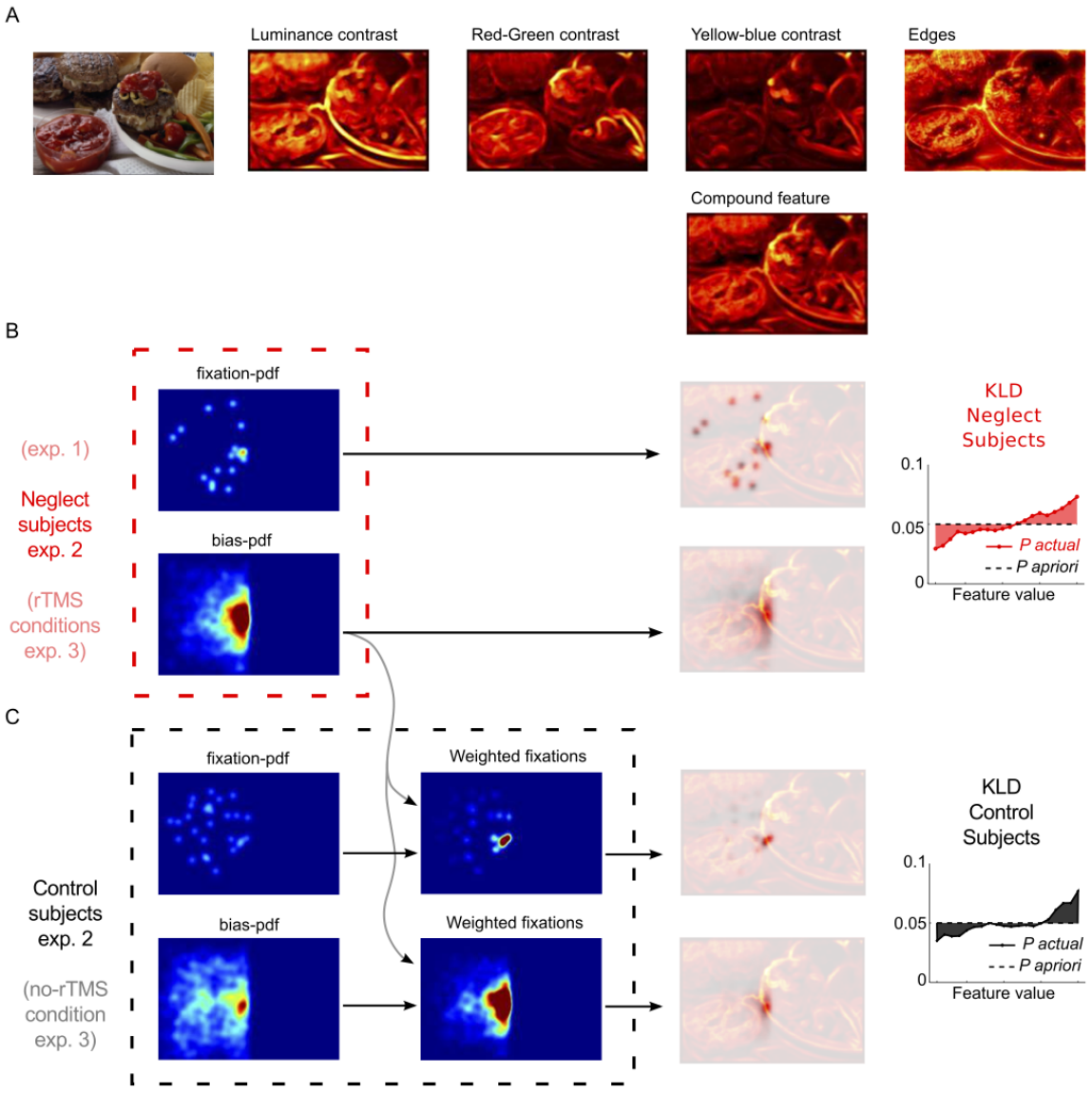

Figure 2.1: Data analysis. (A) Example of a feature analysis of one image. From the original image, 4 features maps are calculated and then combined in a compound map. (B) Examples of analysis. This example is taken from the data of neglect patients in Experiment 2, but it shows the same procedure used for the data analysis in Experiment 1 and for the rTMS conditions in Experiment 3. For every image, a fixation-pdf is computed, and the bias-pdf is taken from the exploration over all images. The fixation-pdf is the probability to fixate in different locations in a given image, and this map is used to extract the distribution of probability to fixate different feature values (exemplified here as a mask over the compound feature map, second column). The bias-pdf is obtained by taking all fixations done by the patients in all images; this map is used to extract the distribution of a priori values. This distribution of a priori values is whitened to a distribution of 20 bins with different spaced features interval but with the same probability to be fixated (third column, $P_{apriori}$) and the same bins are used for the actually fixated values (third column, P_{actual}). Finally, the KLD divergence is calculated between these two distributions (exemplified here as the solid color between P_{actual} and $P_{apriori}$).Analyses are done independently for each hemifield. (C) Example of analysis for the control subject in Experiment 2 and the no-rTMS conditions in Experiment 3. The procedure is similar to (B), but fixation and bias-pdf are further weighted by the overall spatial bias of neglect patients (or the respective rTMS conditions), as seen in the right panels within the dashed black box.

probabilities over locations with feature values falling into twenty equally spaced feature value intervals: $P_{apriori}(a \leq feat < b) = \sum_i P_{fix}(i)$, with a and b as the lower and upper limit of a feature interval and i as the locations with feature values between $(a, b]$. Once the a priori distribution was obtained, it was interpretation of the feature scale. The whitening results in a new individual feature binning with differently spaced intervals $(a_w, b_w]$, but with each one having the same probability of being fixated. A priori distributions were computed for each image separately. Then a final a priori distribution for the subject was obtained by taking the average across images. To generate the distribution of actually fixated feature values, we used the feature map and the actual fixation-pdf of each image seen by each subject. The actual feature distribution was obtained by taking the sum of fixation probabilities on locations with feature values falling into a given feature value interval, but now using the bin intervals obtained in the previous step with

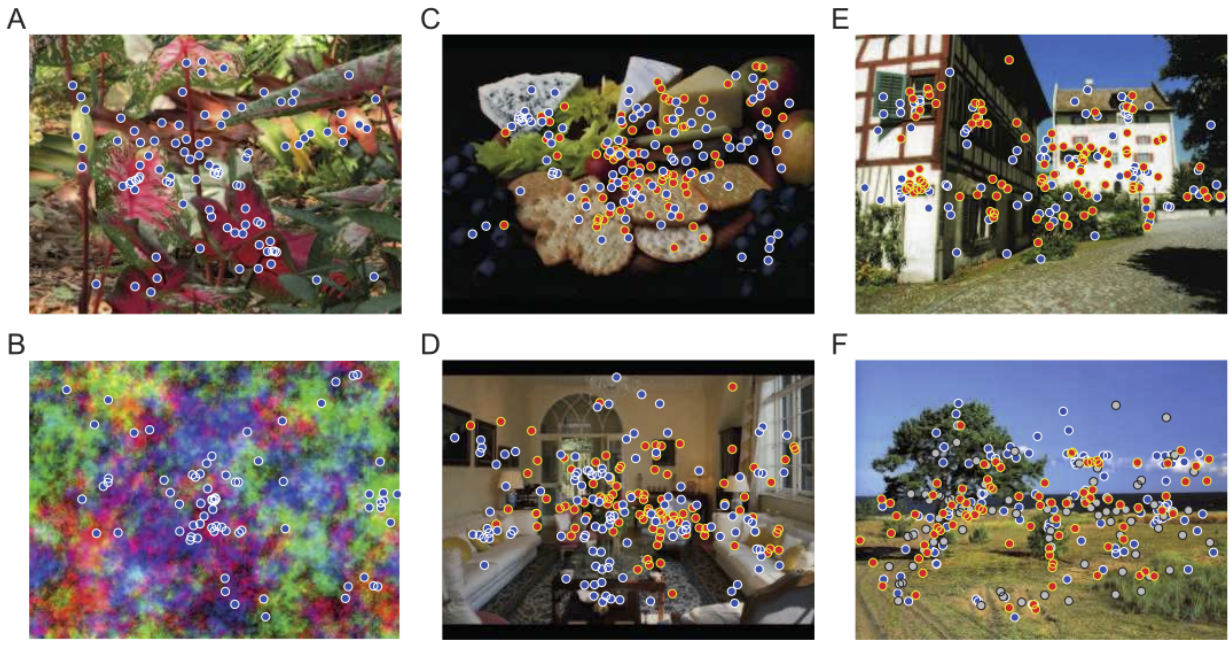

Figure 2.2: Examples of images used and locations fixated. ((A) and (B)) Examples taken from Experiment 1. Blue dots show locations fixated by five subjects in a natural scene (A) and in a pink noise image (B). ((C) and (D)) Examples taken from Experiment 2. Blue dots show locations fixated by 5 control subjects and the red dots show locations fixated by five neglect subjects. ((E) and (F)) Examples taken from Experiment 3. In both images, blue dots show locations fixated by five subjects in the no-rTMS conditions. In (E), red dots show the locations fixated by the same five subjects in the right/left-rTMS. In (F), red dots show locations fixated by the same five subjects in the left-rTMS condition and gray dots in the right-rTMS condition.

the images' a priori distribution: $P_{actual}(a_w \leq feat < b_w) = \sum_i P_{fix}(i)$.

Actual distributions were computed for each image separately, and the final feature distribution for the subject was obtained by taking the average across images. Once the a priori and actual feature distributions for each subject were obtained, the KLD between both distributions was used as a measure of the influence of low-level feature content in fixating behavior for each subject or subject/condition (926):

$$KLD_{apriori \to actual} = \sum_{i}^{n=20} P_{apriori}(i) \ln(P_{apriori}(i)/P_{actual}(i))$$

with i as the bin number corresponding to feature value intervals. As KLD is an asymmetric measure, we took the average between $KLD_{apriori \to actual}$ and $KLD_{actual \to apriori}$ as our final KLD measure.

Statistics: To evaluate differences in the R–L index in the baseline study, individual two-tailed t-tests were evaluated for each image category against the null hypothesis of no horizontal bias ($R - L = 0$). Unlike in experiments 2 and 3, in Experiment 1, the values of the $1/f$ image category were not normally distributed (Lilliefors test, K = 0.16, p = 0.001). Therefore, we used the non-parametric Mann-Whitney U test to contrast between image categories in both hemifields. In all experiments presented here, a significance level of 0.05 was used for all tests, and in the case of multiple comparisons, a Bonferroni correction of the significance level was performed.

2.2.2 Results

We conducted a baseline study in which 48 healthy subjects explored two image categories: natural scenes and pink noise. The pink noise images had the same spatial spectral content as the natural scenes but lacked the phase structure, which defines a scene's high-level content (686, 922). Figure 2.3a-b shows examples of the images used and locations fixated by five subjects. We examined horizontal biases during free-exploration by measuring the difference between the probability of fixating in the left and in the right hemifields. Overall, exploration was biased to the center of the image (Fig. 2.3a-b) and no significant horizontal bias toward the left or the right hemifield was found (R–L$_{naturals}$ = -0.02, $t_{(47)}$ = -1.85, p = 0.069; R-L$_{noise}$ = -0.02, $t_{(47)}$ = -1.01, p = 0.31; Fig. 2.3c). Nevertheless, within single subjects, their

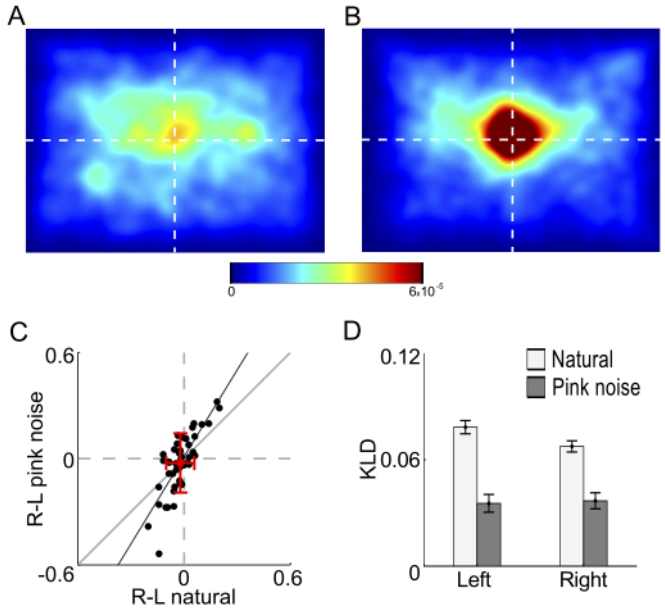

Figure 2.3: Experiment 1: Exploration and low-level feature influence in healthy subjects. ((A) and (B)) Spatial distribution of fixation probability for natural scenes (A) and pink noise images (B). (C) Right-left (R–L) values for the exploration of natural and pink noise images. Each dot represents R–L values of one subject. Red error bars represent population means±SD and the black line is the points' linear fit. (D) KLD values (mean over subjects ± s.e.m.) between feature values at fixated and non-fixated locations for each image category and hemifield. Compared to the exploration of pink noise images, exploration of natural scenes by healthy subjects results in the selection of locations with higher features values in both hemifields.

respective bias values for natural and pink noise images are highly correlated (r = 0.78, $p < 0.001$, Fig. 2.3c) and the slope of the regression line between noise and natural values is positive ($m = 1.63$) and significantly different from 1 (C.I. = 1.25-2.02, $t_{(46)}$ = -3.5, $p < 0.001$), indicating that single subjects deviations from zero bias in natural images are in the same direction and larger for the noise images. Therefore, there are idiosyncratic spatial biases that are consistent across different image categories but stronger when the images lack high-level content.

The influence of a compound low-level feature that includes luminance contrast, color contrast, and edge content was evaluated by measuring the Kullback-Leibler divergence (KLD) between the distribution of feature values at fixated locations and an a priori distribution of the feature values present in the images. For both image categories, the feature values were higher at fixated locations than non-fixated locations but comparatively higher for natural scenes than pink noise images in both hemifields (z_{left} = 6.2, $p < 0.001$; z_{right} = 5.4, $p < 0.001$; Fig. 2.3d). This result is consistent with guidance of attention by low-level features as well as by high-level content due to spatial correlations in complex stimuli. In order to differentiate between these two alternatives, we subsequently examined conditions where top-down control is disrupted.

2.3 Experiment 2: Neglect patients study

2.3.1 Methods

Preliminary behavioral results of the neglect study have been previously published (599). This previous work reported on exploration biases in neglect patients and in control age-matched subjects. In the present study, we investigate the influence of low-level content on the guidance of overt attention.

Subjects: In the neglect patients study, 15 patients from the Division for Cognitive and Restorative Neurology of Bern University Hospital (11 males, mean age: 55.5 years, SD: 9 years) and 8 age-matched controls (6 males, mean age: 48.5 years, SD: 9.5 years) participated in the study. The patients included in the study suffered from left-sided hemispatial neglect after a recent (< 2 months) cerebral damage exclusively confined to the posterior right

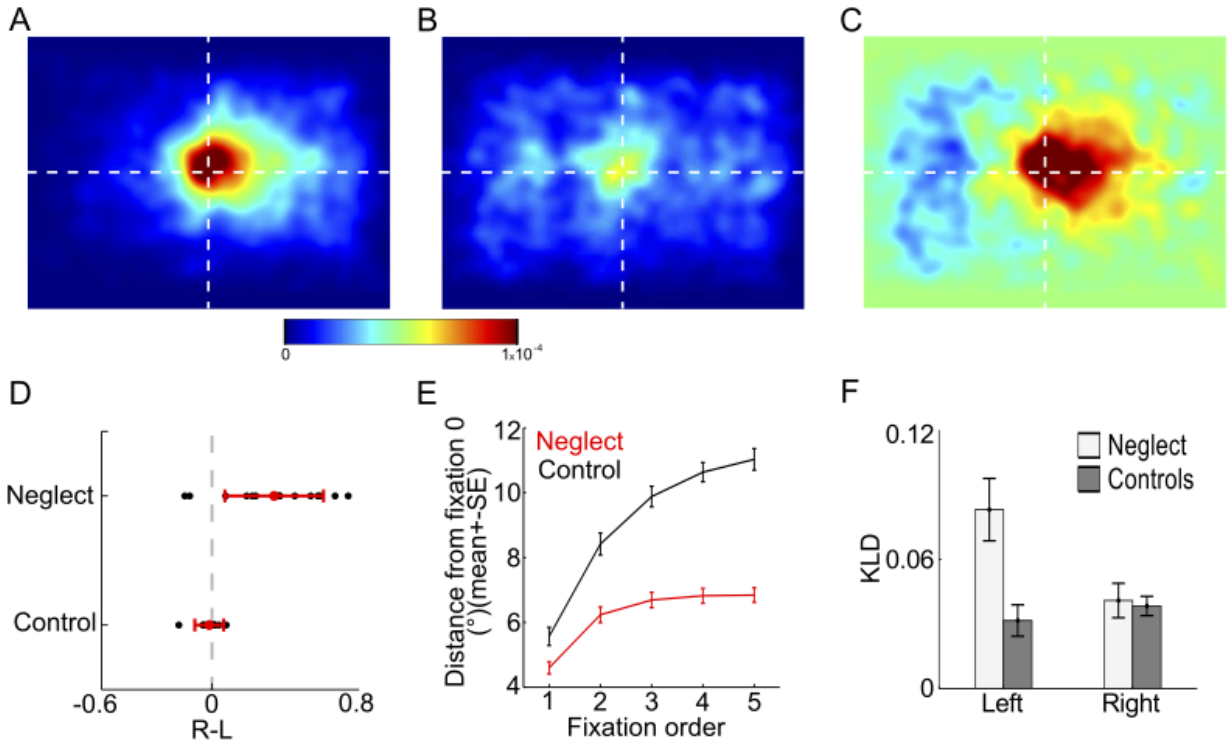

Figure 2.4: Experiment 2: Exploration and low-level feature influence in neglect patients. ((A) and (B)) Spatial distribution of fixation probability for neglect (A) and age-matched controls (B). (C) Difference map between (A) and (B). (D) R–L values for the exploration of neglect and control subjects. Each dot represents the R–L values of one subject. Red error bars represent subjects' mean ± SD. (E) Mean distance of consecutive fixations from a given fixation. For every fixation done (fix 0), we calculated the distance to each of the consecutive five fixations. The error bar represents subjects' mean ± s.e.m. (F) KLD values (mean over subjects ± s.e.m.) between feature values at fixated and non-fixated locations for each subject group and hemifield. Exploration of the left-hemifield by neglect subjects results in the selection of locations with higher feature values than in the right hemifield or in both hemifields by control subjects.

hemisphere (13 ischemic, 2 hemorrhagic). Neglect was assessed by clinical examination and by means of five neuropsychological tests: line bisection (741), Bell's test (287), a subtask of the Vienna Test System (PVT; Dr. G. Schuhfried GmbH, Mödling, Austria), and reading and drawing performance. Neglect was defined as the presence of deficits in at least three out of the five tests. All patients had normal or corrected-to-normal vision, no signs of strabismus, and intact central visual field (i.e. 30°), as assessed by perimetry. Written informed consent was obtained from all participants prior to participation. Experimental procedures conformed to the Declaration of Helsinki and were approved by the ethical committee of the State of Bern.

Stimuli: Thirty-two naturalistic color photographs of everyday scenes were presented in full screen at a 70 cm viewing distance on a 19" CRT monitor (SyncMaster 959NF, Samsung Electronics) at a resolution of 800 x 600. Examples different images used are presented in Figure 2.2.

Eye trackig: Eye movements were recorded with a head-mounted video oculographic eye-tracking system using binocular pupil tracking at 250 Hz (Eyelink I, SR Research Ltd., Mississauga, Canada). Calibration was repeated until the average error fell below 1°(baseline).

Procedure: The procedure was similar to Experiment 1. Images were presented for 7 s instead of 6 s.

Data Analysis: Data analysis followed the same steps as in Experiment 1. The same procedure for generating feature and fixation maps was followed, but unlike Experiment 1, we further weighted the spatial distribution of fixations of the control group to yield comparable measures (see Fig. 2.1c). Given the nature of neglect syndrome, we expected different spatial biases that, to a large extent, are independent of image content (e.g. 370), and therefore we also had to take into account this bias of the neglect group when analyzing the influence of low-level features in the control group. Consequently, in the case of the control group in Experiment 2, both bias-pdf and actual fixation-pdfs of the control group were further weighted by the spatial-bias fixation-pdf of the neglect patient group (see Fig. 2.1b-c).

Statistics: A one-tailed unpaired t-test was used to evaluate differences in the spatial bias between the neglect and control groups (R–$L_{neglect}$ > R–$L_{controls}$). To compare differences in KLD values in the neglect study, a two-way ANOVA with factors subject group (neglect, controls) and hemifield (left, right) was used.

2.3.2 Results

To clarify the role of cortical control in the guidance of attention, we examined the feature values at the locations fixated by 15 patients with left-sided visual hemineglect and by 8 age-matched healthy controls. Before the actual feature analysis, we evaluated patients' oculomotor behavior and bias in exploration. Figure 2.2c,d shows examples of the images used and locations fixated by five neglect (red dots) and five control (blue dots) subjects. As reported previously (599), these neglect patients exhibit a severe spatial bias to the right in the free-viewing exploration of natural scenes when compared to controls (R–L$_{neglect}$ = 0.33, R–L$_{controls}$ = -0.01, $t_{(21)}$ = 3.7, p = 0.001; Fig. 2.4a-d). This spatial bias is the result of less ocular movements done in the neglected field, a two-way ANOVA for the amount of fixations per trial resulted in a main effect of hemifield (F$_{hemifield(1,42)}$ = 14.1, $p < 0.001$) and the interaction between hemifield and group (F$_{hemifield\,x\,group(1,42)}$ = 20.1, $p < 0.001$). Neglect subjects perform significantly less fixations in the left hemifield compared to the right hemifield ($t_{(28)}$ = -6, $p < 0.001$) and compared to controls in both hemifields ($t_{left(28)}$ = -4.32, $p < 0.001$; $t_{right(28)}$ = -3.7, p = 0.001). The bias is present from the beginning of exploration, as patients perform 28% of their first movements to the left in comparison to 60% in the control subjects' movements ($t_{(28)}$ = -4.39, $p <$ 0.001). Patients' oculomotor behavior also shows signs of perseveration. For every fixation, we measured the distance to each of the consecutive 5 fixations (Fig. 2.4e) and found that neglect patients' extent of exploration away from any given fixation is reduced when compared to control subjects (F$_{group(1,21)}$ = 60.2, $p < 0.001$). In summary, neglect patients' exploration is biased to the right and show signs of perseveration.

Neglect patients have a strong spatial bias and exploratory patterns that considerably differ from control subjects. For this reason, comparisons of low-level feature content between subject groups cannot be done without risking distortions due to the inhomogeneous distribution of features in the images. Therefore, prior to calculating the actual and a priori feature distribution of the control group, we further weighted their fixation and bias-pdf by the spatial bias of the neglect group, allowing us to independently investigate feature effects from spatial biases. The two-way ANOVA test shows a main effect for the subject group (F$_{group(1,42)}$ = 5.2, p = 0.02; Fig. 2.4f) and the interaction between subject group and hemifield (F$_{group\,x\,hemifield(1,42)}$ = 4.2, p = 0.04). Critically, we observe that when neglect patients look to the left, they select locations with higher low-level feature values than those of the locations selected in the right hemifield ($t_{(28)}$ = 3, p = 0.0009) or when compared to locations selected by control subjects in both hemifileds ($t_{left(21)}$ = 2.48, p = 0.02; $t_{right(21)}$ = 2.2, p = 0.03). The KLD values in the left-hemifield were not correlated with patients' R–L index (r = 0.07, p = 0.79). To summarize the results of Experiment 1, we found that lesions in the right parietal cortex that produce neglect syndrome lead to a rightward bias in exploration and an unmasking of guidance of visual selection by low-level features in the neglected hemifield.

2.4 Experiment 3: rTMS study

2.4.1 Methods

Preliminary behavioral results of the TMS study were previously published (128). Similar to Experiment 2, here, we investigate the influence of low-level content on the guidance of overt attention.

Subjects: In the rTMS study, ten healthy subjects (9 males, mean age: 31.1 years, SD: 7.34 years) participated in the study. Written informed consent was obtained from all participants prior to participation. Experimental procedures conformed to the Declaration of Helsinki and national guidelines and were approved by the Ethical Committee of the State of Bern.

Stimuli: In the rTMS experiment, another different set of 48 color images of everyday scenes and their respective mirrored versions were used. Images were presented in full screen at 70 cm on a 20" LCD monitor (Dell 2000 FP) at a resolution of 1600 x 1200. Examples of the different images used are presented in Figure 2.2.

Eye-tracking: Eye movements were recorded with a head-mounted video oculographic eye-tracking system using binocular pupil tracking at 240 Hz (HISpeed, SensoroMotoric Instruments GmbH). Calibration was repeated until the average error fell below 0.5°(baseline).

rTMS stimulation protocol: Repetitive transcranial magnetic stimulation (rTMS) was applied using a MagPro R30 stimulator (Medtronic Functional Diagnostics, Denmark), connected to a round coil with a outer radius of 60 mm (Magnetic Coil Transducer MC-125; Medtronic Functional Diagnostics, Denmark). In order to produce cortical inhibition, a continuous theta burst stimulation protocol was used. This protocol produces inhibitory effects on cortical excitability that last for more than 30 min (373, 632). The stimulation consisted in a single continuous train of biphasic pulses delivered in 267 bursts. Each burst consisted of three pulses at 30 Hz and was separated from the next burst by 100 ms. Theta burst stimulation was applied over P3 or P4, the locations of the International 10-20 EG systems that have been reported to lay above left and right posterior parietal cortex, close to the intraparietal sulcus (362). The coil was held over P3 or P4 tangentially to the scalp with the handle pointing backward, with the current flowing in a clockwise direction, as viewed from above. Stimulation was delivered at 100% of the individual resting motor threshold of left small hand muscles. Participants were systematically questioned after the TBS application, and no side effects were reported.

Procedure: In the third experiment, every subject went through four experimental conditions: no-rTMS, right-rTMS, left-rTMS, and sequential right/left-rTMS. The order of the four conditions was pseudo-randomised over subjects. That is, every subject had a different sequence of conditions. These experimental conditions were completed in less than 35 min in different sessions separated by at least 1 week. At this interval, we did not expect any carry-over effect between sessions (634). Each session consisted of 2 blocks of a free-viewing task in which 48 images were explored for 7s. In the unilateral conditions, the rTMS protocol of stimulation was applied over the right PPC (P4) or the left PPC (P3) 5 min before the first block. In the right/left-rTMS condition, the stimulation was applied over the right PPC 5 min before the first block and the stimulation over the left PPC (P3) was applied just before the start of the second block.

Data analysis: The data analysis followed the same steps as in experiments 1 and 2. The same procedure for generating feature and fixation maps was followed, but unlike in Experiment 1, and like in Experiment 2, we further weighted the spatial distribution of fixations of the no-rTMS condition to yield comparable measures that take into account any spatial bias the rTMS condition under investigation might produce (see Fig. 2.1c for an example). Therefore, both bias-pdf and actual fixation-pdfs of the no-rTMS condition were further weighted by the bias-pdf of the respective rTMS condition under analysis.

Statistics: To evaluate differences in the R–L index in the rTMS study, a one-way ANOVA with a factor experimental condition was used. If the null hypothesis of equality of means was rejected (R–L$_{noTMS}$ = R–L$_{rightTMS}$ = R–L$_{leftTMS}$ = R–L$_{right/leftTMS}$), then the t statistic of the specific contrast was reported. To compare differences in KLD values, each rTMS experimental condition was compared to a differently weighted no-TMS condition, thus, three two-way ANOVAs with factor experimental conditions (Right-rTMS vs. No-rTMS; Left-rTMS vs. No-rTMS; Right/Left-rTMS vs. No-rTMS) and side of presentation (left, right) were used.

2.4.2 Results

Although the results with neglect patients are indicative of an unmasking of low-level stimulus-driven control, neglect is a clinically-defined syndrome that comprises a heterogeneous population of patients with different brain lesions and deficits. Furthermore, lesions producing neglect syndrome usually only indirectly affect areas known to be involved in top-down control of overt attention (159). For these reasons, we next attempted to reproduce the results found with neglect patients in a more controlled manner by testing the role of dysfunction of a specific brain area involved in top-down attention control. To test our hypothesis of a stimulus-driven system that is masked in normal exploration, we studied the exploratory behavior of ten healthy subjects who underwent an rTMS protocol designed to transiently inhibit the activity of the PPC. The PPC has been suggested to be involved in both the formation of saliency maps and in the top-down control of visual exploration by selective attention (69, 156, 390). We tested four experimental conditions: no-rTMS, right-rTMS, left-rTMS, and bilateral, sequential right/left rTMS. Every condition was divided into two blocks. In the last condition of bilateral, sequential rTMS, the first block was after a right rTMS and the second block after a left rTMS. Fig. 2.2e-f shows examples of the images used and locations fixated by five subjects under the different experimental conditions.

Resembling the behavior of neglect patients, right-rTMS significantly biased exploration to the right (R–L$_{right-TMS}$ = 0.11, R–L$_{no-rTMS}$ = 0.04, $t_{(76)}$ = -2.14, p = 0.01; Fig. 2.5a, b and e). This bias was associated with less eye-movements in the left hemifield when compared to the right hemifield ($t_{(18)}$ = -3.32, p = 0.003), but we did not find a significant difference in the percentage of first movements to the left when compared with the other conditions (F$_{exp\,cond(3,39)}$ = 0.56, p = 0.6) or signs of the perseveration behavior we found in neglect subjects (Fig. 2.5d). In comparison to unilateral right-rTMS, unilateral left-rTMS did not produce a horizontal bias (R–L$_{left-rTMS}$ = 0.03, R–L$_{no-rTMS}$ = 0.04, $t_{(76)}$ = 0.47, p = 0.68; Fig. 2.5a,c,e) or a difference between the amount of movements done in the left or right hemifield ($t_{(18)}$ = -1.14, p = 0.26). In the low-level feature analysis, when compared to the no-rTMS condition, neither unilateral right-TMS (F$_{exp\,cond(1,36)}$ = 0.09, p = 0.76, Fig. 2.6a) nor left-rTMS (F$_{exp\,cond(1,36)}$ = 0.59, p = 0.44, Fig. 2.6b) on their

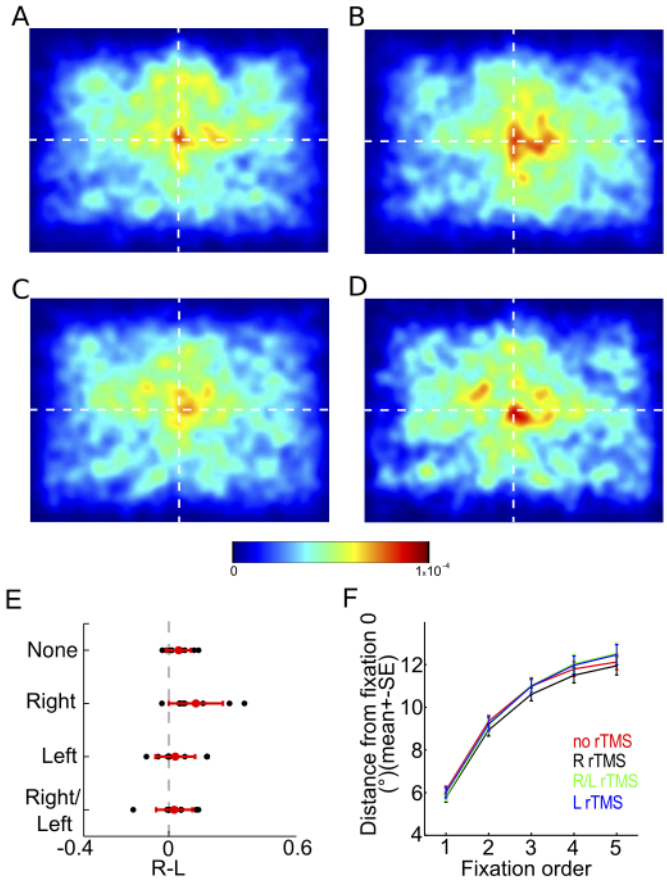

Figure 2.5: Experiment 3: Exploration of healthy subjects after rTMS over PPC. ((A)-(D)) Spatial distribution of fixation probability for conditions: no-rTMS (A), right-rTMS (B), left-rTMS (C), and right/left-rTMS (D). (E) R–L values for the exploration of subject in the different rTMS conditions. Each dot represents R–L the values of one subject. The red error bar represents the population's mean $\pm$ SD. (F) Mean distance of consecutive fixations from every fixation. For every fixation done (fix 0), we calculated the distance to each of the consecutive five fixation. The error bar represents subjects' mean $\pm$ s.e.m.

own reproduced the result of higher feature values at fixated locations in the hemifield contralateral to stimulation. These KLD values were also not correlated with the R–L bias index in the right-rTMS condition (r = 0.55, p = 0.09). Results for unilateral rTMS conditions were the same when both blocks were analyzed (reported here) and when the analysis was only performed on the second block.

As the bilateral rTMS condition was sequential, only the second block of the session corresponded to a bilateral inhibition of the PPCs. Three behavioral results indicate that the right-rTMS effect lasted until the end of the session, thus allowing us to consider the period after a left-rTMS at the start of the second block in the right/left-rTMS conditions as bilateral PPC stimulation (128). First, there was no significant difference in the exploration bias between the first and the second half of the experiment in the case of unilateral right-rTMS (R–L$_{right-rTMS,block1}$ = 0.09, R–L$_{right-rTMS,block2}$ = 0.12, $t_{(18)}$ = 0.51, p = 0.6). Second, there was still a significant right-sided bias in the second half of the unilateral right-rTMS condition when compared to the second half of the no-rTMS condition (R–L$_{right-rTMS,block2}$ = 0.12, R–L$_{no-rTMS,block2}$ = 0.03, $t_{(18)}$ = 2.12, p = 0.04). Finally, left-rTMS at the start of the second block in the right/left-rTMS condition reversed the exploration bias produced by the right-rTMS at the start of that experimental session (R–L$_{right/left-rTMS,block1}$ = 0.15, R–L$_{right/left-rTMS,block2}$ = 0.02, $t_{(18)}$ = 2.7, p = 0.01). In fact, right/left-rTMS produced neither an evident bias on exploration (R–L$_{right/left_rTMS}$ = 0.02, $t_{(76)}$ = 0.51, p = 0.69; Fig. 2.5d and e), nor a change in the amount of fixations

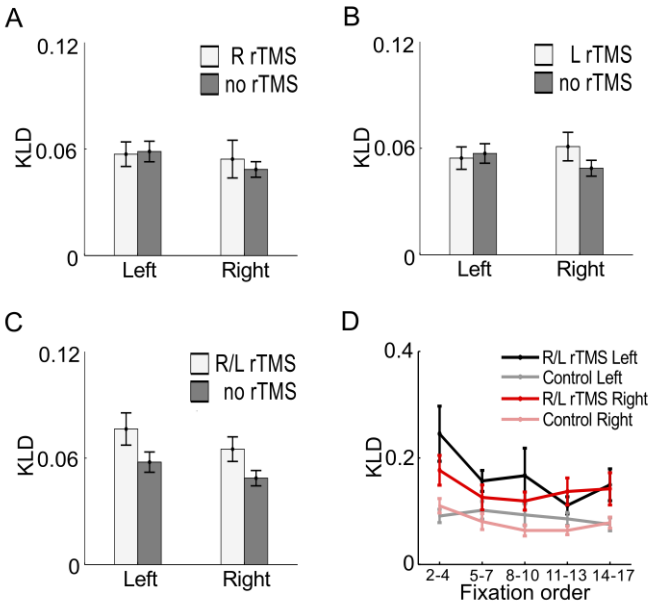

Figure 2.6: Experiment 3: Low-level feature influence in healthy subjects after rTMS over PPC. ((A)-(C)) KLD values (mean over subjects $\pm$ s.e.m.), between feature values at fixated, and non-fixated locations for right-rTMS (A), left-rTMS (B), and right/left-rTMS (C). Only in the right/left-rTMS condition do subjects' selected locations have higher features values than in the no-TMS condition in both hemifields. (D) KLD values for different intervals during the exploration of the images in terms of fixation order, which was calculated for the right/left-rTMS and no-rTMS condition in each hemifield.

done in the left or right hemifield ($t_{(18)}$ = -1.02, p = 0.31) nor the perseveration behaviour observed in neglect patients (Fig. 2.5f). However, when compared to the no-rTMS condition, it resulted in the selection of locations with higher feature values in both hemifields ($F_{exp\,cond(1,36)}$ = 6.73, p = 0.01; Fig. 2.6c). We looked into the temporal progression of low-level feature dependence for the bilateral-rTMS in more detail by analyzing KLD values at different moments of exploration (Fig. 2.6d). A three-way ANOVA resulted in a significant main effect for experimental condition ($F_{exp\,cond(1,180)}$ = 36.2, $p < 0.001$) and fixation order ($F_{fix\,order(4,180)}$ = 2.8, p =0.02) but not for the factor hemifield. Multiple comparisons only result in significantly higher values for the comparison between the first (2nd to 4th fixation) and fourth intervals (11th to 13 fixation)($t_{(18)}$ = 2.5, p = 0.01). To summarise, results of the rTMS experiment showed that both the spatial bias and the dependence on low-level content found in neglect patients are reproducible after selective inhibition of PPC. However, in contrast to the effects seen in neglect patients, spatial biases and low-level guidance can be elicited independently. The right rTMS condition, intended for reproducing the effects seen in neglect patients, produces a spatial bias, whereas only after bilateral rTMS does an increased dependence on low-level features occur.

2.5 Discussion

2.5.1 Influence of low-level features in normal and pathological conditions:

Low-level saliency is an effective drive of both covert and overt visual selection. This effect has been demonstrated in numerous experimental paradigms that show that targets can be detected faster when distinguishable in one feature dimension or can play the role of effective distracters that capture attention regardless of subjects' goals (for an updated review, see 845). Its influence is less clear when visual stimuli do not present the rather restricted feature and spatial configurations that result in attentional capture effects. To address the influence of low-level features in more complex stimuli configurations, models that compute local saliency across multiple feature dimensions have been proposed (389, 450). The results from Experiment 1 suggest that in normal conditions of free-viewing exploration, low-level visual content can drive visual

selection. We used pink noise images that preserved the spectral content of natural scenes but scrambled their phase structure to render high-level content unrecognizable (686, 922). Such a modification nevertheless preserves the first and second-order statistical properties, which, in theory, drive neurons in early visual areas (251). Indeed, various studies have shown that these low-order statistical properties produce multiunit, LFP, and BOLD responses in V1 that are comparable to the responses to natural stimuli (423, 645). Therefore, in the absence of high-level content, we show that low-level features still drive visual selection, supporting the idea of a saliency map that can drive attention. However, it is not possible to fully disentangle low-level influence from images' high-level content since natural scenes present even higher KLD values. Although high-level content is absent in pink noise images, they might lack low-level properties that underlie the higher KLD values for the natural images, such as recognizable collinear edges or solid color blobs, making it impossible to ascertain if the higher influence of low-level features in natural scenes are due to features absent in the noise images or due to the spatial correlation between high-level and low-level content. Several researchers have proposed that the last alternative holds during the exploration of complex stimuli in which visual selection is mainly guided by task requirements (222, 404, 480, 836, 945). In this view, selection by low-level features content has a role only when it is instructed and behaviorally relevant. However, studies of different clinical conditions have suggested that stimulus-driven, feature-based mechanisms play a role when high-level visual processing and goal-oriented control is impaired, regardless of task. For instance, in the case of visual agnosia, a condition that produces a severe impairment in object recognition, patients still select low-level salient locations when exploring natural scenes (266, 531). In the case of the neglect patients in the present study, we see an increased fixation of locations with higher low-level feature values in the neglected hemifield. This result can be interpreted in at least two ways compatible with low-level guidance in the spontaneous exploration of complex visual stimuli: (1) Both patient and healthy controls show the same guidance by low-level features, but patients lack the competition for guidance by high-level features, and (2), there is no competition as such but selection by low-level features is, in the normal case, inhibited by top-down control. This result is in agreement with the reports of patients with visual agnosia and in a recent free-viewing study with neglect patients, where correlations between fixation locations and low-level features were also reported (704). In contrast to these studies of agnosia and neglect patients, we controlled for spatial biases that change the distribution of features that can be fixated, thus making the results of feature effects independent from the spatial bias. This is a relevant methodological change since neglect patients present a strong bias that, to a large extent, cannot be attributed to image content (e.g. 370). Neglect patients also show signs of viewing perseverance, a deficit that is not present in the third experiment (rTMS) and might reflect non-spatial deficits (380) which may be another factor causing the reduction of orientation to high-level cues. We also found an increased effect of low-level features in the right/left-rTMS condition and this effect was, in general, more pronounced at the beginning of image exploration. This temporal dependency is a prediction of bottom- up saliency models, but it might also be related to methodological limitations of the computation of feature maps that do not take into account inhomogeneous retinal properties. In normal conditions, visual selection by high-level content or by other top-down constraints might be an important factor and create difficulty in determining the exact influence of low-level features. However, here we show that when the integration of high-level content for top-down control is impaired, low-level features are able to guide attention.

2.5.2 Inter-hemispheric and intra-hemispheric interactions for spatial and content selection

In the rTMS experiment, we found evidence for a double dissociation between exploratory spatial bias and the control of attention by image content: After unilateral right rTMS, subjects exhibited a right bias without showing signs of an increased influence of low-level features. On the other hand, after bilateral rTMS, we observed the opposite: There was no evident horizontal bias, but an increased influence of low-level features became apparent in both hemifields. Further evidence for an independent mechanism for bias and content guidance is reflected in the KLD values, which do not correlate with the R–L bias values. In Experiment 3, we also find that guidance by low-level features tends to be stronger at the beginning of exploration (although not specifically for the right/left rTMS condition), which suggests that low-level

features are selected by a more automatic bottom-up mechanism.

We propose that the results of the experiments are an expression of the dynamics of intra- and inter-hemispheric competition within the attentional and oculomotor control system. Ever since the seminal work of Sprague in cats (814), it is known that biases in attention and exploration produced by cortical lesions can be reverted by further lesion or inhibition of contralateral areas. This reversion occurs after a lesion or inhibition of both homologous, as well as non-homologous areas. This reversion effect has been subsequently shown in cats (508, 734), monkeys (516), and humans (159, 642, 643, 901, 917). The current explanation for this phenomenon is that cortical lesions that produce the neglect syndrome also produce an inter-hemispheric imbalance in activity between the lesioned area and its contralateral homologue. This imbalance ultimately leads to absolute or relative contra-lesional hyperactivity and heightened ipsilesional inhibition of other structures that are part of the cortico-subcortical system underlying attentional and oculomotor control. These structures include a network of temporal, parietal, and frontal cortical areas that a large body of neurophysiological and neuroimaging studies has identified as the locus of top-down attentional and oculomotor control (156). Specifically, the PPC plays a special role in spatial priority maps (69) and the right temporoparietal junction for the detection of behaviorally relevant events (160). On the other hand, the primary visual cortex (499) and the superior colliculus (774) have been suggested as the locus of low-level saliency maps that could drive visual selection in a bottom-up way, and both areas are also indirectly inhibited after ipsilateral parietal lesions (159, 734).

Within this framework, spatial biases are the result of an inter-hemispheric imbalance of activity between left and right superior colliculus (44, 361, 669). Thus, in the case of the neglect syndrome and after unilateral right rTMS, a further inhibition of ipsi-lesional bottom-up control and oculomotor areas is expected, resulting in an inter-hemispheric imbalance that produces the spatial bias. It is important to note that the bias is at the expense of fewer movements in the left hemifield and therefore the result of an imbalance between the hemispheres drive, rather than local intra-hemispheric phenomena. This inter-hemispheric imbalance might also be involved in effects like attentional capture by ipsi-lesional distracters (703, 799) and impairments in disengagement of attention from the ipsi-lesional field (696). In contrast, in the case of bilateral rTMS, both PPCs are inhibited and thus no inter-hemispheric cortical or subcortical imbalance is produced and therefore no spatial bias is observed.

The increased influence of low-level visual content could be the result of a change in the intra-hemispheric relationship between the afore mentioned top-down and bottom-up areas. In neglect syndrome, inhibition of top-down as well as ipsi-lesional bottom-up areas is expected. However, because of the severe impairment of top-down control using high-level information, putative bottom-up centers remain the only control system available to select contra-lesional locations. As shown, this results in few fixations to the left but directed to locations with high feature values. These results are in agreement with studies that show that cortical lesions result in both a defect in goal-oriented behavior and stimulus-driven behavior in both hemifields (49, 703, 799). Contrary to our expectations derived from the results obtained with neglect patients, unilateral right rTMS did not result in an increased influence of low-level features. We speculate that in this case, the inhibition of high- level processing and top-down control is only partial, as evidenced by the smaller bias of exploration. Therefore, inhibited bottom-up areas may still have to compete with residual ipsilateral top-down control, resulting in no significant change in the feature values at fixated locations. Finally, bilateral PPC rTMS results in symmetrical inhibition of top-down cortical areas, but not in further inhibition of bottom-up areas. This releases the bottom-up control that is normally masked by the ipsilateral PPC or by contralateral areas as in the case of the unilateral rTMS conditions.

2.6 Conclusion

We show that the impairment of parietal cortical control results in the selection of locations with higher feature values when natural visual stimuli are explored. This result is consistent with the action of a bottom-up system for the guidance of attention, which is based on low-level feature extraction and is mediated by early visual areas and/or sub-cortical structures but not by the PPC. Furthermore, the pattern of effects described are in line with a distributed system for visual

selection that depends on (a) the inter-hemispheric balance between homologous areas with regard to spatial biases and (b) the intra-hemispheric balance between areas when selecting between low-level and high-level content for the guidance of attention.

Chapter 3

Irrelevant tactile stimulation biases visual exploration in external coordinates

Abstract

We evaluated the effect of irrelevant tactile stimulation on humans' free-viewing behavior during the exploration of complex static scenes. Specifically, we address the questions of: (1) whether task-irrelevant tactile stimulation, presented to subjects' hands can guide visual selection during free viewing; (2) whether tactile stimulation can modulate visual exploratory biases that are independent of image content and task goals; and (3) in which reference frame these effects occur. Tactile stimulation to uncrossed and crossed hands during the viewing of static images resulted in long-lasting modulation of visual orienting responses. Subjects showed a well-known leftward bias during the early exploration of images, and this bias was modulated by tactile stimulation presented at image onset. Tactile stimulation, both at image onset and later in a trial, biased visual orienting towards the space ipsilateral ti the stimulated hand, both in uncrossed and crossed hand postures. The long-lasting temporal and global spatial profile of the modulation of free viewing exploration by touch indicates that cross-modal cues produce orienting responses, which are coded exclusively in an external reference frame.

This chapter was published as a peer reviewed article: **Ossandón JP**, König P, Heed, T. Irrelevant tactile stimulation biases visual exploration in external coordinates. *Scientific Reports*, **5**, 10664 (2015).

3.1 Introduction

The selection of where we direct our gaze, by moving eyes and head, depends on the interaction of multiple factors that can be divided into three major types: bottom-up or stimulus-driven, top-down or goal-driven, and spatial biases (455). The decision process of how these aspects determine visual selection has been suggested to occur in a topographic "priority" map in which these different factors are integrated (69, 306, 390). Whereas bottom-up and top-down processes affect visual selection in dependence of the stimulus and task, spatial viewing biases, by definition, direct exploration independently of image content and task goals. For instance, humans tend to explore more the center of the visual display while scanning complex scenes (758, 833, 871) and are biased to start the exploration of a new stimulus predominantly on its left side (197, 267, 658).

Most of the research on contingent factors of visual exploration has focused on the visual characteristics of the viewed scene. However, it is often necessary to direct gaze based on information from other senses like audition and touch. Both auditory and tactile cues can direct spatial attention (115, 429, 553) and eye movements to precise locations (72). These sensory modalities can also provide information about spatial locations at the far periphery and outside of the visual field, and may thus extend spatial priority maps beyond of what is accessible from only the visual domain (344, 748, 832, 836). Multimodal signals not only provide localized cues for covert attention and saccades, but they may, in addition, generate global orienting responses. Picture yourself, for example, on a hike through a forest. Songs by various birds may incite you to search the trees. The feeling of softness and obstacles under your feet, in contrast, may guide you to direct your gaze just ahead on your path to avoid stumbling. In these cases, sensory information does not direct gaze to its source. Instead, viewing behavior is biased more generally towards some region of the world, reminiscent of the above-mentioned leftward bias during free viewing. Such general orienting effects have been observed in several cross-modal tactile-visual covert and overt attention tasks. For example, tactile cues that are spatially uninformative result in faster responses to visual targets presented on the same side as the tactile stimulation, compared to targets presented in the opposite hemifield (809). Similarly, tactile signals can effectively orient responses in real life scenarios, for instance, as warning signals to avoid collisions while driving (807). In free viewing, auditory information, too, can modulate exploration. When participants heard lateralized auditory information (e.g. bird-singing), their exploration of natural scenes images was globally biased towards the side of the sound (651, 706). This effect of sound was additive to the effect of low-level visual saliency, consistent with the idea that auditory and visual information were integrated in a supramodal priority map.

In the present work we focused on how tactile cues are integrated for the guidance of free-viewing behavior. The integration of spatial cues from touch can lead to conflict depending on the reference frame used to encode the tactile stimuli, a problem that does not apply to auditory stimuli. Touch is initially coded relative to the skin, for example, in the primary somatosensory cortex's homunculus. However, because our body is flexible, the location of a touch in space crucially depends on the body's posture at the time of touch. Therefore, the external touch location must be derived by integration of skin location and posture (343). For experimental investigation, hand crossing allows dissociating the two reference frames. For instance, when the right hand (skin-based reference frame) is then located in left space (external reference frame). When a saccade is made towards a tactile stimulus on crossed hands, some saccades are initially directed towards the wrong hand, but are corrected in-flight (660); for example, when the crossed right hand has been stimulated, the saccade starts towards the left hand that lies in right space, but ultimately lands at the correct (right) hand in left space. Similarly, a tactile cue can facilitate a visual decision when tactile and visual stimuli spatially coincide. When the time interval between tactile cue and visual stimulus was short, facilitation occurred on the side to which the stimulated hand belongs, independent of hand crossing. When the time interval was long, however, facilitation occurred on the side of space in which the stimulated hand was located (31). Thus, facilitation appears to be guided initially by a skin-based reference frame, but later by an external one.

Yet, other findings suggest that the brain does not simply switch from using a skin-based to an external code, but that it retains the original, skin-based location and derives a location estimate by integrating both reference frames (34, 214, 345). With crossed hands, tactile decisions can be deteriorated, and such findings have been suggested to indicate a conflict

in the integration of mismatching information stemming from different reference frames (343, 779, 944). Accordingly, if touch can be integrated into a putative priority map in a similar way as audition, then the effect of touch may be mediated in skin-based or in an external reference frame, or in both.

Here, we addressed three questions about the effect of tactile cues on visual selection. First, we evaluated whether tactile cues modulate eye-movement behavior in a general, modulatory way as shown before for auditory cues (651, 706). To this end, we provided random, task-irrelevant tactile stimulation to subjects' hands (Fig. 3.1a,c), while they freely viewed complex scenes (Fig. 3.1b). Second, we addressed whether such a potential effect of touch would be restricted to viewing behavior that is contingent on stimulus content and task, or whether it could also modulate the leftward viewing bias that is present during early exploration of complex scenes (658). Because it is known that visual exploration is spatially biased for some time after appearance of an image, we evaluated the effect of touch in two different time intervals. First, tactile stimulation was delivered early, at exactly 150 ms after image appearance. The effect of this early stimulation could be compared with the effect of touch later during image viewing (occurring randomly between 500 and 6000 ms after image appearance), when the exploration bias has subsided. Finally, by presenting tactile stimulation in two different hand postures, uncrossed and crossed (Fig. 3.1c), we evaluate the question of which spatial reference frame would underlie these effects of touch on visual selection.

3.2 Methods

Subjects: Forty-seven right-handed subjects (29 females; mean age: 21.8 years; range: 18-29; SD: 2.3) with normal or corrected-to-normal vision participated in the study. Handedness was evaluated with the Edinburgh handedness inventory (639). In all experiments presented in this article written consent was obtained from each participant, and the experimental procedure conformed to the Declaration of Helsinki and national guidelines.

Stimuli: Following previous work (652, 658) four different kinds of visual stimuli were used: The first category (naturals) included 64 scenes taken from the Calibrated Colour Image Database (646) depicting outdoor scenes without man-made objects or buildings. The second category (man-made) included 192 urban scenes, 64 of them from public spaces around Zrich taken with a high resolution camera (Nikon D2X) and 128 taken from the LabelMe database (735). Urban scenes did not include text. The third category included 64 fractal images.

The fourth category included 63 1/f noise color images that were generated from the images of the three other categories: images belonging to each category were transformed to the Fourier space, and their average power spectra were combined with random phases taken from a uniform distribution. The complete image set was duplicated by mirror reversing the images. Each subject was presented with only one version of each image. Image category as a factor did not result in significant effects in the linear model explained below, and was therefore excluded from the models we report here.

Images were presented at a distance of 80 cm on a 21" CRT monitor (Samsung SyncMaster 1100 DF, Samsung Electronics, Suwon, South Korea) at a refresh rate of 85 Hz and a resolution of 1280x960. The active part of the screen subtended a visual field of 28° horizontally and 21° vertically. One visual degree was equivalent to 45.6 pixels.

Eye-tracking: Eye movements were recorded with a head-mounted video oculographic eye-tracking system using binocular pupil tracking at 500 Hz (Eyelink II, SR Research Ltd., Mississauga, Canada). Eye position was calibrated with a 3x3 grid until the average measurement error was below 0.5°. Fixation locations were calculated by the eye-tracker using the system default parameters, defining fixation periods as the complement of blink and saccade events. Saccades were defined from a minimum deflection threshold of 0.1°, a velocity threshold of 30 °/s and an acceleration threshold of 8000 °/s^2.

Tactile stimulation: Tactile stimulation consisted of vibratory stimulation at 200 Hz for a duration of 50 ms to the back of subjects' hands. It was produced by Oticon bone conductors (Oticon Ltd, Milton Keynes, UK, part number 461-012, size about 1.6x1.0x0.8 cm). Stimulators were controlled by custom-built hardware triggered through the parallel port for millisecond precision timing. Subjects wore earplugs to block the noise of the tactile stimulators.

Procedure: Experiments comprised 394 images and were completed in single sessions of approximately one hour duration. Figure 3.1a depicts the setup. Subjects sat in front of the monitor in a darkened room. Their hands were placed comfortably on a table in front of them in either an uncrossed or a crossed (left over right) posture. The distance between the two hands was 30 cm in all conditions. Images were presented in 16 blocks of 24 images each. Eye tracker drift correction was performed before the first image of a block, and the first image was never analyzed (see Fig. 3.1b for a description of one block). Eye-tracker calibration was renewed every other block. Hand posture was altered every 4 blocks, with the starting posture balanced across subjects. Before the experiment, a training block of 10 trials was run, but not analyzed.

Each image was presented for at least 6 s. After this period, the appearance of the next image was contingent upon subjects' gaze position: the next image was presented after a fixation had begun in an area inside 6° around the images' vertical meridian. Concurrent with the free viewing task, tactile stimulation was delivered at different moments. When early stimulation occurred, it was always delivered at 150 ms after an image change. Late stimulation could occur randomly at any moment between 500 ms after an image change and the end of the trial (6 s).

To ensure that the subjects could not reliably predict whether an early tactile stimulus would occur, tactile stimulation was presented in only half of all trials. In these trials, stimulation occurred either left, right, or bilateral (Fig. 3.1c). To ensure that late stimulation was unpredictable, ISI were sampled from an exponential distribution with a minimum value of 500 ms and a median equal to the trial duration of 6 s, resulting in a constant hazard function. Accordingly, a tactile stimulus occurred in only half of the trials on average. Any stimulus had the same probability to be presented either to the right, the left, or to both hands. Thus, for both early and late stimulation, there were 32 stimuli for each combination of stimulus location (left, right, bilateral) and hand posture (uncrossed, crossed).

Data analysis: The effects of stimulation were evaluated by applying a linear model to the dependent variable gaze position for every gaze sampling point. Two mass-univariate models were calculated for each subject at every gaze sample, one to evaluate effects occurring after image change and early stimulation (from 0 to 3s after image change and stimulation, 1500 samples), and the other to evaluate effects of late stimulation that occurred later during image exploration (from the moment of stimulation to 1.5 s after stimulation occurred, 750 samples). The temporal extent of the analysis window for late stimulation was reduced to 1.5 s as a compromise between having a period of analysis long enough to include several eye-movements after stimulation, and thus allowing to detect long-term biases, with also being able to include as many possible occurrences of late stimulation, considering that stimulation occurred at random times during the interval between 0.5 and 6 seconds and that only complete periods of time after stimulation were to be included in the analysis. Thus, we effectively analyzed viewing biases for tactile stimuli occurring between 0.5 and about 4.5 s after image change. Dummy coding was used to evaluate the influence of main factors tactile stimulation and hand posture against the reference group (constant term) of no-stimulation and hands uncrossed. The interaction of tactile stimulation x hand posture was included to address the possible effect of stimulation in different reference frames. Finally, we included the average gaze position before stimulation, relative to the midline, as a covariate. For early stimulation, we used the 100 ms before an image change, as this gaze position triggered the new image. For late stimulation, we used the 100 ms directly preceding stimulation. In the case of the late model, the reference group of values of no-stimulation was taken randomly from trials without stimulation, at the same moments tactile stimulation occurred in the stimulation trials.

Second level analyses were performed across subjects by testing the regression coefficients associated to each factor and time sample with a one-sample t-test against the null hypothesis of no effect. This results in 1500 (early stimulation) and 750 (late stimulation) t-tests for each factor. To control for the possible elevated family-wise error rate (FWER), we calculated threshold free cluster enhancement values (TFCE) (797) for each sample and factor, and compared them to an appropriate null distribution of control values. TFCE calculates the cluster-like local temporal support of every t-value, and is given by the sum of all sections in time that are underneath it. This local temporal support is the sum of all samples that are not beyond and higher than any local minima that is between them and the sample under calculation. For the gaze position data, this is calculated by: $TFCE(x,t) = \sum_{h=0}^{h_{(x,t)}} e(h)^E h^H$ For every gaze sample (t), the TFCE value equals the sum of the score of all sections underneath it, which is in turn defined by its height (h in t-statistic units) multiplied by its extension (e in sample units). Extension and height are raised to the power of parameters E=0.5 and H=2 respectively (797). TFCE values were calculated separately for positive and for negative t-values, and grouped together afterwards as only positive values. TFCE values for each factor and sample were compared against a null distribution obtained by taking the maximum TFCE value of 1000 permutations of coefficients sign across subjects.

3.3 Results

Forty-seven right handed subjects participated in a free viewing task while their eye movements were recorded and tactile stimulation was provided at different moments of visual exploration (Fig. 3.1a-c). Subjects were instructed to "study the images carefully" and told that the tactile stimulation was irrelevant to the task. The dependent variable was gaze position, and the independent variables were baseline bias (i.e., the model's constant term), the presence of tactile stimulation (none, left hand, right hand, or bilateral), and hand posture (uncrossed or crossed). In the model, we also evaluated the interaction between tactile stimulation and hand posture, in order to disentangle skin-based from external coding, and a position covariate that took into account gaze position before the moment of stimulation (see an example of gaze data in Fig. 3.1d,e and a scheme of the linear model analysis in Fig. 3.1f,g). This analysis procedure resulted in time courses of the estimated model parameters over the duration of the image viewing trial. Four different sets of models were evaluated corresponding to biases in the horizontal and vertical dimensions during early or late stimulation events.

3.3.1 Early exploration and the modulatory effect of touch

We first evaluated whether subjects presented an early horizontal viewing bias (197, 267, 658) in the absence of tactile stimulation. As expected for a right-handed sample, subjects exhibited a baseline bias to initiate exploration of new images on the left side. This bias is evident in Figure 3.2a (gray line), which shows the progression in time of the constant baseline term of the linear model used to fit horizontal gaze position, corresponding to the condition of no tactile

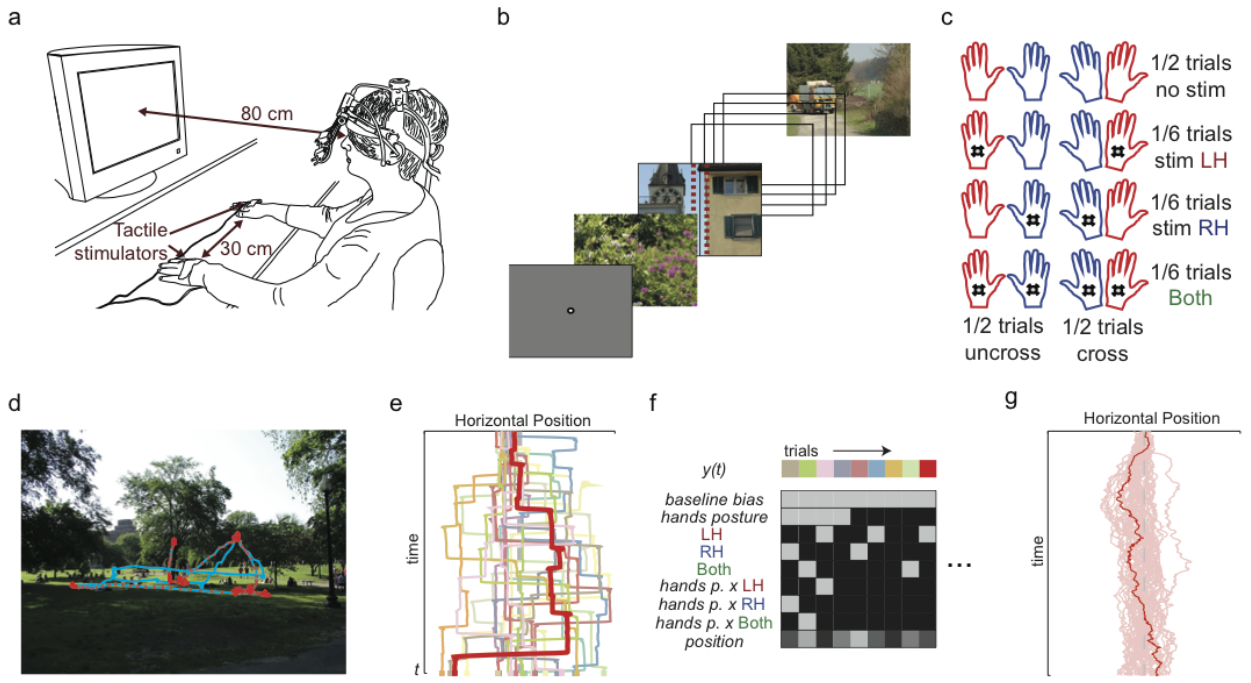

Figure 3.1: Setup and methods. (a) Illustration of the experimental setup in uncrossed hand posture. (b) Per block, 24 images were presented in succession. The first image appeared after a center drift correction. Afterwards, image changes occurred after a minimum delay of 6 s and contingent upon a fixation in the horizontal center of the screen (red dashed lines, not shown during the actual experiment). (c) Schematics of hand crossing and early and late stimulation conditions. Stimulation at image appearance was presented in 192 of 384 trials (32 left, right, and bilateral for uncrossed and crossed postures). Late stimulation, between 0.5 to 6 s, was controlled by a random process such that the expected number of stimuli for each condition were the same as for early stimulation. (d) Example of one trial. The gaze scanpath is shown in light blue for the complete period of 6 s, red dots are the actual gaze data for the first 3 s, sampled at 500 Hz, as used in the analysis. (e) Gaze horizontal position of the trial is shown in red in (d); other traces are examples taken from other trials of the same subject. (f) Example of the design matrices used for the linear model. Dependent variable is gaze position for a given time point and the independent variables are coded using a dummy scheme in which uncrossed hand posture and no stimulation are the reference conditions. The linear model is separately fitted for every time sample. (g) Example of the resulting baseline bias term at all time points for the subject (dark red) used as an example in previous panels and for the other 47 subjects that participated in the experiment (light red).

stimulation with the hands uncrossed. The constant term deviated significantly from the image midline in the interval between 270 and 1240 ms after image change. The main effect of hand posture was not significant at any time point after image appearance. Therefore, hand crossing did not, by itself and in the absence of tactile stimulation, result at any time in a significant change in gaze position (Fig. 3.2a, orange line). Figure 3.2b shows the effect of the covariate, which corresponds to the gaze position prior to image change (not shown in the figure), and therefore starts with a value of 1 at the exact time of image change. Thus, the leftward baseline bias described above was independent of, and not explained by, the eye-position at the time of image change. The influence of the covariate was significant up to 474 ms (Fig. 3.2b), then changed sign, and petered out in a small but significant effect in the opposite direction (616-1190 ms after image change). Thus, subjects showed a horizontal leftward bias during early exploration, and tended to explore the contralateral side more than the ipsilateral region relative to their initial gaze position.

Next, we evaluated the effect of tactile stimulation to test whether touch modulated early visual exploration and the observed leftward bias. As the linear model included the interaction between factors tactile stimulation and posture, a significant main effect of tactile stimulation indicates an additional bias directed to the stimulated hand in the uncrossed condition. Please note that in this condition anatomical and external coordinates are congruent and we cannot differentiate between left-hand side and left side of space. The effect of tactile stimulation (indicated with a dotted line in Figs. 3.2 and 3.3), delivered always at 150 ms after image change (indicated as time zero in Figs. 3.2 and 3.3), resulted in an additional bias in the horizontal dimension that was directed to the side in space of the stimulated hand (Fig. 3.2c, tactile stimulation). The effect size was comparable for left and right tactile stimulation, although the effects on viewing were more variable for

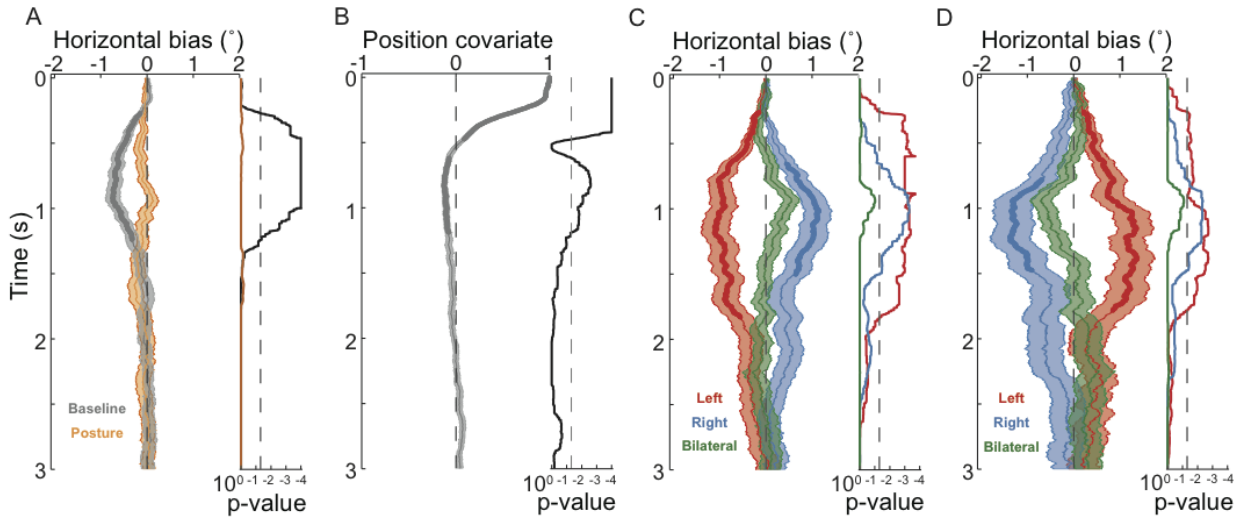

Figure 3.2: Results of the linear model for gaze horizontal position after image change ("early tactile stimulation"). Graphs show the progression of the different factors, and the light-color filled areas represent the estimated standard error. Associated p-values are displayed on the right of each panel on a logarithmic scale. Significant periods are shown by ticker lines that indicate p-values below 0.05. After image start (time zero), the early tactile stimulation always occurred at 150 ms (horizontal dotted line). (A) Baseline bias and hand posture factors. (B) Covariate of gaze position before image change. (C) Tactile stimulation factor. (D) Interaction between tactile stimulation and hand posture.

right than for left stimulation across subjects. As a consequence, the touch-induced bias was significant from 108 to 1680 ms after left tactile stimulation, whereas it was significant from 656 to 1502 ms after right tactile stimulation. In contrast, bilateral tactile stimulation did not induce a significant bias. However, in Figure 3.2c a tendency to the right after bilateral stimulation is apparent (lowest corrected p-value = 0.094). In summary, tactile stimulation produced a viewing bias that modulated the previously known, early leftward baseline bias by an additive component of comparable magnitude.

As a next step, we controlled for potential eye movements directly targeting the tactile stimulus. First, visual examination of the 2-D density of fixation probability over the images in the different stimulation conditions (Fig. 3.3a), evaluated in the interval between 150 and 2000 ms after image change, did not reveal a pattern of saccades directed downward or in the approximated direction from the midline to where the stimulated hand was positioned. Second, a linear model analysis of gaze position with vertical eye position as dependent variable, and with the same factors as in the analysis of horizontal image exploration, did not reveal any significant effects (see Figs. 3.3b,c). Thus, subjects did not perform targeted eye movements towards the region of the tactile stimulus on their hands. Consequently, the horizontal viewing bias induced by tactile stimulation was not a reaction towards tactile stimuli, but a true modulatory effect on image exploration.

The horizontal bias following tactile stimulation may be related to two different spatial reference frames. First, saccades may be biased towards the visual hemifield of the body side to which the tactually stimulated hand belongs. Thus, right hand stimulation would lead to a right visual exploration because the right body side has received tactile stimulation (anatomical reference frame). Alternatively, saccades may be biased towards the hemifield in which the tactually stimulated hand is currently located. Thus, right hand stimulation would lead to visual exploration of the right side of the image, because the right hand was located in the right side of space (external reference frame). Presenting tactile stimuli to crossed hands can disentangle these two accounts. If the effect of tactile stimulation were mediated in an anatomical reference frame, then the model's interaction term of tactile stimulation with hand posture should not be significant and, accordingly, not modulate the viewing bias, given that we coded the side of tactile stimulation in anatomical space. In contrast, if the effect of tactile stimulation were mediated in an external reference frame, then the model's interaction term should be significant and reverse the viewing bias expressed in the main effect of tactile stimulation. Indeed, the interaction between hand posture and tactile stimulation factors was significant (Fig. 3.2d) and resulted in viewing bias pattern that was opposite to that of the factor tactile stimulation on its own (Fig. 3.2c): for left hand tactile stimulation,

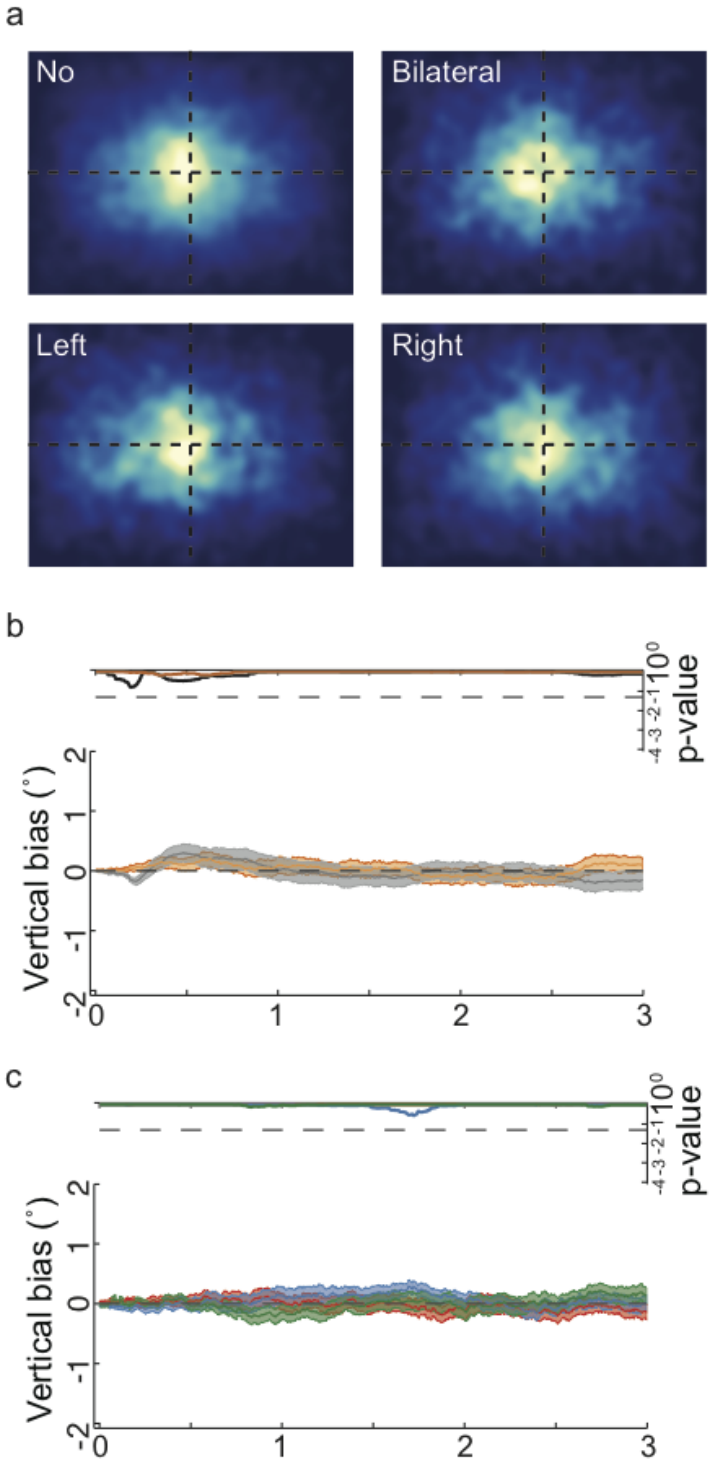

Figure 3.3: Effects of stimulation on the gaze vertical position ("early tactile stimulation"). (A) Fixation density map for fixation locations between 150 and 2000 ms after image change (stimulation occurs at 150 ms). (B) Baseline bias and hand posture factors for deviations of the gaze in the vertical dimension. (C) Tactile stimulation factor.

gaze tended to deviate towards the right in the crossed hand condition (that is, to the external location at which the hand was currently located), and vice versa for the right hand. Bilateral stimulation did not result in a significant bias, but again

a trend is apparent in Figure 3.2d (lowest corrected p-value = 0.08), this time directed to the left side (right-hand). This trend suggests that an orienting response directed to the external position of the dominant hand (here, the right) might exist when both hands are stimulated. However, as the model terms for bilateral tactile stimulation did not reach significance, and we did not test a group of left-handers, this interpretation is currently speculative. In summary, we found that early tactile stimulation biased free viewing behavior exclusively in an external reference frame.

3.3.2 Effects of late tactile stimulation

Examining the effect of tactile stimulation later during image exploration (occurring at random times from 500 to 6000 ms after image appearance) allowed us to evaluate crossmodal effects independent of viewing biases and other effects of a sudden image change event. Late stimulation resulted in a viewing bias pattern similar to that of early stimulation. However, by design, gaze location at the time of stimulation was different for early and late stimulation. Early stimulation was yoked to fixation around the image center (because presentation of a new image depended on this criterion). In contrast, because late stimulation occurred at random times, gaze could be at any position on the screen at the time of stimulation. Consistent with the fact that late stimulation did not coincide with an image change, the baseline term of the linear model (no stimulation and uncrossed hands) did not show any initial bias (see Fig. 3.4a, gray line). Similarly to the early stimulation results, the hand position factor did not reveal a bias (Fig. 3.4a, orange line). For almost the complete evaluated period of 1.5 s following tactile stimulation, the covariate of pre-stimulation gaze position resulted in a strong centering effect (Fig. 3.4b) that simply indicates that the further current gaze position was from the image's center, the more likely the gaze was directed towards the image center. All other factors of the linear model showed a similar pattern of results as that for early tactile stimulation. Tactile stimulation (time zero in Fig. 4) biased exploration in the direction of the stimulated hand in the uncrossed condition, from 31 to 1300 ms for left stimulation, and to the right from 277 to the end of the evaluated period (1500 ms) for right stimulation (see Fig. 3.4c). Bilateral stimulation did not result in a significant bias. The interaction between hand posture and stimulated hand reversed the pattern for the viewing bias observed for the factor tactile stimulation (Fig. 3.4d) in the crossed posture condition, indicating that touch affected free viewing in an external reference frame. Stimulation of the crossed left hand resulted in a gaze bias to the right from 337 to 733 ms and stimulation of the right hand resulted in a gaze bias to the left from 311 to 1047 ms. As for early stimulation, we did not observe any significant effects of tactile stimulation on the vertical saccade direction (data not shown), indicating that for late stimulation, too, biases were not due to reflective orienting towards the stimulated hand. In summary, just like early tactile stimulation, late tactile stimulation of the hands biased visual exploration, indicating that the induced viewing bias did not depend on gaze being centered on the screen.

3.3.3 Effects of stimulation and image change in saccade programming

Tactile stimulation could affect saccade programming at different stages. Reorientation of the direction of a saccade could occur when it is already on course (660), or by changing the spatial target of a saccade that is already being programmed, or by entirely resetting any potentially ongoing saccadic programming. The current experimental design prevented analysis of in-flight saccade redirection, because explicit saccade start and end points would have to be known to assess deviations from a default trajectory, but are not available in a free-viewing task. We were able, however, to evaluate the resetting option by evaluating saccade latencies after tactile stimulation. Because image change has an effect on saccade re-programming (658), any re-programming effect of tactile stimulation cannot easily be disentangled from the effect of image change at the beginning of a viewing trial. Instead, we analyzed latencies for stimulation late during image viewing.

The distribution of saccade latencies after tactile stimulation (i.e. the time from stimulation to movement) was bimodal with an early peak at 45 ms, a second peak at 165 ms (Fig. 3.5) and the antimode at 105 ms. This distribution strongly differed in pattern from a control distribution constructed with saccade latencies in no-stimulation trials, sampled at

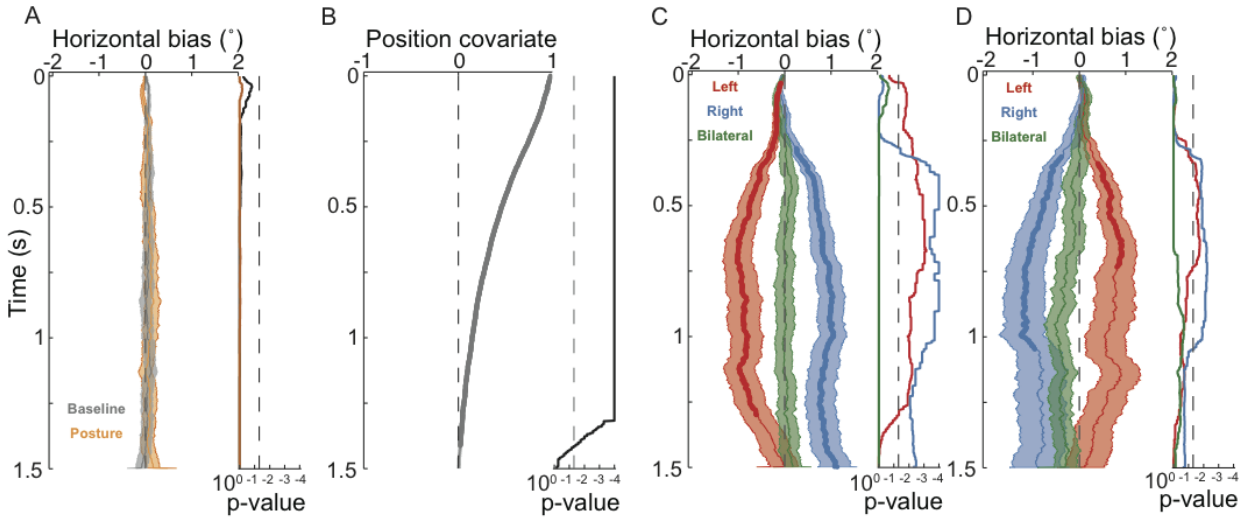

Figure 3.4: Linear modeling results for gaze horizontal position after stimulation during image viewing ("late tactile stimulation"). Graphs show the progression of the different factors, and the light-color filled areas represent one standard error of the mean in each direction. Associated p-values are displayed on the right of each panel in logarithmic scale. Significant periods are shown by thicker lines that indicate p-values below 0.05. Here time zero corresponds to the moment of stimulation, or in baseline no-stimulation hand-uncrossed trials, to the same times in which tactile stimulation occurred in stimulation trials (A) Baseline bias and hand posture. (B) Covariate of gaze position before image change (from -100ms to image change). (C) Tactile stimulation factor. (D) Interaction between tactile stimulation and hand posture.

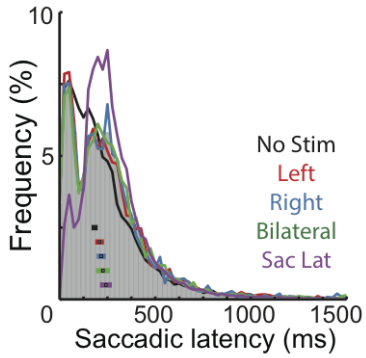

Figure 3.5: Distributions of saccade latencies after tactile stimulation. The bar histogram displays the grand total distribution of saccadic latencies of all stimulation conditions. The curves display data of different conditions; black squares within the histogram correspond to conditions median values plus/minus the absolute median deviation. Two control distributions were used to evaluate saccadic resetting: the no stimulation control (black, No Stim) corresponds to latencies of saccade onsets in trials without stimulation sampled at the same times as stimulation occurred in stimulation trials. Saccadic latency control (purple, Sac Lat) corresponds to the latency of saccades in trials without stimulation.

the same times stimulation occurred in stimulation trials (see Fig. 3.5, black trace; χ^2 goodness of fit test, comparison between no-stimulation control and pooled stimulation conditions: $\chi^2_{(61)}$ = 304.5, $p < 0.0001$). Distributions median values were also significantly different (No/left, z = -4.01, $p < 0.0001$; No/Right, z = –4.63, $p < 0.0001$; No/Bilateral, z = -4.44, $p < 0.0001$). Stimulation conditions did not differ from each other (all $p > 0.05$). This result suggests that the programming of saccades was affected by the occurrence of a tactile stimulus. Yet, if tactile stimulation always resulted in a resetting of saccade programming, the distribution of latencies should resemble a shifted normal saccadic latency (i.e. fixation durations) compared to when no stimulation occurred (Fig. 3.5, purple line). However, this distribution also had a different shape from the stimulation conditions (normal saccadic latency against pooled stimulation conditions: $\chi^2_{(61)}$ = 1308.6, $p < 0.0001$) as well as a higher median value (No/left, z = -3.74, p = 0.0002; No/Right, z = -3.13, p = 0.0009; No/Bilateral, z = -2.38, $p < 0.017$), suggesting that, although touch affected saccade programming, it did not always induce reprogramming. This result is in line with the finding that a programmed saccadic movement cannot be stopped later than 124 and 145 ms before it starts (335). Therefore, tactile stimulation occurring in this final interval of the

programming of a saccade presumably could not stop an already triggered movement. The most plausible explanation for the bimodal shape seen here is, therefore, that tactile stimulation resulted in a resetting of saccadic programming, but left unaffected a population of saccades that were already beyond their stopping point, and that are represented by the first mode of the distribution.

3.4 Discussion

We showed that task irrelevant tactile stimulation resulted in a long-lasting free viewing bias. This bias was directed globally to the images' side ipsilateral to the location of stimulation in external coordinates. It was present both during the initial period of image viewing in which there is a strong horizontal spatial bias, as well as during later viewing which is dominated by contingent, content-based, exploration of the images.

Tactile stimulation has previously been shown to affect the orienting of spatial attention in covert and overt attention tasks. In contrast to previous research, we presented a description of the effect of touch during free viewing behavior, which is closer to how we explore the visual world outside of experimental settings. The fine-grained spatial and temporal analysis used here allowed us to investigate in which reference frame touch affects free viewing. Tactile location has been demonstrated to be represented both in skin-based, anatomical and external reference frames in a wide variety of tasks (32, 31, 336, 337, 343), including when the touch is the target of an eye movement (99, 321, 660). In contrast, the biasing effect of tactile stimulation on visual exploration in the present study was exclusively coded in an external reference frame.

Although many studies have reported effects of both anatomical and external reference frames, several studies suggest that, in some tactile tasks, behavior is predominately modulated by an external reference frame (428, 429, 811). Such variability in the use of different reference frames is consistent with the suggestion that spatial location in touch is derived by weighted integration of information from different reference frames and may be highly task-dependent (35, 345). In fact, whereas studies in which subjects were required to make saccades to tactile targets have reported the use of both anatomical and external reference frames (321, 660), a study in which touch co-occurred with saccades, but was not the saccade target reported that the enhancement of touch by saccade planning was mediated in external coordinates (728). Here, we investigated the reverse link of an influence of task- irrelevant touch on saccade planning, and again observed the use of only external coordinates. Yet, the idea that only external coordinates are relevant whenever touch is not task-relevant cannot be generalized, as other paradigms that did not involve saccades, have reported mixed reference frame use for task-irrelevant touch (808).

The fact that anatomical guidance occurred only for short-latency saccades in Overvliet and colleagues' study led us to expect that we should find an anatomical bias for saccades occurring early after tactile stimulation, and an external effect for saccades occurring later. Analysis of late saccades in the present study suggested that saccade planning was reset by tactile stimulation, suggesting that saccades directed to tactile stimuli (660) and saccades merely evoked by tactile stimulation (present study) should be readily comparable. However, we did not observe a change of reference frame in the time course of the viewing bias with respect to hand posture, suggesting that, in fact, the reference frame used to guide the viewing bias in natural scenes was selectively external. Yet, incorrectly directed saccades occurred only infrequently in Overvliet and colleagues' study even for early saccades. Therefore, it appears possible that some saccades in the present study, too, were modulated in an anatomical reference frame, but that this influence was not observable in our bias measure that aggregated over a large number of saccades.

The external spatial effect of touch on visual selection lasted for several seconds, that is, it affected several saccades that followed tactile stimulation. This temporal profile is reminiscent of endogenous attentional orienting, which is characterized by late latency, long-lasting orienting responses to non-local symbolic cues (594, 716, 775, 940). In comparison, exogenous cueing is said to be characterized by short latency, short-lived responses to peripheral local cues (594, 775, 939, 940). In the present study, the tactile stimulus was spatially localized, and it was non-symbolic. However, its effects were spatially generalized, directed towards one side of space, and not restricted to the location of the touch. This generalized

spatial orienting effect is also characteristic of endogenous responses and similar to the effect of auditory cues during free viewing (651, 706). Together with the temporal profile of the tactually induced bias, the current results therefore suggest that touch was integrated like an endogenous attentional cue, rather than as an exogenous one.

In our experiment, tactile stimulation was unrelated to the task and occurred outside the defined spatial area for exploration, with the hands placed underneath the monitor. This setting probably resulted in an internal framing of spatial attention, which is a mechanism suggested for the absence of capture by salient external events when they are localized elsewhere (60, 848). It is therefore possible that we did not observe saccades to the location of tactile stimulation because the hands were outside subjects' window of attention. This may also be a relevant factor for the occurrence of tactile orienting in a purely external reference frame in the present study.

To conclude, our results demonstrate that exploratory viewing behavior can be spatially biased for extended periods of time by short, irrelevant tactile stimuli. As sound can also bias free viewing in a similar, spatially generalized manner, our results suggest that non-visual stimuli can exert surprisingly extensive biases on spatial orienting behavior when the perceived stimulus is not selected as a direct target for visual fixation. Together with previous research, our results support the idea that visual selection is based on the integration of multisensory local cues, global orienting signals, and of non-sensory bias signals, possibly in some type of unique priority map (69, 210, 306).

Chapter 4

Spatial biases in viewing behavior

Abstract

Viewing behavior exhibits temporal and spatial structure that is independent of stimulus content and task goals. One example of such structure is horizontal biases, which are likely rooted in left-right asymmetries of the visual and attentional systems. Here, we studied the existence, extent, and mechanisms of this bias. Left- and right-handed subjects explored scenes from different image categories, presented in original and mirrored versions. We also varied the spatial spectral content of the images and the timing of stimulus onset. We found a marked leftward bias at the start of exploration that was independent of image category. This left bias was followed by a weak bias to the right that persisted for several seconds. This asymmetry was found in the majority of right-handers but not in left-handers. Neither low- nor high-pass filtering of the stimuli influenced the bias. This argues against mechanisms related to the hemispheric segregation of global versus local visual processing. Introducing a delay in stimulus onset after offset of a central fixation spot also had no influence. The bias was present even when stimuli were presented continuously and without any requirement to fixate, associated to both fixation- and saccade-contingent image changes. This suggests the bias is not caused by structural asymmetries in fixation control. Instead the pervasive horizontal bias is compatible with known asymmetries of higher-level attentional areas related to the detection of novel events.

This chapter was published as a peer reviewed article: **Ossandón JP**, Onat S, König P. Spatial biases in viewing behavior. *Journal of Vision*, **14**(2):20, 1-26 (2014).

4.1 Introduction

Viewing behavior is not determined only by the stimulus and task at hand; it is also influenced by other factors. Overt visual exploration is studied with eye-tracking experiments, which reveal the temporal and spatial structure of ocular movements responding to a variety of tasks and stimuli. The observed exploration patterns are highly variable and usually interpreted in terms of "goal-oriented" behavior: Locations on the visual field are selected based on their low- or high-level content in the context of task requirements (67, 390, 836). Viewing behavior is nevertheless not exhausted by factors that depend solely on goals or stimulus content; eye movements display temporal organization and spatial biases that seem to be independent of such determinants (455).

For instance, temporal organization that is independent of stimulus content is present in fixation durations and saccade amplitudes. Fixation durations increase and saccade amplitudes decrease as a complex scene is explored. Because this pattern persists during different tasks, even when it is not the optimal viewing strategy, it has been proposed as evidence of a global-to-local visual exploration strategy (659, 879).

On the other hand, spatial structure in eye movements that is independent of stimulus and task can be defined as viewing bias. One spatial bias is the tendency to look at the center of visual stimuli during the free exploration of images (833, 871). Besides this prominent bias, there is some evidence for an asymmetric horizontal spatial bias. Eye-tracking studies about face perception have shown that perceptual biases are often accompanied by an initial exploratory bias to the left (46, 112, 327, 328, 489, 565, 680). Other studies have also shown this leftward bias in the initial exploration of complex scenes, but these studies were not investigating this and so did not control for image content asymmetry (489, 665, 834). Only recently have two studies confirmed this early leftward bias with controlled stimuli: one on constructive memory errors (197) and the other on the relationship between viewing bias and the perceptual bias of "pseudoneglect" (267).

This leftward bias could be the result of hemispheric lateralization, or dominance, in high-level brain areas. The cortical network involved in attention is one of the clearest examples of where hemispheric lateralization has the potential to bias visual exploration. Neuroimaging and lesion studies indicate this network involves regions in the parietal, frontal, and temporal lobes, roughly divided into two subsystems: a bilateral dorsal network dedicated to the voluntary control of overt and covert attention and a ventral network lateralized to the right hemisphere and involved in the detection of behaviorally relevant novel stimuli (160, 156). The disruption of this ventral subsystem leads to the severe inattention to and reduced exploration of the left hemifield seen in neglect syndrome (157). Besides attention, hemispheric dominance of brain areas dedicated to the analysis of different visual content, such as text or faces, could also cause bias. Face processing is particularly interesting because it is usually right-dominant (952) and because a series of perceptual biases for left-hemifield content has been associated with biases in viewing behavior. As these different functional systems, the attentional network and the modules for the processing of different visual content, may each cause bias, we cannot attribute viewing bias to the lateralization of a single brain area or functional system.

Regardless of the underlying cause of these biases, understanding their manifestations is essential to avoiding systematic experimental errors when studying viewing behavior by itself or as a marker of other cognitive processes.

Here we present a series of experiments to confirm horizontal asymmetry in the spatial structure of viewing behavior, independent of image structure. We further intend to characterize its properties and investigate contributing factors. We avoid confounding behavioral bias with bias of stimuli properties by comparing free-viewing behavior of static complex scenes with their mirror images. In Experiment 1, we run a baseline, in which many subjects freely explore static visual stimuli of different categories. In Experiment 2, we check if the horizontal bias is related to handedness or to general visual processes that are lateralized in the brain. In Experiments 3 and 4, we control for the possibility that the bias could be the result of asymmetries in voluntary inhibitory control caused by fixating a drift correction dot before each stimulus.

4.2 Experiment 1: Asymmetric spatial bias in the exploration of various visual stimuli

Horizontal bias in viewing behavior has been reported mainly in face-viewing experiments. However, only two of these controlled for content asymmetry, either by using mirror-reversed versions (565) or by artificially making the faces perfectly symmetric (112). These studies investigated only the first few fixations on an image and focused on perceptual bias in face recognition and not on the general structure or progression of viewing bias. In the case of real-world scenes, studies have found an early bias to the left using mainly indoor and outdoor scenes with manmade structures. This kind of stimuli activates ventral visual areas such as the parahippocampal and occipital place area. Although activation is usually bilateral, as with faces, activation is stronger on the right (3, 232). The associated neuropsychological deficits, landmark agnosia and anterograde disorientation, result from bilateral or right-hemispheric lesions, which agrees with the neuroimaging results (4). With both faces and scenes, spatial bias may be caused by lateralization of a visual processing module to the right. Therefore, it is highly relevant to explore the generalization of bias to other types of stimuli. The goals of Experiment 1 are to confirm previous results about asymmetric bias in visual exploration, to evaluate the generalization of the bias to other kinds of complex stimuli that share low-level properties with complex scenes but lack their high-level cognitive content, and to describe in detail the bias' overall spatial and temporal pattern.

4.2.1 Methods

Subjects: Forty-three subjects (21 males, mean age: 24.1 years, SD: 6.1 years, range: 19–48 years) with normal or corrected-to-normal vision participated in the study. Only right-handers were included. Additionally, ocular dominance was assessed by the Miles test (575). In all experiments presented here, an informed written consent was obtained from each participant. Experimental procedure conformed to the Declaration of Helsinki and national guidelines. Part of the data from Experiment 1 has been used in previous publications regarding limitations of models of fixation selection (926) and as a comparison group in a study of low-level visual guidance on the free-viewing behavior of neglect patients (655).

Stimuli: We used four different kinds of visual stimuli (Fig. 4.1): natural, urban, fractal, and pink noise. The natural category included 64 scenes from the Calibrated Colour Image Database (646) depicting outdoor scenes without man-made objects. The urban category included 64 high-resolution photos of public spaces around Zrich (taken with a Nikon D2X, Japan). The fractal category included self-similar computer-generated shapes with second-order statistics similar to real-world images from three different web databases: Chaotic N-Space Network (http://www.cnspace.net/html/fractals.html), Elena's Fractal Gallery (http://www.elena-fractals.it/, accessible in http://web.archive.org), and Maria's Fractal Explorer Gallery (http://www.mariagrist.net/fegal). We generated chromatic pink noise images from the images of the three other categories, transforming each to the Fourier space and combining their average power spectra with random phases taken from a uniform distribution to generate 63 noise images (21 per category). Mirror-reversing each image duplicated the complete set.

We presented the images at 80 cm on a 21-in. CRT monitor (Samsung SyncMaster 1100 DF, Samsung Electronics, Suwon, South Korea) at a refresh rate of 85 Hz and a resolution of 1280 x 960, corresponding to 45.6 pixels/$^\circ$ and a visual field of 288 x 218.

Eye tracking: Eye movements were recorded with a head-mounted video-based eye-tracking system using binocular pupil tracking at 500 Hz (Eyelink II, SR Research Ltd., Mississauga, ON, Canada). Eye movements were defined using system default parameters, and a standard calibration procedure was performed to achieve an average error below 0.3° (651).

Procedure: We presented the 255 stimuli in sessions about 1 hr long. Subjects sat in a dark room in front of the monitor and were told to "study the images carefully." Each image was presented for 6 s (Fig. 4.1b). First, a fixation dot appeared in the centre of the screen, and the trial started after the eye-tracking system performed an automatic drift correction. Subjects explored a mixture of original and mirror-reversed images. Each explored one and only one version, original or reversed, of each image. Subjects were paired with one partner getting the original version and one getting the mirror version.

Analysis: The goal of the following analysis is to describe patterns of bias independent of spatial asymmetry in image content. We generated fixation-density maps that display the overall distribution of fixations on the images. We smoothed the maps with a circular convolution kernel, $\mathrm{FWHM}_{(x,y)} = 0.5^\circ$. We generated spatiotemporal maps (STMs) to display the temporal progression of horizontal exploration, $\mathrm{FWHM}_{(x)} = 2^\circ$, $\mathrm{FWHM}_{(t)} = 20$ ms. Fixation-density maps and STMs were generated separately for both the normal and mirror-reversed viewing conditions. To evaluate the exploration bias, we computed the difference between the original STMs and horizontally flipped STMs of the mirror-reversed image (Fig. 4.1c). We calculated an asymmetry index (AI) in the following fashion (Fig. 4.1d): For each time point, we counted the difference in fixations between the left hemifield of the original image and the right of the mirrored one and, likewise, between the right hemifield of the original and left of the mirrored. These pairs of differences show the excess of fixations produced by spatial bias in the respective hemifields. Normalizing by the total amount of fixations for a given time gives an estimate of the fraction of spatially biased fixations over all fixations. Finally, we average the estimate of the left hemifield with the negative of the right hemifield to obtain a single AI value. Confidence intervals for the asymmetry index were calculated by bootstrapping (250 samples with replacement).

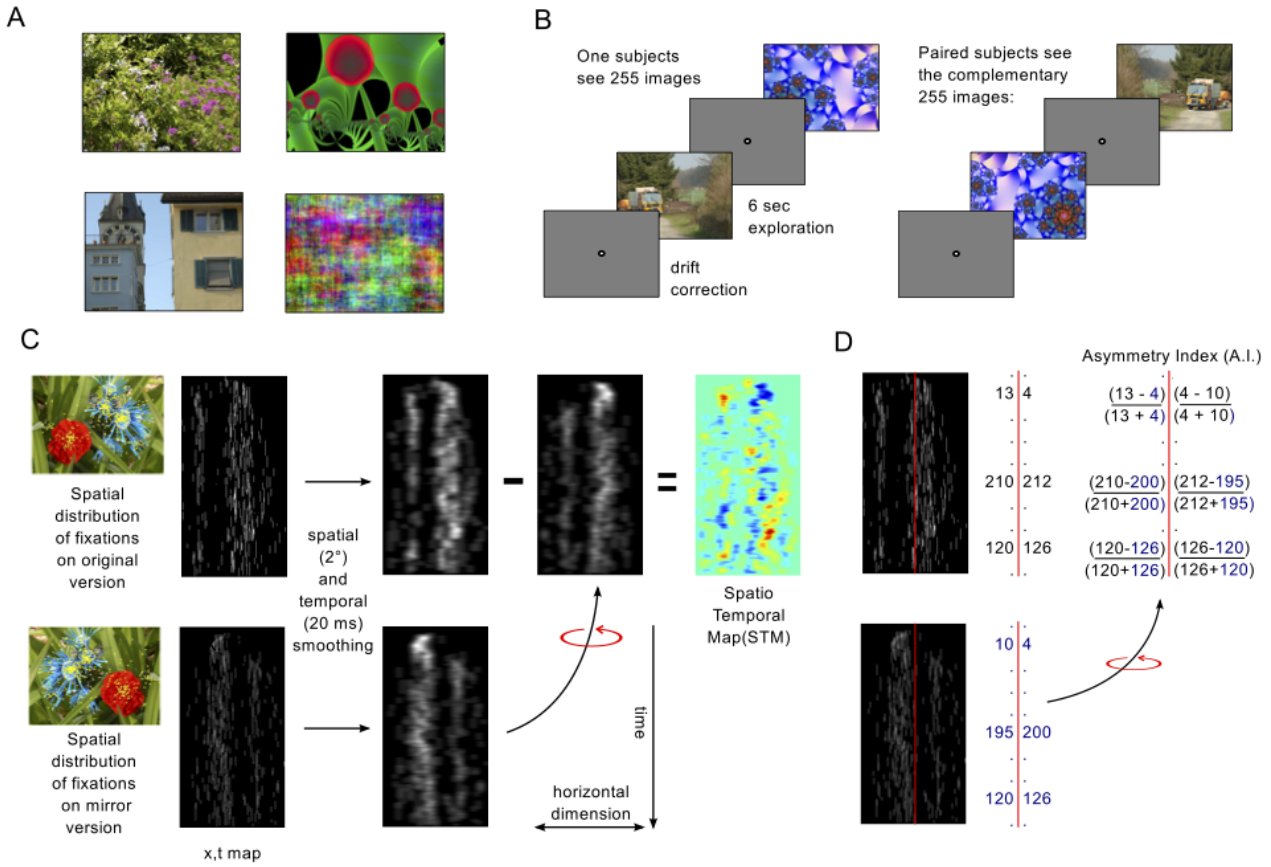

Figure 4.1: (A) Example of images from categories naturals, urban, and pink noise. (B) Experiment 1 procedure: Subjects explored static images presented for 6 s. Images appeared suddenly after subjects fixated on the center of the screen to correct for drift. Images were presented in their original or mirror versions but never both for one subject. (C) Generation of STMs: All fixations on the original or mirror versions were included in 2-D matrices of size (trial duration) x (horizontal length) at their respective time and spatial bins. An example of such matrices is shown in the black boxes (second column, "x,t maps"), where every fixation is shown as a vertical line that marks its horizontal position and duration. Temporal and spatial filters smoothed original and mirror-version matrices to create STMs for original and mirror trials. Finally, we subtracted the flipped version of the mirror matrices from the original version, correcting for a potential bias in image content and getting the final difference STM used in the following figures. (D) We calculated the AI by collapsing data of each hemifield of the unsmoothed x,t maps, then subtracting fixation counts of the flipped mirror-version images from the originals and normalizing by the total of fixations in a given time. Final values are obtained from the average of both hemifields and were calculated for each time sample and also for successive periods of 1.5 s.

For further testing of asymmetries in viewing behavior, we calculated the AI for consecutive time windows of 1.5 s. In the different experiments presented here, we assessed significant differences between conditions with repeated measures or mixed ANOVAs of the AI. The unit of observation was images because individual subjects saw only one version of each. Prior to statistical tests, we checked normality with the D'Agostino-Pearson test and sphericity with the Mauchly test. Of the 72 different data subgroups presented here (all experiments), only two were not normally distributed. This is fully compatible with the expected false positive rate, and neither of these two groups was part of a significant contrast. Hence, the ANOVA was an appropriate statistical method. Homogeneity of variance was preserved and sphericity violations (measured with Mauchly's test) corrected. We used custom MATLAB functions and the SPSS package for all analysis.

4.2.2 Results

All 43 subjects viewed each image either in its original or mirror-reversed version. Wilming et al (926) showed that a number of subjects higher than 20 do not noticeably increase inter-subject predictability of fixation locations. Therefore, we considered the images' fixation-density maps to be stable descriptions of their viewing behavior. Inspection of fixation-density maps, obtained by pooling across all subjects, fixations, and images, revealed an overall mirrored pattern of exploration when comparing the exploration of the images' original and mirror versions (Fig. 4.2a). Both image versions' explorations also showed a center bias. Its strength differed among categories, being stronger for the noise images and

weaker for urban ones.

We then looked for general spatial asymmetries in exploratory behavior due to factors independent of image content. First, we looked at the horizontal center of gravity (mean horizontal position) of all fixations over each image (Fig. 4.2a). The paired comparisons of centers of gravity across images showed no difference between original and mirror version trials (all images: t = 0.9, p = 0.32; natural: t = -0.5, p = 0.59; fractal: t = 1, p = 0.32; urban: t = -1.53, p = 0.11; noise: t = -0.05, p = 0.96). However, when examining in detail the first five fixations after trial start, we see that the first two fixations on the images were clearly biased to the left (Fig. 4.2b). We then calculated STMs of image-viewing behavior (pooled across subjects and image category). Subtracting the horizontally flipped STM of the mirror version from the original version's STM (see methods, Fig. 4.1a) cancels out the probability of fixation due to image structure but preserves the probability of fixation due to an asymmetric spatial bias. Figure 4.2c shows this difference map averaged over all images, and Figure 4.2d (black line) shows the continuous AI value as a function of time. Both STM and AI plots showed a marked initial spatial bias to the left for approximately the first 1.5 s. Afterward, a smaller bias to the right continues until the end of the trial. According to the AI, up to 50% of fixations at the start of exploration can be attributed to the spatial bias to the left (the other half being distributed left/right according to chance). This demonstrates that, although there was no asymmetric bias in all fixations, there was a substantial bias to the left at the beginning of exploration, independent of image structure.

To further test the temporal progression of AI, we performed a mixed-effect ANOVA. The unit of observation was images, and we used one between-group factor for image category (four levels) and one repeated-measure factor for time interval (four levels). Additionally, we included a further repeated-measure factor to test gender differences in image viewing (two levels). Images with outlier values within an experimental group (>3 SD) were removed (3/64 natural, 3/64 fractal, 2/64 urban, and 1/63 noise images). We observed a main effect of time interval, $F_{(3,726)}$ = 275.6, $p < 0.001$, and an interaction between time interval and image category, $F_{(9,726)}$ = 2.74, p = 0.004. Gender was not significant, $F_{(1,242)}$ = 1.07, p = 0.3. Post hoc tests showed significant differences only for the main effect of time interval between the first and all other intervals ($p < 0.05$ corrected, Fig. 4.2f). There were no significant differences in direct contrasts between image categories within the same time interval. The difference closest to significance was between fractal and noise images in the second interval (corrected p = 0.07). Trend analysis indicated a cubic trend for the interaction between time and image category, $F_{(3,242)}$ = 4.82, p = 0.003, thus reflecting the combined differences between image categories with respect to the strength of the early bias, the subsequent bias to the right, and its reduced strength at the end of the trial. This confirmed a temporally structured exploratory bias that is independent of image content and present in all categories with differences in fine-grain structure depending on image type. The bias was leftward starting at the beginning of exploration (<1 s), then switched sharply toward the right and remained slightly biased to the right until trial's end.

The early asymmetric bias could be mainly produced by a bias of the first fixation. To test this possibility, we created two surrogated data sets that preserved the temporal structure of the original data (fixation-saccade intervals) but shuffled the spatial structure. We did so by sampling saccade orientations and amplitudes from distributions generated with all saccades done from the fourth fixation on (fixation groups that did not show differences in AI, analysis not shown). In the first surrogated set, the random sampling was for every movement order. We generated the second set similarly but preserved the spatial information of the first-pair saccade fixation. Figure 4.2d shows the results. When all saccade amplitudes and orientations are taken randomly from their parent distributions (brown line), there is no apparent bias at any moment. This holds both for the early strong leftward bias as well as the weaker rightward bias after 1.5 s. On the other hand, when the spatial information of the first fixation was preserved (dark blue line), the AI mimics the original data (black line) with a left bias at the beginning, then drifts back to the center more slowly than in the original data. Therefore, the swift return to no or right bias is somewhat independent of movement statistics. The early bias also depended on the latency to move: Movements started later after image presentation were less biased that those started in the first 300 ms (Fig. 4.2g). These results show that the first saccade indeed produced most of the spatial bias, which depended on the latency of this first movement.

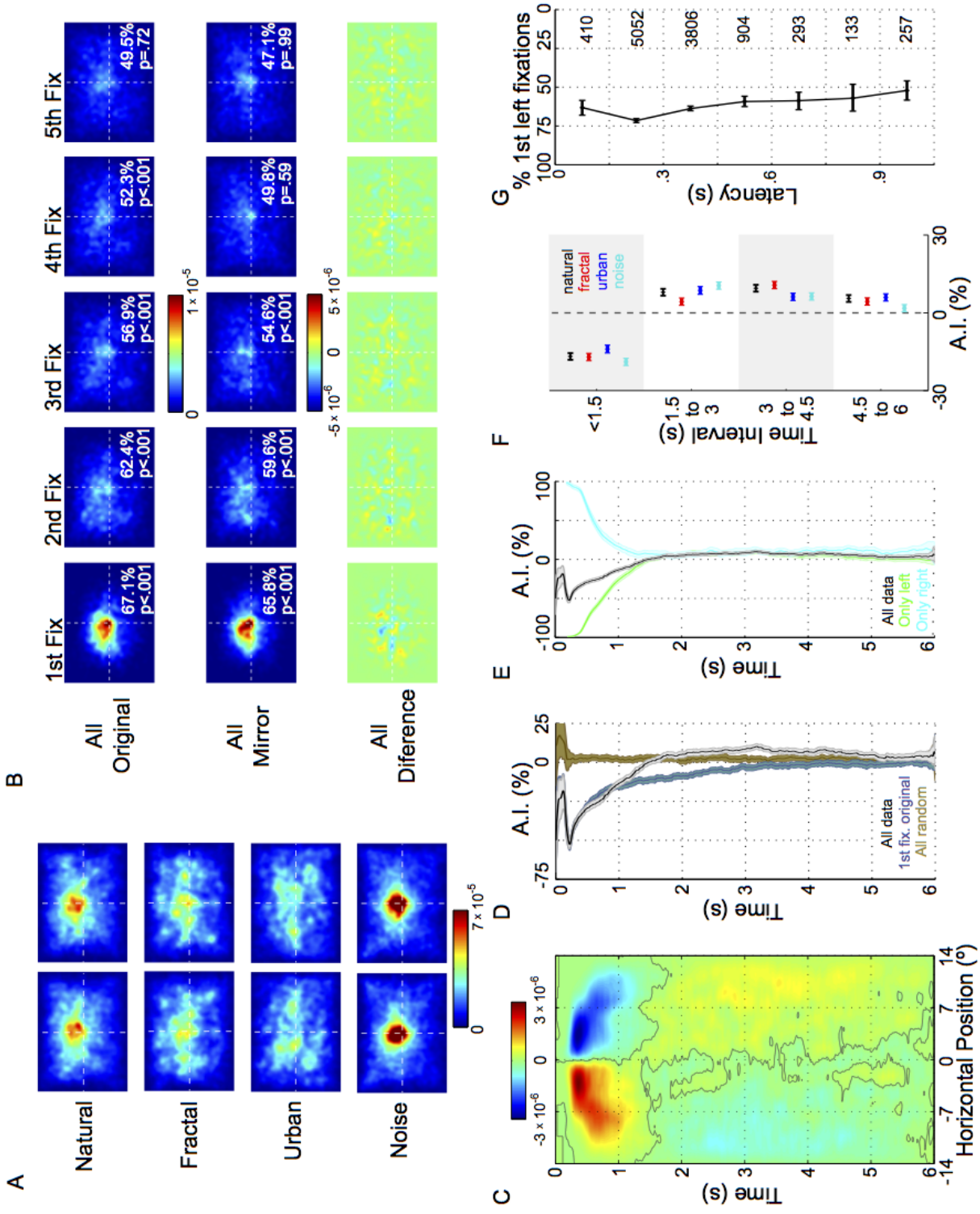
A
Natural
Fractal
Urban
Noise
B
1st Fix
2nd Fix
3rd Fix
4th Fix
5th Fix
All Original
All Mirror
All Diference
67.1% p<.001
62.4% p<.001
56.9% p<.001
52.3% p<.001
49.5% p=.72
65.8% p<.001
59.6% p<.001
54.6% p<.001
49.8% p=.59
47.1% p=.99
C
Time (s)
Horizontal Position (°)
D
A.I. (%)
All data
1st fix. original
All random
E
A.I. (%)
All data
Only left
Only right
F
Time Interval (s)
natural
fractal
urban
noise
A.I. (%)
G
% 1st left fixations
Latency (s)
410
5052
3806
904
293
133
257

Figure 4.2

Figure 4.2 ***(previous page)*****:** (A) Fixation-density maps for all images within a category separated by exploration of original (left column) or mirrored versions (right column). (B) Spatial distribution of fixation in both versions for different fixation orders after trial start. The bottom row shows the difference between both maps. Insets report the amount of fixations to the left of midline. P values are the probabilities associated with that fraction k assuming a binomial distribution f(k; n, p) with parameters n equal to the amount of fixations and p = 0.5. (C) Difference map between the STMs for all original images minus the horizontally flipped STMs of the mirror trials. Positive (red) values represent the excess of fixations that remain after removing fixations that are over the same stimulus content. (D) Continuous AI for original data and surrogated sets. The AI expresses the fraction of all fixations attributable to an excess of biased fixations to the left (negative) or right (positive) with corresponding bootstrap CI in light color. The surrogate sets preserve the temporal structure of the original trials but take the spatial information of saccade orientation and size randomly from the overall distribution of saccade orientations and amplitudes. The black line corresponds to the original data pooling across all images and subjects (corresponding to the difference STM in C). The dark blue line represents the surrogate set that preserves the spatial information of the first fixation; the brown line represents the set that does not. (E) Continuous AI for original data and subsets all-left (green) and all-right (cyan). We generated the subsets by taking only trial pairs in which the exploration in both the original and in the mirror versions started in the same hemifield. (F) Asymmetry index by time interval and for the different image categories. (G) Fraction of first saccades to the left of the midline by latency to move. Numbers on the right of the figure are the quantities of fixations in each temporal bin and error bars are the bootstrap CIs.

After discounting the initial leftward bias, the following rightward bias could be a consequence of the statistics of saccade orientation and amplitudes. We discarded this unlikely alternative, in which the saccades' parameters are decided randomly, independent of task or content, by the analysis of the surrogated set shown in Figure 4.2d (dark blue line): Starting from the initial leftward bias, randomly sampling saccade orientations and amplitudes does not produce a subsequent bias to the right. The second alternative is that the rightward bias compensates for the early leftward one in terms of information gathering. To test this alternative, we created two new data subsets based on whether initial movement was directed exclusively to the left or to the right in both original and mirror-version trials. Figure 4.2e shows the results, by definition in an initial AI of -100% and 100%, respectively. If the subsequent bias compensates for the initial one, the AI should drift to the opposite side. This is not the case; the left subset did not result in a stronger rightward bias, and the right subset did not result in a leftward bias. Instead, both data partitions result in a later bias to the right as in the complete data set. This result suggests that the late rightward bias is a non-compensatory, independent phenomenon.

We demonstrated a strong bias by comparing image-viewing between original and mirror-reversed versions; now we look at subject variability. Because subjects saw only one version of the images to avoid memory effects, we could not calculate the same STM and AI measures for individual subjects. However, as the first movement could explain most of the initial bias, we used the fraction of first fixations to the left of the midline of the image as a measure of each subject's bias. On average, the fraction of leftward-directed first movements was 66% (range 37%–92%, SD = 14%), significantly different from 50%, $t_{(42)}$ =7.6, $p < 0.001$. This fraction of first fixations is not the same as the AI used previously. The AI measures the percentage of all fixations in a given interval attributable to an asymmetric spatial bias as opposed to the percentage of first fixations. The fraction of first fixations takes into account all first movements, including biased but also content-responsive movements. As we had an equal number of original and mirror-version trials per image, the values should show the same tendency.

The strength of the leftward bias negatively correlated with subject latency to make the first saccade (Fig. 4.3a, N = 43, r = -0.381, p = 0.01). The strength of leftward bias also correlated with the horizontal center of gravity of the endpoint of those leftward saccades (Fig. 4.3b, N = 43, r = -0.382, p = 0.01). In other words, the subjects with more first movements to the left were also the ones in which those saccades to the left ended in more leftward locations, possibly indicating an increased guidance by low-frequency spatial content. Subjects showed high half-split reliability as well as high correlation between percentages of first fixation to the left across different image categories (Fig. 4.3c). In summary, horizontally biased behavior was highly consistent.

By looking into a subject's measure of bias, we could also evaluate other factors that might be related to the bias, such as handedness (investigated in Experiment 2), ocular dominance, and gender. Subjects did vary with respect to their ocular dominance, so we explored the influence of this factor on the horizontal bias. In three subjects, this was not possible due to inconsistency between the two versions of the Miles test used. Of the remaining 40 subjects, 10 had left ocular dominance (Fig. 4.3a,b). Subjects with left ocular dominance were less biased to the left (N = 10, 60%) than those with right ocular dominance (N = 30, 69%), which might be interpreted as a consequence of the monocular parts of the visual field at high eccentricity. However, this difference is not significant, $t_{(38)}$ = 1.76, p = 0.08, and we refrain from further discussion.

Patterns of brain lateralization and dominance usually differ in male and female subjects [273, 303, 467, 920]; therefore, we

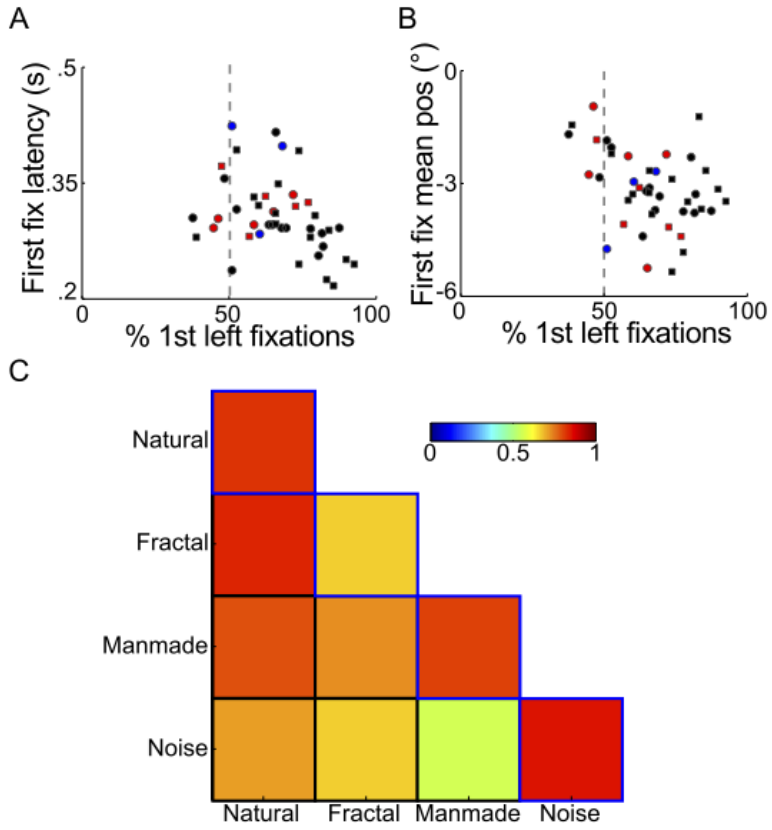

Figure 4.3: Subjects' spatial bias. Fraction of first movements to the left against mean latency (A) and mean horizontal position (B). Every dot represents the average value across trials for one subject (circles: female subjects, squares: male subjects; black: right ocular dominance, red: left ocular dominance, and blue: unclear) (C) Correlation of subjects' first fixation bias between different categories, and in the diagonal (boxes with blue borders) the half-split reliability for each category is shown (all correlation p values are below 0.005).

also looked into gender differences (Fig. 4.3a,b squares and circles, respectively) but found none at the image level (see the above AI ANOVA results for the gender factor) or in percentage of first fixations to the left, Mean males = 69%, Mean females = 63%, $t_{(41)} = 1.47$, $p = 0.14$. In summary, the analysis of subject bias confirmed the strong bias to the left at the beginning of exploration.

4.2.3 Discussion

Results from Experiment 1 show a marked horizontal bias to the left followed by a smaller one to the right that continues until the trial's end. The early bias was mainly due to the first saccade done in the image. Because spatial bias changes during exploration, it was undetectable unless one took into account the temporal dimension; the mean horizontal position of all fixations was not biased to either side.

The leftward bias has been reported before, mainly in eye-tracking studies with face stimuli and, more recently, with complex scenes. However, the later bias to the right was an unexpected finding. Foulsham et al. (267) reported the progression of the bias up to the 10th saccade, approximately 3.5 s into the trials in our experiment, long enough to detect the bias to the right. This difference with our study might be explained by the measures used (absolute location vs. gaze direction) and/or in the small size of the effect. The late rightward bias could explain some inconsistencies between previous reports that aggregate behavior over different time windows.

A common explanation of behavioral bias is that perceptual and exploratory biases follow the hemispheric dominance of specific visual-processing modules in the brain. For instance, in the case of faces, behavioral evidence shows that human

subjects, presented with chimeric stimuli composed of two half-faces, report identity, gender, and emotion based on the features appearing in the left hemifield (107, 112, 135, 296, 348, 494, 513, 548). In tasks with text stimuli, the right hemifield is dominant (98, 354, 437), and the left hemifield dominates in choices between identical but mirror-reversed asymmetrical images, such as those showing different gradients of brightness (548, 619) or distributions of dots (513, 514). Interestingly, in contrast to these examples of left-hemifield bias, the bias in reporting of content is to the right when the task is to judge the aesthetics of pictures or paintings. Right-handers prefer images with the most important content located to the right (138, 177, 493) . Some explanations for this discrepancy have been attempted, such as the idea that the rightward content of the picture balances the subject's leftward attentional bias (493) or that attracting the gaze to the right leaves most of the image in the left visual field to be evaluated by the right hemisphere (50). All these behavioral studies agree, though, that the left and right hemispheres process visual content differently.

Behavioral studies are consistent with neuroimaging experiments. Left-hemifield dominance for face content and right-hemifield dominance for written content matches the asymmetry of visual processing of faces producing higher activation in the right face fusiform area (e.g., 413, 705) and text producing higher activation in the left occipito-temporal area (e.g., 149, 677). These neuroimaging studies also agree with clinical studies that show lesions in the same areas produce deficits in facial and text recognition (e.g., 148, 180).

In the present study, we investigate asymmetries in several general categories, including naturalistic photos, fractals, and pink noise images. The purpose of using such sets of images was to investigate whether the bias was general or restricted to faces and static real-world scenes. The images used in the previous studies that found a leftward bias as well as in most neuroimaging studies about scene recognition are usually similar to the images we included in our urban category. We included a natural category of landscapes with fewer or no man-made objects. More importantly, we include fractal and noise images, which share first- and second-order statistics with natural stimuli but none of their cognitive content. In this way, we show the bias is present in a broader variety of stimuli and not dependent on specific content, such as faces or human environments. All of the image categories show the same general bias structure although an interaction between image category and time is present, indicating differences of bias strength between categories. When our results are considered together with other stimulus studies, it is clear that a leftward bias exists for most stimuli. This may be due to lateralization of category-specific modules or lateralization of a more general visual-processing mechanism. The second alternative seems most likely because pink noise and fractals are not natural types, and it is improbable that category-specific modules exist for their processing. In Experiment 2, we explore one such general mechanism: the differential processing of global and local features through both hemispheres.

We found no gender differences in bias. Previous reports showed a stronger bias for males on other laterality effects. The biggest meta-analysis so far conducted on laterality effects, including 266 studies, confirmed gender differences in visual paradigms (899). However, the consistency of the effects did not resist analysis for publication bias. Moreover, the small magnitude of the reported differences casts doubt on their relevance (899). It is possible that the variability in the differences between males and females in visual bias depends on the menstrual cycle (e.g. 339). No information about menstrual cycles or hormone levels was recorded in our study, so it is not possible to address this hypothesis here.

In addition to the findings reported above, Experiment 1 also found lesser bias in first movements that were initiated later. Such diminution has been found before but only for short image presentations (500 ms) and not for longer presentations as used here (197). This trade-off between bias and saccadic latency may reflect the processing speed of the different pathways involved in eye movements. Several pathways involved in visual processing and programming of eye movements have parallel components: subcortical versus cortical eye-movement control, magnocellular versus parvocellular pathways, and dorsal versus ventral streams. In Experiment 2, we explore the role of latency with a forced delay between image onset and the initiation of exploration, which we hypothesized would reduce bias.

In summary, in Experiment 1, we established a strong early leftward bias, which is consistent with previous studies. In the following three experiments, we attempted to uncover the possible mechanisms underlying it. To this end, we probed the influence of different visual processes known to show hemispheric lateralization or dominance and, therefore, which

could cause bias.

4.3 Experiment 2: Brain dominance and viewing biases

One possible general mechanism underlying viewing bias is the process of hierarchical evaluation of visual content. "Global precedence" is a phenomenon in which global visual features show priority over local features (616). Multiple studies have shown a behavioral advantage for processing global content presented in the left hemifield and for local content presented in the right (e.g., 139, 768, 886). Neuroimaging supports this pattern, showing a corresponding differential activation in the right hemisphere for globally directed attention and in the left for locally directed attention (254, 333, 538). Further evidence stems from clinical cases showing deficits in globally directed attention following right-hemisphere injury and deficits in locally directed attention following left-hemisphere injury (183, 392, 722). Global and local visual features can usually be mapped to low- and high-frequency spatial content. Therefore, behavioral differences in the processing of hierarchical stimuli could also be explained in terms of differential hemispheric processing of low and high spatial frequencies. This applies for both simple stimuli (140, 392, 768) and complex natural scenes (640, 760). Neuroimaging studies have also shown differential hemispheric responses for low and high spatial frequencies of naturalistic stimuli similar to those used here (678, 679). This kind of stimuli follows a 1/f frequency spectrum (251, 865), concentrating most of the power in the lower frequencies. Therefore, exploratory bias could be rooted in differential hemispheric activation produced by heterogeneous spatial frequency distribution in stimuli. Furthermore, in Experiment 1, subjects with more biased behavior produced larger initial saccades. Because high-frequency content cannot be processed at high eccentricity, these saccades are probably driven by lower frequency content. If the right hemisphere processes lower frequency content, this would explain the saccades' leftward bias. To test this, Experiment 2 uses low-pass (LP) and high-pass (HP) filtered stimuli to change the availability of local or global content.

Experiment 2 evaluates not only right-handers, as in Experiment 1, but also left-handers. The latter present weaker perceptual asymmetries and higher between-subject variance (98, 296, 348, 494, 513). Moreover, identification of local versus global features depends on homologous areas in the posterior parietal cortex (PPC), the lateralization of which is opposite for left-handers (569). Focus on local information depends on the right PPC for left-handers and on the left PPC for right-handers. If the horizontal bias were dependent on differential activation of the hemispheres because of the processing of global and local features, we would expect the bias to be reversed for left-handers.

Experiment 2 also explores whether the salience of the sudden onset of stimuli might cause the bias. The reduction in bias at increased saccadic latencies seen in Experiment 1 could reflect other structural or functional constraints that shorten latency responses. Stronger bias at early latencies might indicate a bias produced by asymmetries in pathways with shorter latencies in the visual system, such as the direct subcortical path through the superior colliculus (SC) or the magnocellular pathway (756, 757). Alternatively, as mentioned, the bias might be caused by the asymmetry of the ventral attentional system for salient events (e.g., the presentation of a novel image), a system that seems situated along the faster visual dorsal stream (e.g. 756). In all cases, a delay between image onset and initiation of exploration could mitigate the competition between faster and slower mechanisms. Therefore, in Experiment 2, we included a condition in which we only allowed subjects to explore the image after a delay of 1 s following onset.

4.3.1 Methods

Subjects: Forty-eight new subjects participated in the study. All had normal or corrected-to-normal vision and participated for either credits or monetary reward. Handedness was determined by subjects' self-report and additionally by the Edinburgh handedness inventory (EHI, 10 questions with a final score between -100 and 100; 639). Subjects belong to two different groups: right-handers (N = 31, 15 males, mean age: 22.5 years, SD: 2.2 years, range: 19-28 years) and left-handers (N = 17, nine males, mean age: 22.8 years, SD: 2.3 years, range: 19-28 years).

Stimuli: We used images in the natural and urban categories described above and created two new versions of each image by spatial LP and HP filtering with a Gaussian filter with a cutoff of 0.6 cycles/$^{\circ}$ (302). Such low cutoff changes eye-movement parameters (322) but preserves clear visual content in

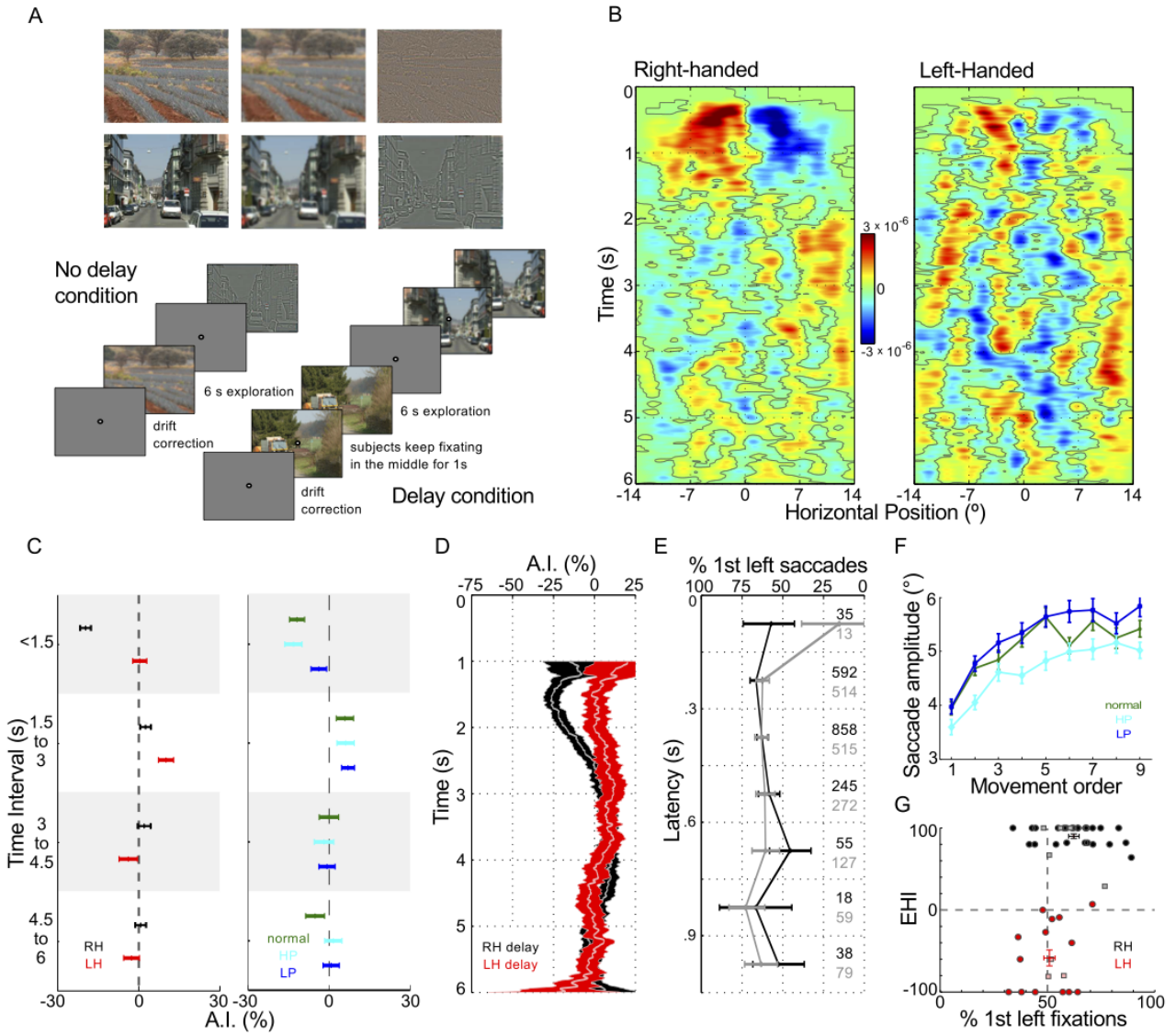

Figure 4.4: (A) Top: Examples of visual stimuli. Original images in the left column, LP in the middle, and HP in the right. Bottom: Subjects explored images after a drift-correction procedure. With the no-delay condition, the procedure was the same as in Experiment 1. With the delay condition, the dot used for drift correction remained visible for 1 s after image appearance, and subjects were instructed to keep fixating on it until its disappearance. (B) Difference STMs for right- and left-handers. (C) Asymmetry index by time interval divided by handedness (left) and image filtering (right) trials. (D) Continuous AI for the delay condition separated by handedness. (E) Fraction of first saccade to the left of the midline by latency to move. The latency is from image appearance in the no-delay condition (black line) and from fixation dot disappearance in the delay condition (gray line). Numbers to the right of the figure are the numbers of fixations in each temporal bin, and error bars represent bootstrap CIs. (F) Saccade amplitudes at different movement orders after image appearance in the three different filtering conditions. (G) Relationship between subjects' spatial bias and EHI values. Red and black markers identify left- and right-handers, respectively (according to the dominant hand used for writing). Square markers identify subjects with first-degree left-handed familiars. Dots with error bars show the groups' mean $\pm$ SEM.

both LP and HP images (Fig. 4.4a). To avoid identifying differences in exploration due only to differences in overall luminance between LP and HP images, the HP version preserved the mean luminance of the original images. Image presentation and eye tracking was identical to Experiment 1.

Procedure: Procedures were similar to those of Experiment 1 with the exception that, in half of the trials, the fixation dot remained on for 1 s after the stimulus onset, and we requested subjects to keep fixating until it disappeared (Fig. 4.4a). If a subject's gaze moved away from a radius of 1° from the center, the trial terminated, and a feedback message was delivered. We blocked delay and nondelay trials and balanced the order of blocks across subjects.

4.3.2 Results

Experiment 1 results came from a population of only right-handers; therefore, we wanted to investigate whether the bias was also present in left-handers. We looked at the overall pattern of exploration by making difference STMs as in the baseline experiment (Fig. 4.4b). We reproduced the main result of the baseline experiment; the left spatial bias was visible for right-handed subjects but almost absent for left-handers. However, although left-handers did not present a leftward bias, they also did not present a mirrored bias.

We evaluated the role of handedness and image filtering in a repeated-measures ANOVA with factors subject group (right-handers and left-handers), filter (none, LP, HP), and the already known effect of time interval (four levels). Only in 93 of 128 images was there complete information for every level of the different factors. In the others, the general reduction in exploration with filtered images led to sparser data (657), which could not be included in the analysis. The assumption of sphericity was violated in the main effect of time, Mauchly's test $\chi^2_{(5)}$ = 13.9, p = 0.016, and in the interaction between time and handedness, Mauchly's test $\chi^2_{(20)}$ = 28.7, p = 0.001; therefore, we corrected degrees of freedom using Greenhouse-Geisser estimates of sphericity (e = 0.9 and 0.89, respectively). We found a main effect of time, $F_{(2.7,249.2)}$ = 12.5, $p < 0.001$; handedness, $F_{(1,92)}$ = 10.0, p = 0.002; and the interaction between the two, $F_{(2.6,247.1)}$ = 9.2, $p < 0.001$ (Fig. 4.4c). Notably, the filtering factor was not significant, $F_{(2,184)}$ = 1.86, p = 0.16 (Fig. 4.4c). For the interaction between time interval and group, we found significant differences between images explored by left- and right-handed subjects only in the first time interval, <1.5 s, $t_{(184)}$ = 6.06, $p < 0.001$. Image filtering did cause other changes in viewing behavior, especially in saccade amplitudes (Fig. 4.4f). An ANOVA with a single factor, filtering, was significant, $F_{(2,273)}$ = 14.1, $p < 0.001$, distinguishing HP images from normal, $t_{(273)}$ = 3.18, $p < 0.001$, and LP images, $t_{(273)}$ =5.01, $p < 0.001$, but not normal from LP, $t_{(273)}$ =1.82, p = 0.03 uncorrected. We conclude that only handedness but not spatial scale results in a significantly different exploration bias.

We then evaluated whether the spatial bias was related to the sudden presentation of the image. In half of the trials, we asked subjects to keep fixating on the middle of the screen for 1 s after image onset. When subjects failed to fixate on a central region of 18 radius, the trial stopped and the experiment continued with the next trial (7.2% of trials). Of the trials that continued, 8.7% still showed eye movement before the go signal, but this movement was smaller than 18. In the no-delay condition, right-handers showed a strong initial bias to the left and left-handers remained unbiased. The introduction of a forced delay in movement after image appearance did not change the spatial bias pattern seen in Experiment 1 or in the no-delay condition (Fig. 4.4d). The relationship between latency to move and amount of bias seen in Experiment 1 was also present in the no-delay condition (Fig. 4.4e, black line) in Experiment 2 but was absent when subjects had to withhold movement for 1 s (Fig. 4.4e, gray line). We performed a second repeated-measures ANOVA for the delay condition data with the same factors as in the no-delay data but with the time interval factor reduced to only three levels. Only 80 of the 128 images could be included in the analysis due to the lost trials and the reduction of exploration of filtered images. The results for the delay data were in full concordance with the no-delay condition. We found a main effect of time, $F_{(2,158)}$ = 9.3, $p < 0.001$; handedness, $F_{(1,79)}$ = 13.9, $p < 0.001$; and an interaction between time and handedness, $F_{(2,158)}$ = 12.3, $p < 0.001$. Introducing a delay in movement did not change the early leftward bias.

Finally, we evaluated how the results obtained using images as units of observation are expressed in terms of subjects' behavior. As in Experiment 1, we used the fraction of first fixations to the left as a measure of subject bias. This analysis revealed again a left bias in the first fixation with a mean percentage of left saccades of 58.2% (range 31.9%-89%, SD = 13). Percentages of first fixation to the left (Fig. 4.4f) are significantly different from 50% for right-handers, N = 31, 62.2%, $t_{(30)}$ = 5.0, $p < 0.001$, but not for left-handers, N = 17, 50.9%, $t_{(16)}$ = 0.35, p = 0.72, and both groups also differed, $t_{(46)}$ = 2.97, p = 0.004. To better understand the relationship between handedness and viewing bias, we evaluated the correlation between the fraction of first fixations to the left and subjects' EHI value. To compare both groups, we compared the score of right-handers against the negative of the value of left-handers (grouped by self-report of dominant hand). Right-handers scored higher than left-handers, mean right-handers 89.9%, mean left-handers -58.4%,

$t_{(46)}$ = 3.87, $p < 0.001$. Unsurprisingly, EHI and percentage of first saccades to the left correlated when accounting for both groups (N = 47, r = 0.37, p = 0.009). However, correlations within each group were not significant (right-handers N = 31, r = 0.27, p = 0.13; left-handers N = 16, r = 0.21, p = 0.4). This absence of correlation might be only an effect of the reduction in the number of subjects or in the within-group range of scores. In conclusion, although handedness was related to left-ward bias, the bias strength was not clearly correlated with an index of motor dominance.

4.3.3 Discussion

In Experiment 2, we demonstrated that the leftward bias reported in Experiment 1 is observed only in right-handers and largely absent in left-handers. This agrees with behavioral studies showing differing visual perceptual biases between right- and left-handers (98, 296, 348, 494, 513). Those differences were not straightforward reversals. Likewise, here, the bias of left-handed subjects is not a reversal of the bias of right-handed subjects. Early bias strength did not correlate well with the EHI, suggesting that the bias is not the result of a pure motor effect. The EHI mainly measures motor dominance and not attentional biases, such as those found with the line-bisection task or cued-attention paradigms. We did not ask our subjects to perform either one of those tasks, so we cannot determine if they are correlated with the viewing bias shown here. However, Foulsham et al. (267) subjects that presented early leftward biases when exploring scenes also showed leftward error in line bisection. They also tended to start exploration from the left, supporting the idea that the leftward bias correlates with other attentional biases.

To investigate whether leftward bias results from right hemispheric dominance in the processing of global visual content, we presented filtered images. If it did, we would expect a decreased leftward bias for HP filtered images and an increased bias for LP images. The filtering cutoff used here is in the lowest range of spatial frequencies usually tested in contrast-sensitivity functions. It nevertheless clearly affects fixation frequency and saccade length. As shown previously with texture stimuli (322), HP images produced shorter saccades than LP images, suggesting that visible content in the periphery is necessary for saccades to that region. In other words, saccades seem not to be directed to image areas for which no information is available even if content seems likely to be there given normal scene structure (657). Image-filtering did not result in the expected change in bias pattern. The lateralization of spectral processing depends, however, not on the absolute frequencies present in the image but on their distribution (141, 349, 440, 441). Therefore, bias could still depend on the spectral content. Filtering does nevertheless effectively reduce the amount of global (HP filtered images) or local content (LP). This indicates that leftward bias cannot be explained in terms of opposing hemispheric processes oriented to global or local processing. Likewise, as magnocellular and parvocellular pathways are also segregated in their spectral response, with the faster magnocellular division being much more responsive to low-frequency content (187), our results suggest the bias is not due to differences in the processing speed or lateralization profile of these pathways.

Global precedence effects can also be reversed by making global features less salient (255, 256, 333, 477, 570). In a series of behavioral, transcranial magnetic stimulation, and neuroimaging studies, Mevorach et al. used modified hierarchical stimuli to independently assess the effects of local and global content and saliency (as determined by stimulus spectral power). This modification left differences in behavior and activity between right and left hemispheres better explained by lateralization, not of global or local processing, but of the processing of salience (572, 570, 571). The relevant cortical structure for this kind of control is within the PPC and not in the ventral stream where specific category processing modules are. Based on these results, an alternative hypothesis has been proposed to explain global precedence and hemispheric spectral precedence. This hypothesis holds that there are opposing, lateralized systems for the selection or avoidance of salient stimuli (570), a proposition compatible with the results shown here.

The presentation of a static visual scene, even after filtering, is a salient event and salient stimulus. Therefore, it could cause an attentional bias by activating right temporoparietal and frontal areas that are involved in the response to behaviorally relevant salient stimuli (160). As the lateralization of selection and avoidance of salient stimuli relates to handedness (569), the difference in bias we show here is to be expected. In summary, the exploratory bias could reflect

attentional bias produced by the stimuli's overall salience. The closer a saccade is to stimulus onset, the stronger the influence of salience (887, 888). This results in a dependency between viewing bias and movement latency. This holds for the sudden onset of images in Experiment 1 and the no-delay condition of Experiment 2. However, a forced delay in movement initiation in Experiment 2 did not reduce the bias, and after a delay, the bias did not seem to depend on the latency of the first movement. These results cast doubts on the attentional explanation and raise the question of whether forced fixation before image appearance causes the early bias. We evaluate this question in Experiments 3 and 4.

4.4 Experiment 3: Bias and fixation control

In the previous experiments, the images displayed directly after the disappearance of a fixation drift-correction point. Almost all of the cited reports on perceptual or exploratory biases use similar procedures. This explicit requirement to fixate on a visual anchor might result in inhibitory processes related to voluntary control that could underlie the observed bias.

Cortical and subcortical mechanisms involved in the voluntary inhibition of response seem also to be dominant in the right hemisphere. Multiple studies have implicated right frontal and right cingulate cortical areas in the inhibition of response, usually in go/no-go and stop-signal tasks (732, 826). Subcortical pathways also show asymmetries. One of the main neural routes in the voluntary control of eye movements from the frontal cortex to the SC goes through the basal ganglia (360). The latter circuit shows left-right asymmetries in dopamine content that have been found to correlate with other, monocular, exploratory biases (179, 963). If any of these asymmetries inhibits the left SC more than the right before the beginning of exploration, it will facilitate saccades to the left. As the inhibition will probably decay with time, saccades initiated later should be less biased.

One way to control for inhibition related to voluntary fixation is to introduce a gap between fixation and stimulus onset. This procedure reduces the latency of eye movements to the extent that a second population of very fast "express" saccades appears (258, 737). This gap effect is mediated by changes in the activation profiles of motor neurons in the SC (204, 205). Accordingly, it is absent after SC lesions (746) and becomes more prominent after frontal cortical lesions (84, 324, 682). We used the gap effect paradigm in Experiment 3 to evaluate the asymmetry-of-inhibition hypothesis as an explanation for the early bias described above.

4.4.1 Methods

Subjects: Twenty-four new subjects participated in the study (18 females, mean age: 22 years, SD: 2.5 years, range: 19–28 years). All subjects were right-handed, had normal or corrected-to-normal vision, and participated either for credits or monetary reward.

Stimuli: Natural and urban images from Experiment 1 were used. Image presentation and eye tracking were identical to Experiment 1.

Procedure: Procedures were similar to those in Experiment 1, but we introduced temporal gaps between fixation dot disappearance and image appearance, creating four experimental conditions: 0-ms no-gap, 300-ms gap, 600-ms gap, and 900-ms gap (Fig. 4.5a). During the temporal gap, the screen was at the gray scale level of the drift-correction period, and the gap duration was randomized across trials. Subjects did not receive any instruction in relation to the existence of a gap.

4.4.2 Results

In Experiment 3, we evaluated the role of inhibition control in the production of exploratory biases. Subjects' median latency to the first movement after image appearance (Fig. 4.5b) was not different between any of the gap conditions (gap 0 = 297 ms, gap 300 = 320 ms, gap 600 = 314 ms, gap 900 = 317 ms, Kruskal-Wallis χ^2 = 1.28, p =0.73, data only from subjects with more than five events per gap). The first movement sometimes began during the gap period with increasing frequency as the gap lengthened (gap 300: 16.3%, gap 600: 37%, gap 900: 54.7%). These first movements done during the gap period peaked at a similar time to the no-gap condition and then progressively decreased until about 150 ms after stimulus onset. The difference STM plot shows that introducing a gap did not change the overall pattern of bias after

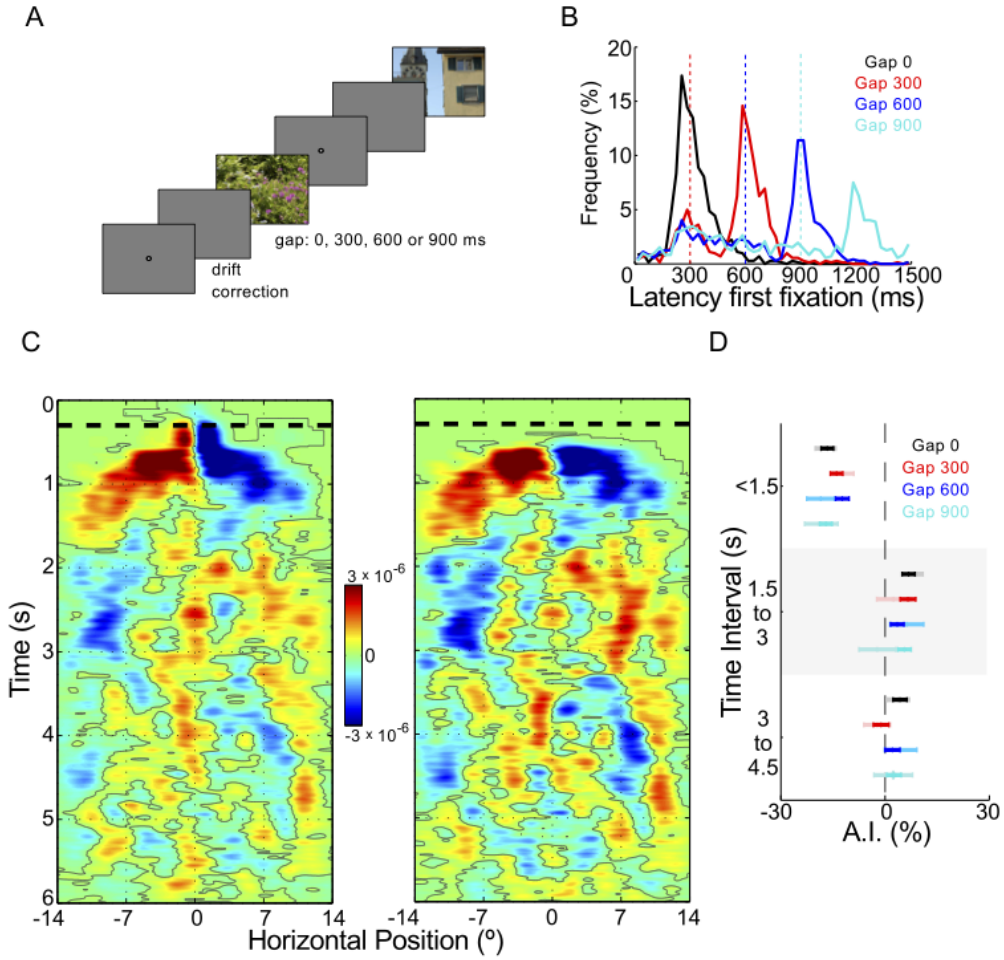

Figure 4.5: (A) Trials started with a requirement to fixate a dot in the center of the screen. Once subjects were fixating in the middle, the screen turned blank for a variable gap interval and then the image appeared. (B) Distribution of first movements' latency after fixation dot disappearance for the different gap conditions. Vertical dashed lines show moment of image appearance for the different conditions. (C) Difference STM for the 300-ms gap condition for the complete data set (left) and for only the trials without movement prior to image onset (right). (D) Asymmetry index by time interval and gap condition. The time interval starts at image onset. Saturated colors represent all trials, and the lighter colors are used for only the trials without movements prior to image onset.

image appearance (Fig. 4.5c, example for the 300-ms gap condition). The bias was also present for movements during the gap period.

We evaluated the role of the gap in a repeated-measures ANOVA with factors gap length (no-gap, 300 ms, 600 ms, and 900 ms) and time interval (three levels, starting at the moment of image appearance). The data from one image, <abs(3 SD), was considered as an outlier and removed from analysis. We found only a main effect of time, $F_{(2,236)} = 99.8$, $p < 0.001$, with a post hoc difference between the first interval and the other two (Fig. 4.5d). There was no effect due to gap modification. As this analysis also included the trials in which an eye movement began before image appearance, we performed a second ANOVA only with trials in which subjects refrained completely from eye movement until after image appearance (Fig. 4.5b, light colors). The result was again only a significant main effect for time interval, $F_{(2,102)} = 28$, $p < 0.001$, similar to the one with the complete data. In summary, gaps between fixation dot disappearance and image appearance did not change the spatial bias.

Analysis based on a subject measure was performed for the fraction of first fixations to the left in two analyses: one if the movement was performed before image presentation and one for movement after. The fraction of first fixations after image presentation was biased to the left for all gap conditions, gap 0 = 68.6%, $t_{(18)} = 5.2$, $p < 0.001$; gap 300

= 69.4%, $t_{(18)}$ = 5.29, $p < 0.001$; gap 600 = 66.8%, $t_{(18)}$ = 5.09, $p < 0.001$; and gap 900 = 67.8%, $t_{(18)}$ = 6.0, $p < 0.001$. A repeated-measures ANOVA with a main factor of gap condition did not show difference between the groups, N = 19/24, $F_{(3,54)}$ = 0.65, p = 0.58. Saccades in the absence of stimuli during the gap period were also biased to the left in all conditions (gap 300 = 73.8%, gap 600 = 69.3%, gap 900 = 67.6%). A repeated-measures ANOVA with a main factor of gap condition did not show a difference between groups, $F_{(2,16)}$ = 0.42, p = 0.66.

4.4.3 Discussion

In Experiment 3, we evaluated the role of fixation control by introducing a temporal gap between fixation and image onset. This modification reduces reaction time in reflexive saccade tasks. Despite our expectations, the gap did not reduce movement latencies or cause the appearance of a bimodal distribution. Although this was unlikely for the 600-ms and 900-ms gaps, a 300-ms gap is within the optimal gap range (200–300 ms) for producing express saccades in humans (550, 737). The two longer latencies were tested to compare with the observed effect of movement latency seen in Experiment 1. Express movements initially appear only in a fraction of trials but increase greatly in frequency with training (259). However, most subjects do show short-latency saccades already in the first experimental session, so a lack of training with the task is unlikely to explain the lack of express movements in Experiment 3. This absence of latency reduction disagrees with the literature on reflexive-saccade experiments but agrees with one previous report about the gap effect in free viewing in monkeys (747). In that experiment, a gap before stimulus in a free-viewing task using complex scenes also failed to reduce movement latency. Moreover, the sudden appearance of a complex background prevented monkeys from producing faster saccades to targets even after an optimal gap. Considering the long movement latency after onset compared to the movement latency in reflexive saccade paradigms and our absence of a gap effect, we speculate that the sudden onset of a complex scene increases inhibition of the motor layers of the SC and overrides the disinhibition elicited by a gap (204).

Regardless, the visual fixation anchor was removed for periods up to 900 ms, but the bias remained. Therefore, this result does not support the hypothesis that the exploratory bias is produced by the requirement to fixate in the center prior to exploration start. However, as no gap effect was produced, we cannot exclude the possibility that the inhibition remained despite the gap. For this reason, in Experiment 4, we tested the role of voluntary and explicit fixation control by entirely removing the requirement to fixate.

4.5 Experiment 4: Bias and continuous image presentation

In Experiment 4, we tested the role of voluntary and explicit fixation control by changing the images unexpectedly during the exploration of a previous image. In this way, we eliminated resting intervals between trials and avoided the explicit requirement to fixate on the center of the screen before changing the images. This experimental setting also allowed us to test whether the bias effect was produced only by image changes occurring during a fixation period or also when the image appears during a saccade. This distinction allowed us to investigate whether the inhibition of visual processing during saccades influences the bias pattern.

4.5.1 Methods

Subjects: Seventeen new subjects participated in the study (10 females, mean age: 22.8 years, SD: 2.5 years, range: 19–29 years). All subjects were right-handed, had normal or corrected-to-normal vision, and participated for either credits or monetary reward.

Stimuli: In Experiment 4, we used different original images than in the three others, 165 images from the "LabelMe" database (735) and mirror-reversed them as above. We did this to ensure the bias was not bound to a specific image set. We took care that the images did not include cues (e.g., text) that could make subjects aware that some images were mirror-reversed. Image presentation and eye tracking was identical to Experiment 1.

Procedure: Each experiment was completed in less than 1-hr sessions in which the 165 scenes were presented. Each session was divided into five blocks, which used 33 images each. Each block started with an image presented after a drift-correction point, but after that first image, the next 32

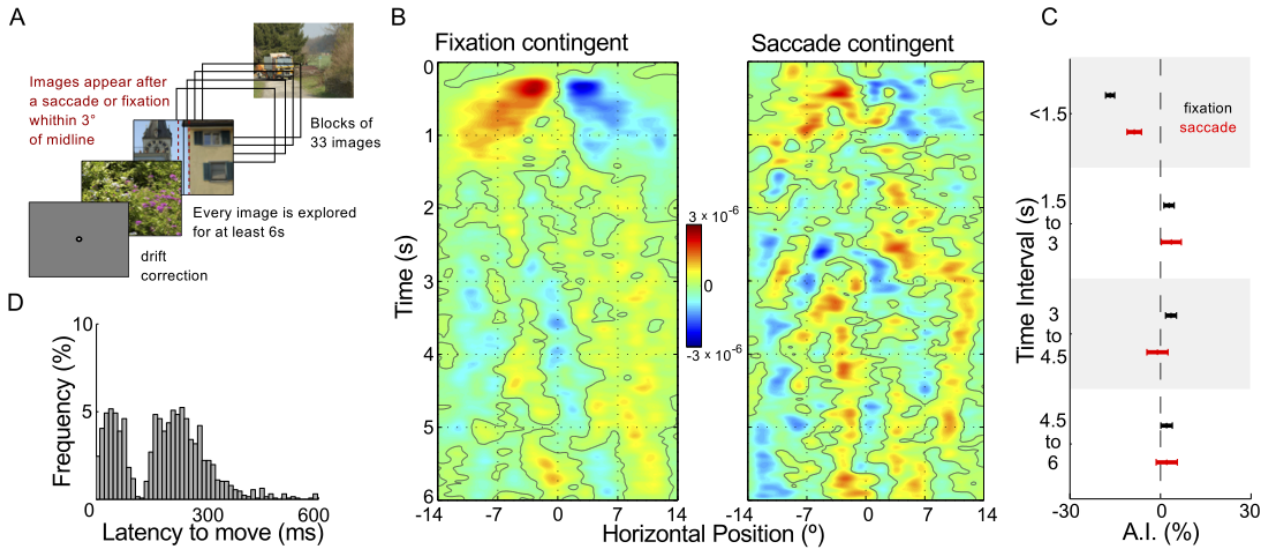

Figure 4.6: (A) Experiment 4 procedure. Images appeared in blocks of 33, one after another, without intervening blank screens or drift-correction procedures. After the first image in the block, successive image changes occurred after at least 6 s of exploration and contingent on the start of a fixation or saccade within 38 of the horizontal midline (shown in the third image by black and dashed red lines that were not present during image viewing). (B) Difference STM for the fixation and saccade condition. (C) AI by time interval for the two conditions. (D) Latency to move after image change in fixation-contingent trials.

images appeared in sequence without intervening fixation points. The experiment was set to obtain image changes during a saccade half the time and, in the other half, changes during a fixation period (50 to 140 ms after fixation start). Image change occurred after two criteria had been fulfilled (Fig. 4.6a): (a) The previous image was explored for at least 6 s, and (b) gaze was within 3 visual degrees of the image's horizontal center (fixation start position for fixation-change trials and previous fixation end position for saccade-change trials). The combination of criteria ensured that subjects could not predict exactly when a new image would appear. Subjects explored a set of original and mirror-reversed images with each exposed to only one version of each image, paired as in Experiment 1.

Due to hardware limitations and the uncertainty of when a saccade or fixation would end, saccade- or fixation-contingent changes did not always occur as planned. In only 44.3% of the saccade-contingent trials did the change occur during a saccade; the rest were right after the end of the saccade. Overall, change during a saccade occurred when the saccade was longer or during saccades associated with blinks. During fixation-contingent trials, in 92.6% of the trials, the change was achieved during a fixation. Data were reassigned offline to the correct saccade- and fixation-contingent conditions.

4.5.2 Results

In Experiment 4, we evaluated the role of fixation control in relation to the subjects' instruction in Experiments 1, 2, and 3 to fixate in the middle of the screen before exploration of the stimuli. In Experiment 4, image changes occurred suddenly while subjects explored the previous image. STM profiles show that this did not change the overall pattern of bias (Fig. 4.6b), but it seems reduced in the saccade-contingent trials.

We evaluated the role of the sudden change of images during saccade or fixation periods with a repeated-measures ANOVA with factors time interval (four levels, starting at the moment of image appearance) and movement condition (two levels, change of images during a fixation or during a saccade). Due to the fewer saccade-contingent trials, only 134 of 185 images yielded sufficient information on every level of the different factors to perform the repeated-measures analysis. We found only a main effect of time, $F_{(3,399)} = 16.5$, $p < 0.001$, with a post hoc difference between the first interval and the other three (Fig. 4.6c). There was no significant difference between images appearing during a saccade or during a fixation period.

Analysis based on subject measures was performed for the percentage of first saccades to the left after image change in two different conditions: saccade- and fixation-contingent changes. The percentage was higher than chance in each condition, fixation =60.3%, $t_{(16)} = 4.27$, $p < 0.001$; saccade = 57.7%, $t_{(16)} = 3.02$, $p = 0.008$, and similar in both, $t_{(32)} = 0.72$, $p = 0.47$. During fixation-contingent trials, latency for the next movements showed a marked bimodal distribution

(Fig. 4.6d). Based on the literature of counter-manding tasks in monkeys and humans, in which the time needed to cancel a movement is between 125 and 145 ms (335), this bimodal distribution suggests that movements begun before 125 ms of image change were responses to targets in the previous image that could not be stopped. When taking into account only the movements in the fixation-contingent trials that started after 125 ms, the fraction of saccades to the left increased from 60.1% to 63.7%. Nevertheless, the comparison between fixation- and saccade-contingent trials remains nonsignificant, $t_{(32)} = 1.43$, $p = 0.15$.

4.5.3 Discussion

The results of Experiment 4 confirmed that the exploratory bias is not caused by the explicit requirement to fixate. The pattern of viewing bias remained in both fixation- and saccade-contingent trials. However, after excluding the left-handed group of Experiment 2, the fraction of first fixations to the left was the smallest of all four experiments, and the saccade condition showed the smallest bias of all. It is important to note that Experiment 4 also differed from the other three in the image set used. Because the methods in all four experiments were chosen explicitly to demonstrate that the bias does not depend on actual content and we have already shown that the leftward bias is present in different types of images, we think the new image set is unlikely to have caused changes in bias.

The processing of visual stimuli is actively suppressed during eye movements. This is known as "saccadic suppression" (730). This inhibition makes the detection of major changes in visual scenes difficult (e.g., 320, 367). If the bias is driven by visual attention, and saccadic suppression reduces the saliency of the onset of a new image, then changes during saccades should result in less bias. This was observed in our data. In agreement with this view, changes are detected faster in the left hemifield in the change-blindness paradigm (515, 813). This has been shown in detection experiments in which scenes were flickered and has not yet been investigated in saccade-contingent paradigms. Neuroimaging and transcranial magnetic stimulation studies show that change-detection performance correlates with activity in the right parietal and right dorsolateral prefrontal cortex (52, 51). The fact that bias appears to be reduced in saccade-contingent trials compared to the first three experiments suggests that saliency could be the crucial factor driving the leftward bias.

4.6 General Discussion

We presented four experiments that showed an asymmetric exploratory bias during the initial exploration of complex visual stimuli. This bias was robust to different experimental conditions. Across the four experiments, we tested a total of 132 subjects. The only ones who did not exhibit a leftward bias were the 17 left-handers of Experiment 2. A second bias to the right following the initial bias to the left and continuing until trial's end was evident in Experiment 1. These biases were independent of each other, of image asymmetries, and of image type. The rightward bias was small and could not be confirmed in the other three experiments: Its existence and relevance need to be confirmed before considering it a consistent effect. The first saccade mostly explains the early bias. This bias was unlikely to result from a predominance of global features or an asymmetry in inhibitory control. We found a trade-off between movement latency and the bias of the first movement. Importantly, the general bias pattern was not changed by a number of experimental manipulations that removed the explicit requirement to fixate in the center or that disentangled the first saccade from image onset. These experiments demonstrate a horizontal bias in visual exploration under a wide variety of experimental conditions. This is not explained by previously reported differences of hemispheric lateralization of the processing of visual content. Instead, the simplest explanation is that the bias is driven by hemispheric asymmetries in the attentional system.

4.6.1 Bias and stimulus

There are different ways in which spatial viewing bias can depend on stimulus content. For instance, one usual explanation of the center bias described in Experiment 1 is that the features of the stimuli itself are concentrated in the center.

This is also known as the "photographer bias": The photographer centers the composition on the content rich in features. This can explain the observed centered distribution in at least two ways. In the first case, the empirical distribution is the direct result of visual selection being driven by the actual stimulus features, which, in most cases, are centered, and therefore, aggregated behavior will show it correspondingly. In this case, the real bias is the inhomogeneous distribution of features in the visual stimuli and not in the behavior. In the second case, the empirical distribution is truly biased, i.e., it does not entirely depend on the distribution of features in the currently presented stimulus but is a strategy based on learned stimuli statistics. Evidence supports both views with experiments showing that the empirical fixation distribution is dependent on the actual feature distribution (871) or independent of it (833).

The asymmetric bias described here cannot be explained by the location of features in the stimuli because mirror-reversing the images controls this. Therefore, we observed true behavioral bias. This bias could still be a learned strategy based upon the statistics of content distribution. However, it is also not the case that the overall exploration is biased to the left: The bias is restricted to the start of the exploration of a new scene. As a learned strategy this early bias might be useful for text or other kinds of structured stimuli, such as web pages (67). As the biases shown here are asymmetric, there is another possibility of stimulus-driven bias: It may be caused by hemispheric dominance of visual-processing modules for specific stimulus content. We discuss in the next two sections both alternatives: strategic sampling of the stimulus as in the example of reading and lateralization of visual-processing modules.

4.6.2 Role of strategic sampling

The prime example of strategic sampling is reading scanning habits. Although we did not test this directly, several reasons make this explanation unlikely. First, left-handers would have the same reading bias; nevertheless, they do not show the same bias pattern. Second, 6-month-old humans and animals, such as monkeys and dogs, also present such viewing bias (327). Third, horizontal exploratory asymmetries also appear in other behaviors, such as head-turning biases in neonates (e.g., 147, 500) or kissing (326), which seem to have little to do with reading. Fourth, studies about the dependence of perceptual asymmetries on reading show that subjects still present leftward bias despite reading from right to left although the bias is often smaller, especially for subjects literate only in a right-to-left language (138, 296, 342, 558, 620, 882). Finally, although a learned strategy from reading might generalize to other behavior, the stimuli in our and other experiments do not involve any text. Therefore, if viewing bias is secondary to reading habits, this implies that a strategy associated with reading has become an automatic process that cannot be overridden by task-specific requirements, at least in experiments that use sudden stimulation on computer monitors. It seems more plausible that, if bias were related to reading, it would be the result of spatial priming from reading instructions on the screen. Such a carryover effect has been shown before for successive unrelated tasks (e.g. 267) and should be tested directly in further work. Altogether, these different considerations suggest that the viewing bias is not primarily based on learned reading strategy or normal monitor-scanning strategies.

4.6.3 Role of lateralization of visual-processing modules

The hemispheric specialization hypothesis is supported by perceptual bias experiments that show opposing hemifield advantages for different kinds of stimuli. The best examples are the advantage of the side of the face presented in the left hemifield and the advantage for text presented in the right hemifield in accordance with right and left hemisphere dominance for the respective stimuli. Moreover, when faces appear upside down, making recognition more difficult, exploratory biases shrink (46, 112, 154, 327, 489). This suggests that hemispheric dominance does play a role in both perceptual and exploratory bias. On the other hand, perceptual bias seems to be highly dependent on exploratory patterns: The left-field bias for faces correlates with the number of fixations on the left (112), and free-viewing paradigms result in stronger perceptual biases than tachiscopically presented stimuli (114). There is also less perceptual bias when images appear too briefly to be explored and when exploration time is much longer than the period of leftward bias (113, 680). Our results also argue against a simple effect of lateralization of visual-processing modules: The exploratory bias is present with a

variety of stimuli, making hemispheric specialization as a single factor unlikely. Moreover, even for perceptual biases directed to the right hemifield, as in the case of text, there is still a left-hemifield bias when stimuli appear simultaneously in both fields (354). In summary, although the use of stimuli that is processed asymmetrically in the brain might modulate exploratory asymmetries, general evidence speaks against lateralization of specific visual-processing modules as the cause of bias.

4.6.4 Role of attentional control

An alternative cause of leftward bias is brain asymmetries in attentional control related to the salience of new stimuli. Attentional mechanisms are lateralized in the brain with the most striking example being neglect syndrome, in which one hemifield, usually the left, is unattended after injuries to the contralateral hemisphere. Healthy subjects present plenty of other behavioral evidence of attentional bias in different phenomena, such as spatial memory errors (109, 184), boundary extension in scene memory tasks (e.g. 197), multi-tracking of stimuli (9), and feature-based attention capture (211).

These different attentional or perceptual biases are observed in both tachiscopic and free-viewing conditions; thus, it is not easy to address whether attention or perceptual biases follow scanning biases or the other way around. For instance, in the line-bisection task, a standard test of attentional bias in clinical settings, healthy subjects consistently show a slight bias or "pseudoneglect," usually to the left side. However, there is large variability on this subtle bias, depending both on subject characteristics and task details (394). Structurally, it seems that the strength of bias in this task depends on inter-hemispheric asymmetries in the attentional network: Individual behavioral biases correlate both with neural activity asymmetries in frontoparietal areas (829) and with anatomical asymmetries in the white-matter tracts that connect the parietal and frontal cortices (851). One of the most relevant behavioral parameters that affects the bias direction and strength is whether visual scanning is allowed or not (394), making it possible to partly differentiate between contributions of covert and overt attention. Some of the largest effects in line bisection are seen in experiments that manipulate the direction of scanning with the largest effect seen when subjects are forced to start scanning from the left (95, 387). Similarly, the studies about perceptual asymmetries in face-perception bias show an enhancement of the bias for the left hemifield when scanning is allowed (112). This suggests that attentional and perceptual biases follow viewing biases.

On the other hand, attentional and perceptual biases also appear when eye movements are not possible or can be dissociated from them. For instance, one study of change blindness showed faster detection of changes in the left hemifield but unrelated to early viewing biases (515). In another example, boundary-extension errors appear only when subjects are prevented from exploring the images and not when they do explore, but a marked viewing bias to the left nevertheless remains (197). In the case of asymmetries in the perception of visual stimuli, one study found that while controlling for premotor, scanning, and attentional biases, only attention could modify these biases (620). Therefore, there is evidence for causation in both directions with covert attention and content processing on one side and overt eye movements on the other.

To differentiate between these two alternatives is experimentally and conceptually challenging because overt and covert attention are strongly linked. The cortical and subcortical networks of overt and covert attention overlap to a large extent (155, 622). This organization results in both obligatory pre-saccadic shifts of attention being produced by the programming of eye movements (191) and small saccadic movement in the cued direction being produced by covert attention (226, 331).

Different aspects of our results support an attentional explanation of the early leftward bias. The onset of a complex scene is a salient event, and a spontaneous delay in exploring a new image lessens bias. This agrees with the dependence of saccade latencies on low-level salience (887, 888). Further support for this view is that the smallest bias occurs when the image appears during a saccade, a period in which processing of visual stimuli is actively inhibited and salience presumably reduced. However, this last conclusion needs to be taken with caution because the unexpected image change during saccade or fixation periods did not differ significantly in Experiment 4. Therefore, it is likely that the high saliency

of the appearance of a new complex stimulus might partly explain the strong exploratory bias shown here. However, another manipulation that might have reduced the saliency of new stimuli by preventing subjects from exploring until 1 s after stimulus onset did not change the bias pattern. We found a clear effect of handedness, which may be linked with asymmetries in the salience selection mechanisms in the PPC (570), which also supports an attentional cause. However, these are indirect post hoc explanations that need to be tested in the future by looking for evidence of an association between viewing bias and other attentional biases and between the viewing bias and structural or functional asymmetries in the subjects' attentional network.

4.7 Conclusion

Although the exploration of static scenes is a limited example of how visual stimuli are encountered in the real world, we have presented here evidence for a strong early leftward bias and a late rightward bias that are probably present in many other task contexts. Because the early leftward bias is a robust finding, we believe it will now be relevant to evaluate how it could affect the results of any research that includes visual attentional components. This is especially the case for tasks with noncontrolled asymmetric stimuli or when differences between left- and right-handers are found. Finally, these biases indicate asymmetries in the structure of the visual-selection system that might not have a functional role but that need, nevertheless, to be taken into account when modeling the organization of the visual system.

Chapter 5

The influence of DBS in Parkinson's patients free-viewing behavior

Abstract

In contrast to its well-established role in alleviating skeleto-motor symptoms in Parkinson's disease, little is known about the impact of deep brain stimulation (DBS) of the subthalamic nucleus (STN) on oculomotor control and attention. Eye-tracking data of 17 patients with left-hemibody symptom onset was compared with 17 age-matched control subjects. Free-viewing of natural images was assessed without stimulation as baseline and during bilateral DBS. To examine the involvement of ventral STN territories in oculomotion and spatial attention, we employed unilateral stimulation via the left and right ventralmost contacts respectively. When DBS was off, patients showed shorter saccades and a rightward viewing bias compared with controls. Bilateral stimulation in therapeutic settings improved saccade length but not the spatial bias. At a group level, unilateral ventral stimulation yielded no consistent effects. However, the evaluation of electrode position within normalized MNI coordinate space revealed that the extent of exploration bias correlated with the precise stimulation site within the left subthalamic area ($p=0.037$). These results suggest that oculomotor impairments but not higher-level exploration patterns are effectively ameliorable by DBS in therapeutic settings. Our findings highlight the relevance of the STN topography in selecting contacts for chronic stimulation especially upon appearance of visuospatial attention deficits.

This chapter is taken from a manuscript currently under review: Fischer P, **Ossandón JP***, Keyser J, Gulberti A, Wilming N, Hamel W, Koeppen J, Buhmann C, Westphal M, Gerloff C, Moll CKE, Engel A, & König P. Amplification of attentional bias in Parkinson's disease by unilateral STN-DBS during free-viewing. *Shared first authorship.

5.1 Introduction

Patients with Parkinson's disease (PD) develop a wide range of impairments other than the well-known skeletomotor symptoms. Among them, abnormal eye-movements and deficient spatial attention can potentially impair the sampling of visual information and impact patients' quality of life.

Previous research has shown that ocular movements are affected in Parkinson's disease (reviewed in 684, 824). The most common finding is a reduction of saccade amplitudes and an increase in the latency to initiate a saccade. These changes in saccade parameters are more evident for tasks with stronger volitional components, like memory or antisaccade procedures, than for tasks of a more reflexive type. In how far these findings are related to impairment of attentional control, or the interrelation of oculomotor with other cognitive deficits, is still not well understood.

Visuospatial attention biases have mainly been reported for patients with left hemibody onset of motor symptoms (895, 817, 215, 486, 484). Left-dominant expression of parkinsonian symptoms is related to more severe neurodegeneration in the contralateral (right) basal ganglia and is often accompanied by orientation biases towards the right. While right hemispheric dysfunction is also found in patients with chronic visual neglect, attentional biases of Parkinson's disease patients are less pronounced. However, even subtle attentional deficits may exert significant impact on daily life activities, and may partly explain behavioral anomalies, such as poor driving performance (875, 146) or predisposition to bump into objects or doorways (175). Therefore, the study of visuo-spatial deficits is clinically important. Additionally, it provides an opportunity to improve our understanding of how the basal ganglia are involved in eye-movement and attentional control.

The effects of bilateral deep brain stimulation (DBS) of the subthalamic nucleus (STN) on oculomotor parameters, like saccade amplitude and latency, has been tested with tasks allowing only very specific patterns of movement. Reflexive tasks involving saccades to targets appearing in predictable positions suggest that STN-DBS improves saccade latencies and amplitudes (738, 953, 839, 840, 243, 17, 18). However, such effects have not always been found (720, 507). STN-DBS can improve amplitude and latency of saccades also in memory and anti-saccade tasks (720, 953, 243), relying again on simple stimuli and specific movement goals. It is less clear whether similar improvements can be observed when patients are allowed to explore freely, and whether attentional deficits would recede or appear more pronounced.

The effects of STN-DBS on attentional deficits have previously been tested in a reaction time task (930) and during free-viewing of complex scenes (752). These studies included unilateral and bilateral stimulation conditions but did not include comparisons to a control group. In both tasks, only exclusive stimulation of the left electrode resulted in a small attentional bias to the right hemifield. Surprisingly, patients showed no attentional bias in the reaction time task in a baseline condition where the stimulation was switched off. Unilateral left stimulation therefore introduced a bias not present without stimulation. In the free-viewing task, no baseline condition (without DBS) was recorded, in which biases might have been easier to detect because of decreased compensatory cognitive control in comparison to the reaction time task. On the contrary, it has been reported that oculomotor deficits were less obvious during the exploration of line-drawings of increasing complexity (544). Thus, unconstrained exploration of complex stimuli might generally result in compensation of motor and attentional deficits in Parkinson's. This raises the question whether patients with predominantly left-sided symptoms are biased during exploration of complex visual stimuli at all – a task closer to the demands of oculomotor control patients are facing in daily activities.

In the present study, we evaluated oculomotor performance and aspects of visual attention in Parkinson's disease patients with left symptom onset during a free-viewing task. In order to establish visuospatial deficits inherent to the disease, we measured patients during a baseline condition (medicated but without DBS) and compared them to a group of age-matched control subjects. Additionally, we evaluated bilateral and unilateral STN-DBS. Similar to nonhuman primates (546), the oculomotor territory of the human STN is located within the ventral region of the nucleus (242). In contrast to previous studies, in which unilateral DBS was directed at dorsal skeletomotor STN territories (930, 752), we attempted to selectively manipulate activity within the ventral oculomotor STN region and the subjacent substantia nigra pars reticulata (SNr).

ID	Age	Gender	LED	PD Dur	DBS Dur	UPDRS	Asymmetry	Therap. Stim Right	Therap. Stim Left	veR Volt	veL Volt	CO Age	Gender
1	32	m	631	2.0	0.8	13.0	73.3	-10/+11, 60, 130, 2.5V	-2/+C, 60, 130, 2.3V	2.8	1.5	30	m
2	42	m	567	7.5	2.1	47.0	54.9	-9/-10/+C, 60, 180, 2.0V	-1/-2/+C, 60, 180, 2.1V	N/A	N/A	40	m
3	45	m	1249	7.5	0.3	39.5	61.4	-10/+C, 60, 130, 2.7V	-2/+C, 60, 130, 2.3V	2.6	4.0	51	f
4	48	f	1082	12.0	0.8	34.0	66.7	-9/+C, 60, 130, 3.8V	-2/+C, 60, 130, 2.8V	2.4	2.0	51	m
5	49	m	809	9.0	2.3	32.0	77.8	-10/+C, 60, 90, 3.2V	-2/+C, 60, 90, 2.0V	2.4	5.0	53	f
6	53	m	624	0.0	0.3	48.0	53.1	-10/+C, 60, 130, 2.7V	-2/+C, 60, 130, 2.7V	1.4	2.8	53	m
7	58	f	1341	12.0	2.0	14.5	93.8	-10/+C, 60, 150, 2.6V	-2/+C, 60, 150, 2.5V	0.8	1.6	54	m
8	58	m	1203	20.5	3.0	22.5	45.2	-9/-10/+C, 60, 130, 3.0V	-1/-2/+C, 60, 130, 3.3V	3.4	4.3	54	f
9	60	m	1027	19.8	3.8	45.5	60.9	-8/+C, 60, 160, 2.0V	-1/+C, 60, 160, 2.4V	2.5	2.9	56	f
10	60	f	967	22.5	5.8	46.5	47.2	-10/+C, 90, 130, 3.9V	-1/+C, 60, 130, 3.6V	N/A	N/A	56	m
11	60	f	1038	8.5	1.8	42.0	65.4	-10/+9, 90, 130, 3.2V	-2/+C, 60, 130, 2.0V	2.8	1.4	57	f
12	60	m	550	10.0	3.2	55.0	55.3	-9/+C, 60, 180, 4.0V	-1/+C, 60, 180, 4.5V	3.2	2.4	61	m
13	62	m	926	11.5	1.3	52.0	53.9	-10/+C, 60, 160, 3.7V	-2/+C, 60, 160, 3.5V	1.6	3.2	63	m
14	65	m	566	16.7	3.0	25.0	75.6	-10/-9/+C, 60, 130, 3.9V	-1/+C, 60, 130, 1.5V	3.2	3.2	68	f
15	69	f	508	15.2	0.8	26.0	89.5	-10/+9, 60, 180, 2.5V	-2/+C, 60, 180, 2.8V	N/A	N/A	68	f
16	72	m	1111	12.2	2.0	27.5	64.3	-10/+9, 60, 130, 4.0V	-2/+1, 60, 130, 3.5V	3.6	4.0	76	f
17	73	m	537	20.5	7.5	31.0	63.0	-10/+C, 60, 130, 3.1V	-2/+C, 60, 130, 3.1V	4.0	5.6	76	m

Table 5.1: Demographic information and disease history of patients (left) and age-matched control subjects (two rightmost columns). LED = Levodopa equivalent daily dose (conversion factors after 860, PD Dur = Disease duration in years past diagnosis, DBS Dur = DBS Duration (years past electrode implantation), UPDRS = UPDRS-III score during DBS OFF, Asymmetry = Symptom severity of the left side relative to severity on both sides (UPDRS-III 20-26 left-sided items / [left-sided items + right-sided items] * 100), Therap. Stim Right/Left = Therapeutic stimulation settings of the right or left electrode (Negative poles/positive pole [C = case, 0 and 8 are the ventralmost contacts for the left and right electrode respectively], pulse width (μs), frequency (Hz), intensity (V)), veR Volt = Voltage during unilateral ventral right stimulation, veL Volt = Voltage during unilateral ventral left stimulation, CO = Control subjects.

We evaluated three hypotheses under these conditions. First, we hypothesized that oculomotor and attentional deficits observed in simple well-defined tasks should also be present during free-viewing of complex scenes. Specifically, patients without DBS are expected to make shorter saccades with a viewing bias to the right in comparison with controls. Second, we hypothesized that bilateral clinical stimulation, in addition to the known and desired clinical effects, would improve these deficits. And third, we predicted that unilateral stimulation in the ventral STN region would bias exploration towards the contralateral site.

5.2 Methods

Participants: We collected eye movement data of 19 PD patients with left hemibody symptom onset, and of 19 age-matched healthy control subjects. Two patients and two controls were excluded because the two patients participated only in one of our four experiment conditions, and the control subjects' calibration accuracy was insufficient. Three of the 17 remaining patients participated only in two of four conditions: during regular clinical stimulation and when stimulation was OFF. Handedness was evaluated with the Edinburgh handedness inventory (639). All participants were right-handed except for one ambidextrous patient. Demographic and clinical data are presented as meanSD in this section and in Table 5.1. Mean age was 56.8 $\pm$ 10.9 for patients (12 males) and 56.8 $\pm$ for control subjects (9 males). Two patients and two control subjects showed deficient color vision according to the Ishihara Color Vision test. Patients were generally suffering from advanced PD (mean years post-diagnosis = 12.2 $\pm$ 6.4; mean Levodopa equivalent daily dose = 867 $\pm$ 284mg; mean UPDRS-III in OFF = 35 $\pm$13)and had undergone bilateral stereotactic implantation of DBS electrodes in the STN (model DBS 3389, Medtronic Inc., Minneapolis, MN, USA) on average 2.4 $\pm$ (range 0.3-7.5) years before the experimental investigations. The degree of symptom lateralization is quantified by the fraction of left-sided symptoms relative to symptoms on both sides, which was on average 64.8% (Table 1). Values around 50% show that as a result of disease progression symptoms have appeared bilaterally and become more symmetric.

We obtained the present data in two different locations using the same equipment. All healthy control subjects and 13 patients were recorded at the Dept. of Neurophysiology and Pathophysiology at the University Medical Center Hamburg-Eppendorf, Germany. Four additional patients were recorded at a neurologist's practice (Dr. med. Oehlwein). All participants gave their written informed consent to participate in this study and were paid 10 per hour for their participation. Our study complied with Helsinki Declaration guidelines and was approved by the local ethics committee (Nr. PV4298, Ethik-Kommission der Ärztekammer Hamburg).

Setup and Procedure: Participant's eye movements were recorded using a remote video-oculographic eye tracker system (EyeLink 1000, 500 Hz sampling rate, SR Research Ltd., Mississauga, Canada). Subjects' sat central in front of a 24" flatscreen monitor at an eye-screen distance of 65 cm. Patients' average calibration error was 0.6°(STD = 0.38°) and for controls it was 0.48°(STD = 0.19°).

Patients performed the visual exploration task described below in four different DBS conditions. For the baseline condition stimulation was switched off (OFF). The bilateral condition employed standard therapeutic stimulation parameters (ON), and the remaining two experimental conditions consisted of unilateral monopolar stimulation of the most ventral DBS electrode contacts (unilateral ventral left, veL; unilateral ventral right, veR).

	LEFT							RIGHT						
ID	x	y	z	SE	%Ri	InitB	ΔSac	x	y	z	SE	%Ri	InitB	ΔSac
1	-11.9	-13.4	-7.1	TC, DYS	36.8	-1.01	1.1	10.4	-14.0	-7.1	PAR, DYS	44.3	-0.08	0.0
3	-11.9	-14.9	-6.9	TMC, DA	85.3	0.62	0.0	11.8	-14.6	-7.2	TMC	26.9	-1.32	0.2
4	-10.0	-13.5	-9.5	DYS, TC, MO	51.9	-1.19	0.2	10.3	-13.6	-6.4	PAR, DA	56.8	-0.52	0.2
5	-9.4	-14.4	-7.3	PAR	71.0	2.42	-0.3	10.6	-15.8	-7.1	PAR	58.6	1.97	-0.5
6	-11.1	-14.1	-6.9	PAR	47.5	0.14	0.2	11.7	-12.2	-8.1	PAR	60.6	0.88	-0.2
7	-8.4	-14.2	-11.0	PAR, DA	59.6	2.97	-0.6	11.0	-13.6	-6.7	DA	56.2	3.91	-0.2
8	-11.9	-12.2	-8.1	DYS, AUT	54.3	-0.50	-0.2	12.1	-14.0	-7.6	PAR, AUT	51.0	1.32	-0.1
9	-10.8	-13.8	-11.3	N/A	49.6	-1.25	0.8	9.4	-16.6	-8.4	N/A	50.0	-1.24	1.1
11	-10.2	-15.3	-8.4	TC, PAR, DYS	42.7	-1.61	0.3	12.7	-13.3	-7.8	MO, TMC	40.3	-2.96	-0.7
12	-6.0	-15.6	-12.6	PAR	80.4	3.60	0.5	11.0	-10.6	-5.9	PAR	76.7	2.36	0.2
13	-10.9	-12.8	-6.7	TMC, DYS, PAR, DA	40.7	-2.95	1.0	10.6	-14.5	-6.4	TC, DA, PAR	85.0	1.34	3.4
14	-9.0	-16.3	-7.7	PAR, DA	79.6	5.64	0.5	11.9	-14.6	-5.2	PAR, DA	69.0	1.60	1.1
16	-8.5	-15.6	-6.1	AUT, PAR	73.0	1.14	0.2	9.8	-15.1	-4.6	AUT, PAR	40.6	0.21	-0.5
17	N/A	N/A	N/A	N/A	57.1	-0.64	-0.8	N/A	N/A	N/A	N/A	55.1	-0.42	-1.1

Table 5.2: Electrode positions (mm). x = medio-lateral axis (+: right, -: left), y = antero-posterior axis, z = dorso-ventral axis. %Ri = % right side explored, InitB = initial bias ($^\circ$visual angle, negative values are left of the midpoint), ΔSac = saccade length difference (right - left direction). Side effect (SE) abbreviations: DA = dysarthria, PAR = paresthesia, DYS = dyskinesia, TC = torticollis, TMC = tetanic muscle contractions, AUT = autonomic side effects (dizziness or lightheadedness), MO = mood change, N/A = not available. Patients were ordered by age starting with the youngest as in Table 1.

For all conditions in which stimulation occurred, the pulse width and stimulation frequency remained unchanged from patients' clinical settings. In the unilateral conditions, the voltage was adjusted as follows: First, the threshold for the occurrence of persisting side effects was determined clinically (e.g. stimulation-induced paresthesias or tetanic muscle contractions). Table 5.2 provides a summary of the side effects encountered. Stimulation voltage was then reduced by 20% of the previously determined side-effect threshold. Because of this procedure neither patients nor experimenters were blinded to the conditions. Stimulation intensities did not differ significantly between the two unilateral ventral stimulation conditions (veL: 3.14 $\pm$1.31V; veR: 2.62 $\pm$ 0.88V, paired t-test: $t_{(13)}$ = 1.62, p = 0.13). Conditions were randomized such that the orders of ONc and OFF, and the order of veL and veR were balanced across patients.For eight patients the very first recording was in ON due to time constraints, whereas the other nine patients were measured first either in OFF (3 patients), veR (3 patients) or veL (3 patients). Recordings started at least 30 minutes after DBS parameters were changed.

In the first part of the experiment, participants carried out a visual search task (10 to 20 minutes) that will be reported separately. After a short break, the free-viewing experiment followed. Participants were instructed to examine the pictures as if they were in a museum or viewing a picture book. Completion of the free-viewing task took six to seven minutes excluding calibration. In every stimulation condition, 35 images of natural or urban scenes were displayed for eight seconds each. Each stimulus onset was triggered by the experimenter to ensure that patients were fixating a dot presented in the middle of the screen prior to each trial. An example image with the scanpath from one subject and a fixation density map depicting the pooled patient data are shown in Figure 5.1a-b. In order to avoid viewing biases caused by an asymmetrical distribution of image content, we randomly presented images from a pre-selected pool of pictures. The images were balanced with respect to averaged spatial fixation behavior observed in previous experiments with healthy subjects (658).

Ventral subthalamic DBS can result in restricted eye motility due to accidental stimulation of the oculomotor nerve (55). Therefore, we carefully assessed eye motility for each experimental condition and asked the patients for the occurrence of double vision. Clinical STN-DBS and attentional bias examination of eye movements was routinely carried out before the start of each session. Furthermore, we took photographs after completion of each experimental condition while participants shifted their gaze into nine different directions without moving their head. Importantly, none of our patients reported double vision or showed restricted eye motility.

Finally, at the end of each condition block, an experienced movement disorder specialist (CKM) evaluated patients' motor impairments according to the motor subsection of the Unified Parkinson's Disease Rating Scale (UPDRS-III). Patients usually completed two conditions in a row. One session comprising two conditions, took approximately three hours. Patients, who participated in all four stimulation conditions, completed the experiment on two different days. The order of events was kept identical for control subjects, including the 30-minutes breaks between trials to control for tiring effects.

Electrode positions in standard space: Pre- and post-operative computerized tomography (CT) scans and pre-operative magnetic resonance imaging (MRI) scans were used to determine the position of the ventralmost contacts used for the unilateral stimulation conditions. Imaging data from one patient had to be excluded from this analysis because the CT scans were too distorted to ensure accurate co-registration.

For each patient the post-operative CT scan was co-registered to the MRI scan in two steps. First, the pre-operative CT scan was aligned with

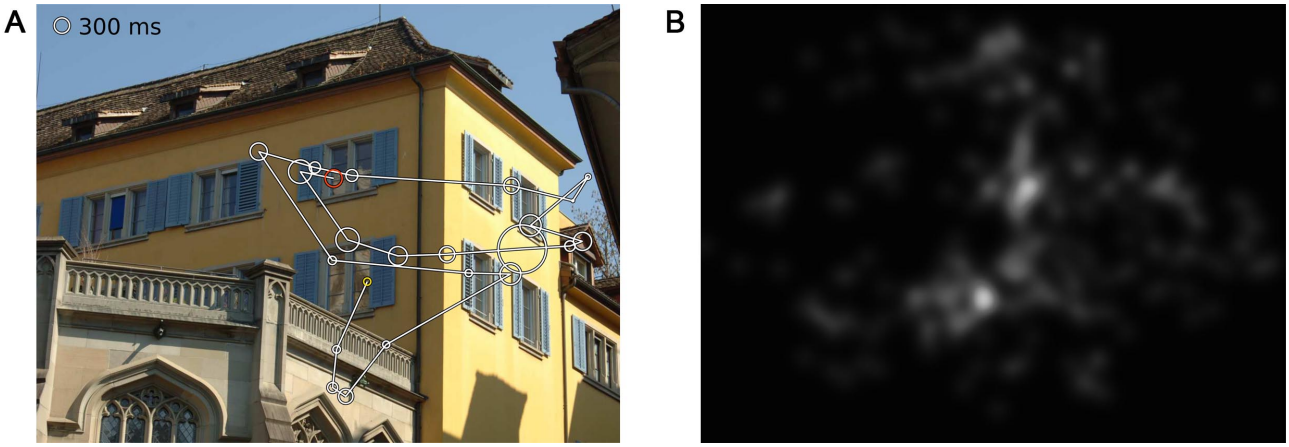

Figure 5.1: Example of exploration. (a) Scanpath of one subject in one trial. The yellow circle depicts the first fixation and the red circle the last one. Circle sizes illustrate fixation durations. (b) Fixation density map of all patients viewing this image.

the MRI scan (General Registration BRAINS, implemented in 3DSlicer 4.3.1, www.slicer.org, 245). Since the pre-operative CT was void of electrode artefacts this allowed accurate co-registration. In a second step, the post-operative CT scan was aligned with the co-registered pre-operative CT scan using manual and automatic transformations. For the subsequent normalization and electrode localization we used the MATLAB Toolbox LEAD DBS (Horn and Khn, 2015). MRI and CT scans were normalized to MNI (Montreal Neurological Institute) space (SPM New Segment nonlinear method, www.fil.ion.ucl.ac.uk/spm/software/spm8, 23) and electrode trajectories were reconstructed automatically, visually checked and corrected. To determine whether the electrode positions were related to individual exploration biases, a linear regression model ($bias = \beta_1 x + \beta_2 y + \beta_3 z$) was estimated with the demeaned electrode positions as predictors and the z-transformed bias data as predicted variable. The three regression coefficients determine a vector along which exploration biases change most in MNI space. We examined the size of the effect of electrode positions by computing correlations between the individual exploration biases and changes along the vector determined by the linear regression.

Visuospatial bias: To identify whether viewing behavior was biased, we computed three measures: (1) The median horizontal position of the first fixation in each trial representing the initial bias. (2) The median horizontal position of all fixations after the first one, carrying information about the extent of horizontal deviation. And (3), the exploration time spent on the right hemifield, as assessed by the fraction of spatio-temporal fixation density maps falling onto the right side of the image. The spatio-temporal fixation density maps were 2D maps generated by weighting all fixations after the first one by their duration and then spatially smoothing fixation locations via a 2-dimensional convolution with a Gaussian kernel (std = 0.5° visual angle). This way, both fixation spread and durations were taken into account. Subsequently, we took the median of the trial-wise fraction to get robust subject estimates.

Statistical analyses: To detect disease-related impairments independently from DBS effects, we tested measures obtained in the OFF condition against the average of both runs of control subjects (which were not statistically different). In addition to testing differences between patients in OFF and controls, we tested for within-patients differences between the four DBS conditions. Only when a condition differed from OFF it was further compared with the values of control subjects.

We employed two statistical models of Bayesian analyses: BEST (466), as a robust substitute for t-tests, and an ANOVA-like extension of its concepts to four conditions (465). Model specifications are described in the Supplementary Material. Unlike a t test, BEST uses Bayesian estimation to provide posterior probabilities of group or condition means and mean effect sizes. Results were obtained using R (version 3.0.3, http://www.r-project.org/; R Core Team, 2014) and JAGS (version 3.4.0, http://mcmc-jags.sourceforge.net/; (Plummer, 2014)) and are presented as group/condition means and their mean differences, both with their respective 95% Highest Density Intervals (HDI) (465), and with estimates of mean effect size (466) $((\mu 1 - \mu 2)/\sqrt{((\sigma 1 + \sigma 2)/2)}$ when appropriate. HDIs are defined as the smallest interval of the posterior probability distribution spanning a given fraction (e.g. 95%) analog to the notion of confidence intervals. This provides an intuitive summary statistic for each group/condition mean and mean effect sizes in the sense that all values within the HDI are more likely than any value outside the HDI. We consider differences significant if their 95% HDI exclude zero showing that the probability of the null hypothesis being true is below 5%. HDIs shown in the figures depict the variability between subjects in individual conditions rather than the condition differences derived from paired comparisons. This resembles classical statistical hypothesis tests, where differences are significant if their 95% confidence interval excludes zero. For ordinal data like UPDRS-III scores, non-parametric tests and Bonferroni-Holm corrected thresholds were applied. All tests were two-tailed.

Several reasons led to the choice of robust Bayesian statistics for drawing inference from our data: First, they allow to present the data in a most comprehensive manner in terms of parameters' joint distributions. This prior knowledge can be incorporated in future experiments, which is especially valuable for studies with patients involving laborious and intricate data acquisition. Secondly, these methods can deal with non-normal data as the one presented here. Furthermore, outliers can be accounted for by incorporating adaptable Student's t-distributions as likelihood functions. Depending on the input data, the t-distribution comprised heavy tails in case of outliers and approximated a normal distribution if there were no outliers. Thirdly,

separate variance model parameters for each condition render our results unconstrained from the assumption of equal variances across conditions. Finally, the BANOVA model (465) provides an in-built solution for the multiple comparison problem by virtue of an overarching distribution across the condition effects: Similar mean parameters among conditions lead to smaller estimated variability between them and thus cause "parameter shrinkage", i.e. different condition estimates get drawn towards the overarching distributions' mean (466, 291). This is important as our experimental design required six pairwise comparisons to test for differences between all combinations of the four DBS conditions.

5.3 Results

We first describe how patients' general motor impairment responded to the altered stimulation settings, and then discuss the effects on oculomotor recordings. Finally, we report about differences in attention with respect to viewing biases.

5.3.1 Skeletomotor symptoms and DBS

We evaluated differences in patients' UPDRS-III motor scores across the four DBS conditions (Friedman ANOVA, $\chi^2_{(3,39)}$ = 19.07, $p < 0.001$). As expected, motor symptoms were least pronounced during clinical stimulation (Fig. 5.2, median ON = 21.5; veR = 26.5; veL = 31.8; OFF = 34.0). Pairwise comparisons showed significant differences between ONc against OFF ($p < 0.001$), veR against OFF ($p < 0.001$), and ONc against veL (p = 0.009). DBS affected the UPDRS-III items of the left body side in a similar manner as it affected the overall sum, i.e. the ordering of scores was identical (Friedman ANOVA, $\chi^2_{(3,39)}$ = 22.47, $p < 0.001$; median ONc = 8.0; veR = 10.0; veL = 14.8; OFF = 16.0). Furthermore, the three pairwise comparisons listed above also indicated a significant improvement of left-sided symptoms (ONc against OFF $p < 0.001$; veR against OFF $p < 0.001$; ONc against veL p = 0.005). Additionally, veR was significantly more effective than veL (p = 0.001). For the right body side the ordering of scores was again identical, but the ANOVA did not reach significance ($\chi^2_{(3,39)}$ = 7.62; median ONc = 6.0; veR = 6.3; veL = 6.3; OFF = 8.5). Note that the motor scores for the right body side in all four conditions compare well to the left counterparts in the clinical condition. Less pronounced symptoms on the right side thus imply that the range for therapeutic effects was more limited for this side, leading to a floor effect. In summary, in agreement with previous reports (356) clinical stimulation (ON) led to significant improvements of motor symptoms while unilateral ventral stimulation was only partly effective.

5.3.2 Eye-movements deficits and the effect of DBS

One of the most consistently affected parameters reported in the literature of eye-movements in Parkinson's disease is reduced saccade length (894, 684). In the current experiment, the mean saccade length in patients in the OFF condition (Fig. 5.3a, mean OFF = 2.79°, 95% HDI [2.30, 3.21]) was significantly smaller than the mean of control subjects (mean difference CTRL-OFF = 1.00°, 95% HDI [0.36, 1.65], effect size = 1.13). The length of saccades did not differ with respect to whether they were directed to the left or right. Clinical DBS significantly elongated saccades in comparison to OFF (mean difference ONc-OFF = 0.29°, 95% HDI [0.06, 0.52], effect size = 0.37). The average saccade length during clinical DBS (mean ONc = 3.14°, 95% HDI [2.58, 3.68]) was still shorter than that of control subjects, but this difference was not significant (mean difference CTRL-ONc = 0.64°, 95% HDI [-0.07, 1.35], effect size = 0.66). Mean saccadic lengths during veR and veL were intermediate between ON and OFF, suggesting only moderate improvement by unilateral ventral stimulation but those changes were not significant in comparison with ON or OFF. Thus, consistent with previous studies our results demonstrate that clinical DBS partially compensates the reduced saccade length in patients.

As a measure of motor flexibility, which is usually reduced in Parkinson's disease patients (384, 689), we evaluated saccade length variation during exploration. Saccade length variability, calculated as the median standard deviation of the saccade length within each trial, was significantly reduced in patients compared with controls (Fig. 5.3b, mean OFF = 2.71°, 95% HDI [2.34, 3.09]; mean difference CTRL-OFF= 0.63°, 95% HDI [0.13, 1.10]; effect size = 0.94). Importantly, the variability of saccade lengths was not significantly improved by ON (mean ONc= 2.89°, 95% HDI [2.49, 3.26]; mean

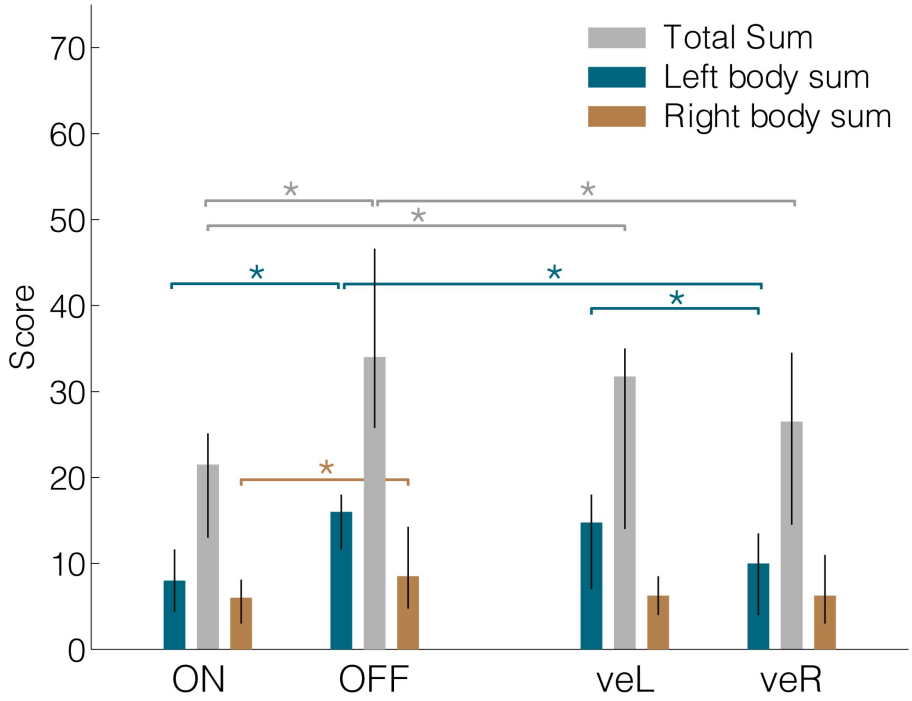

Figure 5.2: Median UPDRS-III total sums, left body sums and right body sums for all four conditions. Lateralized values were derived from items 20-26. ON = DBS On, OFF = DBS OFF, veR = Ventral contact of right electrode active and left electrode off, veL = Ventral contact of left electrode active and right electrode off. Errorbars denote the interquartile range.

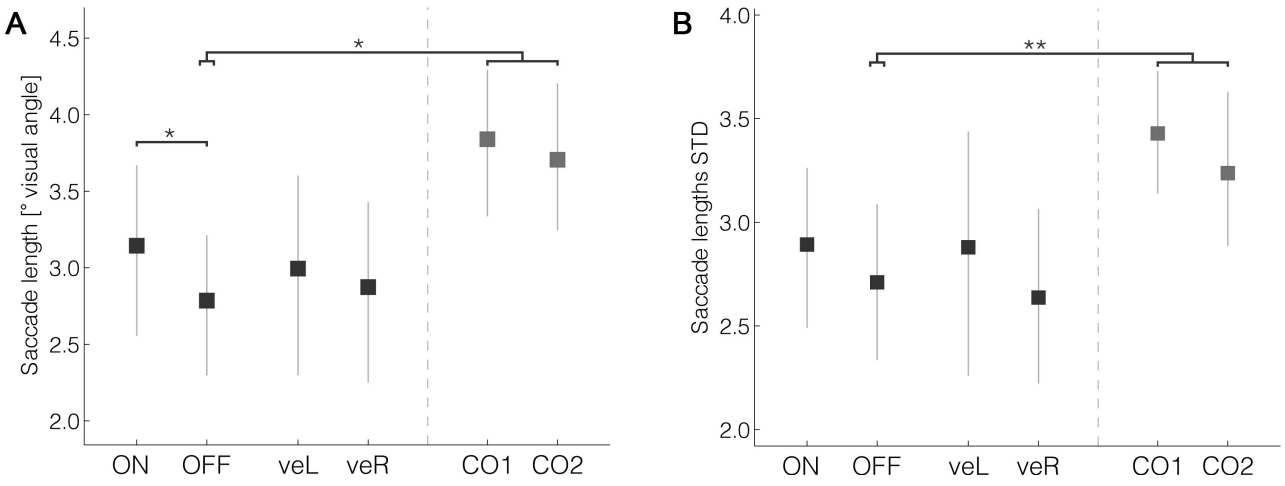

Figure 5.3: Oculomotor parameters. Saccade length and saccade length variability were significantly reduced in patients when compared with controls. Bilateral DBS in therapeutic settings significantly increased saccade length. Errorbars are 95% HDIs.

difference ONc-OFF = 0.14°, 95% HDI [-0.10, 0.38]; effect size = 0.22). This lack of effect of clinical DBS on saccade variability is a first indication that DBS compensates disease-induced alterations of distinct eye-movement parameters to different degrees.

To evaluate differences in saccade velocity it is necessary to take into account that saccade peak velocities are closely tied to saccade lengths, with the latter being broadly distributed during free-viewing. A simple comparison of mean peak velocities could therefore be confounded by patients making smaller saccades than controls. In order to control for this, we evaluated subjects' saccade main sequences. The main sequence is the log-log linear relationship between saccades lengths and velocities. To simplify the analysis of slopes and offsets of this linear function, we evaluated the definite

	ON	OFF	veL	veR	CTRL 1	CTRL 2
Area viewed (%)	17.3 ±3	17.2 ±4	16.9 ±4	16.2 ±5	19.7 ±3	18.9 ±4
Fixation Duration	265 ±35	255 ±32	258 ±41	265 ±48	261 ±23	260 ±29
Fixation Duration Ri-Le	5.2 ±13	3.3 ±19	10.5 ±21	6.0 ±25	-0.1 ±14	2.2 ±9
SMS Peak Velocity Integral	2.75 ±0.1	2.73 ±0.1	2.73 ±0.1	2.72 ±0.1	2.74 ±0.1	2.73 ±0.1
Number of Saccades	682 ±105	691 ±132	690 ±129	647 ±154	739 ±98	716 ±116
% Rightward Saccades	49.7 ±3	50.6 ±4	50.5 ±5	50.4 ±3	49.4 ±4	49.8 ±3
Saccade Length Ri-Le	0.06 ±0.4	0.02 ±0.4	0.20 ±0.6	-0.08 ±0.4	0.17 ±0.6	0.15 ±0.4
Saccade Angle Variability	1.79 ±0.1	1.82 ±0.1	1.80 ±0.1	1.80 ±0.1	1.82 ±0.1	1.79 ±0.1
Median vertical position	0.56 ±0.8	0.60 ±1.4	0.86 ±1.5	0.68 ±1.3	0.59 ±0.9	0.87 ±0.8
Upward bias	59.5 ±11	58.5 ±15	57.9 ±14	60.3 ±17	55.7 ±7	56.3 ±9

Table 5.3: Means and standard deviations of eye-movement measures that did not differ between conditions and subject groups (SMS = Saccade Main Sequence, Fixation Duration Ri-Le = Difference between fixations durations on the right hemifield and durations on the left hemifield, Saccade Length Ri-Le = Difference between lengths of rightward saccades and leftward saccades).

integral of the main sequence between 0.1 and 40° visual angle, the range covering all our subjects' saccades. This integral is proportional to the peak velocity value at a saccade of 2° length (the mean of the integral's bounds in log space). It is of interest to note that saccadic peak velocity, when controlling for their length as assessed via the area under the saccade main sequence, did not differ between patients and controls (mean OFF = 2.73, 95% HDI [2.70, 2.78]; mean difference CTRL-OFF= 0, 95% HDI [-0.06, 0.06]; effect size = 0.01), or between DBS conditions (mean ONc= 2.75 [2.70, 2.79]; mean difference ONc-OFF = 0.01, 95% HDI [-0.02, 0.03]; effect size = 0.13). In summary, when adjusted for length differences, patients' saccades were not significantly slower than controls.

Furthermore, we also assessed a variety of additional oculomotor parameters, where no difference was found between patients and controls, or between DBS conditions (see Table 5.3). Even though the area viewed (percentage of the complete picture) and the amount of saccades tended to be smaller in patients than in controls, these differences were not significant. Patients' rightward saccades (defined as being directed to the right relative to the previous fixation point irrespective of the target hemifield) were not more frequent or longer relative to leftward saccades than in controls. Fixation durations and saccade angle variability were similar across conditions and patient groups. Altogether, these measures indicate that differences in saccade lengths and variability between patients and controls did not cause slower exploration because the number of eye movements and the area covered was not significantly reduced.

In summary, oculomotor parameters under free-viewing conditions were affected in patients in a way that is compatible with previous results obtained in simpler tasks. Patients generally made smaller saccades and showed less saccade length variability than control subjects. Of note, only saccade length was significantly improved by clinical stimulation.

5.3.3 Exploration bias in Parkinson's disease

Previous studies have reported subclinical neglect in Parkinson's disease patients, but its impact on patients' daily activities is still unclear. We evaluated if an exploration bias exists during the scanning and exploration of complex natural scenes and how it can be affected by unilateral STN-DBS. We evaluated patients' horizontal bias in two different ways: by means of the median horizontal fixation positions and via the fraction of exploration done in the right hemifield.

Patients' median horizontal fixation position was in OFF significantly shifted to the right as compared with control

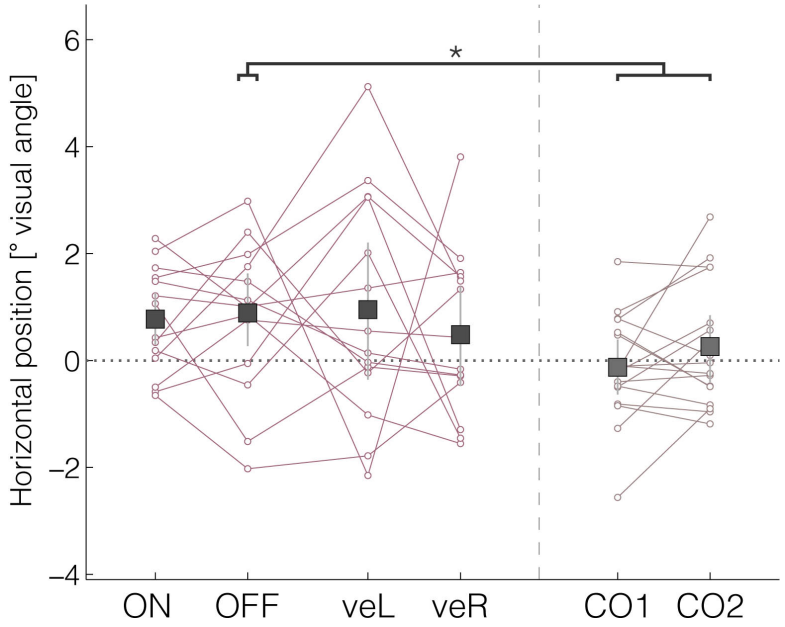

Figure 5.4: Rightward bias of patients assessed by the median horizontal position. Negative values indicate deviations to the left, and positive values deviations to the right.

subjects (Fig. 5.4, OFF = 0.89, 95% HDI [0.27, 1.63]; mean difference OFF-CTRL = 0.88°, 95% HDI [0.05°, 1.75°]; effect size = 0.78). The four DBS conditions did not differ significantly from each other (ONc = 0.77, 95% HDI [0.29, 1.27], veL = 0.95 95% HDI [-0.36, 2.21], veR = 0.48 95% HDI [-0.48, 1.39]). The comparison of patients' percentage of exploration towards the right in OFF with the bias of control subjects resulted only in a trend (OFF = 57.77%, 95% HDI [51.86, 64.43], mean difference OFF-CTRL= 6.24%, 95% HDI [-1.02, 13.37], effect size = 0.66). Nevertheless, the rightward bias of patients in OFF was significantly different from 50%, which was not the case for control subjects (mean = 52.19%, 95% HDI [48.37, 55.53]). The difference between these two measures of bias, together with the absence of altered fixation durations (Table 5.3), indicate that it is the extent of fixation deviation towards the right hemifield, and not the duration of the fixation, what contributed most to patients' rightward bias. There were no significant differences in vertical bias, which was computed similarly to the rightward bias as percentage of summed fixation durations to the upper visual field or as median vertical position (Table 5.3).

During free viewing of static images, healthy subjects explore first the left image sides (658). We assessed whether this early bias is also present in patients by examining the horizontal position of the first fixation relative to the centre. Control subjects tended to direct their first fixation to the left hemifield of the image (CTRL = -1.00°, 95% HDI [-1.72, -0.23]). In contrast, patients' average horizontal position of the first fixation was centered (OFF = 0.14°, 95% HDI [-0.52, 0.87]), and hence significantly shifted to the right in comparison with controls (mean difference OFF-CTRL = 1.15°, 95% HDI [0.14, 2.15], effect size = 0.82). Again, there were again neither significant differences nor trends between different DBS conditions.

In summary, we found evidence of a slight general rightward bias in patients, which is consistent with previous reports of attentional bias in patients with Parkinson's disease, and a reduced early leftward bias. In contrast to the reduction of saccadic impairments seen in the previous section, clinical DBS did not change this bias pattern. Contrary to our initial predictions, unilateral stimulation directed at ventral subthalamic regions did neither reduce the bias nor reverse the direction at the group level.

5.3.4 Individual analysis

As the variability between patients appeared to be increased during unilateral stimulation of the ventral subthalamic area (Fig. 5.4), we hypothesized that an effect of unilateral ventral DBS might have been concealed by variability in the electrode position among subjects. We reconstructed the positions of subjects' ventralmost DBS electrode contacts in normalized MNI space. As expected, these stimulation sites were concentrated in ventral STN (Fig. 5.5, upper panel), along with more ventral and posteromedial spots in SNr and prerubral area, respectively. We then performed a multiple regression of the measures of bias with the electrode position in three dimension as predictors. For unilateral left DBS, the bias of the first movement showed a significant dependence on the position of the electrode (Fig. 5.5, $F_{(3,10)}$ = 4.2, p = 0.037, r^2 = 0.56), which was only close to significance in the case of global bias measured by median horizontal fixation positions ($F_{(3,10)}$ = 3.3, p = 0.067, r^2 = 0.5). Correlations between the predicted values – assuming this is the most relevant direction – and the actual bias values were highly significant in both cases (initial bias p = 0.003; general bias p = 0.007, r^2 are equivalent to regression results above, and the smaller p-values reflect the reduction in degrees of freedom). Similar regressions for unilateral right DBS were not significant (p = 0.54 and p = 0.89 respectively). Figure 5.5 shows that the predicted direction extends most along the posterior-anterior direction, followed by the medial-lateral directions (upper panel) implying that the position along this direction contributed most to the differences in biases.

While in both unilateral conditions more than half of all patients spent approximately 50% of their exploration time on each hemifield, some patients were strongly biased towards one side (see Table 5.2 and Fig. 5.5). One of those patients (#13) showed stimulation-induced torticollis upon identifying the voltage threshold for side effects. His head turned towards the ipsilateral side of stimulation, i.e. to the right upon ventral right stimulation. In a second patient the head turned to the left upon increasing the voltage for veL (#11). Voltage was lowered until the muscle contractions fully receded, yet their fixations were still shifted towards the turning direction (Table 5.2). Interestingly, both patients received stimulation at similar sites – at the posterior border of the STN (Fig. 5, diamond with a dot markers). Remarkably, another patient's head (#1) involuntarily turned to the contralateral side upon determining the voltage threshold for unilateral left stimulation. Even though his head was turning to the right, his gaze was deviating towards the left. During the subsequent experiment he explored predominantly his left visual field, but surprisingly his rightward saccades were notably longer than his leftward saccades in comparison with most other patients (Table 5.2, ΔSac). The length of saccades seemed to be biased towards the direction of the neck torsion and dissociated from the leftward deviation of the gaze and the left-directed exploration bias. A fourth patient's head (#4, diamond marker) turned slightly to the right when increasing the voltage prior to veL, but this patient showed no general viewing bias (51.9%).

Our results indicate that DBS can cause substantial shifts in attention depending on the stimulation site. Especially the electrode location within the antero-posterior axis in the left STN seems to correlate with the extent of the rightward bias.

5.4 Discussion

Bilateral clinical and unilateral ventral right DBS – applied contralateral to the initially most affected body side – alleviated patients' left-dominant skeletomotor symptoms. In contrast, patients' saccades were not lateralized (e.g. more frequent or longer when directed to the right), and were significantly improved only by bilateral stimulation. The extent of this improvement ($\sim$40%) was similar to the change in motor symptoms measured with the UPDRS-III scale ($\sim$37%), indicating similarities between the responsiveness of the skeletomotor and oculomotor systems. However, patients' attention bias displayed during OFF was not counteracted by clinical stimulation. Only unilateral left stimulation modified biased exploration behavior, depending on the precise electrode location within the ventral subthalamic area.

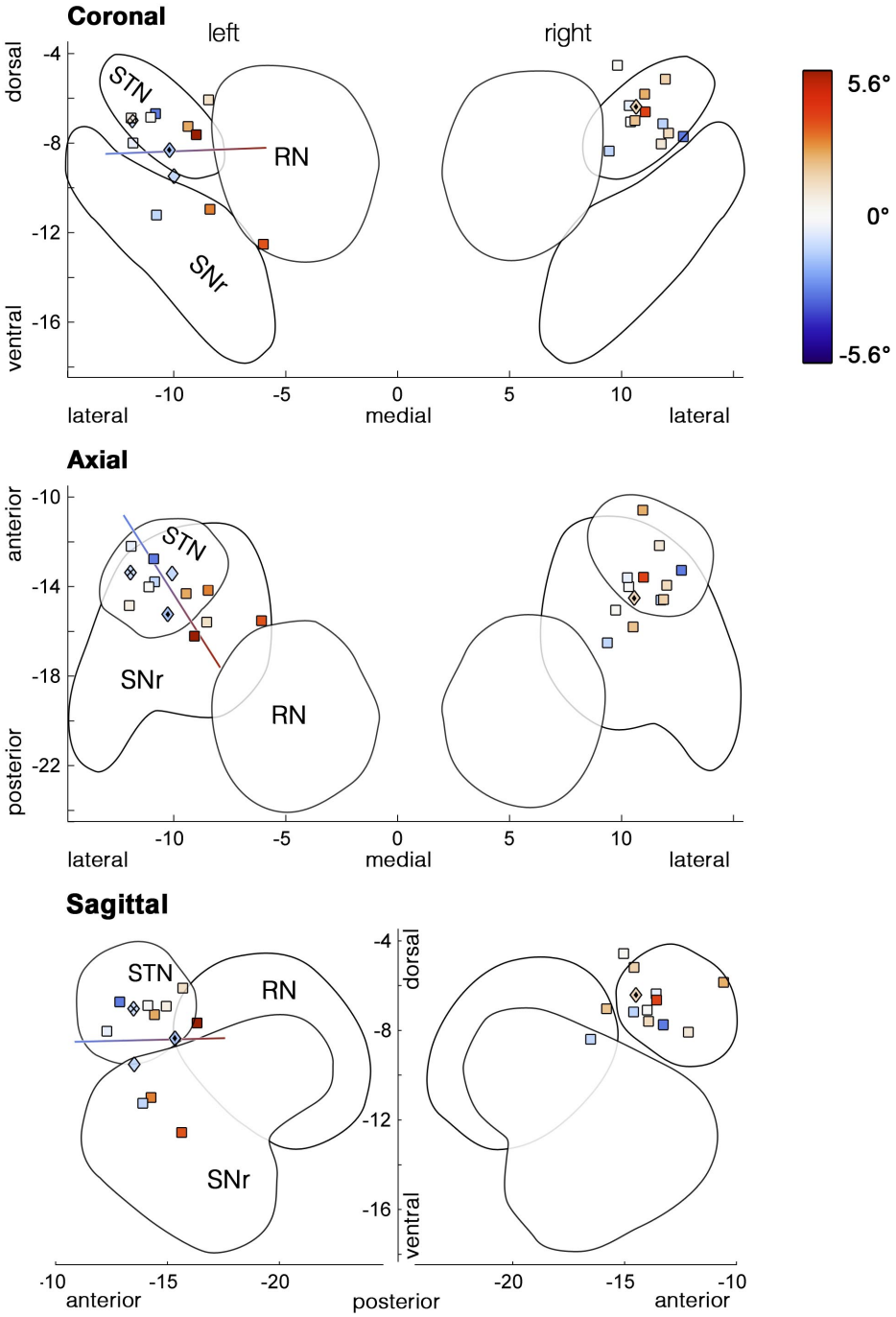

Figure 5.5: Marker colors code the amount of initial bias (°visual angle) with cool colors representing deviations to the left and warm colors deviations to the right. Stimulation sites, where increased voltage induced torticollis prior to determining the side-effects threshold, are depicted as diamond-shaped markers. The line represents the outcome of the multiple regression model, i.e. the best direction for predicting the bias during unilateral left stimulation. Variability of the location along the antero-posterior axis explained most of the bias variance, followed by the medio-lateral direction. Outlines of subcortical structures are based on 3D models of the ATAG Atlas (433).

5.4.1 Limitations

This paper provides a set of observations on the basis of explorative data analysis. One limitation of our study is that neither patients nor experimenters were blinded to the experimental conditions because the threshold for side effects in

the unilateral stimulation condition had to be determined. However, patients were not aware of the initial hypotheses of our study.

Attention deficits might have been more pronounced after medication withdrawal. However, we had to omit initial plans to conduct the study after withdrawal of anti-parkinsonian medication because discomfort resulting from severe Parkinson's disease symptoms caused a large drop-out rate after the first recording session.

5.4.2 Oculomotor impairments in PD

This positive effect of clinical STN DBS on saccade lengths is in line with previous reports of improvement by DBS in saccade lengths during volitional memory-guided tasks (720, 243), anti-saccade tasks (953, 243, 89), smooth pursuit (621) and visually triggered saccade tasks (738, 953). As early neurophysiological studies in monkeys showed no involvement of the basal ganglia in spontaneous exploration (359), it was not certain that effects seen in those simple tasks would generalize to free viewing behavior. Only recent studies in humans (783), are more in line with our findings, showing that the basal ganglia are active during free-viewing, and that exploratory visuomotor behavior thus can be affected in Parkinson's disease as a consequence of basal ganglia dysfunction.

Our results extend the ones from a previous report about free viewing behavior and the effects of DBS in patients with PD (752). In agreement with their results, we did not find significant changes in saccade lengths between bilateral and unilateral stimulation conditions. However, as we also evaluate the behavior of a control group and of patients in a "baseline" condition without DBS, we were able to show that saccade length during free-viewing is reduced in the parkinsonian state and improved by clinical stimulation. Furthermore, patients showed reduced saccade length variability in comparison with controls. However, the impact of these oculomotor alterations on behavior is not clear since the total explored area was not reduced.

5.4.3 Exploration bias during free-viewing behavior

In agreement with previous research showing attentional biases in patients with left-dominant symptoms in other tasks (895, 817, 215, 486, 484), our patients also showed a slight rightward bias during free viewing. The difference to control subjects was most pronounced during the first eye movements, which are usually biased to the left in healthy right-handers (658). This attentional bias was neither explained by a directional bias in saccade lengths (i.e. rightward saccades were not significantly longer or more abundant than leftward saccades) nor by differences in fixation durations between hemifields. The exploration bias was not compensated by clinical stimulation even though it decreased markedly the discrepancy between left and right motor symptoms. In the study by Schmalbach et al. (2014), Parkinson's disease patients did not show biased free-viewing behavior during clinical stimulation. This discrepancy may be explained by the small size of the bias, which became evident only by comparison with a control group. Moreover, Schmalbach et al. included patients with both left- and right-dominant symptoms whereas we evaluated only patients with left hemibody onset of symptoms, who are more likely to show attentional bias. As mentioned above, the bias was not improved by clinical bilateral stimulation like some of the oculomotor parameters highlighting an important difference between the lateralization of skeletomotor, oculomotor and attentional functions.

Other than expected, unilateral stimulation in the ventral subthalamic area caused no consistent shifts of viewing biases but higher variability. Unilateral left stimulation did not only induce shifts to the right but also to the left. This ipsilateral leftward shift was unexpected. A rightward bias after left STN-DBS as reported by Schmalbach et al. (2014) would have been in agreement with the assumption of a disinhibitory effect of DBS and the known circuitry of the basal ganglia ocular movement control. In this model, inhibition of the STN results in decreased excitatory input to the SNr and consequently in a reduced inhibitory tone to the ipsilateral superior colliculusbiasing viewing behavior to the contralateral right visual field. Although we did not find an effect of unilateral stimulation at the group level, the multiple regression analysis revealed a dependency between bias and the position of the activated electrode contact within the left STN. Those patients who were

stimulated in the posterior part of the STN showed a stronger bias towards the right. To understand this relationship it is necessary to look into the fine-grained topographic organization of the basal ganglia circuit, which is still not completely clear, especially in humans. Previous studies in non-human animals showed that the efferents from the STN to the SNr are similarly arranged, especially in the latero/medial axis (663, 798, 399). Additionally, in monkeys and cats, projections from the SNr to the superior colliculus include abundant uncrossed and broadly distributed projections, as well as less numerous crossed projections to the contralateral SC departing from the anterolateral SNr (54, 395). Assuming a similar organization of the human STN/SNr more anterior STN stimulation (i.e. disruption of pathological hyper-synchronization) should result in reduced activity of the corresponding anterolateral SNr, with an impact on both crossed and uncrossed projections. In contrast, more posterior stimulation of the STN should result in reduced activation of the uncrossed population. This would cause, in the case of ventral left posterior stimulation, a bias to the right due to exclusive disinhibition of the ipsilateral SC, whereas more anterior stimulation would result in more balanced disinhibition of both SC and consequently no bias. Yet it is unclear why this occurs only for left stimulation, even if it is not surprising considering the known association of attentional deficits with right cortical lesions.

An important question is whether visuospatial attention is biased in Parkinson's disease patients to an extent that would affect them in everyday activities. The average bias observed at the group level was rather small, and thus has probably only limited impact on daily life. Nonetheless it could impact patient's ability to drive (875, 146) and increase the incidence rate of bumping into objects (175). Individuals might experience more pronounced visuospatial deficits, which is why individual assessments of driving capabilities would be advisable (100). Clinical DBS provides no simple remedy for such impairments, yet trying to select different electrode contacts for stimulation might restore balanced attention and recover normal exploration behavior. On the other hand, in the light of the association between posterior sites and bias presented here, we would recommend to routinely evaluate whether an attentional bias has been induced by DBS, especially in rare cases of unilateral stimulation or when the posterior subthalamic area is targeted as has been suggested for the treatment of tremor suppression (700, 687, 943).

5.4.4 Conclusions

In summary, patients with Parkinson's disease made shorter saccades with a reduced variability in lengths, and were slightly biased towards the right in comparison with controls. Saccade length was significantly improved by clinical stimulation, whereas the effects of unilateral stimulation of the ventral subthalamic area on exploration were dependent on the individual stimulation site. The findings presented provide new evidence for the involvement of the basal ganglia in self-directed visual exploration and will hopefully guide further research on the treatment of patients with visuospatial attention deficits or cervical dystonia.

Chapter 6

Combining EEG and eye tracking: identification, characterization, and correction of eye movement artifacts in EEG data

Abstract

Eye movements introduce large artifact to electroencephalographic recordings (EEG) and thus render data analysis difficult or even impossible. Trials contaminated by eye movement and blink artifacts have to be discarded, hence in standard EEG-paradigms subjects are required to fixate on the screen. To overcome this restriction, several correction methods including regression and blind source separation have been proposed. Yet, there is no automated standard procedure established. By simultaneously recording eye movements and 64-channel-EEG during a guided eye movement paradigm, we investigate and review the properties of eye movement artifacts, including corneo-retinal dipole changes, saccadic spike potentials and eyelid artifacts, and study their interrelations during different types of eye- and eye-lid movements. In concordance with earlier studies our results confirm that these artifacts arise from different independent sources and that depending on electrode site, gaze direction, and choice of reference these sources contribute differently to the measured signal. We assess the respective implications for artifact correction methods and therefore compare the performance of two prominent approaches, namely linear regression and independent component analysis (ICA). We show and discuss that due to the independence of eye artifact sources, regression-based correction methods inevitably over- or under-correct individual artifact components, while ICA is in principle suited to address such mixtures of different types of artifacts. Finally, we propose an algorithm, which uses eye tracker information to objectively identify eye-artifact related ICA-components (ICs) in an automated manner. In the data presented here, the algorithm performed very similar to human experts when those were given both, the topographies of the ICs and their respective activations in a large amount of trials. Moreover it performed more reliable and almost twice as effective than human experts when those had to base their decision on IC topographies only. Furthermore, a receiver operating characteristic (ROC) analysis demonstrated an optimal balance of false positive and false negative at an area under curve (AUC) of more than 0.99. Removing the automatically detected ICs from the data resulted in removal or substantial suppression of ocular artifacts including microsaccadic spike potentials, while the relevant neural signal remained unaffected. In conclusion the present work aims at a better understanding of individual eye movement artifacts, their interrelations and the respective implications for eye artifact correction. Additionally, the proposed ICA-procedure provides a tool for optimized detection and correction of eye movement-related artifact components.

This chapter was published as a peer reviewed article: Plöchl M, **Ossandón JP**, König P. Combining EEG and eye tracking: identification, characterization, and correction of eye movement artifacts in electroencephalographic data. *Frontiers in Human Neuroscience*, **6**: 278 (2012).

6.1 Introduction

Neural activity measured with electroencephalography (EEG) or magnetoencephalography (MEG) yields a relatively weak signal, with amplitudes typically in the order of a few microvolts or femtotesla, respectively. At the same time, such measurements at scalp level are prone to electrical artifacts originating from non-neural sources such as the eyes, muscles or electrical devices in the surroundings. Compared to signals resulting from neural processes these artifacts can be several magnitudes larger in amplitude. Thus, cerebral activity may be buried in noise and remain undetectable even when a large number of trials is averaged.

A common strategy to circumvent this problem is to discard artifactual epochs from the data. This however often leads to considerable data loss, which in turn reduces the signal-to-noise ratio improvement that results from averaging techniques and therefore also the ability to detect neural activity. Additionally, this approach entails methodological constraints: in standard EEG or MEG experiments subjects are required to not move their eyes, thus adding unnatural cognitive loads to the experimental task and precluding the realization of EEG and MEG studies under more natural viewing conditions. Furthermore, the direct study of overt attention dynamics, by exploiting the temporal resolution of non-invasive electrophysiological methods, is rarely pursued. In studies that attempt to do so, the common practice is to analyze only the epochs before or after the eye movement and in this way to avoid problems arising from eye movement artifacts. However, some artifacts can extend to periods before and after saccade on- and off-set, respectively, and thus the analysis of those periods may be confounded (849, 53).

Likewise, studies that are not directly related to eye movements are also potentially impaired: when undetected, even small but systematic artifacts can add up over trials, thus distorting the analysis and the conclusions drawn from it (363). In this context small involuntary eye movements during fixation, usually referred to as miniature eye movements (733) or microsaccades (539, 227), have recently received considerable attention, as they have been shown to vary systematically between different cognitive or perceptual states and in this way to introduce systematic biases in the analysis of neural activity (954, 430).

In order to overcome such limitations and biases, several procedures have been proposed in order to remove or at least reduce artifacts present in the data. These procedures include averaging, filtering (511), linear regression (225, 167, 168, 751), principal component analysis (503, 434), independent component analysis (ICA) (408, 385, 405, 496, 541), dipole modeling (63, 503) and frequency methods (167, 168). Most of these approaches have been shown to effectively remove artifacts whose respective sources are well defined and whose spectral and statistical signal properties (e.g., amplitude, variance, frequency range, kurtosis etc.) differ considerably from those of neural activity. Averaging procedures for example substantially reduce random noise of moderate amplitude and therefore are standard in most electrophysiological experiments (511). Furthermore slow signal drifts caused by changing electrode properties, line noise and high frequency muscle activity can relatively easily be removed from the data by applying appropriate filters. Other muscle artifacts are reliably isolated into ICA components that can then be excluded from the data (525, 408, 385). For eye movements on the other hand there is no standard correction procedure established yet, although several proposals do exist and are extensively discussed with respect to their efficiency (167, 168, 169, 751, 366).

The difficulty to identify and correct eye movements can be largely attributed to the fact that a single eye movement produces several artifacts in the form of signal offsets and transients. These artifacts do not only emerge from different mechanisms but also differ in their statistical and spectral properties, depending on size and direction of the movement: while artifacts produced by eyeball rotation are the consequence of a direction change of the corneo-retinal dipole and therefore change roughly linearly with movement size and direction, blink artifacts are generated by the cornea being short-circuited to the extra ocular skin, thus being independent of corneo-retinal dipole orientation (547, 16, 137). In addition, the amplitude of the (pre-)saccadic spike potential, an artifact that most likely emerges from extra-ocular muscle activity, changes only marginally with saccade amplitude or direction (430, 121). Therefore it may confound the data even during very small eye movements (i.e., microsaccades) that do not produce clearly visible corneo-retinal dipole offsets (954). Another

difficulty for the general characterization of eye movement artifacts is that there are also non-physiological factors that may alter the signal when eye movements are present in the data. As a result of high pass filtering during EEG recording, step-like signal changes, as they occur during eyeball rotation, cause the signal to slowly drift back toward its initial value according to the filter's cut-off frequency. Such drifts may confound the data up to several seconds after the actual saccade. Finally, re-referencing the data (e.g., to the average activity of all scalp electrodes) can change the sign and amplitude of a given artifact component at different recording sites, thus rendering its identification difficult.

In the literature different types of eye artifacts are usually reviewed individually (849, 137, 502, 503, 430). To our knowledge a comprehensive overview that also accounts for their interrelations during different saccade types does not exist.

Moreover, the heterogeneity of sources contributing to signal contamination by eye movements has important implications for correction procedures. Algorithms that assume that eye movement artifacts originate from a single sourceor ignore that the relative contribution of different artifact sources to the signal may vary depending on the respective recording site and movement directionwill generally over- or under-correct the signal even if being accurate at one particular site. On the other hand, algorithms that can account for multiple and independent artifact sources (e.g., blind source separation methods) often depend on subjective decisions, as for example which of the isolated components relate to eye movements and therefore should be excluded from the data (525, 408).

In the following, using EEG and eye tracking during a guided eye movement paradigm, we will first review different types of artifacts produced by eye movements and investigate their projections to different electrode sites during a variety of saccades. Subsequently we will point out the advantages and disadvantages of different approaches to eye artifact correction and then propose a cleaning procedure to remove eye artifacts in an effective and objective manner.

6.2 Methods

Subjects: We simultaneously recorded EEG and eye movements from 14 subjects (7 male, 7 female; age range: 20–31 years) after they were informed about the procedure and purpose of the study and had signed an informed consent. Experimental procedures conformed to the Declaration of Helsinski and national guidelines. All subjects were students at the University of Osnabrück and received payment or course credits for their participation. All subjects reported normal or corrected-to-normal vision.

Stimuli Presentation: The participants sat at 60 cm distance from a 30" TFT monitor (Apple LED Cinema Display, refresh rate 60 Hz, resolution 2560 x 1600 pixels). Due to the range of the eye tracker only a square region of 960 x 960 pixels ($\sim 23^\circ$x 23°) in the center of the screen was used for stimulus presentation. The stimulus itself constantly covered about $3^\circ$of the visual field and consisted of black and white rings, which continuously contracted toward the center at a rate of 2 Hz (i.e., when the outer ring started contracting into the center it was replaced by the next ring of the other color).

Experimental Procedure: Previous to each block of the actual experiment, subjects performed a short pre-experimental procedure in order to calculate the regression coefficients (751) and to complement the data for ICA decomposition (see below). This pre-experiment consisted of 16 trials of 15 s duration in which subjects were asked to perform different eye movements over a gray screen (RGB 127/127/127). Every subject performed four trials for each of the following movements: blinks, vertical movements, horizontal movements, and blinks plus vertical movements. On average each subject performed 169 blinks, 561 vertical, and 312 horizontal saccades during the pre-experiment.

After the pre-experiment the participants performed the task illustrated in Figure 6.1: a white fixation cross (size $\sim 1.5^\circ$) appeared on a gray screen (RGB 127/127/127) in one of nine possible locations arranged in a three by three square. The respective trial started as soon as the subject started fixating the fixation cross. After a variable time (500–800 ms) the stimulus was presented in one of the other eight remaining positions on the screen (Fig. 6.1a).

In one condition (saccade condition) the fixation cross disappeared after another 500–1000 ms, thus providing the cue for the subject to make a saccade to the stimulus location (Fig. 6.1b). In the other condition (fixation condition), instead of the fixation cross disappearing, the stimulus disappeared in its original location and replaced the fixation cross on the fixated position (Fig. 6.1c). Thus, at each location stimulus foveation could result from either an eye movement or the sudden appearance of the stimulus. The stimulus was presented for 1200 ms after disappearance of the fixation cross (saccade condition) or relocation of the stimulus (fixation condition), respectively. Each experimental block consisted of 480 saccade trials and 480 fixation trials, which were randomly interleaved. All subjects performed at least two pre-experimental and two experimental blocks.

Eye Tracking: Eye movements were recorded with a remote video eye tracking system using monocular pupil tracking at 500 Hz (Eyelink 1000, SR Research Ltd., Mississauga, Canada). To calibrate eye position a 13-point grid was used and the calibration procedure was repeated until the average error was below 0.5°. Saccades were defined using a velocity threshold of 30°/s, an acceleration threshold of $8000^\circ/s^2$, and a minimum deflection threshold of 0.1°.

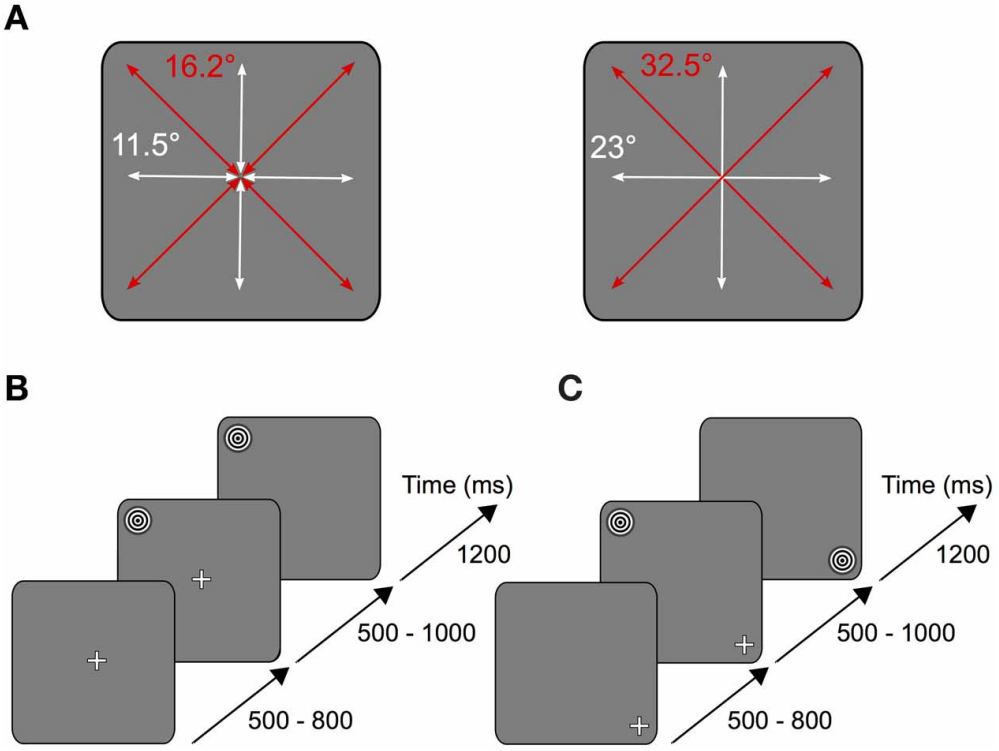

Figure 6.1: Experimental task. (A) Depending on the stimulus location relative to the fixation cross, subjects performed horizontal and vertical (white arrows) or oblique (red arrows) saccades on the screen. Left: short saccades (11.5° vertical and horizontal, 16.2° oblique) were either performed from the periphery to the center or from the center to the periphery. Right: long saccades (23° vertical and horizontal, 32.5° oblique) were performed from the periphery to another peripheral point located opposite across the center. (B) Each trial started as soon as the subject began to fixate the fixation cross located in one of nine possible locations on the screen. After a variable time of 500–800 ms the stimulus was shown in one of the other eight remaining locations on the screen. In the saccade condition the fixation cross disappeared after another 500–1000 ms, thus serving as the cue for the subject to make a saccade onto the stimulus. (C) In the fixation condition, instead of the fixation cross disappearing, the stimulus was relocated onto the position where the subject fixated.

Microsaccade detection: Using an algorithm published by Engbert and Mergenthaler (227), microsaccades were defined as intervals in which the recorded eye movements exceeded a relative velocity threshold of six median-based standard deviations for a duration of at least six samples (12 ms) and had an amplitude between 0.1° and 1°. Microsaccade detection was only performed on fixation trials that did not contain any saccades larger than 1° (according to the criteria described in "Eye Tracking").

EEG recordings: EEG-data were recorded using an ActiCap 64-channel active electrode system with a BrainAmp DC amplifier (Brain Products GmbH, Gilching, Germany). 61 of the electrodes were placed equidistantly on the scalp, one was placed on the forehead (approximately 25 mm above the nasion), and another two on the left and right infraorbital rim, respectively. The impedance of all electrodes was reduced below 5 kΩ. The data were recorded at a sampling rate of 1000 Hz and online band-pass filtered between 0.016 Hz and 250 Hz. During recording all electrodes were referenced to a nose tip electrode.

Preprocessing and analysis: All data were preprocessed and analyzed in Matlab (Mathworks) and using FieldTrip (653) and EEGLAB (185).

EEG data were down-sampled to 500 Hz in order to match the sampling rate of the eye data and low-pass filtered at 100 Hz. Eye- and EEG-data were then aligned by cutting them into trials according to the triggers that were simultaneously sent to both, the EEG and the eye tracking system. We visually inspected the EEG data and removed trials containing high amplitude noise, as it typically arises from muscle activity related to larger body movements, as well as blinks and other easily identifiable confounds such as sudden electrode drifts and jumps. Trials containing saccade-related artifacts were not excluded from analysis unless (1) they were not related to the task and exceeded 2° of visual angle in the saccade condition or 1° during fixation trials, (2) there was no stable fixation within 400 ms after the cue, or (3) they were not located in a window of 2° around the center of the stimulus. Where explicitly stated in the results section, the EEG data were re-referenced to the average activity of the 61 scalp electrodes.

Event-related potentials: For the analysis of event-related potentials (ERPs) the trials were cut into 1 s long epochs ranging from -500 to +500 ms around the event of interest (i.e., saccade on- or off-set in the saccade condition and stimulus relocation in the fixation condition). Subsequently the trials were baseline corrected to the pre-event interval and then averaged for each condition over all subjects. Deviations from this procedure will be detailed in the respective result sections.

Time-frequency analysis: Time-frequency analysis of the gamma frequency band ($>$ 30 Hz) was performed using a set of complex Morlet wavelets with a width of five cycles per frequency. The spectral estimate was obtained for frequencies ranging from 30 to 100 Hz in steps of 2 Hz.

For the analysis of the frequency bands below 30 Hz we used Fast Fourier Transform instead of wavelet analysis in order to obtain a constant frequency resolution. More specifically we segmented each trial into 200 ms long overlapping data windows, advancing in 5 ms steps from -500 to +500 ms. We then multiplied each data segment with a Hanning window before the Fast Fourier Transform was computed.

Finally, in order to obtain power changes with respect to baseline, all time-frequency bins were normalized to the average pre-stimulus power in each frequency bin and then averaged over trials and subjects.

Independent component analysis: We performed ICA to identify and extract ocular artifact components from the data. ICA is a blind source decomposition algorithm that enables the separation of statistically independent sources from multichannel data. It has been proposed as an effective method for separating ocular movement and blink artifacts from EEG data (408, 385, 366). ICA was performed using the Infomax ICA algorithm (58) as implemented in the EEGLAB toolbox (185). In order to optimize the ICA decomposition with respect to eye movement- and blink-related components, we appended the experimental data with data from a pre-experimental procedure during which each participant performed blinks and vertical and horizontal saccades within the same region of the gray screen that would later be used for stimulus presentation (see experimental procedure). Then, for each subject individually, we decomposed the preprocessed data from all 64 channels into 64 statistically independent components (ICs). To differentiate ICs that are related to eye movements and blinks from the ones produced by neural activity and other sources, we followed the procedure that is illustrated in Figure 6.2b: first we partitioned every trial into saccade and fixation epochs. Saccade epochs were defined as the time between saccade on- (Fig. 6.2b, green dotted lines) and off-set (Fig. 6.2b, red dotted lines) as given by the eye tracker. To ensure that both, spike potentials and post-saccadic eyelid artifacts were comprised by saccade epochs as well, we additionally included the intervals 5 ms before and 10 ms after saccade on- and offset, respectively. Conversely, fixation intervals were defined as the time between saccade epochs. Subsequently, for each trial, we computed the variance of the respective IC activations during saccades and during fixations (note that in Fig. 6.2 for illustration purposes we show IC ERPs instead of IC activations during single trials). If for a given IC the mean variance of saccade epochs was at least 10% higher than the mean variance of fixation epochs (i.e., $variance_{saccade}/variance_{fixation} > 1.1$), the IC was classified as eye-artifact-related and subsequently removed from the data. The threshold of 10% was introduced to avoid that components with constant variance over both, saccade and fixation epochs, might be misclassified due to random fluctuations.

Note that here we only rejected eye-artifact-related ICs, while ICs related to non-ocular artifacts (e.g., muscle activity) were not excluded from the data.

Regression: We used two different linear models for regression-based artifact correction. In both models electrooculogram (EOG) channels were used as the independent variables that convey the signal of a single artifact source for both eyes. As the movement of the eyeball with respect to the head can be explained with only two spatial components, the first model only takes vertical and horizontal EOG measurements into account: $EEG(t)_{observed} = EEG(t)_{source} + \beta_1 vEOG(t) + \beta_2 hEOG(t)$. It has been proposed that artifacts related to eyelid movement, which are independent of eyeball movement could be modeled as the third spatial component (radial) of the same single source that explains artifacts produced by eye movements (225, 167, 751): $EEG(t)_{observed} = EEG(t)_{source} + \beta_1 vEOG(t) + \beta_2 hEOG(t) + \beta_3 rEOG(t)$. For the model based on two spatial components, horizontal and vertical EOG channels were obtained using a triangular montage, consisting of one electrode on the forehead (e1) and two on the left (e2), and right (e3) infraorbital rim (751). For the three spatial components model, besides the triangular montage a left (e4) and a right (e5) temporal electrode were included to generate the radial component (225) according to $e1/2 + (e2 + e3)/4 - [(e4 + e5)/2]$.

The coefficients for both models were obtained from the eye(lid) movements in the pre-experimental periods described above. The subjects' individual coefficients were then applied to the data of the experimental conditions in order to correct eye movement-related artifacts.

Statistics: To test for statistical significance and at the same time to control for multiple comparisons, we used a cluster-based non-parametric permutation test that is described in detail in (533). The rationale behind this test is summarized as follows: if for example the difference between two ERPs yields 20 samples that reach significance (e.g., according to a t-test), they are more likely to represent a difference in neural processing when they occur adjacent in time, as compared to when they occur at 20 independent time points (which rather would suggest random fluctuations in the signal). If at the same time significant values are also observed in several neighboring electrodes, the likeliness of these values being the result of neural activity is even higher. Following this rationale, ERP differences or time-frequency differences that exceed a predefined threshold (here two standard deviations from the mean) are clustered and summed across adjacent channels, time points and, for time-frequency analysis, across frequency bins. By randomly exchanging conditions in a random subset of subjects, i.e., flipping the sign of the observed values in both conditions before averaging and clustering, an alternative observation is obtained. Repeating this procedure multiple times (n = 1000) yields a reference distribution under the null hypothesis. It now can be tested how often clusters of the observed size are expected to randomly occur under the null hypothesis. Additionally, for statistical comparisons between multiple factors we used repeated-measures ANOVA.

6.3 Results

6.3.1 Stimulus Response

We aim at investigating the impact of different types of eye movement artifacts on EEG data and evaluate the efficiency of regression and ICA-based artifact correction methods. As a reference for distinguishing neural activity from confounds

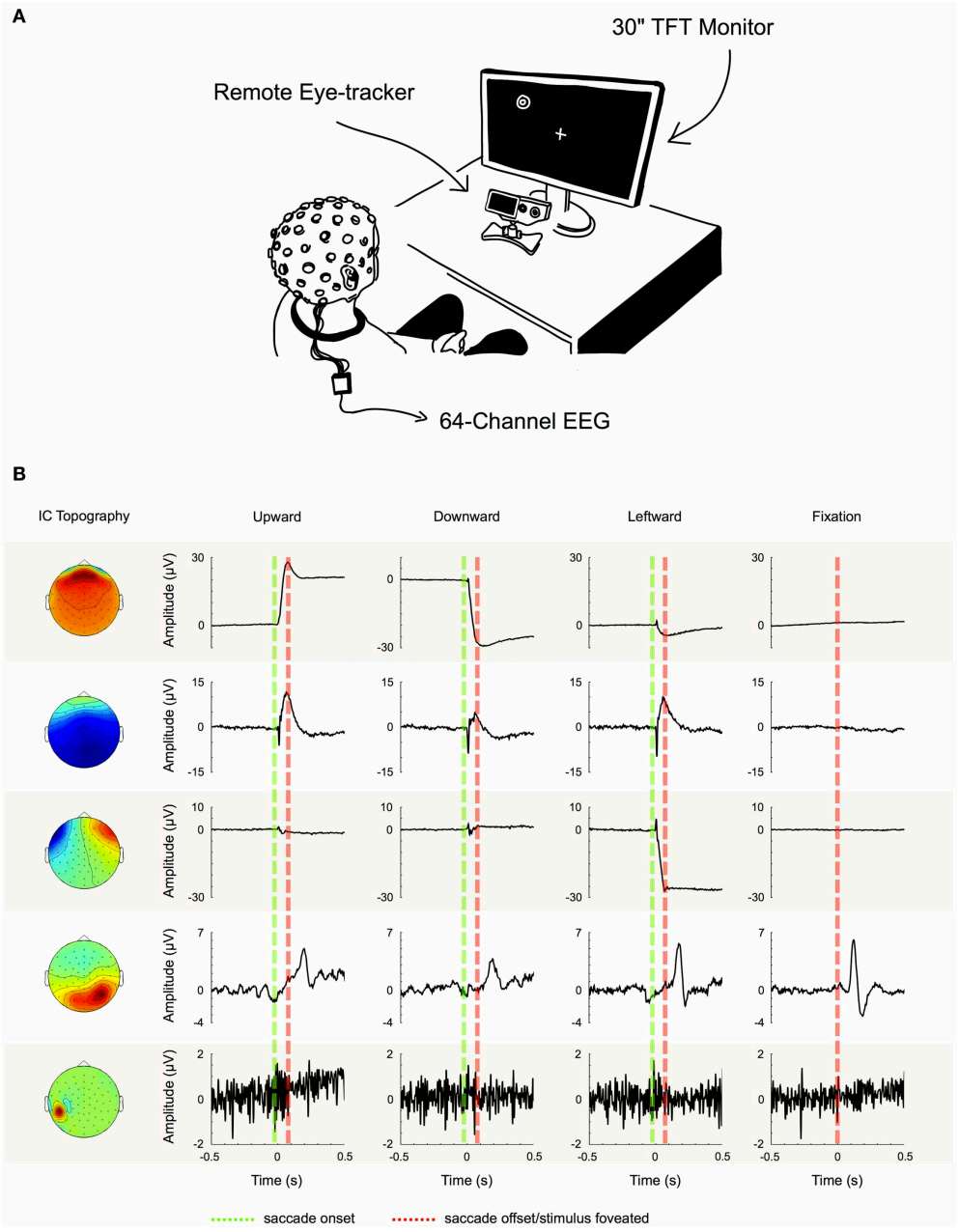

Figure 6.2: Component examples and correction procedure. (A) Experimental setup. (B) Examples of five typical IC topographies and their activations, as we found them similarly for all of our subjects. The first three ICs can be classified as eye movement-related as their activations display high variance during saccade intervals (between green and red dotted line), while being inactive during fixation periods (left and right of green and red dotted line). IC 4 on the other hand displays its largest variance during fixation. Therefore, it cannot be attributed to artifacts produced during saccade execution, but instead to neural activityin this case the time locked visual response to the stimulus. Finally, the topography and signal properties of IC 5 suggest that it emerges from muscle activity or other noise sources at one particular electrode site. The component's activity is not systematically related to saccade execution or stimulus presentation and thus displays similar variance during both, saccade and fixation intervals. Based on these observations we used the variance difference between saccade and fixation periods in each IC to objectively differentiate eye artifact-related ICs from those related to neural activity and other sources.

induced by ocular artifacts we first assessed EEG responses to a standard visual stimulus during fixation. The stimulus of choice consisted of black and white contracting rings, because they are known to generate both, a clear visual ERP and a distinct gamma band response in human EEG and MEG signals (368, 276, 452).

The results for the nose-referenced data are shown in Figure 6.3a. The average ERP over occipital electrode sites (top panel) displays a transient visual response followed by a prolonged increase in amplitude, which lasts throughout

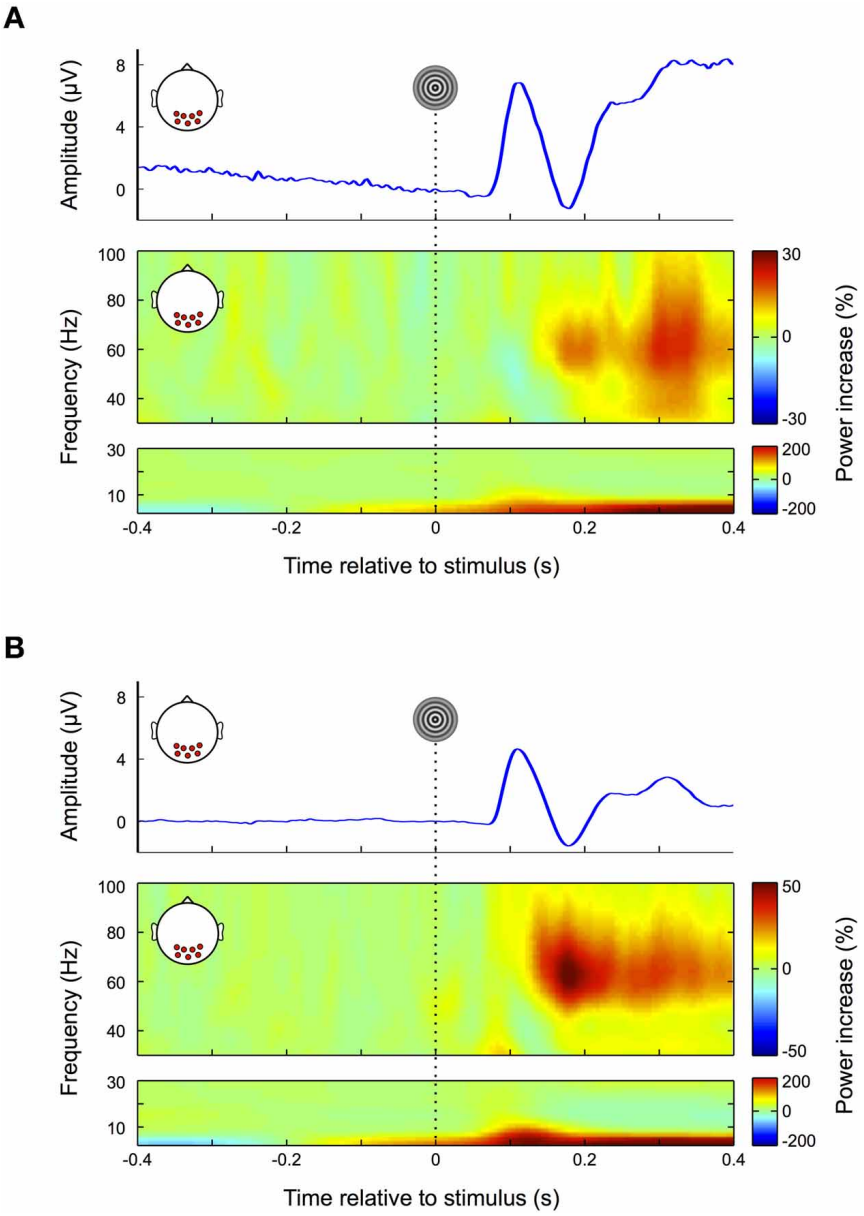

Figure 6.3: Visual response. (A) Nose-referenced data. During fixation trials the average ERP over occipital electrode sites displays a clear visual response (upper panel), i.e., an early transient response, followed by a prolonged increase in amplitude. In the gamma frequency range (30–100 Hz, middle panel) power increases from about 180 ms until the end of the trial. Unlike similar responses in earlier studies at source level the power increase here is not restricted to a defined frequency band over its whole time course but also spreads over the whole gamma range in the later portion of the trial. The power increase in the lower frequency range (0–30 Hz, lower panel) broadens in bandwidth coinciding with the transient response in the ERP. (B) Average-referenced data. Similar to (A) the ERP displays an early transient and later prolonged response; however, the signal is smoother with lower amplitudes (upper panel). Compared to the nose referenced data, the prolonged response in the gamma frequency band is now more pronounced and confined to a relatively narrow frequency range (middle panel). Similarly the early visual response in the low frequencies is more pronounced.

the remainder of the trial. The slow signal drift observed prior to stimulus onset is most likely due to eye movements in previous trials, which due to the high-pass properties of the recording system cause the signal to slowly drift back toward its initial value. We observed a steady increase in power for frequencies below 5 Hz (Fig. 6.3a, bottom panel), which reflects the general positive trend of the signal over the whole trial (see also Fig. 6.3a top panel). Between approximately 80–160 ms a peak in the alpha range (8–14 Hz) appears to be partially occluded by the lower frequency power increase. Due to its time and frequency range this alpha peak can be attributed to the transient visual response in the ERP. In the

gamma band (Fig. 6.3a, middle panel) power increases up to 20% with respect to baseline (<0 ms). In accordance with previous findings the early (150–250 ms) and the late part (380–400 ms) of this response are confined to a frequency range between ∼50–80 Hz. However, in the time interval between 250 and 380 ms the bandwidth of the power increase broadens and expands over entire gamma frequency range (30–100 Hz).

As this latter finding differs from earlier studies using MEG, ICA, and invasive animal recordings (368, 276, 452) we average-referenced the data to make it more comparable to these reference free methods (630). The results are shown in Figure 6.3b: the slow signal drift in the ERP disappears and the peak amplitude of the early visual response is decreased (Fig. 6.3b top panel). Moreover, the early visual response becomes more pronounced in the low frequencies (<30Hz) (Fig. 6.3b bottom panel) and extends to the lower gamma frequency range (<40 Hz, Fig. 6.3b middle panel). Similarly the prolonged gamma band response is substantially increased and confined to a well-defined frequency range that is in concordance with earlier studies using source level analysis (368, 276, 452). As a result the visually evoked gamma increase now becomes distinguishable from the transient and broadband increase in gamma activity ($\sim 30 - 100$ Hz; see also section "Microsaccades") that is observed in association with fixational eye movements (276, 954).

6.3.2 Corneo-retinal dipole movement

Large ocular movements result in prominent transients and off-sets in the EEG signal. These are caused by an orientation change of the eyeball and thus of the corneo-retinal dipole produced between the negatively charged retina and the positively charged cornea. The impact of corneo-retinal dipole changes on the EEG signal is illustrated in Figure 6.4.

Figure 6.4a shows the ERPs for small (∼11.5°, gray traces) and large (∼23°, black traces) vertical saccades measured at a mid-frontal electrode (Fig. 6.4a inset, red circle). Figure 6.4b shows the same for saccades in the horizontal axis when measured at a right temple electrode (Fig. 6.4b inset, red circle). Depending on whether the cornea moves toward or away from the electrode the signal displays prominent positive and negative offsets, respectively. Within the investigated range, the relationship between movement size and corneo-retinal dipole offset is roughly linear, that is doubling saccade size results in a signal offset of twice the amplitude. Offset topographies are presented in the right column of Figures 6.4a and 6.4b, which illustrate the offset amplitude for different movement directions across the scalp normalized to the mid-frontal (vertical movements) or right temple electrode (horizontal movements). If linearity holds for all electrode sites, the only difference between saccades in the same direction but of different sizes should be in signal amplitude, while the general topographic pattern (i.e., the normalized topography) should stay the same. A direct comparison using a cluster-based permutation test did not reveal any significant differences between the normalized topographies of small and large saccades ($p > 0.05$, Fig. 6.4c, middle and left column). Thus, the relationship between saccade size and signal offset can be considered linear over all electrode sites.

To compare movements of the same size but opposite horizontal directions, we mirrored the topographies of leftward saccades along the midline and subtracted them from the topographies of rightward saccades. Again, we did not observe significant topographic differences (Fig. 6.4c, upper right). In the vertical dimension, however, a change in movement direction results in a significant difference in voltage, which extends over all electrode sites ($p < 0.05$, Fig. 6.4c bottom right).

6.3.3 Eyelid-induced artifacts

Blinks occur spontaneously or can be elicited at will. During blinking the eyelid slides down over the cornea, which is positively charged with respect to the forehead. Thereby the lid acts like a "sliding electrode," short-circuiting the cornea to the scalp and producing artifacts in the EEG signal (43, 547, 16, 502, 503). Blink artifacts are easy to identify even in raw data and show a topographic distribution mostly over frontal electrodes. As shown in Figure 6.5a and demonstrated in earlier studies (e.g., 502, 503), their amplitude differs ($p < 0.01$) between voluntary blinks (obtained from the pre-experimental procedure)

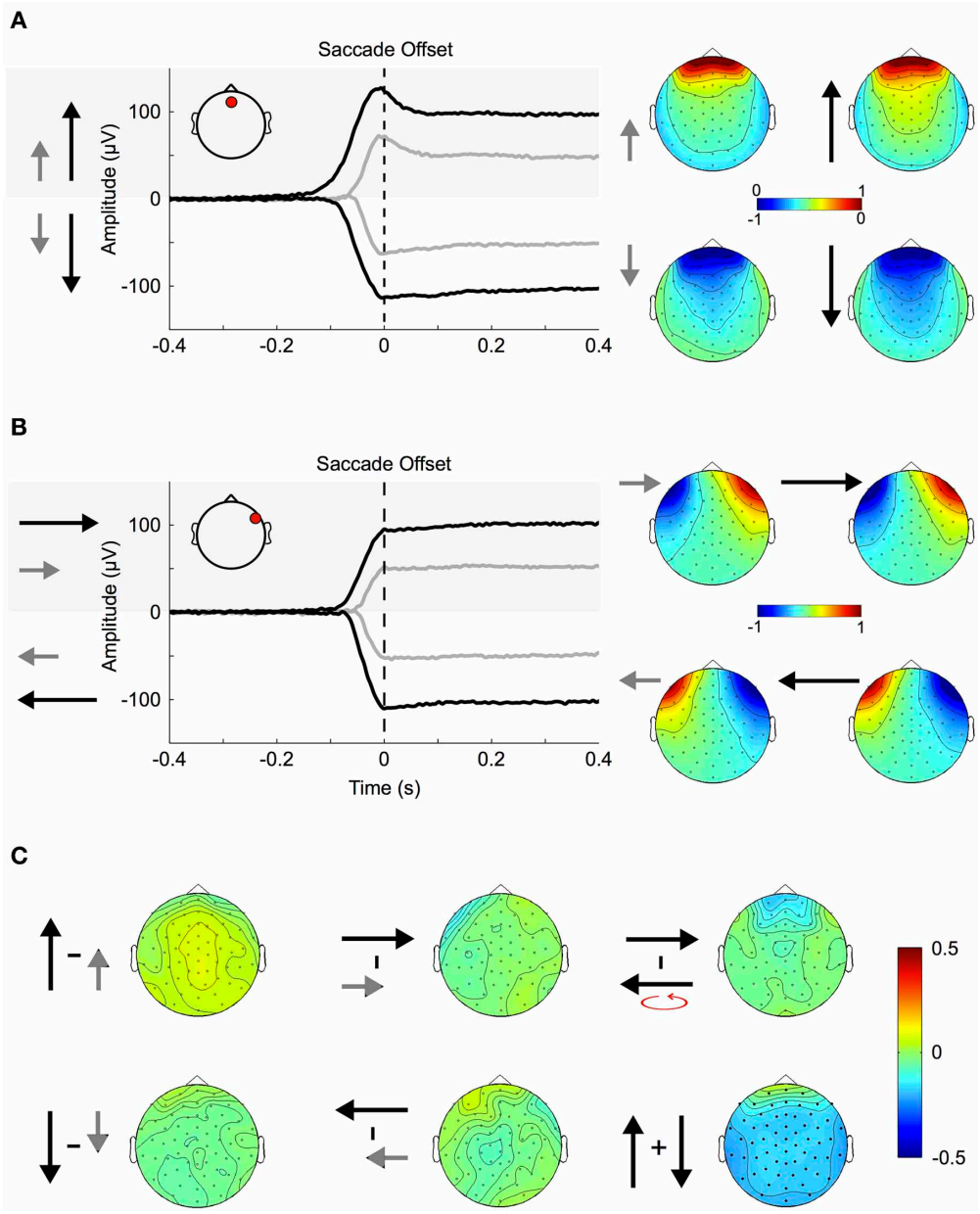

Figure 6.4: Corneo-retinal dipole offsets. (A) Left: ERPs during small (gray traces) and large (black traces) up- and downward saccades as measured at a fronto-central electrode (inset, red circle). The traces show that amplitude and duration of corneo-retinal dipole offsets scale about linearly with saccade size. Right: The normalized topographies during small and large saccades. (B) Small and large horizontal saccades. Same conventions and results as in (A). (C) Topographic differences between different types of saccades: The normalized topographies of small and large saccades in the same vertical (left column) and horizontal (middle column) direction do not display any significant differences, indicating that the linear relationship between saccade size and signal offset holds for all electrode sites. The same is observed for horizontal movements of the same size but opposite directions (right column, top). In the vertical dimension, however, downward saccades produce a significantly larger offsets than upward saccades of the same size (right column, bottom; significant electrodes marked by bold black dots).

and spontaneous blinks (obtained from excluded trials of the main experiment), while their normalized topographies, and thus their propagation factors onto the scalp, do not (Figs. 6.5a and 6.5b).

Although blink artifacts are well-known in cognitive research, other eyelid induced artifacts occurring during and after saccades are often neglected. As illustrated in Figure 6.4 during upward saccades, the corneo-retinal dipole offset reaches its maximum when the saccade ends (time 0 ms, = fixation onset). However, after this offset change, a smaller second change of opposite polarity can be observed. This latter change exceeds saccade duration and it is known to be produced

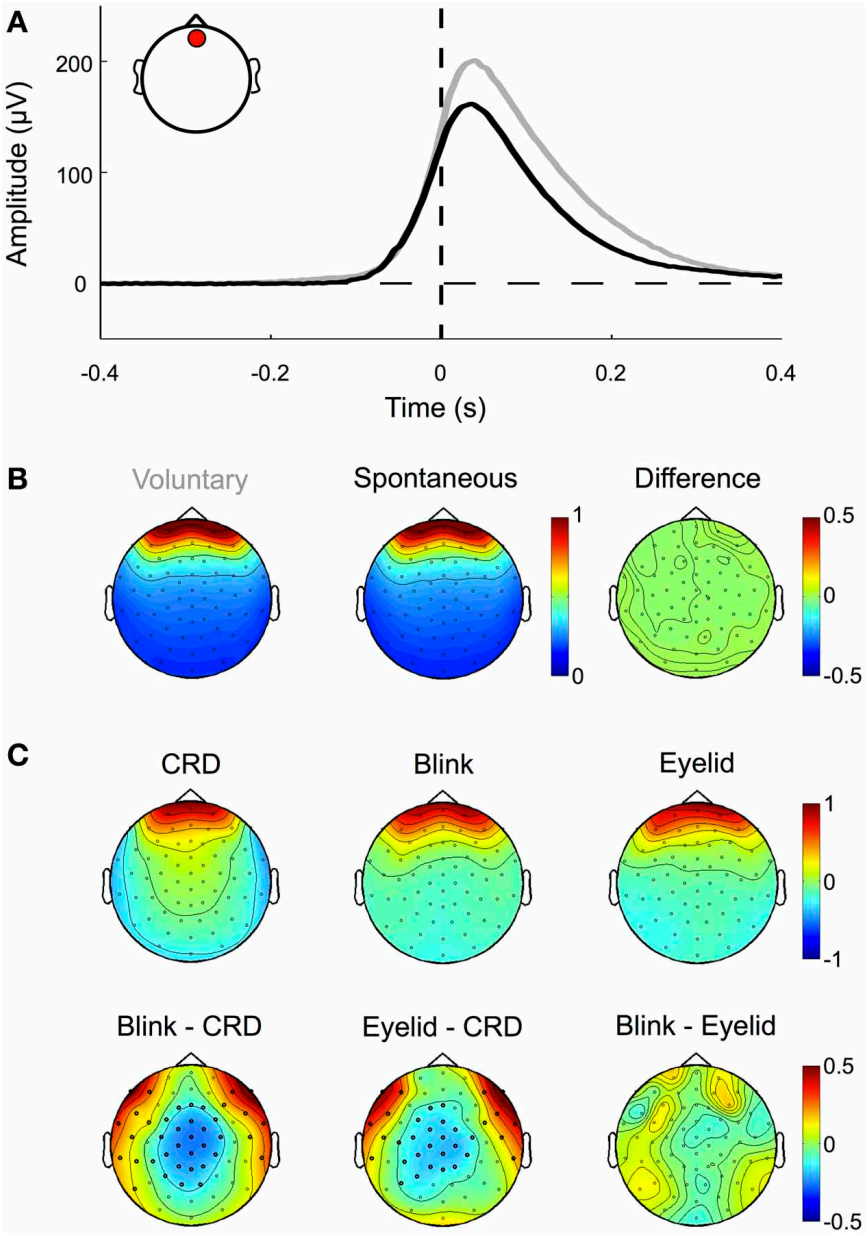

Figure 6.5: Eyelid-induced signal changes. (A) ERP traces for voluntary (gray) and spontaneous (black) blinks measured at a frontal electrode (inset, red circle). Voluntary blinks are of longer duration and result in higher amplitudes than involuntary blinks. Note that blink onset as defined by the eye tracker (time 0, vertical dashed line) corresponds to the point at which the pupil is not visible anymore. The actual eyelid movement already starts around 100 ms earlier, when the signal deflects from the zero line (horizontal dashed line). (B) Although spontaneous and voluntary blinks differ in amplitude and duration, they share the same topographic pattern (i.e., the normalized amplitude distribution across the scalp). (C) Topographic patterns of corneo-retinal dipole offsets related to upward saccades, blinks, and post-saccadic eyelid movements (upper row) and the differences between them (lower row). Bold black dots indicate electrode sites with statistical significant differences. The results show that corneo-retinal dipole offsets produce a topographic pattern that differs from both, blinks and post-saccadic eyelid movements, while no differences were found between the latter two. This suggests that blinks and post-saccadic eyelid movements are produced by the same electrophysiological source.

by eyelid movements that go along with the saccade [43, 137]. More specifically, saccades are accompanied by ballistic eyelid movements, so called eyelid-saccades, which occur in synchrony with the rotation of the eyeball and therefore are not distinguishable from the corneo-retinal dipole offset in the raw data. In other words, during upward saccades for instance, eyelid and eyeball move upwards with approximately the same speed. However, after the termination of both, eye- and eyelid saccades, the eyelid continues to slide more slowly for another 30–300 ms and produces a signal change

that is observable particularly after upward saccades (43, 53). In contrast to eyelid artifacts that co-occur with the saccade, this post-saccadic signal change, although well-established in ophthalmology, is rarely mentioned or described in relevant publications in cognitive sciences (cf. 430, 201).

To confirm previous findings and to investigate how this post-saccadic eyelid artifact affects our data, we compared the difference between the signal amplitude measured at a frontal electrode (see inset Fig. 6.4a) at the time of saccade offset and the signal amplitude at the same electrode but 100 ms later, when the eyelid-induced signal change has reached its final level (as for example seen in Fig. 6.4a). A Two-Way repeated-measures ANOVA (three movement types: periphery to center, center to periphery and periphery to periphery; four movement directions: up, down, left, and right) revealed that amplitude differences between saccade offset and eyelid offset depend on both, movement type (F = 25.63, $p < 0.001$) and movement direction (F = 42.47, $p < 0.001$). We observed significant amplitude differences between long and short saccades ($p < 0.001$) and found that eyelid-induced amplitude changes were significantly larger ($p < 0.01$) for upward saccades than for all other movement directions. Together with the finding that there is an interaction between type and direction of the movement (F = 2.55, $p < 0.01$) this confirms earlier reports that eyelid-induced amplitude changes are most prominent after upward directed eye movements (see also Fig. 6.4a, 43, 53).

Next, we compared the normalized topographies of blink artifacts, corneo-retinal dipole offsets and post-saccadic eyelid artifacts. As blink- and saccade-related eyelid artifacts are produced by the same mechanism, namely the eyelid sliding over the cornea, their activity projects to the scalp with the same topographic pattern (Fig. 6.5c). Topographies related to corneo-retinal dipole offsets on the other hand differ from both, those of blinks and those of post-saccadic eyelid movements, with significant differences clustered around the central and fronto-lateral regions ($p < 0.05$, Fig. 6.5c). Effectively these results indicate that eyelid induced artifacts and corneo-retinal dipole offsets arise from two different electrophysiological mechanisms that cannot be modeled as a single source.

6.3.4 Spike Potential

In early studies the saccadic spike potential has been described as a "monophasic potential appearing just before saccade onset" (849). However, concordant with earlier studies (718, 614, 430), high-pass filtering the data at 10 Hz and thereby removing corneo-retinal dipole offsets reveals that the saccadic spike potential actually displays a biphasic waveform, starting around 5 ms prior to saccade onset and consisting of a larger positive deflection followed by a smaller negative deflection (Fig. 6.6). Note that in the present study, as compared to the above-mentioned ones, the polarity of the waveform is inverted. This is because we describe the properties of the saccadic spike potential at scalp electrodes rather than at EOG channels (430) and because we used a nose reference, while other studies referenced to an electrode attached to the temporal bone (849, 718). Since in the unfiltered data the negative deflection of the saccadic spike potential is largely occluded by the corneo-retinal dipole offset (Fig. 6.6, insets) the following analysis will only focus on the positive peak of the saccadic spike potential.

To investigate amplitude and topography of the saccadic spike potential for saccades of different sizes and directions, we relate the data to a 5 ms baseline before the onset of the spike potential (i.e., -10 to -5 ms relative to saccade onset). Figure 6.7a shows the topography of the positive peak of the spike potential averaged over all saccade directions. When the data is average-referenced, the topographic pattern stays the same while the magnitude is shifted from central-parietal electrodes to electrode sites surrounding the eyes (Fig. 6.7a, 430). For the remainder of the analysis of saccadic spike potentials we used nose-referenced data exclusively.

To compare the topographic pattern of spike potentials between eye movement directions we normalized the respective topographies to the maximum amplitude over all saccade directions. The difference between spike potentials accompanying up- and downward saccades shows that during upward saccades at almost all electrodes the measured potential is significantly lower ($p < 0.05$) than during downward saccades (Fig. 6.7b, left). A possible explanation is that at the onset of a downward saccade the eye, and thus the positive pole of the corneo-retinal dipole, is directed upward, conse-

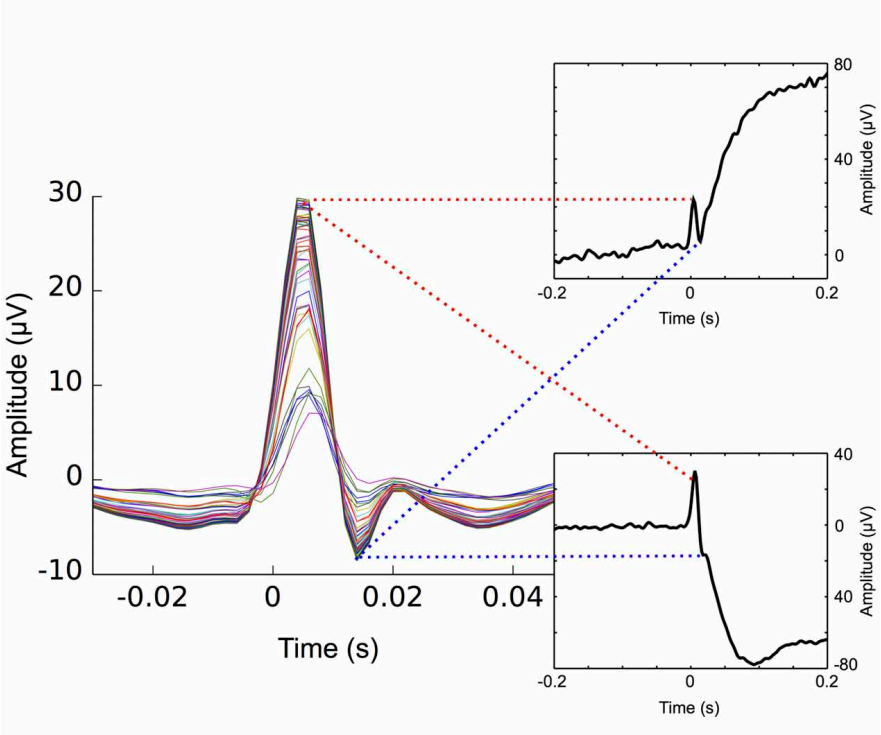

Figure 6.6: Saccadic spike potential. After removal of the corneo-retinal dipole by high pass filtering the data at 30 Hz, the spike potential displays a biphasic shape at all scalp electrodes (colored traces). Without filtering the ERP traces for up- (upper inset) and downward (lower inset) saccades show that the negative deflection of the spike potential is largely occluded by the manifold larger corneo-retinal dipole offset.

quently leading to a more positive topography as compared to the onset of upward saccades where the positive pole of the corneo-retinal dipole is initially directed downwards. This is also supported by the observation that topographic differences between left- and rightward saccades become significant ($p < 0.05$) at electrodes around the eyes and thus close to the corneo-retinal dipole (Fig. 6.7b, middle). We found no differences between the topographic patterns of ipsi- and contralateral saccades (i.e., the topography of leftward saccades versus the horizontally flipped topography of rightward saccades, Fig. 6.7b, right).

Next we compared how the amplitude of saccadic spike potentials changes depending on the type of eye movement. Figure 6.7c shows the respective amplitudes and topographies for different saccade sizes, directions and initial eye positions, that is up-, down-, left- and rightward saccades performed from the periphery to the center, from the center to the periphery and from the periphery to the opposite peripheral region (i.e., long saccades). For each of these classes we determined the highest peak at central-parietal electrodes during a time period ranging from -5 to +10ms relative to saccade onset. A Two-Way repeated-measures ANOVA revealed that the amplitude of the saccadic spike potential depends on both direction (F = 13.05, $p < 0.001$) and type of the movement (F = 29.06, $p < 0.001$). It significantly differs between vertical and horizontal saccades ($p < 0.05$, Bonferroni corrected) and movements within the vertical dimension (i.e., upward and downward saccades, $p < 0.001$), but not between left- and rightward saccades. The amplitude of saccadic spike potentials has been shown to increase non-linearly with saccade size up to 1.28°before reaching its final maximum [(21)]. However, as saccade sizes in our experiment exceeded this threshold, we did not expect any amplitude differences between spike potentials related to long ($\sim$23°) and short ($\sim$11.5°) saccades. But interestingly the amplitudes observed for short saccades from the center to the periphery were significantly different from those accompanying long saccades ($p < 0.001$). This difference, however, cannot be attributed to saccade size, as it was not observed between long saccades and short saccades from the periphery to the center.

To check whether this rather surprising finding could be a result of filter-induced slow signal drifts in the recording, as

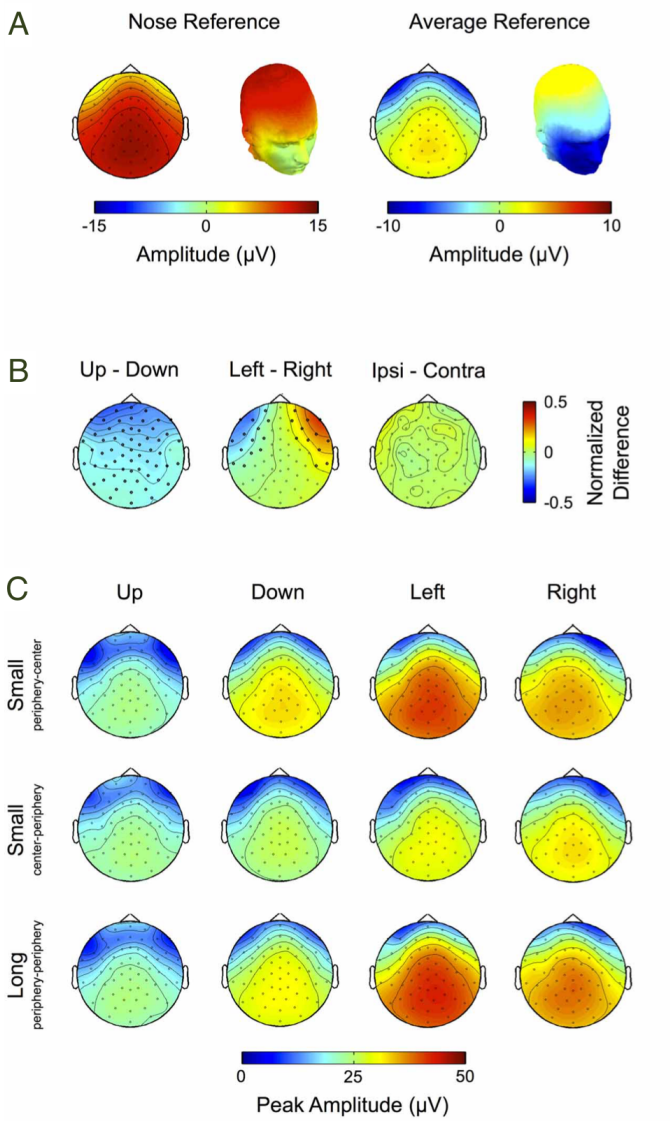

Figure 6.7: Saccadic spike potential. (A) Average referencing reduces the amplitude of the spike potential at scalp electrodes and leads to increased negativity around the eyes. (B) Differences of topographic patterns for spike potentials related to saccades in the same axis but opposite directions. Comparing spike potentials related to up- and downward saccades of the same size results in significant amplitude differences at almost all scalp electrodes, indicating that downward saccades produce higher spike potential amplitudes. The difference between left and rightward saccades yields significant values at electrode sites close to the eyes. However, no significant differences were found between spike potentials related to ipsi- and contralateral saccades, suggesting that the topographic differences for saccades with the same size and along the same axis may be not so much related to the spike potential's amplitude itself but rather to eye position (i.e., the direction of the corneo-retinal dipole) before saccade onset. (C) Spike potential topographies for different saccade directions (columns) and sizes (rows). A two-way ANOVA reveals that peak amplitudes of the spike potential are higher for down- than for upward saccades while they are not significantly different between left and rightward saccades. Smaller saccades from the periphery to the center result in higher spike potential amplitudes than saccades of the same size but performed from the center to the periphery. Surprisingly saccades from the periphery to the center do not show significant differences to long saccades (i.e., saccades performed from the periphery across the center to another peripheral location). This indicates that the peak amplitude of spike potentials may depend on initial eye position, rather than on saccade size.

described above (i.e., saccades to peripheral screen positions are generally larger and therefore might produce larger drifts when the signal returns back to baseline), we repeated the analysis after high pass filtering the data at 10 Hz, and in this way eliminating such drifts. However, using filtered data yielded the same results as using unfiltered data. This suggests that for saccades larger than $\sim$11.5° the amplitude of the saccadic spike potential depends on the initial eye position, rather than on saccade size per se.

6.3.5 Microsaccades

Microsaccades are small eye movements that occur during fixation. They distinguish themselves from regular saccades not only in amplitude but also in that they are performed involuntarily.

In the fixation condition we detected a total of 4252 microsaccades over all trials and subjects, which corresponds to an average of 1.07 microsaccades per trial. Note that although sometimes other or additional criteria (e.g., larger or smaller amplitude range, involuntary performance etc.) are applied, here we defined all eye movements with amplitudes between 0.1 and 1° of visual angle as microsaccades. To ensure that the detected movements were indeed microsaccades and not noise in the eye movement recordings, we investigated the relationship between their amplitude and velocity. In agreement with previous descriptions (539), the microsaccades detected in our data follow a linear relationship when plotted on a log-log scale (i.e., the "main sequence," Fig. 6.8a).

Microsaccades typically occur with a frequency of 1–2Hz (227). The probability of their occurrence, however, is not equally distributed over time but follows a typical temporal pattern with respect to stimulus onset: after stimulus presentation their rate initially decreases to its minimum at around 150 ms. Thereafter it rapidly increases again reaching its maximum at about 350 ms (226, 200). When we investigated the distribution of microsaccades over all fixation trials and all subjects, we found that it matched this pattern very closely (Fig. 6.8b).

To study the impact of microsaccades on the EEG signal, we segmented the data into epochs time-locked to microsaccade onset. The ERP of these epochs displays the same biphasic waveform as the saccadic spike potential of larger saccades, although its amplitude is substantially smaller (Fig. 6.8c). In the time-frequency analysis of our data this pattern manifests itself as a transient burst between 40 and 100Hz (Fig. 6.8d), which is in concordance with earlier studies (954, 430). Altogether these findings confirm, that microsaccade-induced confounds in the EEG are mainly caused by spike potentials occurring at microsaccade onset, while orientation changes of the corneo-retinal dipole only play a minor role.

6.3.6 Artifact correction

In order to evaluate the efficiency of different approaches to eye artifact correction we compared the performance of a two and a three component regression model (225, 751) and ICA (408).

In order to objectively distinguish eye movement-related from non-eye-movement-related ICs we employed a selection procedure based on eye tracking information. More specifically, we compared every IC's activation during saccade and fixation periods. If the respective IC displayed a higher activation during saccades than during fixation, it was classified as eye movement-related and rejected from the data (see section "Independent Component Analysis" and Fig. 6.2 for more details). Following this procedure we found between 3 and 11 artifactual ICs for each subject, accumulating to a total number of 74 (out of 896) rejected ICs.

To test how well the automated selection algorithm performed in comparison to visual selection by experienced researchers, we asked two independent experts to tag all ICs in our data that they considered as eye movement-related. The classification was done in three steps: (1) we asked both experts to identify eye movement-related ICs solely based on their respective topographies. Over all subjects and components, Expert 1 classified 36 ICs as eye movement-related, while Expert 2 identified 41 ICs as related to ocular artifacts. (2) Next we asked the experts to repeat their evaluation but this time based on both, the ICs' topographies and their activations during three example trials, each of which contained an eye movement in a different direction (up, down, and left). Given the additional information about the ICs' activations, Expert 1 rated 16 additional ICs as eye movement-related. Similarly, Expert 2 tagged 16 more ICs as eye artifacts but additionally revised his previous judgment about four components, which he removed from his selection. Now, in total 52 ICs were tagged by Expert 1 and 53 ICs by Expert 2. Notably, apart from the one additional IC identified by Expert 2, both experts' selection of eye movement ICs was identical. This strongly suggests that including IC activations as a decision criterion leads to a substantial improvement in effectiveness and reliability of IC classification. (3) In a last step we determined all ICs that had a variance ratio (i.e., variance of saccade intervals vs. variance of fixation intervals; see

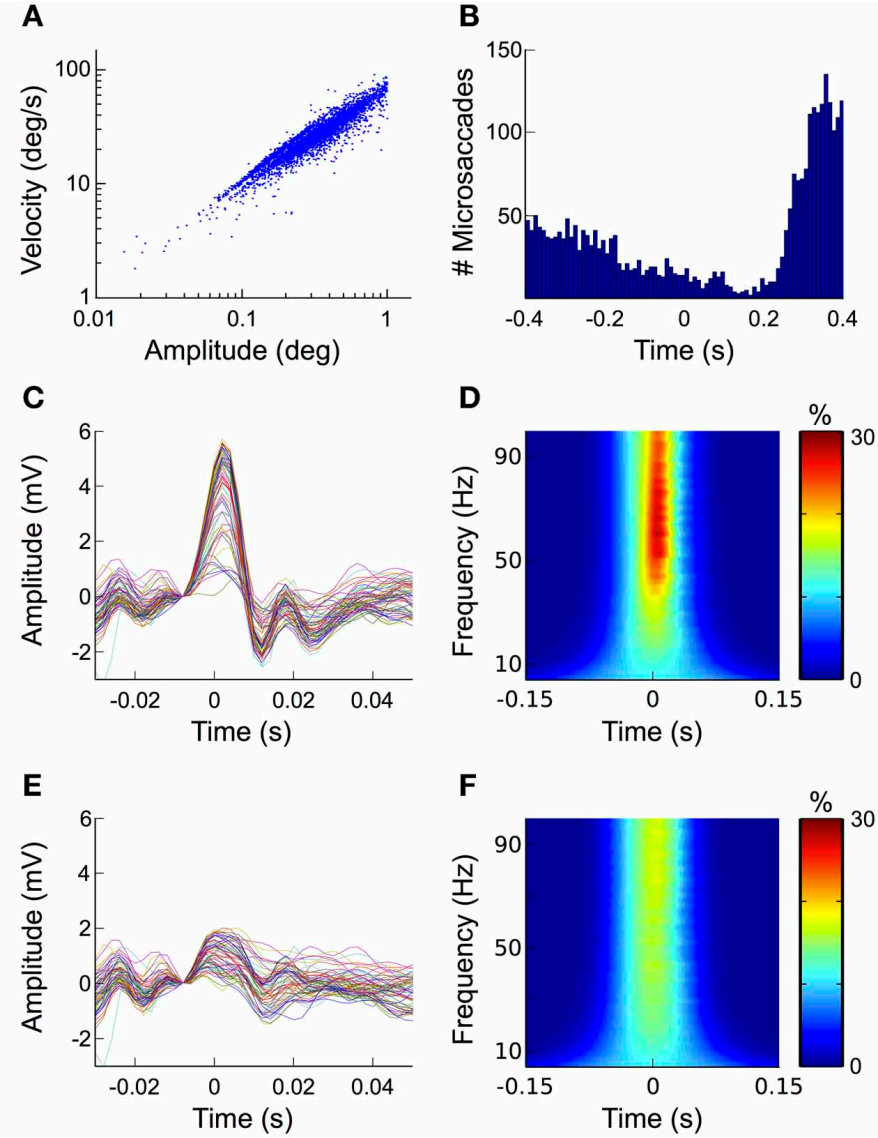

Figure 6.8: Microsaccades. (A) Mainsequence. Plotting microsaccade amplitudes against microsaccade velocities results in a straight line on a log/log scale (i.e., the main sequence). This relationship is a signature for ballistic eye movements, thus confirming the physiological origin of the microsaccades detected here. (B) Histogram of the microsaccade distribution over all fixation trials. After stimulus onset the frequency of microsaccades decreases, followed by a rebound starting at around 200 ms and peaking 370 ms after stimulus onset. (C) ERP aligned to microsaccade onset. At scalp electrodes microsaccades display a similar biphasic pattern as the saccadic spike potential, suggesting that the most prominent contribution of microsaccades to the signal measured on the scalp is produced by spike potentials going along with eye movement. (D) Time-frequency signature of microsaccades. The sharp peak of the microsaccade-related spike potential results in a transient broadband power burst that spans over the entire gamma frequency range (30–100 Hz). (E) Reduction of microsaccade-related artifacts in the time domain. The ICA-based correction procedure proposed here diminishes the microsaccade-related spike potential to about one third of its original amplitude. (F) Reduction of microsaccade-related artifacts in the frequency domain. Corresponding to what was observed for the ERP, the correction procedure substantially reduces the spike potential-related frequency signature in the gamma band.

section “Independent Component Analysis” and Fig. 6.2) above one and that the respective expert had not tagged as eye movement-related before. For these ICs, next to their topographies, we now provided the activations during all available saccade trials and again asked the experts to classify them as either eye movement-related or unrelated. Now having a large number of trials available, Expert 1 tagged another 16 ICs and Expert 2 another 15 ICs. Thus, in total both experts rated 67 ICs out of 896 as eye movement-related and their assessment was now perfectly congruent.

Out of the 67 ICs identified by human scorers, 64 ICs were also detected by the automated selection procedure. Additionally the algorithm tagged 7 ICs that did not conform to the experts’ assessment. However, as 6 of these 7 ICs

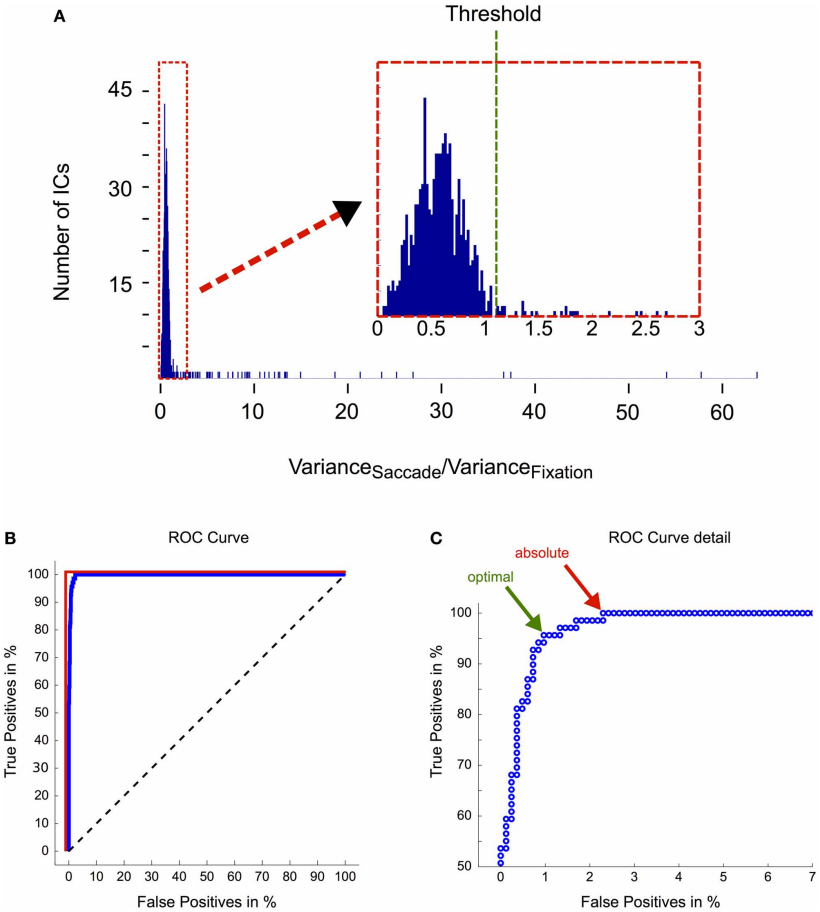

Figure 6.9: Evaluation of the IC selection procedure. (A) Distribution of saccade/fixation variance ratios. The magnification in the inset illustrates that the ratios are not clearly bimodally distributed. Therefore the threshold that optimally separates eye movement-related ICs from non-ocular ICs is difficult to determine. Based on heuristics, that is after inspecting IC activations that had a ratio above one and that we considered likely to be eye movement-related, we set the threshold to a ratio of 1.1. (B) ROC analysis. ROC curves are graphical illustrations of how well two different classes (here: eye movement-related ICs vs. non-eye movement-related ICs) can be separated depending on the threshold of the discrimination criterion (here: the ratio between the variance in saccade and fixation intervals). Each point on the blue curve represents the saccade/fixation variance ratio of one IC starting with the highest (63.71) in the lower left corner and ending with the lowest (0.04) in the upper right corner. If ICs could be unequivocally separated into being eye- or non-eye-related solely based on their variance ratio, lowering the threshold would include more and more eye movement ICs (as determined by expert tagging) until a true positive rate of 100% is reached. Subsequently by further lowering the threshold more and more non-eye movement-related components would be included in the selection. In this case the blue curve would be identical with the red line. Conversely, if the variance ratio would not provide any information about the IC's relation to eye movements, the blue curve would follow the black dashed line. The area under curve (AUC), which is obtained by computing the area between the blue and the black dashed line, quantifies how well eye movement-related ICs are separated from other ICs only based on their saccade/fixation variance ratio. An AUC value of 1 indicates perfect discrimination and a value of 0.5 indicates random performance. Here we observed an AUC value of more than 0.99. (C) ROC curve detail. The green arrow indicates the the optimal threshold for separating the ICs into two classes. It is given by the point at which further lowering the threshold would include more false positives than true positives. Here it has a value of 1.11 and is thus very close to our pre-determined threshold. The red arrow indicates the threshold at which all eye movement-related ICs are included in the selection. The corresponding ratio is 0.99.

were from only one subject and their topographies peaked in neighboring regions of the scalp, we assume that these 6 ICs may have entered the selection due to unusual activity and/or noise in this particular subject's data.

For further quantification of the algorithm's efficiency and to test the adequacy of the pre-determined ratio threshold of 1.1 (Fig. 6.9a), we performed a receiver operating characteristic (ROC) analysis (Fig. 6.9b; see figure captions for a description of the method), where ICs tagged by human experts served as reference (true positives). We observed an area under curve (AUC) value of more than 0.99, which indicates that eye movement-related ICs are almost perfectly separable from other ICs solely based on their saccade/fixation variance ratios. The optimal threshold for this separation is defined by the point at which further lowering the threshold would include more false positives than true positives and is indicated by the green arrow in Figure 6.9c. The respective saccade/fixation variance ratio at this point is 1.11 and the following one (i.e., the first suboptimal threshold) has a value of 1.06. This means that the pre-determined threshold of 1.1 turned

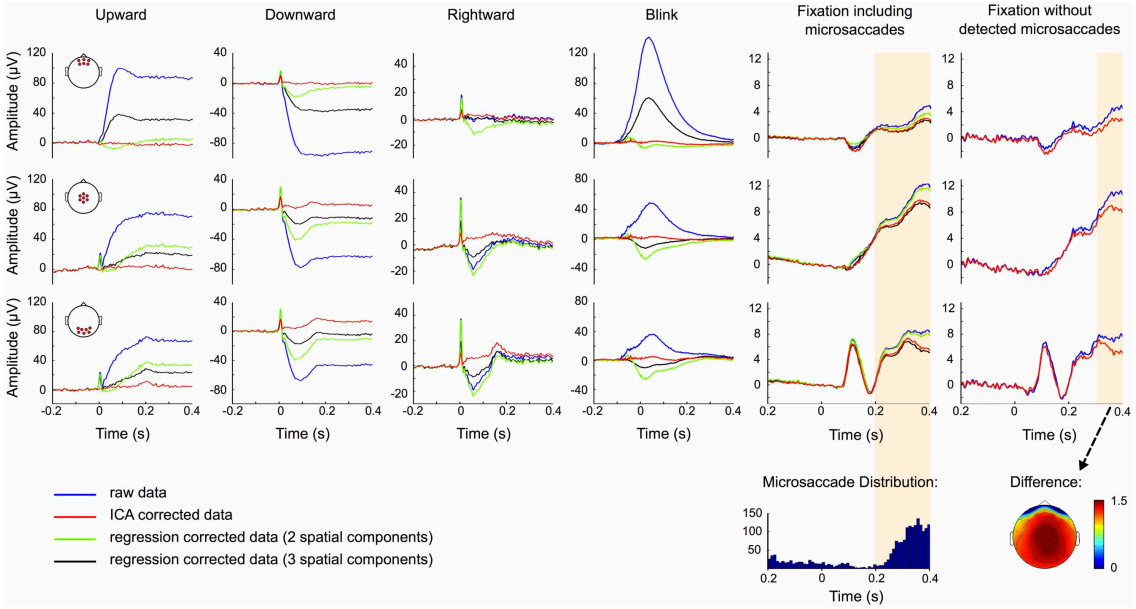

Figure 6.10: ERP correction. ERP traces for uncorrected data (blue), data corrected based on two (green) and three (black) component regression models and ICA corrected data (red). Rows show the ERPs measured at frontal (top), central (middle), and occipital (bottom) scalp locations and the red circles in the head plots on the left indicate the respective electrode sites. Columns correspond to up-, down-, and rightward saccades, blinks and fixation trials with and without detected microsaccades, respectively. Time 0 represents saccade and blink onset as determined by the eye tracker and stimulus presentation in fixation trials. The traces suggest that regression tends to over- or under-correct the data. ICA on the other hand efficiently removes corneo-retinal dipole offsets and eyelid artifacts, while the visual response is still clearly seen in occipital channels. However, ICA fails to entirely remove the spike potential at saccade onset but still reduces it substantially. In the fixation condition including microsaccades the raw and the ICA corrected data display significant differences (shaded area) in the time interval after 198 ms, but the distribution of microsaccades over all trials (bottom row) suggests that a significant portion of these differences can be attributed to the reduction of microsaccade-related artifacts. This is supported by the observation that in fixation trials without detected microsaccades, the difference between raw and ICA corrected data is smaller and only becomes significant after 278 ms. The topography of this difference resembles the one of the saccadic spike potential and may therefore be related to undetected microsaccades.

out to be chosen optimally for the dataset presented here.

Since it is not possible to measure uncontaminated neural activity with EEG, the validation of correction procedures is always suboptimal (167, 168). Simple inspection of corrected raw data by expert scorers as used elsewhere (408, 405, 751) might be insufficient, as small residuals of artifacts may be not noticeable in the raw signal. Averaging over many trials however increases the signal-to-noise ratio and thus facilitates the detection of such residuals. For this reason we evaluated correction performance based on the ERP and the time-frequency response, both time-locked to the saccade.

The results of ERP correction by using 2 (green traces) and 3 (black traces) model regression and the proposed ICA-based procedure (red traces) are shown in Figure 6.10. artifact correction by regression fails to completely remove the offset produced by eye movements or blinks. In any case, apart from spike potential suppression, the correction by the regression model with two spatial components performs better than the one with three spatial components. This probably reflects an excessive introduction of correlated neural activity to the EOG measurements due to the use of temporal channels for the calculation of the axial component of the model. Because regression coefficients were obtained in a period including both eye movements and blinks, regression fails to entirely remove offsets because the regressors that are fit to the data are based on both, corneo-retinal dipole off-sets and eyelid artifacts. As a result the weights that are assigned to each electrode for all movement directions constitute a compromise between these two artifacts. For more posterior channels (Fig. 6.10, 2nd and 3rd row) this results in over-correction for blinking and under-correction for saccades, as blink peaks propagate less to the back than saccade offsets do (see Fig. 6.5c).

ICA on the other hand independently removes both, corneo-retinal dipole offsets and eyelid artifacts, and thus accounts for the fact that their relative contribution to the measured signal varies for different movement directions. However, except for upward saccades ICA failed to entirely remove the spike potential at saccade onset, but nevertheless reduced it by about 75% depending on saccade size and direction (Fig. 6.10, red traces). The visual response is still clearly seen

in occipital channels but due to variations in saccade duration it does not display its distinctive shape (see Fig. 6.3) but manifests itself as a flat and broad peak at around 180 ms.

To check whether the procedure might over-correct the data and thus remove neural signals along with eye movement artifacts, we compared the raw and the corrected data during fixation trials (Fig. 6.10, 5th column). We observed a significant difference ($p < 0.001$, shaded area) between ERPs of raw (blue traces) and ICA corrected data (red traces), comprising a time interval from 198 ms after stimulus onset to the end of the trial. However, the distribution of microsaccades over all trials (Fig. 6.10, 5th column bottom) and the observation that after correction microsaccade-related spike potentials are reduced to about one third of their initial value (Fig. 6.8e), suggest that a significant part of this difference can be attributed to the reduction of microsaccade-related artifacts, rather than to removal of neural activity. To test this assumption we repeated the analysis with only those trials in which we did not detect any microsaccades. As seen in the right-most column in Figure 6.10 the difference between raw (blue) and ICA corrected data (red) is now smaller, especially in central and occipital regions, and only becomes significant 278 ms after stimulus onset, which is 80 ms later than what we observed in trials including microsaccades. The topography of the remaining difference strongly resembles the topography of the saccadic spike potential. We therefore conclude that a large part of this difference may be due to microsaccades that are still present in the data but were not detected in our eye tracking data. Additionally, analogous to average referencing, ICA correction may reduce global noise and power (see also Figure 6.2). This may also be the reason why during fixation trials the regression model with a third spatial component spanning across a large part of the brain is more similar to the ICA corrected than to the raw data (Fig. 6.10, 5th column).

In summary, rejecting ICA components based on eye tracking information resulted in complete removal of corneo-retinal dipole offsets and eyelid artifacts from the ERP. It also reduced confounds related to saccadic spike potentials to a very large extent, without substantially affecting signals from neural sources.

Nevertheless, confounds that are not strictly time-locked to the saccade or that are restricted to a certain frequency range may go unnoticed in the ERP. Therefore we evaluated eye tracking based IC rejection also with respect to its efficiency in the frequency domain. The results are seen in Figure 6.11: in the high frequencies (30–100 Hz) the uncorrected data (left column) display the typical broadband gamma burst-related to the spike potential at saccade onset. Consistent with the topography of this spike potential this burst is most pronounced at central and occipital channel locations. Additionally, as a result of small correctional saccades, a similar but much weaker burst is observed about 180 ms after fixation onset. In frequencies below 10 Hz the corneo-retinal dipole offset leads to a general power increase, which is most pronounced at frontal electrode sites. In concordance with the observation for ERP data, ICA correction (left column) completely removes power changes related to corneo-retinal dipole offsets and eyelid artifacts, and reduces the high-frequency correspondent of the saccadic spike potential by about 85% (Fig. 6.11a). Note that in concordance with earlier studies (430) a similar reduction was also observed for microsaccadic spike potentials (Fig. 6.8f).

Investigating the data at occipital electrode sites on a lower color scale provides a more detailed view on the properties of eye movement confounds and the impact of the correction procedure (Fig. 6.11b). In the uncorrected data (left column) the broadband gamma burst of the saccadic spike potential extends into the low frequency range and together with the power increase related to corneo-retinal dipole offsets, covers the early transient visual response that was observed in the ERP. Additionally, the second broadband burst largely occludes the later visual response in the gamma range (see Fig. 6.3). In the corrected data on the other hand, both, the early transient (after 70 ms) and the later prolonged visual response (after around 200 ms) become clearly visible in the low and high frequencies, respectively (Fig. 6.11b, right column).

Again, we checked whether the correction procedure affects the signal during fixation trials, as in the absence of eye movements there should not be any discrepancies between the raw and the ICA corrected data. Figure 6.12a shows the results. In the uncorrected data (left) we observed a prominent gamma power increase at central electrode sites starting at around 250 ms after stimulus onset. That corresponds to the time and frequency range of the bandwidth increase of the visual gamma band response in occipital channels, which was described above (Fig. 6.3). In the corrected data this broadband gamma increase disappears and the visual response is confined to a frequency band between 50 and 85

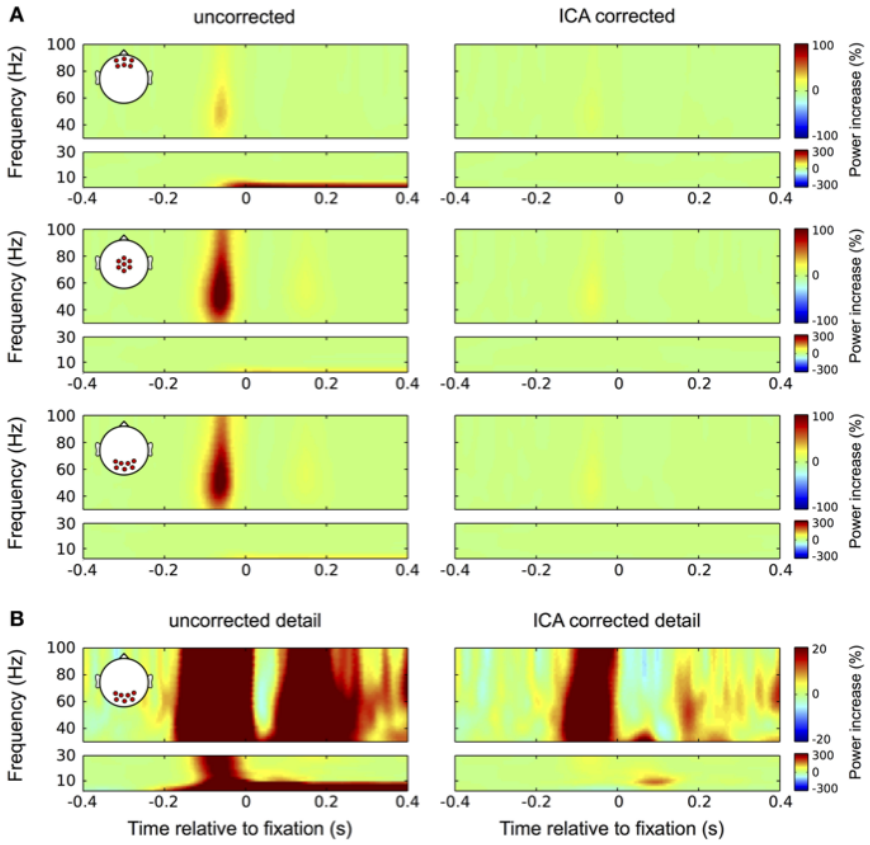

Figure 6.11: Correction in the time-frequency domain. (A) Correction of eye movement artifacts in the high (larger boxes) and low (smaller boxes) frequency ranges at frontal (top panel), central (second panel), and occipital (bottom panel) electrode sites. Left column: In the high frequencies (30–100 Hz) the uncorrected data display the typical broadband gamma burst-related to the spike potential at saccade onset. Corresponding with the topography of the spike potential this burst is most pronounced at central and occipital channel locations. As a result of small correctional saccades, a similar but much weaker burst is observed about 180 ms after fixation onset. In the low frequencies (<30 Hz) the corneo-retinal dipole offset leads to a prolonged increase in power below 10 Hz, which is starting at saccade onset and manifests itself most prominently at frontal electrode sites. Right column: In concordance with the observation for ERP data, ICA correction significantly reduces the spike potential-related gamma burst and completely removes the power increase related to corneo-retinal dipole offsets. (B) Correction of eye movement artifacts at occipital electrode sites on a more detailed color scale. Left column: The second broadband burst in the gamma range, which is caused by correctional saccades occludes the prolonged visual response we found earlier during fixation trials. Similarly, with the more detailed color scale confounds produced by the spike potential are also observed in the low frequency range and together with the corneo-retinal dipole-related power increase, the early visual response that is observed in the ERP is largely occluded. Right column: The more detailed color scale confirms that ICA completely removes corneo-retinal dipole induced power changes, while the spike potential still visible for both, task-related and correctional saccades. However, the removal of corneo-retinal dipole offsets and reduction of the spike potential renders the visual responses clearly visible in both the low and high frequencies.

Hz similar to what was observed in the average-referenced data and reported in earlier studies. Moreover, the peak of this response is now also visible in central channels. In the lower frequency range the corrected data reveal a distinct peak at 9 Hz, corresponding to the early transient response in the ERP. Comparing the difference between corrected and uncorrected data (right column) with the distribution of microsaccades indicates that the significant portions of the observed differences (original color, non-significant bins are grey shaded) follow the pattern of the distribution very closely. The power drop-off in gamma band after stimulus onset seems to be caused by a drop in microsaccade rate relative to the pre-stimulus interval, which here serves as the baseline. The rebound of microsaccade rate after 230 ms coincides with a substantial increase in gamma power, again indicating that the observed differences are caused by miniature eye movements during fixation. Like with the ERP data before, we tested this presumption by repeating the analysis with only those trials in which we did not detect any microsaccades. The results are shown in Figure 6.12b: as compared to trials with microsaccades, the broad-band power increase after 250 ms at central and occipital channels largely disappears, thus supporting the hypothesis that it was caused by microsaccadic spike potentials. We still find differences between the raw and the ICA corrected data, but now being much smaller and starting later at around 300 ms after stimulus

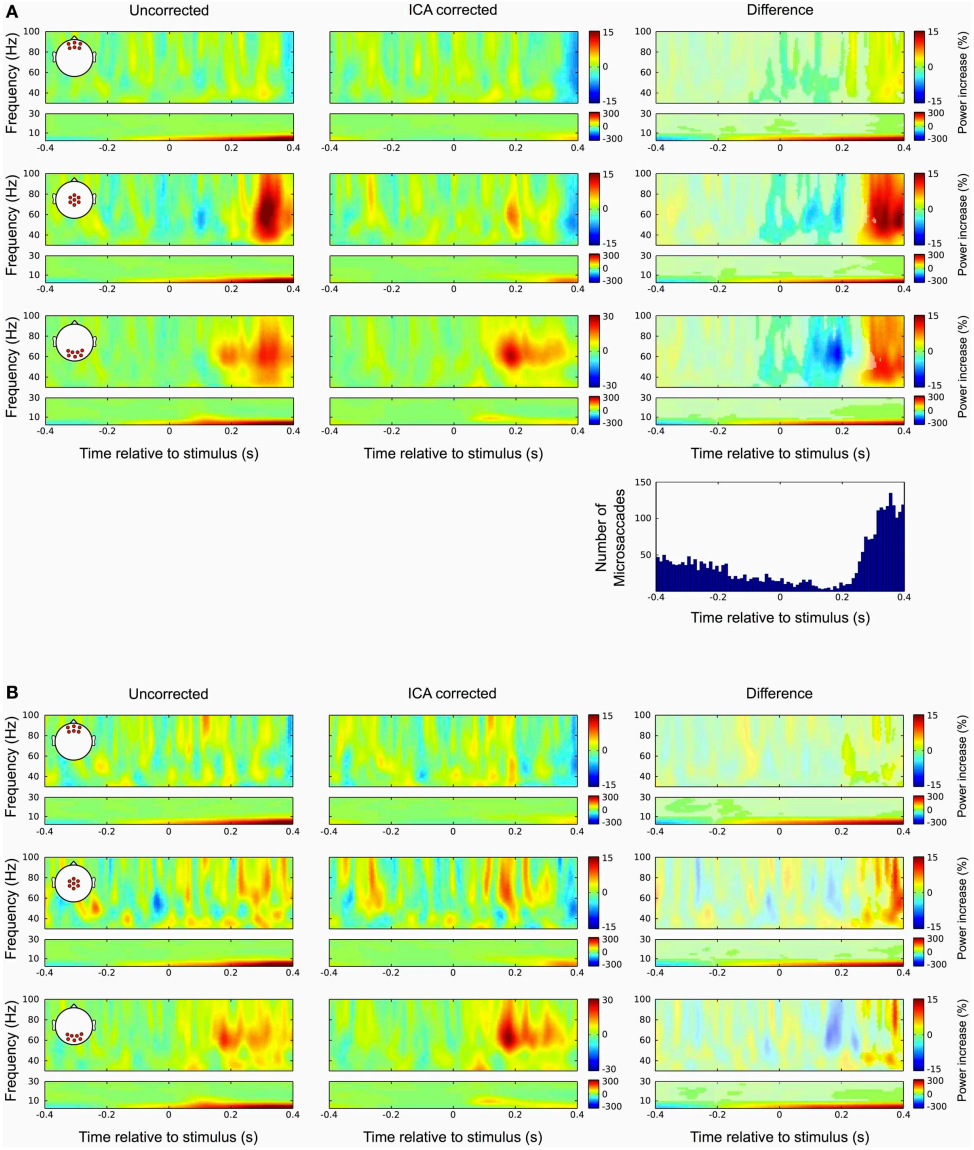

Figure 6.12: Differences between uncorrected and ICA corrected time frequency data during fixation trials. (A) Same conventions as in Figure 9. Left column: In the uncorrected data a prominent broadband gamma power increase is observed at central electrode sites. Occipital channels display prolonged activity in the gamma range corresponding to the late visual response as described in Figure 3. Middle column: In the corrected data the prolonged visual gamma response is confined to a frequency band between approximately 50 and 80 Hz and its peak now also visible in central channels. The low frequencies reveal a distinct peak at around 9Hz corresponding to the early transient response in the ERP. Right column: Comparing the difference between corrected and uncorrected data with the distribution of microsaccades indicates that the significant portions of the observed differences (i.e., bins in original color; non-significant bins are gray shaded) follow the pattern of microsaccade distribution very closely. The negative gamma power difference after stimulus onset results from a drop in microsaccade rate relative to the pre-stimulus interval, which here serves as the baseline. Then coinciding with the increase in microsaccade rate after 250 ms the difference in gamma power substantially increases. (B) In trials without detected microsaccades the largest part of the broadband gamma power increase disappears and smaller differences between raw and ICA corrected data only become significant after 300 ms. Again these residual differences display the spatial and spectral signatures of the saccadic spike potential and therefore are likely the result of undetected microsaccades.

onset. Analogous to our observations in the ERP data we conclude that these differences are mainly caused by undetected microsaccades, rather than by removal of neural activity. This is strongly supported by the frequency signature and scalp distribution of the residual difference, which very closely resemble the ones that we observed for spike potentials and microsaccades, respectively.

6.4 Discussion

We were able to confirm that eye- and eyelid movement-related artifacts arise from several independent mechanisms and showed that their relative contribution to the measured EEG signal depends on the type of eye movement.

We evaluated the performance of ICA and regression-based eye artifact correction methods. As using ICA for artifact rejection generally poses the problem to objectively differentiate between ICs related to artifacts and ICs related to neural activity, we devised a selection procedure that identifies eye artifact related ICs based on eye tracker information. Rejecting these ICs from the data resulted in complete removal or significant reduction of the above-described eye- and eyelid movement artifacts, while leaving the relevant signal emerging from neural sources intact. In contrast, both regression models tested here resulted in suboptimal artifact correction.

Below we will review our findings in the light of previous studies of eye movement artifacts and discuss the resulting implications for artifact correction and data analysis. We discuss why ICA is in principle suited to extract artifacts arising from multiple sources and why regression is likely to fail under these circumstances. Finally we consider neural activity that goes along with eye movements and therefore may have an impact on the data despite artifact correction.

6.4.1 Eye- and eyelid movement artifacts

Eyeball rotation artifacts: Eyeball rotations induce signal changes that depend on both, movement size and direction. The polarity of these changes in turn depend on the orientation of the corneo-retinal dipole, whose axis closely follows the direction of gaze. The corneo-retinal dipole itself is produced by the ionic gradient between the apical and basal surfaces of the retinal pigment epithelium (for a review of the underlying physiology see 19). However, even when the retina is surgically removed, signal changes related to eyeball rotation can still be recorded. Therefore it is probable that other sources also contribute to the generation of the dipole, like for instance potential differences that occur exclusively across the cornea or between the blood and the intraocular fluids (668).

For any given movement direction, the amplitude of the corneo-retinal dipole offset changes roughly linearly with saccade size. However, the magnitude of the corneo-retinal dipole itself is far from static. It has been shown that the potential between cornea and retina changes with illumination (574, 20). This change may occur on a time scale ranging from a few milliseconds to several hours. For instance, illumination of a dark-adapted eye produces a rise in potential that peaks after 10–15 min (503). The respective peak amplitude depends on both, the intensity of the light and the duration of the dark adaptation and it is followed by a damped oscillation that continues for hours (20). Next to other reasons (cf. 201), these fluctuations in response to illumination changes constrain the utilization of the EOG as an absolute measure for gaze position, because a reliable estimation would require recalibration about every 10 s (624). However, changes in the standing potential do not preclude the correction of corneo-retinal dipole-related artifacts since the propagation of the potential through the volume conductor is independent of its intensity (297).

More problematic in this respect is the fact that eyeball rotation can be accompanied by translational or torsional movements of the eye. Such eyeball displacements impede accurately modeling the potential difference between cornea and retina as a single dipole, which in turn leads to difficulties in estimating a single set of scalp propagation factors for a given dipole orientation. Still, in the present study, we found that saccades of different sizes but with the same orientation share the same topographic pattern and thus the same propagation factors of corneo-retinal dipole-related artifacts onto the scalp. This implies that for the movements investigated here, possible displacements of the eyeball do not have significant impact on the measured signal. We also observed that movements of opposite orientation in the horizontal axis do not only result in the same (but mirror reversed) propagation factors but that they also project to the scalp with the same amplitude. Although we found a global difference in amplitude between up- and downward movements, the similarity of their topographic patterns suggests that this is because the reference is not located symmetrical with respect to the plane of eye rotation, rather than because of a difference between their respective propagation factors.

Eyelid artifacts: artifacts emerging from blinks, eyelid saccades, and post-saccadic eyelid movements are produced by the same principal mechanism, namely the eyelid changing the resistance between the positively charged cornea and the forehead. Accordingly lid fixation severely reduces or even prevents eyelid-related potential changes in the EEG (137). Blinks are also accompanied by an active small extorsional, downward, and nasalward eye movement which is followed by a fast passive return to the pre-blinking position due to passive elastic forces (76, 64). Yet artifacts arising from such blink-associated eye movements are usually occluded by the lid induced artifact and therefore only play a minor role with respect to blink-related signal contamination.

Importantly, the distribution of eyelid artifacts at scalp level is independent of corneo-retinal dipole orientation. As our results show, their topographic pattern does not change across different types of eye and eyelid movements, and their related potentials only differ in amplitude and duration (see also, 240, 325, 503, 890). Still, eyelid artifacts are interrelated with the corneo-retinal dipole in the sense that an intact eye globe is necessary for the production of blink potentials. Active or passive movements over a non-metallic prosthetic eye do not result in blinking potentials (547). Conversely, passive eyelid movement over an intact eye results in electrical changes congruent with the ones of blinking and eyelid artifacts (547).

Another important issue concerning the interrelation between eye and eyelid artifacts is that saccadic eyeball rotations are accompanied by ballistic eyelid movements, or "eyelid-saccades," that are performed in synchrony with saccadic eye movements (53, 240, 325, 350). Saccades and eyelid-saccades are coordinated by several brainstem structures and different cortical pre-motor and motor areas (350). Consequently, eyelid-saccade parameters are closely matched with those of eye-saccades (53) and therefore cannot be disentangled in the signal measured at scalp electrodes. However, after the termination of both eye and eyelid saccades the lid continues to slide for another 30–300ms (53). This post-saccadic eyelid movement produces a returning change in offset which, in concordance with both, previous studies and our data, is exclusively observed after vertical and oblique upward saccades (43). However, based on the interpretation of source dipole modeling of eye artifacts, other authors have proposed that post-saccadic eyelid artifacts could also be present for horizontal saccades (503). Although we do not see corresponding changes at scalp level, we cannot discard this possibility, especially as eyelid related ICs display offset changes also during horizontal saccades. Note, that post-saccadic eyelid artifacts are not related to eye movement overshoots as they could be interpreted at first sight (43). This is supported by the observation that the returning change in offset is not present for eye movements performed with eyes closed (377).

Finally, the observation that velocity and duration profiles of post-saccadic eyelid movements and eyelid movements during opening the eyes after blinking are very similar, further argues for the same underlying mechanism (240). However, blinks produce about 5–10 times larger artifacts than post-saccadic eyelid movements. In frontal electrodes, that is about 100 μV for blinks as compared to approximately 20 μV for eyelid artifacts succeeding large upward movements when the recorded data is nose-referenced.

In summary our results confirm that the propagation of eyelid related artifacts onto the scalp is independent of corneo-retinal dipole orientation while their amplitude and latency may change significantly depending on the type of eye and eyelid movement.

Spike potential: The saccadic spike potential is a transient high amplitude potential observed around saccade onset. Its origin has been a matter of debate, but although some authors argue for the saccadic spike potential to emerge from cortical sources (469, 614, 667), it is now generally believed that saccadic spike potentials reflect the recruitment of motor units in extra-ocular muscles (849, 850, 681, 430, 121). The onset of the saccadic spike potential precedes the onset of the saccade about 5 ms and therefore this artifact is sometimes referred to as "pre-saccadic" spike potential (849). However, it has been argued that saccadic spike potentials and saccades actually start at exact the same time but since the latter are usually defined as the eye movement exceeding a certain velocity threshold, their detection lags behind the actual movement onset (430).

Both, amplitude and topography of the saccadic spike potential at scalp level change depending on movement size and direction. Yet, the results in the present study suggest that the observed topographic patterns might reflect a mixture of corneo-retinal dipole orientation and different sequences of muscle activation. More specifically we observed that both, amplitude and topography of the saccadic spike potential, are dependent on initial eye position rather than on saccade

size. This may indicate that at saccade onset the impact of the corneo-retinal dipole on the overall polarity on the scalp contributes more to the observed topographic pattern than the saccadic spike potential itself.

It appears virtually impossible to study the saccadic spike potential's contribution to the measured signal independently of other artifact sources, because, as it was shown here and in previous studies (430), ICA often fails to single out the saccadic spike potential into one or several separate components. One of the reasons, next to its short duration, may be that different ocular muscle units are recognized as different sources, which however are too weak to be isolated into independent components. Moreover, the problem of studying the properties of the saccadic spike potential during different types of eye movements in isolation of other artifacts will also not be easily resolved by using other methods such as source localization, since their spatial resolution is limited and the precise origin of the mechanisms generating the spike potential is not well understood yet.

Microsaccades: Microsaccades are performed involuntarily and their execution is controlled by the superior colliculus (332). Their behavioral purpose is not entirely clear yet but several studies suggest that they play an important role for counteracting visual fading (539) and enhancing fine spatial detail (733). However, it remains an open question how these putative functions of microsaccades can be brought in accordance with earlier findings that microsaccades are sometimes suppressed in high-acuity tasks like threading a needle or shooting a rifle (929, 91).

As pointed out above, the most prominent microsaccade-related confounds in EEG data are produced by the spike potential at microsaccade onset, while offsets that go along with corneo-retinal dipole rotation only have a minor impact on the signal.

Consistent with earlier reports (430), our results show that ICA-correction significantly reduces the amplitude of microsaccade-related spike potentials. Moreover, the finding that during fixation trials the correction procedure leads to a signal reduction that follows the observed microsaccade distribution suggests that microsaccade-related spike potentials do not only affect the induced gamma band response in the frequency domain but also ERP amplitudes. Thus, addressing the question which factors systematically modulate the rate of microsaccades will not only shed light on the behavioral purpose of microsaccades but may possibly also reveal spike potential induced confounds in previous ERP studies.

In summary, the different types of eye artifacts investigated here are largely independent of each other and display different properties with regard to different types of eye movements: amplitude and topography of corneo-retinal dipole-related artifacts are determined by both, eye movement size and direction. Blink-related artifacts on the other hand are independent of eye movements and although small eye movements do occur during blinking, their impact on the signal is minor as compared to the eyelid induced resistance change. As a consequence the only factor significantly modulating the amplitude of blink artifacts is whether a blink is performed voluntarily or involuntarily. In this respect blink artifacts differ from post-saccadic eyelid artifacts, which do depend on both, eye movement size and direction. More specifically, at scalp level they are only observed during upward eye movements and display larger amplitudes after large saccades. However, apart from differences in amplitude all eyelid-induced artifacts produce the same topographic pattern. Similarly, the topography of the saccadic spike potential changes relatively little for different saccade amplitudes and directions and the observed differences in amplitude seem to depend on the initial eye position rather than on the type of movement. Apart from the saccadic spike potential, the contribution of ocular muscle activity to eye and eyelid movement-related artifacts is negligible (592). This holds for both, tonic muscle activity that keeps the eye or eyelid in a given position and phasic muscle activity during blinking.

6.4.2 Correction of eye movement artifacts

Regression-based correction: It is widely recognized that blink and saccade-related artifacts propagate differently onto the scalp (161, 310, 16, 225, 63, 681, 169). Still, some authors advocate that both types of artifacts can be fully corrected by regression methods that are based on only two orthogonal (i.e., horizontal and vertical) EOG measures, thus ignoring the independence of eyelid and corneo-retinal dipole-related artifacts and the topographic differences between them (892, 751).

Other authors that acknowledge these differences argue that in principle artifacts produced by eyelid movement during blinking and upward saccades could be separated from the EOG by including a radial component in the corneo-retinal dipole model (225, 167, 168, 751). However, our results demonstrate that a three-component model does not necessarily result in better correction performance than a two-component model. Therefore it appears doubtful that the effects of eyelid movement on the corneo-retinal dipole can be fully modeled by a single dipole in three dimensions. It has been shown that a correct modeling of both, vertical eye movements and blinks requires at least two current dipoles (16). Also, the best dipole fits for eye movement artifacts are obtained when dipoles are allowed to take different locations and orientations depending on the type of movement. More specifically, dipoles that correspond to blink-related activity should not only be located in front of the vertical eye movement dipole (as it could be modeled by an axial component) but also above it (63, 503). In addition, it is not clear how to estimate an axial spatial component for a single corneo-retinal dipole source most adequately, as it may depend on electrodes at many different locations (630), which are not necessarily symmetric and could contain contributions from neural sources. In the present study we re-referenced channels to mathematically linked temporal channels for calculating the axial component (225, 167, 168). This however resulted in suboptimal correction coefficients for both, blinks and eye movements.

Another problem of regression-based methods is that the regression coefficients are affected by other sources of correlation between EEG channels and EOG channels, principally by brain sources that propagate to both groups of channels and by other electrical artifacts like coherent direct-current shifts (165, 166). Such correlations could "inflate" or "deflate" regression coefficients in a manner that depends on both, the size of the artifacts and the ratio between confounded and artifact-free periods in the data. For example, regression coefficients calculated with small saccade amplitudes will be inflated with respect to those obtained from larger saccades (165, 166). To overpass the problem of inflation it has been proposed to subtract event-related activity from the raw data before calculating the coefficients and in this way to eliminate inflation caused by the forward propagation of time-locked neural signals into the EOG channels (310). An alternative proposal suggests that before the calculation of the regression weights, the data should be averaged with respect to artifact events instead of neural events, thereby reducing inflation that is produced by brain activity that is not time-locked to the ocular movement (165, 166). Although these methods can help to reduce the correlation between EEG and EOG channels, they are not able to completely decorrelate both types of signals. As a consequence inflation of regression coefficients cannot be completely avoided and activity from neural sources may be subtracted from the signal.

To summarize, regression initially appears to provide a straightforward solution for removing eye movement artifacts from the EEG. But as our results show, it is not possible to correct corneo-retinal dipole and eyelid artifacts at the same time. Additionally potential correlations between EEG and regression channels may lead to inflation of regression coefficients and erroneous removal of brain activity from the signal. Note that choosing more advanced regression methods or different regression channels may have yielded better results as the ones presented here. However, the general problems of regression-based eye artifact correction remain and therefore inevitably lead to suboptimal correction performance.

Independent component analysis correction: ICA does in principle not suffer from the limitations that are encountered with regression methods. ICA decomposes the signal measured at scalp level into the activity of the particular sources that contribute to the signal. Thus, in the ideal case, brain and artifact-related activity are clearly separated and can be handled independently. In practice however there are several problems related to this approach.

First, the effectiveness of ICA strongly depends on the quality of the signal decomposition. Not all signal sources may be isolated into separate components and there are no definite means to evaluate whether or not contributions of other sources confound a particular component. However, with optimally prepared data (i.e., sufficient length, cleaned from large amplitude noise and rare artifacts and possibly filtered to the frequency range of interest) this problem can be minimized (524). A large number of studies has shown that ICA is able to isolate all relevant signal sources in a way that the components of interest, as for example brain activity from a defined area and/or related to a certain cognitive task, are not affected by other components, like artifacts or other cortical sources (525, 524, 309, 329).

A second problem is how to objectively identify components related to ocular artifacts. Often this is done based on

visual inspection of the components' topography (408, 385, 524), thus relying on the subjective judgment of the experimenter. Here we have shown, that this approach, not only leads to suboptimal detection and possible misclassification of ICs, but also to divergent results depending on the subjective view of the researcher. Likewise, even more objective methods, like defining ocular artifacts based on their statistical properties may fail to identify all relevant components, as different artifacts display very different features with respect to their propagation pattern, amplitude or frequency range (524). Another conventional method to identify ocular components is to cluster ICs based on their source locations and defining the signals emerging from clusters located in and around the eye and eyelid as eye movement-related (309, 329). However, source clustering might fail in some cases. For example, noisy components often contain eye artifacts but do not display bipolar patterns and thus are likely to be mislocalized.

Here we proposed a procedure to identify eye artifact-related ICs, by comparing their activations during saccade and during fixation intervals, as defined by high temporal resolution eye tracking. In this way we circumvent the problem of how to objectively distinguish artifactual from non-artifactual ICs to a large extent, as this approach does not rely on subjective interpretation of topographies or prior assumptions about artifact properties, such as source location or spectral content. Consequently, the procedure potentially also identifies confounds that are not directly produced by ocular sources but by artifacts that may occur during eye movements in a systematic manner, as for example head or face movement-related muscle artifacts.

We were able to demonstrate that eye movement-related ICs are almost completely separable from other ICs only based on their saccade/fixation variance ratio. The selection algorithm presented here performed more effectively and reliable than human experts, when those had to base their decision on topographies alone or in combination with only a small subset of component activations. The experts outperformed the automated selection procedure when they could assess ICs based on both, their topographies and a large amount of trials. However, given the number of ICs and trials (here: 896 ICs with an average number of 283 trials each) this approach may not be feasible for most experiments. Employing automated IC classification therefore could prove as an efficient alternative, especially since the possibly misclassified ICs in our experiment were most likely related to noise rather than to brain activity.

There are, however, potential drawbacks to the proposed approach: most importantly, brain sources that are mainly active during the saccade interval might be erroneously excluded. But as motor planning and sensory processing usually take place before and after the saccade itself, the exclusion of brain-related components is rather unlikely. In the data presented here, none of the ICs that were identified as eye movement-related appeared to contain contributions from neural sources.

It also has to be noted that the proposed approach, namely classifying ICs according to their activation differences between saccade and fixation intervals, is not entirely free from prior assumptions. As discussed above, small eye movements also occur during fixation and therefore might bias the saccade/fixation variance ratio. However, microsaccades generally occur only in a subset of fixation intervals, and are even less frequent when eye movements are allowed during the experiment. Additionally, spike potentials, which have been identified as the main microsaccade-related confound in EEG data (954, 430), are not likely to contribute as much to the variance of generally longer fixation periods as to the usually much shorter saccade intervals. Beside these assumptions, the ratio-threshold defining whether a given IC is eye movement-related or not, was set based on heuristics. For our data the pre-defined value of 1.1 proved to be optimally chosen. In other experiments, however, the discrimination threshold may have to be adapted. On the other hand here all ICs with ratios lower than 1.1 but above about 0.9 appeared to be exclusively related to muscle activity and noise, respectively. Therefore we conclude that even setting the threshold to 1 is not likely to affect task relevant neural signals.

Another limitation is that the IC selection procedure we suggested here requires high temporal resolution eye tracking, which may not always be available in standard EEG experiments. It may however be possible to extract saccade periods based on typical eye movement signatures in the EOG channels, such as signal deflections and/or the saccadic spike potential (430).

Lastly, effective eye artifact correction using ICA does not only depend on a sufficient amount of eye movements in

the data but also on their amplitude. Applying the procedure on another data set containing fewer and smaller saccades resulted in a suboptimal ICA decomposition. Therefore it is highly recommended to include a variety of eye movements that are performed independently from the task at hand in the ICA decomposition, as we did in our pre-experimental procedure.

6.4.3 Neural activity accompanying eye movements

Studying brain activity in the presence of eye movements entails another, often overlooked aspect that cannot be solved by artifact correction: the contribution of eye- and eyelid movements to the signal measured on the scalp does not only consist of non-cortical sources. They are also accompanied by cortical activity related to motor preparation, perceptual suppression, and sensory responses. As blinks and eye movements are also present in experimental designs that require fixation, their neural concomitants are easily overlooked especially when relying on artifact correction procedures. Thus, in the presence of voluntary or involuntary eye- and eyelid movements, comparisons between experimental conditions may be influenced by systematic variation of brain activity related to eye movement execution, attentional control (299, 600, 160), visual suppression and stability during the saccade (941) or the related visual responses (200, 201, 656). Neglecting these potentially systematic neural signals may lead to an erroneous interpretation of the data. Similar to saccades, blinks and eyelid movements are also partially controlled by cortical structures. In monkeys several frontal and parietal areas have been linked to the control of blinks (301). In humans, activity in the medial frontal gyrus (951) has been related to spontaneous blinking and activity in precentral motor areas to voluntary blinking or the active inhibition of it (420, 951, 144). Furthermore blinking has also an impact on sensory processing, as it causes suppression of activity in visual, parietal and prefrontal cortices (93), thereby leading to a decrease of visual sensitivity around the blinking period (897). Additionally the interruption of visual input while the eyelid covers the pupil, a period that may range from 100 to 300 ms, usually goes unnoticed. This phenomenon, commonly termed as "visual continuity," has been related to activity in parieto-occipital areas during blinking (93). Although not consciously processed, blink-related visual potentials do display differences depending on the degree of illumination (62).

Lastly, due to the occurrence of microsaccades, eye movement-related brain signals are likely to be present even during fixation intervals. Dimigen et al (200) have recently shown that microsaccades are not only accompanied by extra-cortical confounds (i.e., spike potentials) but also by activity emerging from cortical sources. They found that microsaccades generate visually evoked potentials, so called lambda responses, as they typically occur in response to stimulus onset or after larger voluntary saccades (200).

Altogether these findings imply that eye movements influence the recorded EEG in a way that cannot be separated from neuronal processing. Therefore experimenters should be aware that frequency and size of eye and eyelid movements may vary systematically between conditions: saccade rate for instance depends on a variety of aspects like attention, task and image features. Also, the probability of fixational eye movements is known to change in dependency of behavioral task (929, 91), proportion of target stimuli in oddball paradigms (200) and image type (733, 954). Similarly, size, frequency, and timing of blinks were found to depend on different cognitive and experimental factors such as attentional breaks (784, 611), mind-wandering (792), use of startle stimuli (481), and the occurrence of certain saccade types as for instance while changing lines during reading (654).

In summary, relying on artifact correction methods alone would mean to ignore the fact that eye movements do not only introduce artifacts to the EEG but that they also go along with neural activity, which when overlooked may lead to misinterpretation of the data. But eye movements are an essential part of human cognition and experimental setups where they have to be suppressed may not provide adequate information about neural processing under natural conditions. Moreover, systematic variations of eye movements between conditions directly result from differences in cognitive processing and therefore their respective neural signatures cannot be dismissed as "confounds". In many cases, especially when studying overt visual attention, these alleged "neural confounds" constitute exactly the activity of interest.

Thus, eye movements during EEG recordings should not necessarily be considered as interferences but as a part of natural human behavior. Their presence, however, demands the experimenter's awareness and the observed patterns of neural activity have to be interpreted carefully in the sense that they may be linked to visual attention and saccade execution rather than to other cognitive processes that may be the actual focus of interest. Under this point of view simultaneous eye tracking or other saccade detection methods, may help to identify possible biases that arise from systematic differences in probability, size, and timing of eye- and eyelid movements (cf. 434, 954, 430, 201).

6.5 Conclusion

A large number of studies have investigated individual eye movement artifacts under various aspects (e.g., 849, 137, 502, 503, 350, 430) and a variety of different methods has been proposed to correct or reduce their impact on the EEG (e.g., 503, 167, 168, 408, 385, 751). There are efforts to optimize these methods in order to overcome some of their inherent limitations (e.g., 310, 165, 166, 524, 430) and it has been suggested to complement EEG measurements with eye-tracker information in order to address the problems and pitfalls that are connected to recording EEG in the presence of eye movements (e.g., 434, 201). Here, by co-registering EEG and eye movements, we studied a wide range of eye artifacts and reinvestigated a number of previous findings within one single data set. This made it possible to examine eye artifacts not only with respect to their individual properties but also their interrelations, thus making earlier findings more comparable. In addition we assessed the efficiency of regression and ICA based artifact correction methods. Unlike earlier studies we also evaluated their impact on a well-defined visual brain response, which is suited to serve as a reference for direct statistical comparisons in both the time and frequency domain. Finally we propose a procedure for the automated selection of eye movement-related ICs. As the procedure is based on a single quantifiable criterion (i.e., the variance ratio of their activations) it can be equally applied to all types of eye movement-related artifacts, without requiring individual decisions by the experimenter.

Chapter 7

Predictions of visual content across eye movements and their modulation by inferred information

Abstract

The brain is proposed to operate through probabilistic inference, testing and refining predictions about the world. Here, we search for neural activity compatible with the violation of active predictions, learned from the contingencies between actions and the consequent changes in sensory input. We focused on vision, where eye movements produce stimuli shifts that could, in principle, be predicted. We compared, in humans, error signals to saccade-contingent changes of veridical and inferred inputs by contrasting the electroencephalographic activity after saccades to a stimulus presented inside or outside the blind spot. We observed early ($<$250 ms) and late ($>$250 ms) error signals after stimulus change, indicating the violation of sensory and associative predictions, respectively. Remarkably, the late response was diminished for blind-spot trials. These results indicate that predictive signals occur across multiple levels of the visual hierarchy, based on generative models that differentiate between signals that originate from the outside world and those that are inferred.

This chapter was published as a peer reviewed article: Ehinger B, König P, **Ossandón JP**. Predictions of visual content across eye movements and their modulation by inferred information. *The Journal of Neuroscience*, **35**(19):7403-7413 (2015).

7.1 Introduction

The brain is likely to operate constructively, generating probabilistic models of reality that are in continuous testing against sensory inputs. Functionally, probabilistic models can successfully explain a large range of phenomena, like perceptual illusions (919), spontaneous activity representing uncertainty (260), and the optimal integration of multimodal signals (938, 236, 458). To find neural correlates of such processes, researchers look for patterns of brain activity compatible with probabilistic neural computation, in which predictive coding is one of the most popular models.

In predictive coding, higher areas in a brain hierarchy predict the activity of lower areas by inhibitory feedback, whereas lower areas generate corresponding error signals in relation to their own feedforward inputs. In current formulations of predictive coding, the precision-weighted prediction errors are thought to be encoded predominantly in superficial pyramidal cells of the cortex (246, 48), and thus measurable by electroencephalography (EEG). Previous EEG experiments, which revealed neural signatures compatible with predictive coding, have mostly relied on passive tasks, in which the predictability of the stimuli is imposed externally. However, the predictive coding framework can also embrace predictions that are the consequences of agents' self-generated actions, in line with recent proposals of embodied cognition that emphasize the role of the body and self-generated action for perception (229).

Eye movements can be considered as "experiments" in the visual domain, testing hypotheses about visual content through actions (280). Given that there is evidence for predictive coding in early visual areas for passive stimulation (603, 825, 7, 454), it is conceivable that the shifts of the visual input produced by eye movements could, in principle, result in predictable signals in all levels of the visual hierarchy. Moreover, active sensory predictions could also exist for signals that are generated in the absence of actual inputs. This occurs naturally in the retina's blind spot, which is demonstrable in monocular vision as a percept that is "filled-in" from the surroundings' content.

We combined eye-tracking and EEG measurements to evaluate the existence and timing of predictive signals that are caused by human subject's eye movements. Crucially, in our experimental design we measured prediction error responses in the context of both veridical (precise) sensory information and inferred (imprecise) visual cues, presented outside and within the blind spot, respectively. Two alternatives are conceivable in the case of blind spot stimulation: first, feedforward activity of neurons related to filling-in is taken by the brain as if it was actual input, and therefore, no differences should exist between prediction violations inside or outside the blind spot. Alternatively, within the brain's generative models, there is an expected uncertainty about the blind quality of filled-in information; therefore, we would expect to see an attenuated error response when the violations were based upon imprecise filling-in, when stimuli were presented in the blind spot, relative to when they were not.

7.2 Methods

Overview: To find signals compatible with predictive errors that can be differentiated from non-predictive remapping signals, we compared EEG responses with stimuli that were changed or unchanged during the saccade that brought it to the center of the gaze. Our study design has effectively two key factors (Fig. 7.1); namely, a stimulus change during the saccade (or not) and an initial presentation of the stimulus (presaccadic) within the blind spot (or not). The stimulus change involved rotating the inner segment of a circular grating to create an inner visual feature, in which the direction of the grating was orthogonal to the surroundings. Crucially, this visual feature (inset) was smaller than the blind spot resulting in perceptual filling-in when presented within the blind spot. We presented stimuli within the blind spot using monocular stimuli (by using shutter glasses), but alternatively to the right or left eye. This resulted in a design with four factors in total: stimulus change (present or absent), inset (present or absent), blind spot (within or without), and position (peripheral initial presentation, right vs left).

Subjects: Fifteen subjects participated in the study (mean age: 22.5 years, 18–28; 1 left-handed, 6 with a left-dominant eye, 9 female). All subjects gave written consent, and the experiment was approved by the local ethics committee. An additional nine subjects were rejected before their EEG recording either due to the screening procedure (n = 4, see below for criteria); technical problems (n = 2); incompatibility of lenses with the combination of shutter glasses and eye tracker (n = 2); or perceptual problems in the peripheral field-of-view (n = 1).

EEG: Electrophysiological data were recorded using 64 Ag/AgCl electrodes with an equal distance placement system. Scalp impedances were kept below 5 kΩ. EEG data were sampled with 1000 Hz using Cz as recording-reference (actiCap, Brain Products GmbH, Germany) and the ground electrode placed near Fz.

7. Predictions of visual content

Eyetracking: A remote, infrared eye-tracking device (Eyelink 1000, SR Research) with a 500 Hz sampling rate was used. The average calibration error was kept $<0.5^\circ$ with a maximal calibration error $<1.0^\circ$. Trials with a fixation deviation of $>2.6^\circ$ from the fixation point were aborted.

Display:We used a 24 inch, 120 Hz monitor (XL2420t, BenQ) with a resolution of 1920 x 1080 pixels in combination with consumer-grade shutter glasses for monocular stimuli presentation (3D Vision, Nvidia, wired version). The shutter glasses were evaluated for appropriate cross- talk/ghosting using a custom-manufactured luminance sensor sampling at 20 kHz. The measured crosstalk at full luminance was 3.94%.

Change latency: As the main analysis of EEG data were about signals related to saccade-contingent changes, we needed to make sure that the stimulus change always occurred during the saccades. The online detection of a saccade by the eye-tracker took on average 27 ms [SD = 1 ms, 5/95% (22-35 ms)] from the movement start, and the saccade duration was on average 60 ms [SD = 4 ms, 5/95% (48-80 ms)]. An additional 8.75 ms (max = 11 ms) delay occurred from the computer command to the actual stimulus change on the monitor. The slowest detection of a saccade (35 ms) plus the maximum time it took to change the stimulus (11 ms) was faster then the shortest saccade (48 ms). Thus, the stimulus was always exchanged before the fixation onset. Reaction time from go signals to saccade start was, on average, 248 ms (SD = 20 ms).

Stimuli: Modified Gabor patches with a frequency of 0.89 cycles/$^\circ$ and a diameter of 9.6° were generated. Two kinds of patterns were used (Fig. 7.1d): one completely continuous and one with a small perpendicular inset of 2.4°. For comparison, the blind spot typically has a diameter of 4°-5°. The Gabor had constant contrast in a radius of 6.3° around the center. This ensured the same perception of the continuous stimulus outside the blind spot compared with a filled-in stimulus where the inner part is inside the blind spot. To account for possible adaptation effects, horizontal and vertical stimuli were used in a balanced and randomized way over trials. Stimuli were displayed using the Psychophysics Toolbox (83, 445) and Eyelink Toolbox (162).

Calibration of Blind Spot: To calibrate the blind spots, subjects were instructed to use the keyboard to move a circular monocular probe on the monitor, and adjust the size and location to fill the blind spot with maximal size. They were explicitly instructed to calibrate it as small as necessary to preclude any residual flickering. The circular probe flickered from dark gray to light gray to be more salient than a probe with constant color (29). All stimuli were presented centered at the respective calibrated blind spot location. In total, each subject calibrated the blind spot 30 times over two sessions.

In-line with previous studies (931), the blind spots (left and right) were located horizontally at -5.4° (SD = 0.6°) and 15.7° (SD = 0.6°) from the fixation cross. The mean calibrated diameter was 4.9° (SD = 0.7°) for the left and 5.0°(SD = 0.5°) for the right blind spot. Blind spots did not significantly differ in size (p = 0.061, CI = -0.3, 0.0) but they did differ in absolute horizontal position (in relation to the fixation cross; p = 0.005, CI = -0.5°, -0.1°]) with the right blind spot, on average, 0.3° further outside from the fixation cross. There was no difference in the vertical position (p = 0.87, CI = -0.5°, 0.3°). In summary, the properties of the subjects' blind spots were fully compatible with the previously reported values. One exception is that subjects calibrated the left blind spot, compared with the right one, closer to the fixation cross.

Eye movements result in EEG artifacts that differ according to their kinematics. Although we used state-of-the-art procedures to remove this artifact (see below), it is important to evaluate the systematic differences in eye movement that could confound the analysis. The saccades did not differ in amplitude for saccades to the left against saccades to the right. There was a significant difference of amplitude between saccades inside the blind spot and saccades outside the blind spot of 0.3° (SD = 0.1°,p = 0.001,CI = 0.1°, 0.4°). However, this difference was small compared with the overall average saccade amplitude of 13.9° , and the stimulus size of 9.6°.

Screening Procedure: The screening procedure was used to ensure a normal fill-in, absence of problems in the peripheral vision unbeknownst to the subjects themselves, and the ability to sustain a high level of attention. A single stimulus, either continuous or with an inset, was monocularly presented in the periphery at the previously determined blind-spot location (inside the blind spot, temporally) or in the horizontally mirrored position (outside the blind spot, nasally). Subjects indicated via button press whether they perceived a stimulus without inset (left key) or a stimulus with inset (right key) stimulus. A total of 48 trials were shown, and they were fully balanced and randomized. We applied conservative criteria, requesting a 94% performance level in this simple classification task. If an inset stimulus was presented inside the blind spot and thereby eliciting fill-in, it was counted as a correct trial when subjects answered that they perceived the stimulus as continuous.

Responses to saccade contingent changes outside and inside BS: Concurrent EEG and eye-tracking recordings were performed allowing us to induce artificial mismatches between pre-saccadic and post-saccadic stimuli and thus evaluate the differences in EEG responses to saccade-contingent changes. At the start of the trial (Fig. 7.1a-c), the subjects were asked to fixate on a cross in the middle of the screen. A Gabor stimulus, the pre-saccadic stimulus, was presented monocularly either to the left or to the right eye and either outside the blind spot (nasally) or inside the blind spot (temporally). After an average of 525 ms ($\pm$ 225 ms), the fixation cross disappeared and the subjects had to perform a saccade to the center of the stimulus. We called the second stimulus, now in the center of the gaze, the post-saccadic stimulus.

Two key factors were evaluated during the experiment. The first factor was "change." To induce a prediction error, we exchanged the stimulus during the saccade in half of the trials. This change was either from a stimulus with the inset present to one where the inset is absent, or vice versa. Saccades were detected online when the gaze deviated $>2.6^\circ$ from the fixation cross. Saccade-contingent changes occurred equally often for movements to stimuli presented inside or outside the blind spot. The second factor, "inset," related to whether subjects saw a stimulus with or without an inset.

Presenting the stimulus with an inset in the blind spot elicits fill-in and thus is perceived as a continuous stimulus, regardless of the veridical physical stimulus properties. It is therefore impossible to perceive an inset stimulus when the initial pre-saccadic stimulus is presented in the blind spot; thus, we did not record trials in such a condition. Moreover, an inset in the later post-saccadic stimulus, when the previous periphery stimulus was inside the blind spot, can only co-occur with a change.

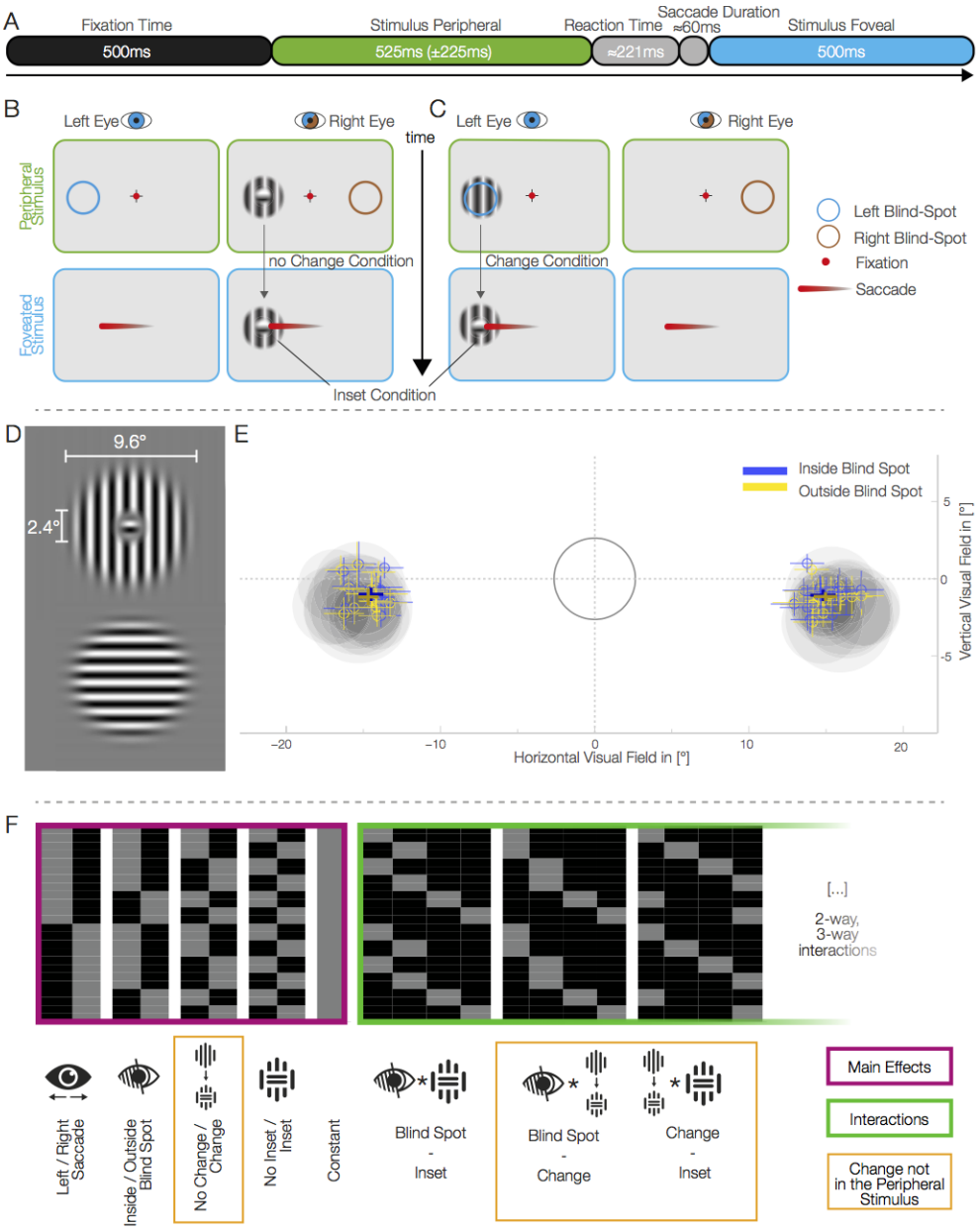

Figure 7.1

In total, 2880 trials were displayed over two sessions with 10 blocks per session. Each condition was displayed in a fully balanced and randomized way for each block.

EEG Processing: Data were analyzed using MATLAB and EEGLAB (185). Data were resampled to 500 Hz and bad channels, which we identified by visual inspection (never more than 1 channel per subject) were excluded from further analysis and interpolated at a later stage (after data epoching, see below) using spherical interpolation. Signals were cleaned visually for coarse motor artifacts and signal drops. An independent-component (IC) analysis (AMICA, standard parameters as implemented in BCILAB v12; 662) was applied on, only for this step, FIR high-pass filtered data (1 Hz, –6 dB cutoff at 0.5 Hz, 1 Hz transition bandwidth, FIRFILT, EEGLAB plugin). ICs were automatically screened for artifacts. For eye artifacts, we used an automatic reliable algorithm (201, 688) that removed, on average, 7.5 eye-artifact ICs (SD = 2.5; low = 4, high = 18) per subject. For muscle-artifact ICs, we correlated the spectrum of the ICs with a prototypical "square-root" spectrum commonly observed in muscle artifacts. A correlation >0.7 was used to identify an IC as a muscle-artifact IC. We found, on average, 6.8 components per subject (2.3; low = 0, high = 15). All rejected ICs were also visually validated by inspecting the topographies, spectra, and activation over time, and confirmed.

Finally, EEG data were low-pass filtered below 50 Hz (–6 dB cutoff at 56.25 Hz, 12.5 Hz transition bandwidth) using a finite impulse response

Figure 7.1 ***(previous page)*:** Experiment setup and eye-movements behavior. A) Trial time course. B-C) Each set of two panels represents what is presented to each eye with the shutter glasses. After a fixation interval, a stimulus appeared monocularly in the periphery (top). After the disappearance of the fixated crosshair, the subjects perform a saccade to the center of the pre-saccadic stimulus, which becomes the post-saccadic stimulus (bottom). The colored circles represent the location of the blind spot in each eye and were not displayed on the screen. B) An example of a trial without change: the inset stimulus, presented outside the blind spot, does not change before and after the saccade. Importantly, presenting an inset stimulus inside the blind spot always leads to fill-in and therefore the perception of a continuous stimulus. We therefore recorded the inset no-change condition only outside the blind spot. C) A trial with change: the continuous stimulus, presented inside the blind spot, is exchanged during the saccade to an inset stimulus. D) Gabor patches used as stimuli; horizontal stimuli were also used. The inset was set to ∼50% the diameter of the blind spot. E) Locations of the blind spots and saccades' end-points. The gray ring encloses the tolerance area for fixation. The gray discs represent the average calibrated blind spot sizes and locations for each subject. Bold crosses represent the winsorized average saccade end locations over subjects of both inside and outside blind spot trials (+-winsorized SD). Small crosses show the same metrics for each individual subject. F) The design matrix used for the single subject GLMs. An over-parameterized model of four main effects (purple), constant, and all interactions (green) was used.

filter. Data were cut into epochs of –300 ms to 500 ms with a baseline of –300 ms to –100 ms and aligned to two different events: the onset of the pre-saccadic stimulus and the start of the post-saccadic stimulus fixation. Trials were excluded from further analysis in three circumstances: subjects made a saccade when they should have maintained fixation, the saccade endpoint was not in an area of 10 around the center of the stimulus, or the reaction time was greater than three times the SD above the mean for each subject. After online fixation control and EEG cleaning, on average, 88% (4.9%; low = 62.9%; high = 96.5%) of the trials entered further analysis.

The complete eye-tracking and EEG datasets, and analysis scripts are available upon request.

Statistics: We used robust statistics wherever possible. Robust statistics are more reliable in the case of small deviations from assumed distributions than their classical statistical counterparts (923, their Chapter 1). If not stated otherwise, all reported descriptive values are 20% winsorized mean followed by 20% winsorized SD in round brackets (923, their Chapter 3.3). When winsorizing, the upper and lower 20% of samples are replaced by the remaining most extreme values, and then the mean or SD is calculated. The influence of outliers is thereby strongly attenuated. The median, arguably least affected by outliers, is equal to the most extreme winsorized mean (threshold of 50%), where all values, except the median value, are declared "outliers." Ranges are reported by (low = X, high = Y). We evaluated one-sample tests with the percentile bootstrap method of trimmed means (20%) with α = 0.05 (923, pp 115–116). For paired two-sample data, we used the same procedure on the difference scores. We used bias-corrected, accelerated 95% bootstrapped confidence intervals of the trimmed mean (20%) and reported them in the text by (CI = XY). All bootstrap tests and estimates were done with 10.000 resamples, except for the EEG multiple-comparison correction (TFCE) where we used only 1.000 resamples.

Single Subject GLM: Using a MATLAB toolbox suitable for mass- univariate generalized linear models (GLM; LIMO toolbox; 670), GLMs were fitted on each electrode and time-point separately for each subject. The analysis of EEG data with GLMs, has previously shown advantages in terms of higher sensitivity and unbiased data-driven analysis (172, 731) and is a standard application of statistical parametric mapping (504). An over-parameterized dummy coding with interaction comparisons was used for the design matrix (Fig. 7.1f). The main factors used were stimulus Change, Blind spot (outside/inside), Position (left/right), and Inset (with and without). All possible interactions were modeled.

The analyzed estimable functions are linear combinations of the parameters of the same experimental factor or interaction. For example, for the main factor position, the estimable function was $\beta_2 - \beta_1$.We tested this statistically by Yuen's t-tests with corresponding H0 centered bootstraps over subjects based on the LIMO toolbox implementation. For an interaction example, Position x Blind spot, the estimable function was $(\beta_{10} - \beta_9) - (\beta_{12} - \beta_{11})$, and tested by a Yuen's t-test with corresponding H0 centered bootstraps over subjects. For the peripheral stimulus we did not model the change contrast, as the stimulus was not exchanged in that time window of analysis.

Group Level Statistics: We used a standard TFCE measure of local responses and permutation testing (797, 671) to control the elevated family-wise error ratio of the multiple electrodes × timeframes tests that were performed. In brief, TFCE bypasses the need to define an arbitrary threshold for sample clustering by establishing the "local support" in space and time for every sample. This local support is given by the sum of all sections in time and space that are underneath it; in other words, the sum of all samples that are not beyond and higher than any local minima that is between them and the sample under calculation. TFCE was calculated for the actual mean factors and for 1000 bootstraps of centered subjects. For each of these bootstrapped samples of subjects, the maximum TFCE value across all samples in time and space is used to construct an H_0 distribution, against which the actual TFCE values were compared. Values above the 95th percentile were considered to be controlled for multiple comparisons at an α level of 0.05. The neighborhood distance was calculated on the default electrode locations.

For a given model and data partition, the procedure described above controls for the family-wise error rate resulting from fitting multiple GLMs to different electrodes and time points. We report only effects that extended over five samples (10 ms) or more. Effect clusters of significant values were reported in the text with their respective timing and median TFCE-corrected p value ($\tilde{p}$).

Shift of factor labels: Due to the nature of our factorial design, one can relabel the factors such that main effects and interactions are exchangeable. For example, a main effect of change can be regarded as an interaction between the presence of an inset before and after the saccade: an inset stimulus before the saccade combined with a change results in a no-inset stimulus after the saccade. Without the change, the stimulus before and after the saccade is identical. This is true in reverse for the no-inset stimulus before the saccade. We, indeed, found a change × inset interaction effect (Fig. 7.4B) even before the saccade ended. We observed this pre-saccadic-offset positive effect from -64 ms to 6 ms (positive betas: -64 – 6 ms, $\tilde{p}$ = 0.019, min-p = 0.004; negative betas: -60 to -34 ms, $\tilde{p}$ = 0.045, min-p = 0.03, and from - 30 ms to 0 ms, $\tilde{p}$ = 0.042, min-p = 0.035). This seems puzzling at first, as the change of the stimuli occurred ∼30 ms before the saccade offset, which is after this observed interaction of change × inset. The effect before saccade offset most probably resembles the main effect of the inset during the pre-saccadic stimulus stimulation and can be explained by this changing of factor labels.

Incomplete Design: Due to the very nature of filling-in at the blind spot, only an incomplete factorial design is possible: an inset stimulus inside the blind spot cannot be perceived. Therefore, we have to assume that the three-way interaction containing the Blind spot factor, the Change factor, and the factor Inset is negligible. We additionally confirmed all results in two reduced subset models, each containing a full-factorial design. For the first full-factorial model, we collapsed the change and inset factors in a combined factor and selected only trials that were available both inside and outside the blind spot. The second model excluded the factor Blind spot (and all of the data with a stimulus inside the blind spot) but included separate factors Change and Inset. This allowed us to confirm our full-factorial model with the limitation of two independent error terms for the two models, instead of one error term. All results were confirmed in the fully balanced designs.

7.3 Results

Fifteen subjects participated in a concurrent EEG and eye-tracking experiment. They were asked to perform an eye movement from the center of the screen onto a Gabor stimulus (Fig. 7.1d) located in the periphery, in either the left or the right visual field (Fig. 7.1a-c). The position of the stimulus was centered at either the left or right blind spot of each individual subject and the diameter of the stimulus itself was larger than the blind spot by a factor of $\sim$2 (see Materials and Methods, Calibration of blind spot). By using a 3-D monitor with shutter glasses, it was possible to present the stimuli either in the blind spot or in the same location, albeit in the nasal non-blind spot field of the other eye. Uninstructed to the subjects, in half of the trials, the stimulus changed during the saccade. Post-experiment debriefing established that all subjects became aware that the stimulus was sometimes exchanged. This consisted in a change of a small inset within the center of the Gabor patch (smaller than the blind spot) from no inset (a completely continuous stimulus) to the stimulus with an inset (during inside and outside blind spot trials) or vice versa (only during outside blind spot trials). This experimental manipulation allowed us to evaluate the presence of EEG responses compatible with error signals to changes in a stimulus that are contingent on subjects' actions.

We analyzed electrophysiological responses that are produced after identical eye movements (Fig. 7.1e) with the same amplitude, direction, and target location (see Materials and Methods, Calibration of blind spot) and that resulted in the foveation of identical stimuli, albeit between trials in which the stimulus was either changed or not changed during the eye movement. EEG responses were analyzed with mass-univariate general linear models (670) that were fitted to each electrode and time-point for each subject. The main factors used were as follows: stimulus Change (with/without), Blind spot (outside/inside), Position (left/right saccade), and Inset (with/without; Fig. 7.1f). On the group level, instead of a classical ERP analysis, we analyzed the estimable contrasts of the parameter estimates from the general linear model of the main factors and interactions. This corresponds to a summary statistic approach to random effects analyses. The reported values, termed "β values" as a shorthand, are similar to difference values of raw ERP, but importantly, they take into account the variance of the other independent variables. We found clusters of significant effects associated with the main effect of interest, change, at four distinctive latencies in the analysis of the data after the saccade offset. The following results are organized in three sections. First, we describe EEG effects of filling-in before a saccade was done. Second, we illustrate the effects related to late prediction signals post-saccade. Finally, we describe early and middle latency effect of post-saccadic predictive signals.

7.3.1 Inferred information in the periphery

A stimulus presented in the blind spot elicits filling-in, in which visual signals are inferred from surrounding information without a direct input from the retina or the outside world. Neural activity related to filling-in has been described previously in areas V1–V3 in neurophysiological studies with primates (257, 457, 545) and in fMRI experiments with humans (861), but not in human electrophysiology. We found that, before the eye movement, after the onset of a peripheral stimulus, there is a main effect for the Blind spot factor (Fig. 7.2a) from 172 to 246 ms (positive betas: 172-244 ms, median p value: $\tilde{p}$ = 0.015, min-p = 0.001; negative betas: 172-214 ms, $\tilde{p}$ = 0.011, min-p = 0.002, and from 216 ms to 246 ms, $\tilde{p}$ = 0.028, min-p = 0.011; positive values represent a positive deviation from the average ERP over all conditions and vice versa). As the presaccadic stimulation was lateralized, we analyzed the main factor Position (Fig. 7.2b) and found two significant

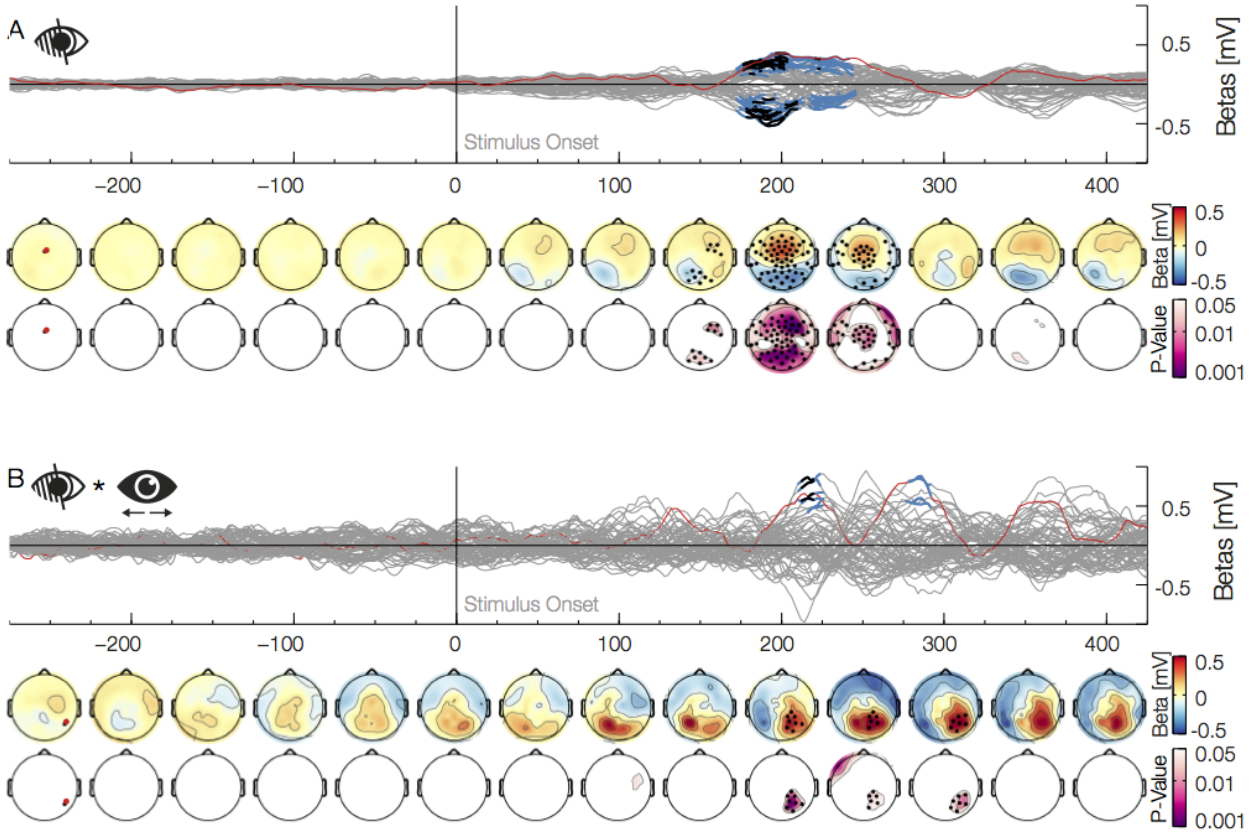

Figure 7.2: Main factor blind spot. GLM analysis of EEG data, aligned to the fixation onset, are presented in these and following figures with a time-series plot of the beta weights of a given main factor or interaction for each electrode in a butterfly plot. All data presented here were baseline corrected from -300 to -100ms. The family-wise error ratio of the multiple electrodes*timeframes tests was controlled with threshold free cluster enhancement statistics (Smith and Nichols 2009; see method section EEG analysis for a detailed description). Blue marked latencies are significant under TFCE threshold of 0.05 and are therefore corrected for multiple comparisons over time points and electrodes. Black marked latencies are significant under additional Bonferroni multiple comparison correction for the multiple tests due to testing multiple factors in one respective model (see methods section Group level statistics). The location of the red highlighted channel is depicted in the first topographic plot below. The first row of the topoplots represents the mean beta weights averaged over 50ms bins. The second row depicts the minimal TFCE-corrected p-values over the same bin. Black marked electrodes represent significant channels in the same bin. A) The Blind spot main effect depicts the difference of a stimulus presentation inside and outside the blind spot which is prominent 200ms after stimulus onset. B) The Blind Spot x Position Interaction depicts a lateral component of the effect shown in A.

effects. The first occurred immediately after the presaccadic stimulus onset from 70 to 114 ms (positive betas: 70-114 ms, $\tilde{p}$ = 0.015, min-p = 0.003; negative betas: 72-106 ms, $\tilde{p}$ = 0.017, min-p = 0.005). As to be expected, a stimulus in the right or left periphery elicits stronger activation in the contralateral occipital electrodes. A second effect can be seen from 362 to 408 (positive betas: 362-408 ms, $\tilde{p}$ = 0.022, min-p = 0.01; negative betas: 386-404 ms, $\tilde{p}$ = 0.018, min-p = 0.004). Importantly, processing of the blind spot filling-in could be lateralized as well. Therefore, we analyzed the interaction Blind spot $\times$ Position (Fig. 7.2c) and found two significant positive effects. The first was from 210 to 226 ms ($\tilde{p}$ = 0.022, min-p = 0.003), and the second one was from 276 to 292 ms ($\tilde{p}$ = 0.03, min-p = 0.011). The first of the lateralized effects started and ended during the main effect, whereas the second one started $\sim$30ms after the main effect. The overall blind spot results are in-line with previous studies with intracranial recordings of V1 neurons that have receptive fields which include the blind spot, and that show differences in activation after 100 ms (545, their Fig. 9B) or after 200 ms (457, their Fig. 9A). These two effects shown here establish an EEG correlate for the difference in visual processing of peripheral stimuli when they are veridical (outside the blind spot) or inferred (inside the blind spot).

7.3.2 Prediction signals over saccades

Our main goal was to find an EEG effect compatible with error signals related to the prediction of specific visual content across eye movements. In contrast to the results described above, all subsequent effects are for the postsaccadic stimulus. The violation of a predictive signal that is independent of specific low-level visual content (which would show in the interaction with position or inset) can be investigated by the main effect of the Change factor. Such a main effect was present from 248 to 498 ms after the end of the saccade (positive betas: 248–498 ms, $\tilde{p}$ = 0.001, min-$p < 0.001$; negative betas: 250–482 ms, $\tilde{p} < 0.001$, min-$p < 0.001$). Together, the topographies and timing of these positive and negative effects were compatible with a P3 ERP (Fig. 7.3A). The P3 component is usually found after infrequent or unexpected events, independently of sensory modality. Our data are therefore consistent with a high-level prediction error, associated with a prediction based on peripheral visual input and the subjects' eye movement.

After establishing the presence of a signal compatible with post-saccadic prediction error, we investigated whether this error signal was different depending on whether the pre-saccadic visual input was veridical (outside the blind spot) or inferred (filling-in inside the blind spot). The Change $\times$ Blind spot interaction (Fig. 7.3b) was significant from 190 to 382 ms (negative betas: 190-382 ms, $\tilde{p}$ = 0.007, min-$p < 0.001$; positive betas: 276 ms to 368 ms, $\tilde{p}$ = 0.01, min-$p <$ 0.001). To understand the direction of the interaction effect, we additionally analyzed the raw ERP difference between the conditions change and no-change, once inside and outside the blind spot. To evaluate these data independently of effects due to the inset, we subtracted the inset difference ERP from the change conditions separately for trials inside and outside the blind spot (Fig. 7.3d). The resulting ERPs show how the interaction modifies the P3 component in two different ways. First, and corresponding to the positive cluster of the interaction, there is a reduction of the anterior part of the P3 when the previously peripheral stimulus was shown inside the blind spot compared with when it was shown outside. This correspond to the P3a subcomponent, which is associated with orienting responses due to the processing of unexpected, novel events (275, 691). Second, corresponding to the negative cluster of the interaction, there is an increase in the posterior part of the P3 for blinds pot trials. This corresponds to the P3b sub-component, which has been associated to several different processes like changes in episodic context (202), the processing of statistical surprise (535, 456), and the updating of perceptual evidence (635, 942, 427, 130). In summary, this demonstrates that the brain treats violations of predictions differently, depending on whether they are based on external or inferred information.

We controlled for non-stationary effects, such as those due to learning, by investigating the Change $\times$ Blind spot interaction over the course of the experiment. As a comparison, we looked into a similar correlation but with the main change effect. The interaction is only estimable over multiple trials; therefore, we used trial partitions of the Change $\times$ Blind spot interaction (the difference of differences) and the difference of change and no change for the change main effect. We partitioned the whole experiment into 10 parts and for each part calculated the corresponding ERP difference. We used the interaction β weights (over time and electrodes) of each subject as a template and correlated these 10 parts with the template resulting in 10 correlation values for each subject (Fig. 7.3c). For the change main effect, we observed a significant negative slope of correlation values against trial partition order (winsorized mean slope: -0.012, p = 0.001, bootstrap-CI: -0.022, -0.005). This indicates that the P3 amplitude diminishes over time because subjects get used to the experimental setting and become habituated to the saccade-contingent change (712, 713). However, the slope over trials for the Change $\times$ Blind spot interaction was not significantly different from zero (winsorized mean slope: 0.002, p = 0.8, bootstrap-CI:-0.009, 0.012). Hence, subjects got used to the task and were less surprised by the saccade contingent change, but there was no habituation of the Change $\times$ Blind spot interaction, indicating that the modified error signal for filled-in content was a stationary effect.

In addition to the Change $\times$ Blind spot interaction, we found one additional significant late interaction between the factors Change and Inset (Fig. 7.4b). The interaction was significant from 334 ms to at least 500 ms (positive betas: 342-436 ms, $\tilde{p}$ = 0.016, min-p = 0.005 and from 440 ms to >500 ms, $\tilde{p}$ = 0.035, min-p = 0.019; negative betas: 334-428 ms, $\tilde{p}$ = 0.008, min-p = 0.004, from 434 ms to 468 ms, $\tilde{p}$ = 0.036, min-p = 0.013 and from 472 ms to >500 ms, $\tilde{p}$ = 0.039, min-p

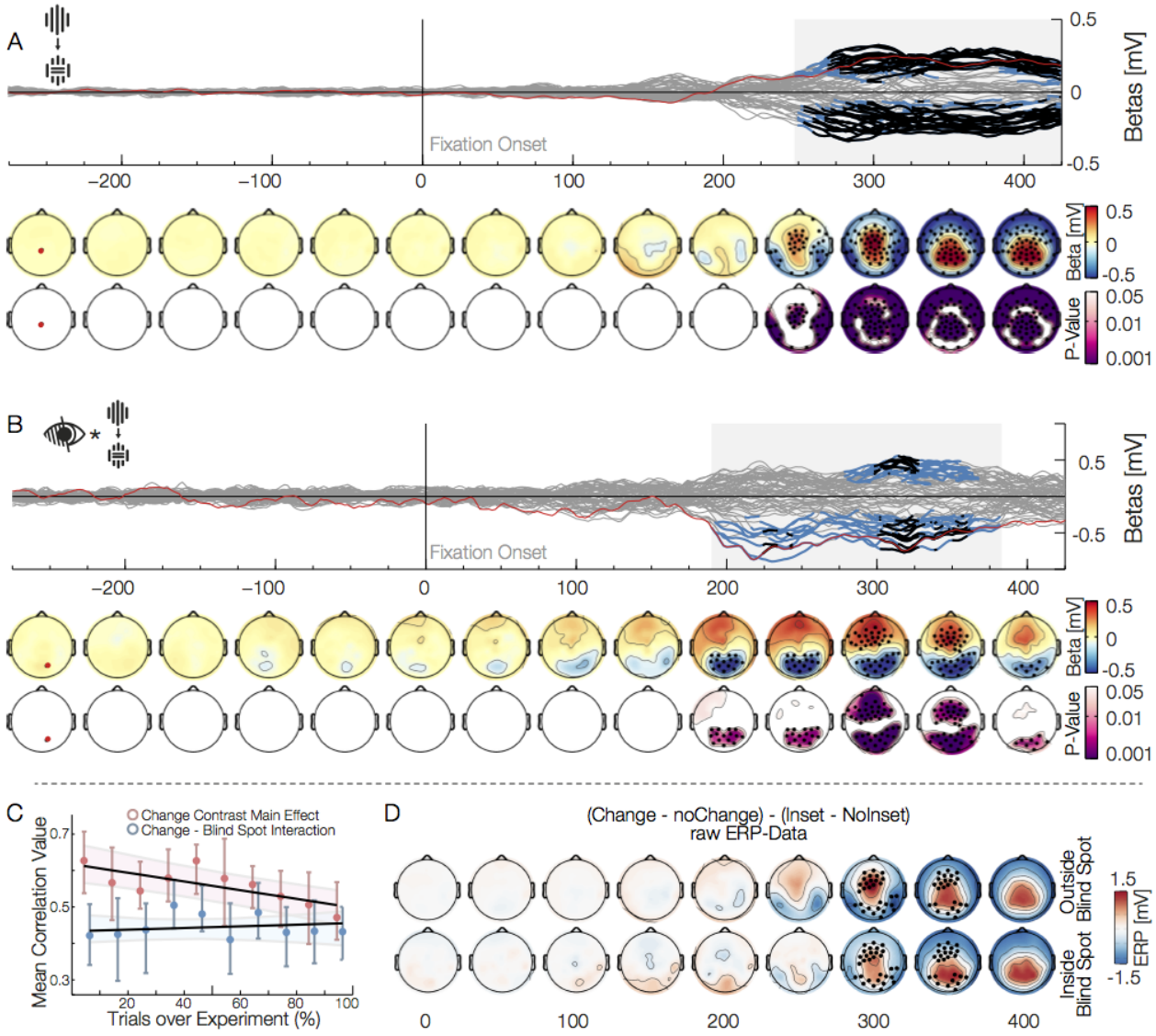

Figure 7.3: Main effect of change and interaction with the blind spot. The depicted data, in this figure, are aligned to the fixation onset. A) The main effect of change is shown, here we are comparing trials in which the stimulus remained the same, with trials, where it changed during the saccade. The effect resembles a prediction error in form of a P3. B) The interaction Blind Spot x Change is shown. This shows a reduction of the prediction error described in A). C) Correlation of each subject effect-template with ERP data over 10 partitions of the experiment. The red correlation shows that the change main effect habituates over the course of the experiment. The blue correlation shows no significant increase or decrease for the Change x Blind Spot interaction and thus stays stationary over the experiment. D) Raw ERP data the contrast in the full GLM model depicted in B). Upper row shows only outside the blind spot, the lower row only inside the blind spot data. The difference of the change effect inside blind spot vs outside blind spot against each other was tested using a bootstrapped Yuens t -test and corrected for multiple comparisons using TFCE. The significant electrodes and time-points can be seen as black dots. A reduction of the P3 can be observed inside the blind spot.

= 0.026). We interpreted this interaction as a consequence of the imbalance in the experimental design (see Materials and Methods, Incomplete design). We showed more continuous than inset stimuli in the periphery (1/3–2/3) due to the physical limitation, as an inset stimulus in the blind spot is necessarily perceived as the stimulus without inset. Due to this imbalance, a change from continuous to an inset stimulus is twice as frequent as a change from inset to a continuous stimulus. This less frequent change, the one to a continuous stimulus, resulted in an increased response compatible with a higher surprise.

7.3.3 Middle and early prediction signals

The main and interaction effects presented above emerge late after the post-saccadic foveation of the stimulus and showed a topography that is consistent with a known high-level associative component. As such, those effects are unlikely to be related to trans-saccadic prediction signals of specific low-level visual input. We search for evidence for this kinds of predictions based on two criteria: effect latency and interaction with low-level stimulus features. Specifically, we would first expect that sensory error signals would be different whether the change was from pre-saccadic no-inset to post-saccadic inset stimuli or vice versa. Second, the pre-saccadic position of the stimulus should also have an effect due to the communication of prediction and error signals between unilateral hemispheric areas and the bi-hemispheric central representation of the post-saccadic foveal stimulus. The change effect had a lateralized component, which was dependent on the stimulus location previous to the eye movement, even though the stimulus was then fixated centrally: we observed a significant Change $\times$ Position interaction (Fig. 7.4a) from 182 to 226 ms (positive betas: 182-226 ms, $\tilde{p}$ = 0.009, min-p <0.001; negative betas: 192-212 ms, $\tilde{p}$ = 0.029, min-p = 0.015, and from 216 ms to 226 ms, $\tilde{p}$ = 0.039, min-p = 0.027). Even earlier effects were observed in an interaction between Change and Inset factors and in the three-way interaction Position $\times$ Change $\times$ Inset. The interaction Change $\times$ Inset (Fig. 7.4b) was significant only for negative values, $\sim$100 ms (90-126 ms, $\tilde{p}$ = 0.03, min-p = 0.011). Lateralized effects of this two-way interaction were found in the Position $\times$ Change $\times$ Inset interaction (Fig. 7.4c): we found a positive effect from 108 to 154 ms ($\tilde{p}$ = 0.03, min-p = 0.001) and a similar effect, albeit negative, on the other hemisphere from 120 to 142 ms($\tilde{p}$ = 0.035, min-p $<=$ 0.006). Note that the interactions that include the factor Position result in topographic effect similar to the one observed for the pre-saccadic stimuli (Fig. 7.2b), thus suggesting that the processing of post-saccadic foveal stimulus include extensive crosstalk with the areas that represented it before a movement was done. Altogether, these middle and early effects of the interactions between saccadic-contingent change, pre-saccadic position, and low-level characteristics of the stimulus indicate the production of error signals to low- level visual predictions.

7.4 Discussion

We investigated the EEG correlates of prediction errors to changes in visual stimulation occurring during an eye movement. We found early ($\sim$100 ms), middle ($\sim$200 ms) and late ($\sim$300 ms) latency "surprise" responses to changed stimuli. These responses can neither be explained exclusively in terms of remapping operations, as movement vectors were equivalent across conditions, nor by differences in the post-saccadic stimulus because we compared responses to identical stimuli. Early and middle latency responses were either lateralized and/or dependent on the Inset factor, suggesting that their sources are processes specific to the visual sensory domain. In contrast, the late latency response resembled a P3 ERP component, thus suggesting it has a source in a high-order process, possibly non-visual, that it is related to the occurrence of an unexpected event. Such dissociation between perceptual and associative predictions have been shown previously in human EEG, with comparable methods, topographies and time courses, but in the context of perceptual decision-making experiments (942, 130). The late response we observed was also present when the stimulus was located inside the blind spot, but it was reduced in amplitude compared with a response outside the blind spot. This modified response to a change in the blind spot indicates knowledge of the unreliability of the filled-in information, occurring only at a late stage of processing.

We observed early, middle, and late latency effects following a change of the stimulus during a saccade. Both early and middle effects are compatible with modality specific processes: they interact with the side of the field in which the movement is directed (early and middle component) and the orientation contrast of the stimulus (early component only). Previously, sensory error signals have been associated in EEG experiment with the mismatch negativity potential (MMN), both in the auditory (285) and visual domain (818). In the visual domain, orientation mismatch, comparable to our saccade-contingent change in orientation of the stimulus, result in MMN with a temporal and topographic profile similar to the

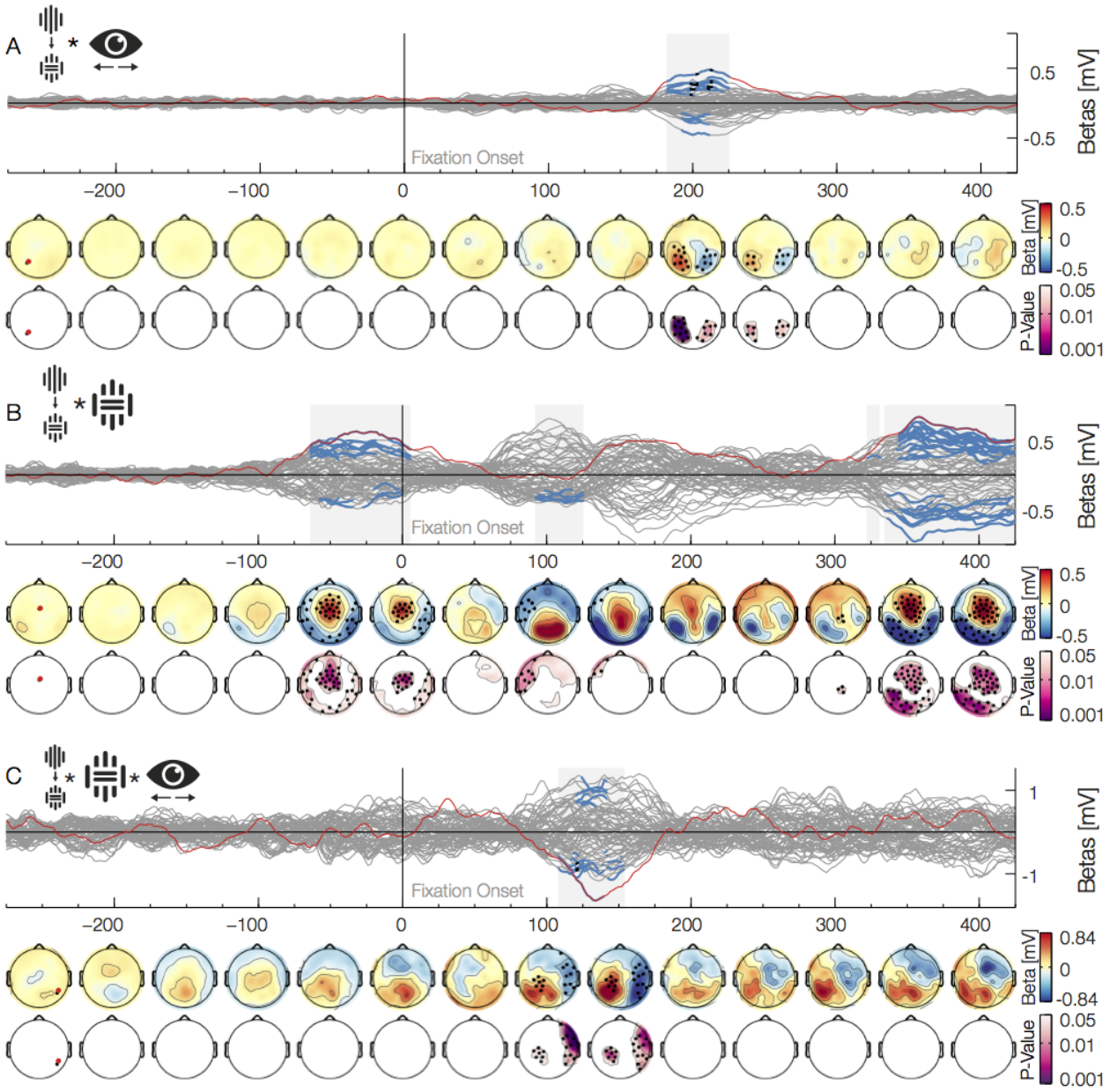

Figure 7.4: Middle and early latency interaction with the change factor. The depicted data, in this figure, are aligned to the fixation onset A) The Change x Position interaction shows a clearly lateralized prediction error at around 200ms B) The Change x Inset interaction shows three separate effects. Detailed descriptions are found in the results sections. C) The Change x Inset x Position interaction shows an early prediction error that is lateralized and also dependent on the low level stimuli properties

early and middle latency change, and change interactions seen here (24). These early effects are, however, unlikely to be related to processes occurring in the primary visual cortex. At 100 ms, the first feedforward–feedback sweep in V1 has already occurred (379, 132). Furthermore, the C1 visual ERP component, which originates in V1 (195), has a latency of 50–60 ms and peaks $\sim$ 90 ms, which is mostly before the effects seen here. The absence of a very early error signal is in concordance with the current knowledge of the extent of remapping in visual areas. Responses related to remapping are present at high levels in the visual hierarchy and are almost absent in the primary visual cortex (610, 564), making it less likely that predictions related to eye movement reach this area. The prediction of foveal, high-spatial frequency content in the primary visual cortex would be, in any case, inefficient due to the limited spatial spectral resolution of peripheral

information (14) and the limited accuracy of eye movements (916). This favors a more restricted role of predictive coding for the primary visual cortex, in which only statistical regularities about the world and the effect of low-level spatial context are taken in account (816, 711, 260), rather than an adaptive, all-encompassing process that also predicts specific content at all cortical areas. Nevertheless, the change-related effects starting at 100 and 200 ms are likely due to other stages of low- and middle-level visual processing.

Previous studies that attempted to uncover error signals to an unpredicted sensory input have been inconclusive regarding how early, or how upstream, prediction signals are produced. In some studies, only late signals related to prediction errors were found. For instance, in the modeling of mismatch negativity signals of auditory stimuli, only the late evoked responses (P3 like here), can be clearly attributed to inhibitory feedback of prediction errors (284). Similarly, a time-frequency analysis shows that high-frequency gamma differences, attributable to prediction errors, start only late, after 200 ms (858), which is the same latency for the effect that occurs in most ERP repetition suppression experiments (for a review, see 319). In contrast, other experiments support early prediction errors. Neuroimaging studies show activity patterns in primary visual cortex consistent with predictive signals for pattern adaptation (319, 825, 217), apparent motion (7), and 3D grouping (603). In electrophysiological experiments, evidence for early predictions exist for the auditory mismatch negativity effect (902), and in the case of a reduction of EEG sensory responses due to "self- stimulation" (537). In this last kind of experiment, the subjects trigger for themselves the appearance of a standard stimulus (740) through a motor action coupled artificially by experimental design, with the appearance of the stimulus. In the case of our experiment, the stimulus was always present, and the subjects' actions were directly related to the modality of stimulation. The stimulus changed its retinotopic location and resolution due to a shift of the visual field that follows overlearned sensorimotor contingencies expected for any eye movement.

The absence of an early interaction between Change and Blind spot factors indicate that filled-in signals, which are inferred from neighbor inputs, are processed by visual areas as if they were the result of an actual input. Such interaction only emerges at a later stage in the form of a modulation of both anterior and posterior subcomponents of the P3. This supports the idea that the exclusively inferred quality of the signals from the blind spot is not lost, and it is taken into account in higher-level associative areas. Even though most of the research showing visual-related P3 components has been done in conditions without eye movements, P3 responses have been recently described in experiment that permit them (171, 410, 422). In contrast to these experiments, in which an infrequent item or a search target produced the P3 component, here the P3 was elicited by a movement-contingent stimulus change. Whereas the MMN potential discussed above is related to low- level sensory processing, the P3 is considered a correlate of a high-level error signal. For instance, P3 responses seem to be a response associated to the processing of global deviants in a stimulus or event succession rather than to local deviants (56, 133), thus depending on the episodic context rather than in specific sensory features (202). A formal interpretation of the P3 is that it corresponds to the processing of statistical surprise (535, 246, 456), and also, especially for the posterior subcomponent, to the update of perceptual evidence (635, 942, 427, 130). The reduction of the anterior sub-component (peaking at 300 ms) in blind spot trials is consistent with predictive coding simulations of attention (246). In these simulations, top-down estimates of reliability (precision) modulate the gain of prediction error units in lower regions of the visual hierarchy. This gain modulation would correspond to attention, where high-precision signals enjoy greater gain and the P3 represents a revision of these precision estimates. Changes in visual stimuli need to be associated with movements or transients to be detected (320, 352). Because this is prevented here by precise experimental timing, it is safe to assume that saccade- contingent changes, even if task irrelevant, are novel events that would result in a revision on the reliability of estimates of stimulus or event constancy, at least in the local context of the experiment. However, in the case of information from the blind spot there is no such context that can change the intrinsic unreliability of filled-in signals, thus resulting in a reduced revision of conditional expectations about the stimulus being stationary. This means that an interpretation of our findings is that we attend away (ignore) visual information from the blind spot; thereby attenuating subsequent responses to violated predictions, when resampling the visual scene.

A modulation of the posterior subcomponent of the P3 in blind spot trials can be observed as well. In contrast to the

modulation of the anterior subcomponent, this difference is not fully consistent with the temporal progression and topography of the change effect. We consider two alternatives interpretations, not necessarily incompatible, of this posterior interaction. First, although the blind spot region remains unreliable, our experimental design could result in a revision, not of the precision estimates, but of the underlying model of the causes of sensory input from this region, normally inferred from the surrounding. In other words, in blind spot trials there is a revision not only of the expectation about the stimulus being stationary (albeit reduced compared with trials outside the blind spot in which the veridical pre-saccadic stimulus has a high reliability), but also of the filling-in model. The second interpretation follows the results of EEG experiments about perceptual decision-making (635, 942, 427, 130), in which a similar posterior topography and time course to the one observed here is seen for the updating of perceptual evidence, indicating that the posterior cluster of the interaction could represent an updating of the perceptual evidence about the contents of the blind spot location. Crucially, these are updates of a decision signal instead of a perceptual one, and thus in our experiment, even in the absence of an explicit task goal, would represent the accumulation of new evidence against the filling-in percept being a reliable model of sensory input.

There are two main conclusions of the present work. First, the sensory consequences of eye movements are actively predicted at multiple levels of the visual hierarchy. This occurs for the prediction of the actual visual content that is present before an eye movement, rather than only for the prediction of general statistics of visual content. Second, the prediction of content that is exclusively inferred differs between levels of the visual hierarchy. Low-level sensory areas process the stimulus as if it originated from an external input source. In contrast, in higher-level processing, the filled-in (and therefore imprecise) nature of the blind-spot information is taken into account. These results suggest that a hierarchy of predictions does not operate in a strictly successive way, in which prediction and errors necessarily propagate all the way down and up, respectively, low- and high-level predictions of the same content can be dissociated.

Chapter 8

General Discussion

8.1 Visual selection

In the General Introduction I highlighted three central elements of visual selection, with a special focus on free viewing: Firstly, that visual exploration is mainly determined by the stimuli' low- and high-level content in a flexible manner that depends on the requirements of the task at hand; Secondly, that stimulus guidance is not restricted to the visual domain but that it can be of a multimodal nature; And thirdly, that several biases exist in visual selection, both normal and pathological. These elements motivated the empirical work presented in Chapters 2 to 5, in which the relative importance and interaction between these factors was addressed in a series of experiments with human subjects.

In the following sections, these alternative mechanisms of visual selection will be placed in relation to existing functional models of attention and their neural substrate. Very generally, subsystems for low- and high-level multimodal guidance and spatial biases are organized in a parallel distributed architecture. Based on the results presented here, I will argue that this parallel architecture goes beyond a given functional divide (for instance, parallel feature channels for low-level visual selection), and exists at various levels of complexity of the decision-making process. In other words, different subsystems seem to be able to select and drive exploration independently of each other. Starting from the lowest order of complexity this comprises biases that are independent of both external stimuli and internal goals, through decisions based on low-level saliency, and up to explicit volitional control of the kind observed in humans.

This view is supported by the results presented in Chapter 2 to 5, which demonstrate biases that are pervasive and strong, and indicate guidance by low-level visual or tactile salience of the stimulus that operates independently of top-down constraints. This description of alternative quasi-independent selection mechanisms is partly at odds with existing functional models of visual selection. These favor, sometimes only implicitly, a serial decision mechanism, in which guidance by low-level cues needs to be vetoed by higher decision areas. Instead, the results of the experiments presented here, in addition to other developmental and functional considerations presented below, support not only parallel visual processing but also parallel decision-making. In this form of organization, areas at the top of the perceptual processing hierarchy can exert considerable control over lower ones, but they are not necessary for normal behavioral control. This functional organization fits well with our knowledge of brain structure, with many subnetworks composed of parallel streams that are often investigated in isolation. By looking in detail at the organization of the brain, it is possible to advance plausible mechanisms for multimodal orienting and the production of pathological and normal biases which are not obvious from an exclusively functional perspective.

8.1.1 Functional models and organizing principles of visual selection

Many functional models have been proposed to explain how visual selection operates. Proposals of attentional models for other modalities preceded visual models. These early models have had a long-lasting influence in subsequent attempts of explaining the functional organization and neural mechanisms underpinning visual selection. These pre-visual models were motivated by the observed ability of people to attend to a single stream of sound from among many streams, the famous "cocktail-party" effect (134). This ability lead to the development of a selection model by D. Broadbent (94) consisting of a filtering mechanism that blocked the sounds coming from the unattended stream from further processing. This

was later categorized as an *early selection* model. However, filtering mechanisms were soon shown to be inadequate by evidence that information from the unattended stream can be reported when it is emotionally relevant or meaningful, for example, subjects' names (587). Subsequent models attempted to accommodate this lingering of non-attended information. For instance, in the *attenuator model* proposed by A. Treisman, basic processing occurs for all inputs and the unselected ones simply have their "energy" attenuated, and are thus ready to receive focus if relevant (868, 867). Other models emphasized *late selection* steps, allowing full processing of stimuli up to the semantic level, leaving selection operations to the moment of competition for access to memory and awareness (193, 623). In general, the emphasis of these models was on how much sensory information was possible to process, but the mechanism of selection itself was not clearly fleshed out. They also presented a type of decision-making organization that is still recognizable in more modern models, in which selection is a one- or two-stage serial process that is controlled by top-down decisions that have been made prior to any event.

Building on these ideas of early- and late-selection processes, U. Neisser introduced the idea of pre-attentive and attentive stages for visual selection (618). In the pre-attentive stage, processing is parallel and automatic, whereas in the attentive stage only a fraction of the stimuli can be processed simultaneously, resulting in effortful and serial processing. These ideas were central in the model proposed by A. Treisman and G. Gelade in the early 80s (869), the Feature Integration Theory, which is probably the most influential model of visual attention to date. This model also comprises two stages of processing. The early stage is pre-attentive, in which features are processed automatically and in parallel across the visual field and feature domains. At this stage, local contrast operations result in texture segmentation and stimulus-driven selection in the form of pop-out effects. In the second stage, features are "glued" together through a serial mechanism that constitutes the basic foundation of object perception.

The influence of top-down factors, usually understood as "goal sets", led to the development of models in which spatial selection by low-level characteristics of the stimuli can be manipulated. This is achieved, for example, by selective weighting of different features maps in the saliency-map model described in the general introduction (450, 391, 389). Similar selective weighting mechanisms were proposed by V. Di Lollo and colleagues in a hybrid model of search, in which features are dynamically filtered to accommodate specific search goals (194). Along similar lines, J. Wolfe developed the Guided Search model in which selection occurs in successive stages, with a first pre-attentive selection stage that reduces in parallel the search space, and a subsequent serial search stage (937, 935). A third approach in this respect is represented by the Selective Tuning model by J. Tsotsos et al. (873, 872) and the Feature Gate model by K. Cave (127). These models allow for the pre-selection not only of a specific feature but also spatial and temporal subsets, and at multiple hierarchical levels and spatial resolutions, thus providing plenty of room for contextual control. The more recent models put an emphasis on how goal-directed selection might operate. This resulted in more complex models that could accommodate the large flexibility of selection behavior. However, the overall architecture of two main stages remains similar to early formulations, with a low-level, parallel selection followed by an effortful, serial search, both determined mainly by top-down constraints.

In parallel to the formulation of functional models, neurophysiological research led to the proposal of basic neural mechanisms capable of the necessary computations. One of these mechanisms is the principle of *biased competition*, proposed by R. Desimone and J. Duncan in the '90s (188). Its basic assumption is that visual objects compete with each other for two reasons: firstly, because processing resources are scarce at later stages of the visual hierarchy where the receptive fields are large; and secondly, because it is only possible in any case to act on one object at any one time, so action goals must necessarily be selected serially. In the original formulation, top-down pre-selections of spatial locations and feature/object templates are assumed to be the principal factors in the competition for resources. For instance, neurons in extra-striate visual areas respond differently to target and distractor stimuli, with no response to distractor elements appearing within their RF if the target location was also within the neuron's RF. The key evidence of biased competition is that neurons do respond to distractors presented within their RF when the target element is outside that RF (586, 512). With respect to feature selection, multiple studies have shown the effect of competition, too. All neurons that are sensitive to a given feature will exhibit increased neural gain if this feature is a target, even if the RF of the neuron falls outside the

spatial area involved in the task $_{(870,540,505,762)}$. Thus, goal-driven selection seems to be determined by gain changes that depend strongly on the presence of competing elements.

In summary, most functional models postulate that low-level guidance is accomplished at an early stage of within-feature local contrast operations. This is combined with some form of biased competition that conveys top-down feature and spatial constraints. The results presented in this thesis exhibit at least three characteristics that are not well explained by these models.

Discussion of functional models

First, these models usually do not define whether low-level selection can operate directly or must be contingent on a top-down goal set. Low-level mechanisms can be operationally independent of higher-level control, evidenced by three facets of our results: firstly, they can be observed when these systems are impaired (see Chapter 2); secondly, by the strong and additive effect of the leftward bias observed in the different experiments presented in Chapters 3 to 5; and thirdly by the orienting effect of irrelevant tactile cues seen in Chapter 3. Independence here means that selection operates locally in the respective submodules and through direct projections to the module responsible for motor control and dynamic selection. This idea is further explained and reinforced in the following two sections (8.1.2, p.130; 8.1.3, p.134) where different element of the underlying brain architecture are discussed.

Second, most functional models do not take into account the existence of biases and so cannot explain them. Some models of bias have been proposed but only for the pathological case of neglect syndrome. As seen in the case of the central bias presented in Chapter 6, and in the pervasive initial leftward bias presented in Chapters 3 to 5, normal human viewing behavior contains biases that are independent of both image content and top-down goals. While it would be possible to construct a model of attention based purely on theoretical constraints, it is of little use to speculate about mechanisms of bias without taking into account the underlying brain structure. Therefore, after presenting various proposals of the brain structure involved in visual selection, I will discuss evidence about connectivity asymmetries of the the systems involved that could explain viewing biases (section 8.1.4, p.136).

Third, functional models of visual attention do not adequately capture the influence of other modalities on viewing behavior. The results presented in Chapter 3 and similar experiments with auditory stimuli (651, 706) indicate that multimodal cues can not only drive local selection but also global orienting. Such dual functionality of multimodal cues is not well captured by functional models of selection but probably plays an important role in real life scenarios, especially for locations outside the visible field. Possible brain mechanisms for crossmodal guidance will be discussed in section 8.1.5 (p.140).

In summary, models of visual selection would be more adequate if they included mechanisms for: (1) independent selection across multiple levels of complexity in the visual hierarchy; (2) the biases that occur in normal human viewing; and (3) non-visual orienting. In the next sections, different proposals of possible brain mechanisms underlying visual selection will be discussed, followed by an exploration of the tension between hierarchical and parallel control of low- and high-level guidance. I will then argue that existing neural models are still greatly incomplete as they ignore multiple subcortical structures that are also involved in visual selection. These structures will be then relevant in the discussion of the brain mechanisms involved in the production of biases and in multimodal selection.

8.1.2 Cortical systems for visual selection

Research on the brain mechanisms of visual selection is roughly divided into two views: those that are mostly cortico-centric (156, 683, 45, 157, 576); and those which also give a prominent role to subcortical structures, beyond merely acknowledging their role in primary motor control (188, 669, 461, 449). The development of functional and computational models of attention was historically accompanied by speculations about the involved brain areas, primarily informed by lesion studies (e.g., 472, 566, 696, 698). It has only been in the last 25 years, as a result of the accumulation of neurophysiological studies on monkeys and the proliferation of neuroimaging studies on humans, that it has been possible to start outlining the responsible neural systems.

Early models

Earlier architectures based on lesion studies lacked definition. Nevertheless they resulted in the development of concepts that have strongly guided subsequent architectures and neuroimaging studies. One of the most influential early

proposals, proposed by M. Posner and colleagues in the '80s (696), combined a functional model with suggestions of possible brain loci for the different functional submodules. This was based on the results of the behavioral cueing tasks described in the General Introduction and on studies with patients with subcortical and cortical lesions (695, 708, 709). According to this model, visual selection consists of at least three basic operations (Fig. 8.1a-b) that occur in order: first, the *disengagement* of attention from a given current location; followed by a *movement* of the focus of attention (overt or covert) to the next location; and finally, the *engagement* of attention at the new location (694, 709). These basic operations were ascribed to the parietal cortex (696), superior colliculus, and the pulvinar nucleus of the thalamus (676), respectively. This orienting network was part of a larger framework including two other subcortical-frontal subsystems for general alerting and target-detection/executive-control. The alerting system included asymmetric projections, with dominance to the right hemisphere, of the subcortical noradrenalin system, whereas the target-detection system was bilateral and composed of the anterior cingulate cortex and the dorsolateral prefrontal cortex (698, 675). Another early proposal, advanced by M. Mesulam, was based on the study of patients with neglect syndrome (566, 568). This model comprised three cortical subcomponents (Fig. 8.1a,c). One posterior parietal component was responsible for attentional shifting and the re-mapping of salient events between coordinate systems. The second, frontal component was involved in selecting specific motor acts, and the third component, located within the cingulate cortex was involved in assessing motivational relevance. Similarly to Posner's model this specific selection network was largely influenced by midbrain and brainstem systems (the "ascending reticular activating system"), including noradrenaline, cholinergic and serotonergic pathways that control arousal and wakefulness.

These two architectures were rudimentary but nevertheless based on a large body of empirical evidence. Although diverging at multiple points, they enabled the recognition of the organizational complexity underlying the process of visual selection by proposing a modular architecture that is structured in a distributed network of brain structures, mostly cortical. This subdivision of functions and areas has been refined, corrected, and extended in the following decades by the accumulated results of neuroimaging studies. In the following section I will present the current prominent cortical architecture for visual selection, proposed by M. Corbetta and G. Shulman. The presentation of this model will advance the discussion in two ways. Firstly, as a basis to question whether such a network, composed mostly of cortical structures that are several steps removed from early sensory areas, can adequately model the basic mechanisms of general orienting and low-level selection. Based on the results presented here on independent low-level selection and biases, the dominant role of this cortical attentional network will be disputed in favor of a more global (i.e., cortical and subcortical) architecture in which selection decisions are distributed among several nodes. Second, the proposed architecture lays the foundation for a model of inter-hemispheric rivalry that seeks to explain pathological and normal biases.

The standard model of (cortical) attentional control

The model of M. Corbetta and G. Shulman is based mostly on neuroimaging experiments with human subjects. The accumulated evidence strongly indicates that two distinct and large cortical subnetworks are involved in the process of visual selection (Fig. 8.1d) (156, 160). The first subsystem is a dorsal fronto-parietal network involved in goal-directed top-down processes and composed of bilateral components in the superior parietal lobe, intraparietal sulcus and dorsofrontal cortex (419, 369, 622, 158, 673). This network is responsible for directing the biased competition process which underlies the proposal by Desimone and Duncan (188) and of several other functional models (194, 937, 935, 873, 127). To put this in relation to the behavioral elements discussed in the General Introduction, this proposed subnetwork would be involved in: (1) the selection of the feature templates that characterize targets in visual search tasks; (2) in the endogenous orienting processes seen in symbolic cueing tasks; (3) and in the spatial framing processes involved in the resistance to attentional capture.

The second subsystem is a ventral fronto-parietal network responsible for stimulus-driven guidance and composed mostly of right-lateralised components located in the temporo-parietal junction, the ventral supramarginal gyrus, anterior insula, and the ventral frontal cortex (158, 673, 519, 129, 438, 781, 782). Importantly, according to this view, this system for stimulus-driven guidance is always contingent on behavioral relevance and is not involved in pure capture by task-irrelevant stimuli.

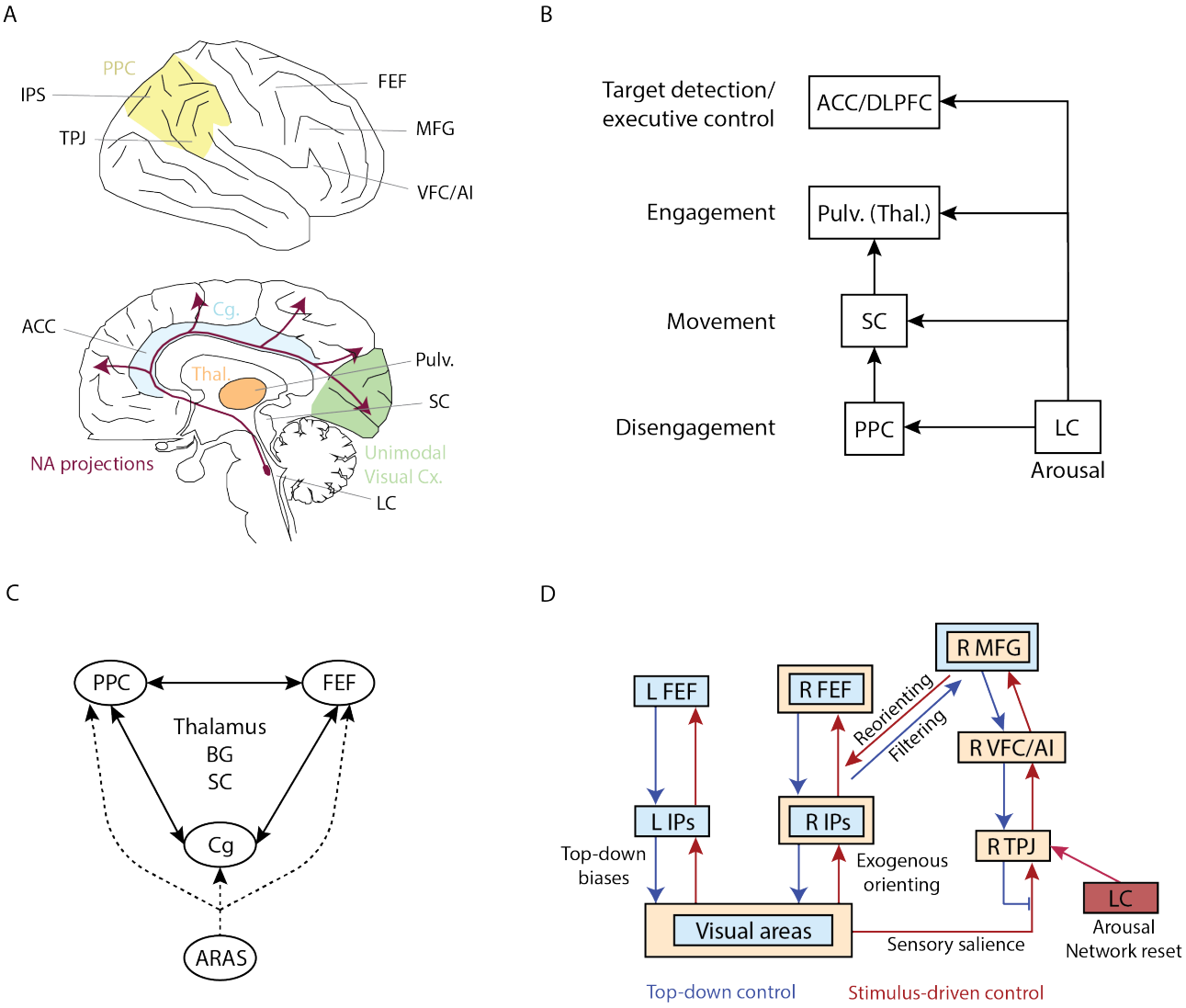

Figure 8.1: Proposed architectures for visual selection (A) Brain schematics of the relevant areas. (B) Posner's model (698, 675). (C) Mesulam's model (adapted from 568). (D) Corbetta & Shulman model (adapted from 156, 160). ACC: anterior cingulate cortex; AI: anterior insula; ARAS: ascending reticular activation system; BG: basal ganglia; Cg: cingulate cortex; DLPFC: dorso-lateral prefrontal cortex; FEF: frontal eye field; IPS: intra-parietal sulcus; LC: locus coerolus; MFG: medial frontal gyrus; NA: noradrenaline; PPC: posterior parietal cortex; Pulv.: pulvinar; SC: superior colliculus; Thal.: thalamus; TPJ: temporo-parietal junction; VFC: ventral frontal cortex.

Therefore, this subnetwork would be involved in the re-orienting to invalid targets in both endogenous and exogenous attentional cueing tasks, in surprise effects to unexpected but relevant events, and in capture effects by distractors that share some of the target features. At odds with the initial proposal, that the ventral network is involved in all stimulus-driven guidance (156) and acts as an exogenous "circuit-breaker" to the dorsal network, subsequent evidence indicates that it does not mediate reflexive low-level selection. Instead, by being relatively suppressed during periods of attentional expectation, it prevents the selection of irrelevant salient stimuli (780), and is only activated by unexpected cues and targets, or by irrelevant distractors that share some feature with the target (764). In contrast, exogenous selection by irrelevant salient stimuli seems only to correlate with activation of the dorsal network and early sensory cortex (207, 178, 438), probably indicating an after-the-fact endogenous re-orienting process. Conversely, an unexpected behaviorally relevant stimulus does engage the ventral network even when its physical salience is low (383).

Notably this dual network architecture also emerges from resting-state imaging studies. In these studies, brain activity is acquired at rest and self-organizing networks are revealed by studying the correlation of activity between areas. Some

of the resulting networks closely match the two attentional sub-networks (269, 270, 341), thus independently confirming their existence.

There are another two important aspects of this model. First, both subnetworks operate with multimodal input (206, 207, 519). This acknowledges the more general role of the attentional system that goes beyond the visual modality, establishing a mechanism for crossmodal cueing and global orienting, such as those described in Chapter 3. The second aspect is the inclusion, in agreement with Posner's and Mesulam's models, of a subcortical component corresponding to the noradrenergic system (160, 157). However, here the role of ascending noradrenergic projections is more confined, taking into account only afferents to the inferior parietal lobe (589). These afferents modulate and "reset" the ventral network during task transitions or after unexpected and behaviorally relevant events (78). The role of these afferents will arise again in the discussion of possible mechanisms of bias.

Discussion of the standard model

There are at least three important points of criticism of this standard model relevant to the results presented here, most of which were recognized by the authors when the model was proposed.

First, the model does not indicate a clear neural mechanism for visual selection based on low-level cues. As pointed out in the General Introduction the existence of functional low-level guidance is well supported by behavioral studies. Furthermore, the results presented in Chapter 2 also suggest independent mechanisms of low-level guidance, which have been found in other recent experiments.

Increased guidance by low-level saliency in neglect syndrome has been reported in four other studies, with both static and dynamic stimuli (704, 49, 521, 248). Similar effects of increased low-level guidance have been reported in another five studies of patients with lesions of the right posterior parietal cortex that did not result in neglect syndrome. This was the case for subjects without neuropsychological deficits (530) and for subjects with deficits other than neglect, namely visual agnosia (531, 266), Balint syndrome (702), and dementia due to posterior cortical atrophy (a subtype of Alzheimer's disease) (772). Results that are compatible with the rTMS experiment presented in Chapter 2 have also been reported in an experiment showing facilitation of bottom-up feature detection after parietal inhibition (644). Together, these studies show that injuries or inhibition of a variety of regions within the dorsal and ventral network, which are associated with deficits of high-level visual processing and selection, result in the unmasking of low-level guidance of visual selection. Therefore this type of selection seems not to be mediated by the network proposed in the standard model.

The second criticism is related to the latency of responses in the involved cortical structures. In the dorsal and ventral network they start at around 100 ms and in some parts, especially in the seemingly vital node of the temporo-parietal junction in the ventral network, the latencies are even longer (i.e. $>$300 ms). This has been recognized as a deficiency of the cortical model, since many of the tasks that result in activation of the two sub-networks can frequently be completed at shorter latencies. This is also the case for free viewing tasks in which the mean latency is between 200-300 ms (figs. 3.5, 4.2g, 4.5b and 4.6d), and even faster for biased behavior (fig. 4.2g).

The temporal aspect leads to the third and probably strongest criticism, that the model does not include subcortical structures that are known to be involved in attention and eye movement control. Subcortical structures are well suited to mediate fast responses, for example, the superior colliculus in the case of express saccades (746, 204, 205). The absence of subcortical areas is likely due in part to the model being based mainly on human fMRI results, a technique that provides good spatial resolution for cortical activity but is ill-suited for studying subcortical structures and for measuring temporal profiles. In contrast, most of the knowledge we have about neural activity in subcortical structures comes from neurophysiological and lesions studies with non-human animals. In these experiments it has been evident for long time that visual selection, and orienting processes in general, can be directed by subcortical structures that might partially or completely be responsible for low-level selection, multimodal orienting, and attentional biases.

8.1.3 Selection outside the cortical attentional network

Intrinsic orienting responses

One big problem of the cortico-centric view is that the brain cortex is in many cases not essential for visual selection. The added value of cortical analysis, related to memory, multidimensional pattern recognition and the integration of complex episodic contexts, in many cases seems not to be necessary for orienting behavior.

Simple orienting responses are ubiquitous in living systems, even for organisms without a nervous system. Motor guidance by light can exist even in the absence of eyes and neurons, like in the case of plants and unicellular microorganisms that with simpler photo-reception machinery are still able to execute photophobic and phototaxis responses (629). Similarly, in organisms with simple nervous systems, light-guided responses in the form of simple approaching or withdrawal behavior can be easily realized by direct coupling between sensory and motor neurons. As we progress to organisms with more developed brains, it is also apparent that even more complex responses are mostly based on low-level cues. In vertebrates, a set of important innate or early imprinted behaviors, like the anti-predator response to overhead stimuli (750, 907), alarm calls (239), and feeding responses (841) can be explained in terms of simple low-level feature detection mechanisms. Classic examples of this are the hawk/goose experiment by K. Lorenz and N. Tinbergen, which showed that geese are alarmed by specific but simple overhead visual patterns that resemble predators (750), and the experiment by N. Timbergen showing the pecking reaction of chicks to the presence of a red patch in their parent's beak (841). The kind of feature detection involved in these responses does probably not require the involvement of the cerebral cortex, and it can be explained even by the output of retinal circuits (490, 950).

Doubts about permanent and pervasive control by the cortex are further supported by lesion studies that show that visually guided behavior is preserved even when large parts of the cortex are removed (103). Oculomotor control is not necessarily impaired by lesions to the frontal and parietal areas that are part of the attentional network (744). Complete bilateral cortical lesions of these areas do not result in major orienting deficit in cats or monkeys (804, 508, 745, 742), which is in stark contrast to the effect of smaller but unilateral lesion (see discussion of Chapter 2). Only when these lesions are accompanied by subcortical ones, specially of the superior colliculus, major deficits occur (745). This supports the existence of multiple autonomous circuits to drive selection, with a prominent role for the superior colliculus and associated midbrain structures.

The role of the superior colliculus in attentional and eye-movement control

Given the position of the superior colliculus (SC) in the circuitry involved in movement control, between the brainstem motor nuclei and the rest of the brain, this subcortical structure was in the past mostly considered as a motor structure. However, in the last decades, with the discovery of its role in covert attention this view has completely changed.

Neurons in the SC are responsive to spatial cues both for overt and covert shifts of attention (470, 382). Micro-stimulation of the SC results in increased sensitivity to visual stimuli, even in the absence of eye movements (557). Arguing against a predominantly motor function of the SC, the inactivation of large parts of it does not preclude eye movements but does impair visual selection (597, 509) and this selection role is independent of its role in eye movements (509, 960).

Together with other associated midbrain nuclei, the SC also provides a complete circuitry to compute saliency and decide between competing stimuli. The SC combines information processed elsewhere, within and between features and modalities, to compute the relative saliency of different spatial locations (449). The mechanisms of this competition have been mostly studied in the owl' optic tectum, the structure homologous to the SC in birds. In the tectum, intermediate layer neurons are inhibited by stimuli occurring outside their movement fields and their sensory responses are tuned to the relative strength between concurrent unimodal or multimodal stimuli, amplifying slight differences in strength in a switch on/off manner (607, 608). The respective neural mechanisms is mediated by a local midbrain circuit composed of the tectum and other near isthmic nuclei (22, 605). The tectum also integrates endogenous attention signals from the cortex. Cortical microstimulation enhances tectum neurons' spatial gain and sensitivity when their RFs match the ones of the stimulated

cortical neurons (927, 928, 605). Moreover, cortical stimulation sharpens the competition between exogenous signals in the SC and bias competition to the signals that are spatially congruent (606). In summary, the SC and associated nuclei form a circuit that is sufficient to execute biased competition, saliency computations, and the integration of top-down spatial cues.

As the SC does not process all types of visual features, it has to nevertheless work in concert with the cortex. Moreover, as described next, saliency is likely computed in multiple cortical areas and influence selection directly through projections to the SC, rather than by engaging the previously described cortical attentional network.

Cortical selection outside the attentional network

In the same way in which some orienting/selection responses are likely driven by subcortical mechanisms, visual selection by the cortex is likely to occur independently in multiple structures, and not restricted to evaluation by areas within the attentional network. In fact, the possibility of selection by early visual cortex was demonstrated by some of the earliest neurophysiological studies about the function of cortical areas. These were electrical micro-stimulation experiments that showed that the stimulation of almost all visual cortices result in eye-movements (739, 906, 904, 426). Although this effect of stimulation of early visual areas could be indirect, the possibility of a direct influence is supported by several anatomical studies that show the existence of projections from almost all visual areas to the motor layers of the SC (308, 277, 918, 837, 838). The projections from visual areas to the SC seem to arise exclusively from cortical layer 5 (277, 918), which is consistent with the observation that the electric current required to elicit saccades from V1 is lower for stimulation at deep layers than superficial ones (837, 838). This kind of projection sends collaterals to the thalamus (77, 323), thus probably establishing an efferent-copy loop (777), which further supports its quality as an action instruction.

If different visual areas are able to control overt selection, on what criteria is the decision made? The proposed answer is that each area pushes for the selection of locations of space that contrast spatially for the given low- or high-level feature such area processes. Thus, structures like the sensory layers of the SC and primary visual cortex would drive selection based on low-level saliency features like luminance and color, whereas other areas would exert selection pressure based on more complex features like high density of edges and conjunctions. This also allows for stimulus-driven guidance based on the identification of complex visual configurations, such as objects and landscapes, without requiring a top-down decision. In all cases, this form of guidance will be of the exogenous type as in the case of direct cueing, 'pop-out' and capture effects described previously, and thus of short-latency, short-lived and mostly independent of task settings (other than spatial framing effects).

An example of this kind of decision making by "sensory areas" is Z. Li's model of low-level visual saliency (497, 498, 499). In this model, the primary visual cortex computes saliency only by means of its intra-area connectivity. This idea is supported by both behavioral and neuroimaging experiments with humans (453, 962). In this model, neurons do not only respond to the presence of a give feature within their RF but their activation is also tuned to the context. This is idea is based on multiple experiments showing that visual neurons responses are extensively modulated by stimuli outside their RF (e.g., 785, 690, 964, 414, 400). This effect is usually referred to as the non-classic RF of the neuron (8) and it would be a plausible mechanism for the computation of local saliency, texture patterns, and the grouping of items following gestalt rules (725). Li's model supports the idea of selection mechanisms that already occur at the structures where the different sensory features are processed. Moreover, the considerations above about projections from visual areas to the SC indicate that such selections can operate independently of the cortical attentional network by sending direct commands to the SC.

Still, the view that saliency can already be computed in early visual cortex is challenged by experiments that demonstrate no role of primary visual cortex (68) or the involvement of areas located higher up in the visual hierarchy. Area V4 (551, 106), different parts of the posterior parietal cortex (around the intraparietal sulcus) (307, 584, 38, 108), and the frontal eye field (853) have also been suggested as the locus of a saliency map. However part of this confusion is due to a loose use of the term, conflating low-level saliency with the selection decision. For instance, lesions of area V4 do not impair the selection of low-level salient objects (743), nor is its activity modulated by low-level salient stimuli that are task irrelevant. Similarly,

other parietal and frontal areas are responsive to salient items only when they will be the target of a movement (853). A more useful approach seems to be the idea of a *priority map* which integrates the "relevance" of both low-level saliency and top-down selection (244, 69). Such a priority map has been proposed to be localized in structures like the posterior parietal cortex or SC (69) or as an emergent property of the complete oculomotor network, similar to the idea of a distributed decision mechanism proposed here (244, 763).

In summary, multiple cortical and subcortical structures seem to be involved in orienting and attention processes. Even when focusing exclusively on visual selection, it seems apparent that the brain network involved is larger and more complex that any of the proposals discussed so far. Therefore it might be worthwhile to develop models that incorporate both cortical and subcortical mechanisms (448, 449) and where these various mechanisms can work mostly independently and in parallel. In the next section, the described cortical and subcortical mechanisms will be further discussed in relation to the production of viewing biases.

8.1.4 Brain organisation and biased exploration

In this thesis, I presented two examples of pathological viewing bias and one of a bias that is present in healthy subjects. In Chapter 2, patients with neglect syndrome showed a marked bias to explore the right side of images, a deficit that is the result of a right-side cortical injury produced by a brain stroke. In Chapter 5, patients with left-onset Parkinson's disease also showed a rightward, albeit smaller, exploratory bias during free viewing. In Parkinson's disease case, the cause is degenerative but also resulting in asymmetrical damage, due to a stronger degeneration of right-side basal ganglia circuits. Finally, in Chapters 3 and 4, a normal leftward bias was demonstrated in a large population of healthy, young subjects, and across five different experiments. In the following section, I discuss some of the different mechanism that have been proposed to explain the cases of pathological bias, why this is usually in the form of a bias to the right after right-side brain injury, and which are the possible links with the leftward bias demonstrated here.

Models of Neglect syndrome

Neglect syndrome is the classic example of attentional bias produced by brain injury. Multiple theories have been put forward to explain how it is produced but only few contenders provide a plausible explanation to the question of why there is a higher prevalence of left-space deficit after right-side injury rather than the opposite, right-side deficits after left injury. One of the most influential models proposes that this is due to a dominance of the right hemisphere for attention (566, 568). According to this view, the left hemisphere would direct attention and exploration exclusively to the right visual field, whereas the right hemisphere would do it to both sides. This organization thus allows a balanced deploy of attention for left-side damage but not for right-side injury. Although this view is largely compatible with the asymmetry of the ventral attentional network described in previous sections, it has lost support in the last years because of two main reasons. First, because it has been demonstrated that the right-lateralized components of the ventral network are mainly non-spatially selective (160, 157). And second, due to the lack of neuroimaging evidence showing asymmetries in the distribution of receptive fields in the posterior parietal areas that form part of the dorsal attentional network (767, 787, 786, 830). Instead, most research supports an alternative model, already presented in the discussion of Chapter 2, in which attentional deployment and visual selection depend on the competition and balance between hemispheres (439). In this view, hemispheres compete, pushing for selection of the opposite hemifield and inhibiting each other. The higher prevalence of left-sided neglect would be given by relative differences in the selection pressure (and contralateral inhibition) exerted by each hemisphere, with a normal stronger bias to the right side of the world by the left hemisphere. This would explain why the deficits in neglect syndrome are seen mostly after right-side lesions.

The hemispheric rivalry hypothesis is supported by several lines of evidence. Firstly, individual behavioral biases are correlated with structural asymmetries of the white-matter tracts that connect the dorsal attentional network, which in turn are likely related to functional asymmetries (851). Secondly, multiple functional studies support the idea of asymmetries

in the activity of two subsystems that conform a bilateral network, instead of one that is completely right lateralized (855, 827, 830, 451, 117, 829). For instance, during covert attention tasks, in the period between the cue and the target, the dorsal attentional network is activated bilaterally for unilateral cues, and the locus of attention can be predicted only by a measure of the relative difference in activity between hemispheres (855, 827, 788). Thirdly, in the pathological case, deficits are not produced only by an inter-hemispheric imbalance restricted to the injured area and its contralateral homologous; indirect dysfunction is also observed as inter-hemispheric asymmetries in the activity of non-injured areas, for example, the primary visual cortex (159, 341). Fourthly, these asymmetries of activity observed in the pathological case can be targeted in order to ameliorate neglect symptoms. This has been demonstrated in the last years through experimental inhibition with TMS of the left, uninjured, posterior parietal cortex of subjects with neglect (642, 643, 92). This procedure's goal is to bring back the lost balance between hemispheres, and it has indeed resulted in partial recovering of attentional deficits (778, 451). Fifth, as shown in the third experiment presented in Chapter 2, this also works in healthy subjects, where the unilateral inhibition of the right posterior parietal cortex, in this case producing an inter-hemispheric imbalance, also results in contralateral inattention (252, 70, 601, 854, 593, 633, 128). As the areas targeted for inhibition are within the bilateral dorsal attentional network, instead of the right-dominant ventral one, and given that the attentional effects happen almost exclusively after right cortical inhibition, these last studies support the idea of attention being mediated by competition within a bilateral, but asymmetric, network. In summary, multiples lines of evidence support the idea that a normal, quasi unbiased, attentional deployment is dependent on the competitive rivalry between the two hemispheres, with each one pushing for selection of their respective contralateral hemifields.

While the right-dominance model lacks of supporting evidence, the hemispheric rivalry model is still unable to explain why does the injury of right-lateralized regions, located in the ventral attentional network, exacerbate asymmetries within the dorsal network (159). Following their cortical dual network model of attention, Corbetta et al. suggested a middle point between dominance and rivalry models (157). In this account, neglect is produced by lesions of the subsystem that is almost exclusively dominant to the right. This ventral subnetwork mediates non-spatial functions involved in the detection of novel or behaviorally relevant stimuli. Its dysfunction results, by itself, in some of the non-spatial deficits that are also characteristic of neglect syndrome, for instance, of sustained attention (380). By some mechanism not yet well understood, impairment of the right-ventral network results in the dysfunction of several other areas involved in visual processing and visual selection. These effects would be larger for components within the dorsal subnetwork and early visual areas, with hyper activation of left-side areas and further indirect inhibition of other ipsi-lesional ones. Thus, although this explanation accommodates most of the neuropsychological and physiological data available to date, and gives an account of why most chronic neglect cases occur after right-side lesions, it still fails in explaining how an injury of the ventral, non-spatial, attentional network results in the pattern of additional imbalances in other non-injured spatial areas.

The hemispheric rivalry hypothesis gets further enriched when considering sources of imbalance at the subcortical level that interact with, and might be instrumental to, the cortical imbalances. Moreover, within the dysfunction of subcortical areas is where it is possible to find the best mechanistic explanations of how indirect asymmetries of cortical activity develop, for instance, through indirect excitotoxic subcortical damage (396). As the role of subcortical structures after injury was already discussed in Chapter 2 (2.5.2, p.34), in the following I will focus on the role of imbalances in two other, also subcortical, neuromodulator mechanisms, the noradrenergic and dopamine systems.

Bias and the noradrenergic system

The noradrenergic system modulates the attentional network and sensory processing areas (263, 698, 567, 160, 736). Noradrenaline (NA) inputs to the brain arise almost exclusively from the Locus Coeruleus (LC), a small nucleus in the brainstem that sends widespread projections to the brain (Fig. 8.1a). The effects of NA are principally neuromodulatory and, in general, result in a reduction of neurons' resting firing rate and in an enhancement of sensory responses, thus increasing neurons' signal-to-noise ratio (263). Together with the other neuromodulatory systems, NA mediates changes in general arousal and in the sleep-wake cycle (263, 661, 66). More specifically, the LC modulates arousal through changes in its phasic

and tonic profiles of activity. These changes result in an enhancement of the sensory processing of salient inputs and in task switching respectively (66, 25).

The NA system is involved in different aspects of attention, with a clear role in sustained attention (793). It is also likely involved in the production of asymmetries in visual selection, both for the pathological and normal case. In the normal case, levels of arousal and vigilance, in part produced by changes of NA tone, are correlated with subjects's spatial biases: the time to react to items in the left increases as general alertness decreases (39, 253), and subjects that show good sustained attention had stronger leftward biases in spatial tasks (59). These effects are likely due to an asymmetrical profile of projections from the LC to thalamus and cortex (637, 638, 316). It is also possible to speculate that changes in arousal produced by the appearance of an image, mediated by an asymmetric NA modulation of the cortex, might be in part responsible of the leftward bias shown here. However, this seems unlikely since we also demonstrated that this biased behavior is more frequent for short-latency movements. This might be too fast to occur through a phasic NA response and thus, if normal biases are linked to the NA system, is rather related to individual differences in NA tone. If this is the case, subject's leftward bias should be correlated with independent measures of sustained attention and it should change through the course of an experiment in such way that increased tiredness and drowsiness should result in less, instead of more bias.

In the pathological case, biases might be partly due to further NA cortical asymmetries secondary to cortical lesions. This has been observed in lesion studies in rats, in which right, but not left, fronto-parietal cortical lesions result in a widespread reduction of cortical NA activity. The reduction of NA is more marked in right-side structures (723), suggesting a link between right fronto-parietal cortex and top-down modulation of the LC, and another possible mechanism for the production of both non-spatial and spatial deficits in the neglect syndrome (157).

Bias and the dopaminergic system

As already mentioned in the General Introduction, circling behavior in animals is related to hemispheric asymmetries in dopaminergic activity. In fact, in the animal model of Parkinson's disease, obtained by unilateral chemical lesions of the basal ganglia dopaminergic system, the appearance of spontaneous circling behavior is the marker of a successful lesion (881, 759). As the basal ganglia circuit is clearly involved in motor control, it is not surprising that the unilateral loss of dopaminergic neurons results in an unilateral motor dysfunction. However, circling behavior is also accompanied by biased orientation responses to the ipsi-lesional side, and these are attributed to a combination of motor and sensory deficits (506, 122, 123, 579).

This influence of the basal ganglia circuit was later confirmed in relation to small, normal, asymmetries of dopaminergic activity. Healthy rats show asymmetries in dopamine between left and right basal ganglia up to 15%, resulting in slight biases of circling behavior to the side with the lower dopamine values (963, 298). Normal circling (and veering) behavior has also been studied in humans by measuring spontaneous full-turns in naive subjects. The results of such studies show the existence of systematic biases in the direction of the dominant hand (81, 82) and, in the case of patients with Parkinson's, contralateral to the most affected body side (i.e., to the side with the most degenerated dopaminergic system) (82). Furthermore, the supplementation of dopamine in healthy subjects, likely balancing the left-dominant basal ganglia activity of right-handers (179), results in less veering to the right in a walking-straight blindfolded task (580). However, circling and veering measures are not always consistent across experiments (580) and different measures of biased motor behavior are inconsistent even within subjects (581), thus these results need to be taken with caution.

Motor and sensory biases related to dopamine activity are also related to eye-movements control. Monkeys with unilateral chemical lesions of the dopaminergic system present a myriad of oculomotor disturbance, with biased spontaneous movement to the ipsi-lesional hemifield and impairment in the production of memory movements to the contra-lesional hemifield (421, 459, 579). In the case of humans' neglect syndrome, the administration of apomorphine, likely reducing normal dopamine asymmetries, reduces spatial bias (261, 292). In Chapter 5, we also show a slight rightward free-viewing bias in patients with left-onset PD which is consistent with other experiments that also show a bias to the side with less dopamine.

Also, partially in congruence with the subcortical/cortical inter-hemispheric rivalry model for neglect syndrome, DBS of the left STN influences viewing behavior, likely by restoring the activity imbalance produced by an asymmetrical dopamine profile. Furthermore, the effects of the dopamine system in viewing biases were also demonstrated by a reduced early leftward bias in patients, supporting the possibility of a strong role of asymmetries in the dopaminergic system in the production of normal biases.

Normal viewing bias and hemispheric rivalry

Normal viewing biases can also be partly explained by the rivalry model. This model assumes a slight imbalance between hemispheres, with a "stronger" left side. Such imbalance could explain some of the biases observed in healthy humans, like the small rightward bias seen in experiment 1 of Chapter 4. However, it fails to explain the multiple cases of normal leftward bias, as in most examples of pseudoneglect (394), and in the case of the strong free-viewing leftward bias shown in Chapter 3 and 4.

The results of recent studies indicate that the pattern of hemispheric rivalry is more complex than simply attributing a stronger weight to one hemisphere. This is revealed already by noticing that different studies with humans subjects disagree in the patterns of inter-hemispheric interactions, even for the same brain regions. For instance, the results of one experiment that used dynamic causal modeling analysis of fMRI data suggested a stronger right-to-left influence between intraparietal sulci (788). This was partly confirmed by an experiment with trifocal TMS that showed a stronger inhibition from a region in the posterior part of the right intraparietal sulcus over the left one (451). However, in a third study, in which the activation of different homologous areas in an attentional task was measured, multiple asymmetries were found (830): one in a region of the superior parietal lobe, which showed attentional activation only in the right; and the others in two regions in the left, the frontal eye field and the intraparietal sulcus, that showed stronger activation than their homologous in the right. Part of the disagreement between studies is likely to be caused by the use of techniques with different spatial accuracy. It is also likely that it reflects samples differences due to the small groups used. For example, in the third studied mentioned above, the subjects' spatial bias in a landmark task was to the right, whereas the general spatial bias seen in healthy subjects is more commonly to the left (394, 61). In summary, as different studies are not congruent, it suggest that there are multiple focus of asymmetric activity in the attentional network and with large variability between subjects.

A more comprehensive and simpler view of inter-hemispheric rivalry is obtained by looking, in a subject-by-subject basis, at the correlation between behavioral biases and a measure of asymmetric activity of the complete attentional network (829). This can be achieved by calculating the sum, in each hemisphere, of all areas "attentional weights", which are obtained by measuring all areas' activation in an attentional task. By comparing the total sum of each hemisphere, it results in an overall measure of functional asymmetry that correlates well with behavioral biases.

The dynamic pattern of biases seen during free-viewing consisted in, first, a strong leftward bias and then a slight rightward one. Considering the rivalry model and the possibility of multiple locus of imbalance between hemispheres, it is possible to speculate that the change in biases are due to changes in the overall distribution of activity between hemispheres. In the case of the free-viewing experiments presented here, the image appearance, a salient onset event in which a novel and complex stimulus appears, might result in the engagement of right-dominant posterior areas of both attentional subnetworks: the ventral-right subnetwork that is engaged by the appearance of a salient, relevant, stimulus, and of other components of the dorsal network that are exclusively present in the right or exert a stronger influence than the left side. All together, the activation of these areas would result in a inter-hemispheric imbalance that leads to a leftward bias. Afterwards, with the role of the ventral network subsiding, the influence of parietal and frontal areas that are stronger in the left hemisphere would bias attention to the right. This represents a more complex view of the rivalry model in which there are multiple nodes involved in the deployment of attention, with some completely lateralized, other stronger in one hemisphere than the other, and others fully balanced, all resulting in biases that change in time depending on the contribution at a given moment of each subcomponent to the global balance between hemispheres.

8.1.5 Tactile guidance of visual selection

The results presented in Chapter 4 demonstrate that touch, even when task-irrelevant, drives viewing behavior by inducing a global orienting response. This type of stimulus-driven guidance is not usually discussed in models of visual selection nor fits well with previous research about crossmodal attention. In our study, the tactile stimulation was unrelated to the task and there was no target stimulus that needed to be discriminated, so by itself this orienting effect does not represent a classical example of crossmodal attention.

In the study of crossmodal attention, in which a cue in a given modality facilitates the detection or discrimination of a target in a different one, it is important to differentiate between unimodal, crossmodal and supramodal mechanisms (210, 810). In the unimodal case, selection occurs independently for each modality; a peripheral cue drives selection exogenously only for posterior stimuli of the same type. However, by virtue of the task structure, for example, when the cue is spatially informative, the exogenous stimulus can also work as an endogenous cue for other modalities and in this way it might facilitate reaction times and discrimination responses. In contrast, in a supramodal mechanism, the cueing effect occurs through a common "workspace" that, in turn, influences the detection of stimuli in any modality (241, 517). These two alternatives are in disagreement with experimental evidence. A pure unimodal mechanism conflicts with the results of crossmodal exogenous cueing and capture tasks. In these tasks, an uninformative stimulus in one modality improves the discrimination of a target in a different modality when spatially congruent, and otherwise impairs it. This happens in a way that is consistent with an exogenous cueing effect (e.g., short-latency) rather than mediated by endogenous processes (806, 809, 811). Similarly, endogenous cueing to a location in one modality result in benefits in other modalities, even when unadaptive (805, 810). These results indicate that selection does not run in parallel for every sensory modality. An exclusive supramodal mechanism is also unlikely, since most of the effects are not symmetrical; it is still easier to detect a target when the cue belongs to the same modality (874). Also, there are both covert and overt reaction time benefits when crossmodal stimuli is used (i.e., coincident), in a way that suggest an integration mechanism rather than only statistical facilitation (321, 900, 272). In conclusion, most behavioral evidence suggest that attentional effects of crossmodal stimuli are the result of some multisensory integration mechanism.

As sensory information from different modalities is initially coded in different reference frames, this also makes necessary some type of multisensory integration, especially in the case of crossmodal tactile-visual tasks. In the case of touch, the position of a tactile stimulus in external coordinates depends on the position of the body and requires the transformation from a skin-based to an external reference frame. Even in the absence of a selection goal, this transformation requires the integration of propioceptive information. Moreover, although the remapping to external coordinates does not require necessarily the integration of visual information, there is plenty of behavioral evidence indicating that visual information bias strongly the judgement of limbs' positions (340, 75, 883, 312, 313). Thus, even without considering crossmodal attentional effects, the orienting to a tactile stimulus in external space requires the integration of information from multiple senses.

The orienting response seen in Chapter 4 does not involve increased discrimination or detection of a specific visual stimulus. Nevertheless, it resulted in an overt viewing bias that is directed to a side of the world instead of to the location where the stimulation occurred. Moreover, and specially in the case of the crossed-hands condition, it requires a transformation of frames of reference since the orienting effect was always to the location of stimulation in an external coordinate system. To understand the possible neural mechanism of this tactile orienting effect, it is therefore necessary to discuss some of the known neural mechanisms of multisensory integration, of the transformation between reference frames, and of crossmodal spatial attention.

Basic neural mechanisms of multisensory integration

The neural correlates of multisensory integration are defined as neural responses to bi or multimodal stimuli that are different from the responses to the most effective single modality, either by showing a significant enhancement or depression (560, 563, 820). This integration is accomplished by the combination of convergent signals from neurons with matching

receptive fields, and therefore, as the information comes from different sources, it usually requires to be transformed from different spatial and temporal reference frames (821, 563, 909, 910).

The first studies that demonstrated multimodal integration at the neural level where performed on the SC of the cat (560, 563, 909), and afterwards in the same midbrain structure in primates (910). In the SC, multisensory neurons are found only in the intermediate/deep motor layers (563, 910), within a cortico-tectal-reticulo-spinal pathway that is well suited for the control of spatial responses (561, 563, 562, 909). Importantly, for multisensory integration to occur at the SC it is necessary the influence of cortical afferents. The signals that are necessary for subcortical integration arise mainly from unimodal neurons that are located within multisensory areas (909). Without this cortical input, SC neurons are still responsive to the individual modalities but the neural and behavioral signatures of integration disappear (908, 924, 397, 398). As multisensory integration also occurs in the cortex but in neurons that are not directly involved on the effects observed in subcortical areas, this suggests that cortical and cortical-subcortical multisensory circuits function in parallel (819). According to this view, multisensory cortical neurons are involved in processes in "high-level" processes like: the transformation of reference frames; the planning of complex motor tasks like reaching and grasping (151, 13, 150); and in perceptual processes that are inherently multimodal as, for instance, in the perception of objects (10) and in the sense of body ownership (344, 71, 219). In contrast, multisensory integration occurring at subcortical structures, but mediated by cortical activity, would be responsible of the more basic crossmodal orienting responses discussed here.

Neural mechanisms of crossmodal orienting

Here, I discuss three possible ways tactile stimuli could influence visual selection: (1) by global orienting to a general body side independently of the external position where the stimulation occurred; (2) by local cueing to the position of stimulation in external coordinates; and (3) by global orienting to the side of external space where the stimulation occurred.

The possibility of the first mechanism is suggested by the neurophysiology of the SC. In both uni- and multi-sensory neurons in the SC, the latency to respond to auditory and somatosensory stimuli is approximately a fifth of the latency of visual stimuli ($\sim$20 against 100 ms) (910). This short-latency activation of the SC could in principle serve for a fast orienting response to non-visual stimuli, even without the benefits of multimodal integration. This fast activation is the result of direct afferents from the ascending sensory pathways. In the case of touch, the RFs of these neuronal responses correspond with the canonical position of body parts (910), which are high-wired from birth (911). Thus, fast orienting guided by the direct projections of the somatosensory pathway to the SC could only result in broad responses to a body side. This could be nevertheless helpful for the generation of fast avoidance responses, but even this type of reaction has been suggested to depend on cortical circuits (314). Moreover, even if the latency of neural response to a tactile stimulus is short in the SC, the latency to produce saccades to somatosensory targets is much slower than to visual ones (321, 617, 72). It is therefore unclear whether this fast activation of the SC plays a role in orienting processes and, in any case, it could not mediate the global cueing effect of touch seen in Chapter 3, which requires a transformation of coordinate systems.

Although the transformation from different reference frames can occur already in subcortical structures, most of our knowledge about sensory remapping comes from studies about the properties of multisensory neurons that are located in the parietal and frontal cortex (151, 150, 820). Specially in parietal cortex, there is a series of areas around the intraparietal sulcus that integrate visual, auditory and somatosensory information. The multisensory neurons that are sensitive to touch respond to visual and auditory stimuli in the peri-personal space. The corresponding visual RFs are coded in different reference frames across these areas, sometimes limb-centered, eye-centered, or in an intermediate reference frame. All together, the remapping of multimodal stimuli across different reference frames makes possible the integration of the different sensory systems and the coordination of different effector systems (13, 150). Besides the role of these neurons in the coordination of tactile and visual information for the manipulation of objects (151), their role in the transformation of reference frames makes them a prime candidate to mediate both local and global orienting effects of tactile stimuli in external coordinates.

Both local and global crossmodal selection might be mediated either by direct exogenous orienting, or by one modality serving as an endogenous cue for the other one. This last effect is likely to be mediated by the attentional network described previously (206, 519, 517, 160). In the case of exogenous crossmodal selection, there are at least three different possibilities. Firstly, again by activation of the cortical attentional network, in a similar way as it is proposed for salient visual stimuli and that was criticized in a previous section (p. 133). Secondly, by the feedback modulation of unimodal visual cortex by multisensory areas (517). This feedback modulation of primary sensory areas has been demonstrated extensively in the last years, in intracranial experiments that show crossmodal influences in primary auditory (294, 475), visual (476) and somatosensory cortex (424). These findings have been confirmed in human neuroimaging studies that demonstrate, for example, that congruent tactile-visual stimulation modulates neural activity in both primary visual and somatosensory cortex (518). This also occurs during saccade programming, independent of the task relevance of the tactile input (520). Therefore, a tactile stimulus, after being encoded in the appropriate external reference frame in a multisensory areas like the parietal cortex, might modulate the response to visual inputs in primary visual cortex and in this way bias selection. In turn, this could result in overt selection through an engagement of the cortical attentional network or by local mechanisms that engage directly with the SC, as discussed previously. Finally, multisensory cortical areas, that to some extent overlap with the attentional network, might mediate selection through the unimodal neurons within, via efferents to the SC.

In conclusion, overt visual selection can be guided by other modalities than vision. Although this is evident from real-life experience and a phenomenon that has been studied extensively with crossmodal attentional tasks with auditory and tactile stimuli, here we demonstrated that tactile cues can also work as global orienting cues. This function of sensory cues is not yet well incorporated in models of visual selection, which mostly deal with local guidance by visual stimuli, and its neural mechanisms are still unclear.

8.2 Visual processing and eye movements

The second part of this thesis deals with the effects of eye movements in the processing of visual information. This was studied with electroencephalography (EEG), and therefore it was necessary to first have a better understanding of the non-neural artifacts produced by eye movements. In Chapter 6 these artifacts were described together with a reliable approach to clean them from the data. In the following section, I will discuss how these advances have resulted in an increasing number of experiments with EEG that allow motion, not only of the eye but of the complete body. Afterwards, I will focus on the implications of the study described in Chapter 7 about the processing of actively-acquired visual information.

8.2.1 Electroencephalography, artifacts and action

EEG experiments that allow movements, and in particular, eye movements, have been performed since the fifties (238, 315). However, most EEG experiments, specially in the field of cognitive psychology, have usually been performed with severe movement restrictions. Experimental subjects were, and still are, usually asked to remain immobile and to avoid eye movements during experimental trials. As explained in the discussion of Chapter 6, this is not only uncomfortable and limits the type of experiments and cognitive processes that can be studied with EEG; it also imposes attentional loads that can potentially interfere with the process under study, and therefore confuse the interpretation of the results. Moreover, the way to deal with the still unavoidable production of movements of body and eyes (e.g. blinks) usually consists in the removal, from the final analysis, of trials containing artifacts, resulting in a reduction of experiments' statistical power.

Things have changed in the last two decades, mainly due to the adoption of advanced analysis techniques, some of them which are relatively new, like Independent Component Analysis (ICA). Crucially, as shown in Chapter 6, these new methods allow an efficient separation and removal of artifacts from the data and without the need to discard entire segments or trials. Many of these techniques, both old and new, were in the past also impractical because they are computationally intensive, and thus have become only recently feasible and available to everyone. In the work presented in Chapter 6, we assessed two different techniques for artifact removal, and following the recommendation of others (408, 385) we have also suggested the use of ICA to clean eye and muscle artifacts. Beyond simply removing unavoidable artifacts, the adoption of advanced cleaning methods like ICA has made possible to carry out experiments in which eye and body motion are not anymore a restriction but a goal, and thus also permitting to evaluate cognitive functions during real-life scenarios.

To study EEG brain activity in complex real-life scenarios it is not enough to have advanced methods for muscular and eye-movement removal. It is also essential to register the dynamics of the increased number of actions that are now allowed. Otherwise it is impossible to proper evaluate the neural correlates of such actions, both in terms of planning processes and of their sensory consequences. To keep track of these increased degrees of freedom, it has becomed necessary to use multiple sensor devices, like eye- and head-trackers, and other motion sensors that can track the movement of the limbs. In addition, all this information needs to be acquired in a format suitable for off-line analysis, a non-trivial problem that has resulted in the development of different platforms for the co-registration of EEG and the motor activity that occurs during eyes, head and whole-body motion (353, 101, 636, 11, 715). Such developments have recently made possible to address scientific questions that were impossible to answer just a decade ago, as for instance: the study of broad-motion control in humans; the decoding of walking kinematics from scalp brain activity (701, 330, 771, 11, 905, 102, 761); the search for neural correlates of arm movement control (186, 11, 436); and the study of neural correlates of human spatial navigation (905, 218).

As with any new technique development, results should be taken with extreme caution. For example, previous works that have demonstrated a linear correlation between EEG activity and limb movements kinematics have been recently challenged because it seems that such correlation was not relying in a brain activity signal (15, 125). Therefore, the development of a better understanding of the characteristics of electrical artifacts is also essential for the identification of

systematic sources of noise that might otherwise get confused with signatures of brain processes. Related to eye movements, two good examples of this are the effect of artifacts on the contingent negativity potential (363) and on estimates of gamma-band activity (954). This last problem has being under heavy scrutiny in the last years, since it seems that the results of many past studies that showed EEG gamma-band activity while performing cognitive functions were probably confused by the systematic production of small eye movements. This was due mostly to the effect of the spike potential, which happens even during microsaccades (364). Consequently, taking in account this type of artifacts has becoming the standard in the literature (124), and much of the earlier research showing wide-band gamma responses in EEG has to be now taken in account with extreme caution (954).

Another set of experiments have focused on validate classic EEG results under less constrained experimental settings. Some event-related potential components that have being used for decades to study sensory and perceptual processing in settings that restrained eye movements have now also been identified in settings that allow them. For instance, the P3 component, related to context updating and probabilistic surprise, has also been found after eye movements as shown in Chapter 7 and in other experiments (171, 96, 422). In the case of visual processing, multiple studies have shown by now that visual evoked responses are similar when eye movement are forbidden or allowed (656, 311, 172), and even during walking (501). All together, these new studies are validating the study of the neurophysiological correlates of cognition in more dynamic conditions. Thus, a new fertile field of study in cognitive science has appeared, in which the results of previous studies can be generalized to conditions closer to real-life scenarios. Moreover, it allows the study of some functions, specially the ones unique to humans, that were impossible to address before.

I would like to conclude this part with two other notes of caution. First, the techniques used for artifact detection and removal, although powerful, are not yet fully understood; their ability to completely remove noise without removing brain sources is still unclear. With respect to the results presented in Chapter 6, it is still necessary to further model the consequences of eye movement and to improve cleaning techniques. The limiting factor for a full validation of such methods is that, short of using a real physical model of the electrical activity of brain and eyes in the head, it is not possible to completely validate a cleaning technique with the certainty of not having also removed some brain activity. The second important thing to note is that as this studies are very recent, the enthusiastic generation of new experimental paradigms results in a risk of producing experiments that are poorly controlled. The inclusion of several degrees of freedom without proper measurement makes very possible, if they result in systematic effects, that they would get confused with effects of the mechanisms that are under study.

8.2.2 Predictive coding and sensory processing

In Chapter 7, I presented evidence that supports the occurrence of trans-saccadic predictions of visual content. These predictions were not limited to veridical content, based on actual retinal inputs, but also to inferred content that is perceived at the location of the blind spot. In the following, the relevance of these results will be discussed in relation to the different types of generative models that could underlie neural predictive coding.

Active visual prediction after eye movements

Previous experiments about the role of predictive coding in sensory processing have mostly consisted on passive tasks in which stimuli are presented in a repetitive, usually rhythmic, stream of identical items (e.g., 284, 825, 217, 858, 902). Although this presentation structure can clearly be learned by the subjects, its relevance to understand general mechanisms of sensory processing might be limited to the artificial conditions of this specific procedure. It is possible that the presentation of a repetitive stream of stimuli results in an ad-hoc adaptation, in which predictive signals are generated because the task consists in a repetitive stream, and not as the expression of a core mechanism of sensory processing. In contrast, in our experiment the stimulus predictability was not a consequence of the task's characteristics but of the regularity that exist between actions, in this case eye movements, and consequent changes in sensory inputs. The putative generative

model that would explain our results is not restricted to what is learned in the experiment but based on sensory-motor contingencies that are exercised every time an eye movement is performed. If such contingencies are learned by the brain, then the incoming sensory input after and eye movement could, in principle, be predicted through forward modeling of sensory content.

For this hypothesized modeling of future sensory inputs to work, it is essential the generation of an *efferent copy* of the eye-movement command. This is a copy of the movement signal sent to the motor centers and its existence has already been proved repeatedly in multiple neurophysiological and behavioral experiments in monkeys (reviewed in 803) and humans (e.g., 191, 727). The experiment presented in Chapter 7 supports the idea that efferent copies are used not only for the motor programming of successive actions (801, 803), or for keeping track of the attentional focus (941, 126), but also to make low- and high-level trans-saccadic predictions of sensory content.

Our results support a view of trans-saccadic prediction that contrast with some of the conclusions of previous research on trans-saccadic remapping, in which there is still controversy about what is actually remapped. In one of two main views, trans-saccadic remapping results in the remapping of specific sensory content. These predictions are nevertheless not considered a general mechanism of sensory processing since they would be selective only for salient objects (559). In contrast, a different position is that what is remapped is only a neural activity level, that is, a baseline pre-activation for the processing of a new stimulus. The role of this pre-activation is conceptualized as some kind of attentional "pointing" (126). In contrast to these two views, we planned and framed our experiment in terms of a general mechanism of neural coding, predictive coding, in which specific sensory content is predicted for every eye movement and attentional differences were discarded by experimental design.

We compared visual evoked responses to identical visual stimuli that are fixated after identical eye movements. Thus, our results are evidence that efferent copies are not only used for attentional remapping, but also for feature remapping. In other words, eye movements are accompanied of specific predictions of visual content. Although experimental evidence for such kind of content remapping during vision already exists (603, 825, 7, 454), in the last years it has been heavily argued against (126), mainly due to contradictory results of behavioral experiments that have failed to replicate early reports of trans-saccadic spatiotopic aftereffects (446, 300). However, in aftereffect experiments the pre-saccadic stimulus usually disappears prior the start of an eye movement and therefore this kind of task is not well suited to study sensory predictions of stable features of the world. In contrast, our experiment preserved the illusion of visual stability and stimuli' changes only occurred during eye movements. Accordingly, the presented results support the view of specific visual content being remapped across eye movements, in the form of spatiotopic predictions of future inputs.

Mechanisms of predictive coding

There is increasing evidence for some form of predictive coding being a fundamental neural mechanism. This is based on theoretical developments and computational modeling (711, 487, 279, 815, 48), as well as on multiple experimental results (e.g., 604, 284, 603, 825, 217, 858, 902, 454, 893, 235).

However, the theory is still unclear with respect to the type and extent of the generative models underlying predictive coding. The results of our experiment advocate for a generative model that produces predictions about transformations of sensory information that are induced by agents' actions. This suggests that a neural generative model is able to: (1) predict temporal changes of an existing sensory object, (2) based on long-term statistical regularities that (3) take in account information of the actions that are being performed. These three elements, and what they entail about the possibilities of predictive coding, are not always explicitly defined or discussed, although they point to possible large differences in the characteristics of generative models and their underlying neural mechanisms.

In the experiment presented in Chapter 7, the observed error signals were a response to an unexpected change of an already-present object. At first sight, this would appear as an intrinsic feature of the concept of prediction, the possibility to predict changes in the temporal domain. However, this simple distinction establishes an important point of difference between empirical and modeling work. As mentioned, most experiments consist in a repetitive stream of stimuli and therefore they test the ability to predict a sensory change in the temporal domain. In contrast, most computational models implement spatial predictions (711, 487, 815). In general, these computational examples of generative models do not predict the characteristics of a specific incoming input but of all possible inputs. In this way, pre-stimulus predictions are fixed, or slowly changing, and based on the learning of the spatial correlation structure of all stimuli that have been experienced by the model. Therefore, this type of computational models are non-adaptive and unable to predict the specific spatial and temporal characteristic of a new sensory input (816). Of course, a computational model can also be made dynamic, either by implementing a fast-changing learning rule, thus making it sensitive to the short-term history of stimulation, or through the explicit learning of the statistics of the transitions between inputs (816, 371, 815, 903). In both cases, a model would be able to produce tailored predictions of the characteristics of a new input but it will still not necessarily incorporate information about the moment of stimulus appearance. This contrasts with most experiments, which usually use auditory stimuli and require both, precise predictions of the short-term structure of transitions between inputs and about the exact timing of stimulation. For this to happen in a computational model, it needs to be explicitly temporal, as for instance with a spiking neural model (903). Thus, it is important when evaluating the results of an experiment or a model of predictive coding to discriminate whether predictions are spatial, or spatial and temporal, and whether temporal prediction means the learning of inputs' transition probabilities, the timing of next inputs, or both.

In the real-world, transitions between sensory inputs can take the form of the appearance or disappearance of a given object or sensory source. However, these are only a subset of all possible real-world transitions and arguably the ones with less predictive power, at least when agents are confronted with new environments. In contrast, changes in the temporal domain that can be reliably predicted take the form of transformations of existing objects. These transformations are the result of objects' movement, object's manipulation, or the movement of the observer (or their sensory surfaces as in the case of eye movements), and all are constrained in an exact way by the laws of physics. Surprisingly, although this type of transitions are ubiquitous, they are almost never tested, whereas a stream of repetitive stimuli without a discernible cause is a rare occurrence in real-life. In this respect, our experiment is almost unique since it test the existence of transformation predictions. Another relevant exception is an fMRI experiment about motion prediction by Alink *et al.* (7) showing that in the primary visual cortex of humans, the violation of predictions about the position of a moving stimulus results in a stronger activation, compatible with the generation of an error signal. These differences in the type of temporal predictions indicate that generative models can be of three types with respect to whether the change is a transformation of an existing object, its disappearance, or the appearance of a new stimulus. The first type is the result of lawful transformations of an existing input due to movement and perspective, and the other two are about contingent regularities that result in the appearance or disappearance of new stimuli. These differences probably imply also different neural mechanisms, with

transformation's predictions being dependent on long-term knowledge about the world structure and how it is transformed by actions, and the other two types depending on local, spatial and temporal, context.

Trans-saccadic predictions of the change an existing object will suffer are based on sensorimotor contingencies that are likely the result of a long-term learning process. In this way, the respective generative model behaves similarly to computational models that incorporate the complete statistics of previously experienced stimuli. In contrast, other experiments test an artificial scenario in which the probabilistic structure is exclusively confined to the experimental setting and the learning process occurs in a time span that goes from seconds to minutes or hours. It is important thus to also discriminate between generative models according to the span of the statistics they contain, whether they predict transformations that are the same in any scenario or if they are dependent on specific contexts. Since effective predictions depends on the statistics of possible inputs being stationary, this means that the most powerful generative models will be the ones that reflect characteristics of the world that are fixed like, for instance in the case of vision, its 3D spatial structure and perspective relationship with the observer. This kind of core predictive knowledge represent a long-term memory that changes only due to structural changes of the body (e.g., change in the distance between eyes or their optical properties). Moreover, it is essential to consider the role of agents' actions in this kind of reliable predictions. For instance, the knowledge about the 3D spatial structure of the world can be truly exploited only in conjunction to the knowledge of how this structure results in different inputs depending on changes in the point of view, changes that are usually a consequence of self-generated action.

Our results also indicate that predictions can be active, a direct consequence of subjects' actions. The role of action in generative models has been studied and discussed previously in relationship to motor control (938, 573) and the discrimination between self- and externally-generated inputs (573, 164, 803). In the first case, forward modeling can be an useful mechanism for the supervised learning of actions and for estimations of the state of the motor system that are necessary for precise motor control (573). In the second case, forward modeling is useful to cancel sensory information that is produced by the agent, for instance the sound of our own voice. In the case of vision, information about eye-movements command is used to produce the phenomena of saccade inhibition discussed in the General Introduction (1.2.1, *During movement effects*). Information about eye movement commands is also used for motor programming. This is most clear in the case of the double-step task, in which the goal is to make two sequential movements to the positions of two briefly flashed stimuli. To land the second movement successfully, it is necessary to integrate information from the first movement which is carried by a neural pathway that goes from the SC, through the thalamus, to the cortex (803). It is likely that, as suggested here, efferent copies are also used for the modeling of sensory information. Our results showed different error signals for movements of the same motor precision and accuracy and that are instead dependent on changes in the composition of the visual target and its reliability. Similar support for active predictions being used in perceptual processing is found in experiments that show spatial and temporal perceptual distortions in the peri-saccadic period. All together, the different lines of evidence indicate that generative models can also be classified in terms of whether they use or not information about motor commands to generate predictions. Furthermore, in the category of active models it is necessary to discriminate between prediction signals that are used either to cancel sensory processing, to control motion, or to predict the next input for perceptual processing. All these differences point also to different neural mechanisms. The suppression of sensory processing is mediated early on, in the case of vision, mostly at the thalamus level. The control of motion is likely mediated by efferent copies generated in the SC and that are integrated within the same structure or in cortical motor centers. Finally, predictive coding involved in sensory and perceptual processing likely occurs at several stages of the visual hierarchy.

To conclude, predictive coding is a mechanism involved in many different levels of motor control, sensory and perceptual processing. The exact type of prediction is produced by generative models with different characteristics in relation of how they integrate information from different spatial and temporal domains. These generative models sometimes work in a closed-loop fashion in which predictions are based on the learned consequences of actions. These functional difference are likely controlled by different neural circuits that are yet to be clearly characterized.

Acknowledgments

My first and greatest thanks goes to my supervisor Professor Peter König, not a single part of this work would have happened without your support, trust and advice. You provide a great working atmosphere of positive interactions among all the people working under you, in which full collaboration and critical discussion is encouraged, always in an ever friendly environment.

All the work presented here is the result of a collaborative effort of many people. Special thanks to the people from the Universities of Bern, Hamburg and UKE, that let me to collaborate with them: Professors Rene Müri and Andreas Engel, Christian Moll, Tobias Heed, Dario Cazzoli, and Alessandro Gulberti. I am deeply thankful of having being able to work with all the members of the NBP group. Some of them participated directly in the work presented here or in other ongoing projects; obviously without their help it would have not been possible to achieve any of this. So many, many thanks to Michael Plöchl, Selim Onat, Benedikt Ehinger, Johannes Keyser, Tim Kietzmann, Niklas Wilming, Petra Fischer, Zaeinab Afsari, Danja Porada and Alper Açık for having worked with me, I hope we can continue doing so in the future.

In my years in Germany I have made more friends that I can list, but I particularly want to mention and thank Saskia, Michael, Rob, Alper, Selim, Gerd, Adina, Tim, Danja, Niklas and Madhu.

Michael, Saskia and Rob proof-read earlier versions of this work and also some of the papers presented here. Thanks a lot for all your help!

Mi ultimas palabras de agradecimiento son para Melanie, por tu cariño y compañía, y para mi familia y superamigos en Chile. Gracias por todo el apoyo incondicional aunque significara tanta lejanía. Aunque estemos lejos, nunca me he sentido solo porque se que siempre puedo contar con ustedes. Un abrazo grande!

Disclaimer

All experiments reported in this thesis conform with the Declaration of Helsinki and have been approved by the ethics committees of the respective institution (University of Osnabrück, University of Bern, University Medical Center Hamburg Eppendorf). I hereby confirm that I wrote this thesis independently and that I have not made use of resources other than those indicated. I guarantee that I significantly contributed to all materials used in this thesis. Furthermore, this thesis was neither published in Germany nor abroad, except the parts indicated above, and has not been used to fulfill any other examination requirements.

Publication List

Articles

- Fischer P, **Ossandón JP** *, Keyser J, Gulberti A, Wilming N, Moll CKE, Engel AK, König P. Effects of dorsal and ventral subthalamic deep brain stimulation on free-viewing behaviour. *In review*
  (* shared first autorship)
- **Ossandón JP**, König P, Heed, T. Irrelevant tactile stimulation biases visual exploration in external coordinates. *Scientific Reports*, **5**, 10664 (2015). doi: 10.1038/srep10664
- Ehinger B, König P, **Ossandón JP**. Predictions of visual content across eye movements and their modulation by inferred information. *The Journal of Neuroscience*, **35**(19):7403-7413 (2015). doi:10.1523/JNEUROSCI.5114-14.2015
- **Ossandón JP**, Onat S, König P. Spatial biases in viewing behavior. *Journal of Vision*, **14**(2):20, 1-26 (2014). doi:10.1167/14.2.20
- **Ossandón JP**, Onat S, Cazzoli D, Nyffeler T, Müri R, König P. Unmasking the contribution of low-level features to the guidance of attention. *Neuropsychologia*, **50**:3478-3487 (2012). doi:10.1016/ j.neuropsychologia.2012.09.043
- Plöchl M, **Ossandón JP**, König P. Combining EEG and eye tracking: identification, characterisation, and correction of eye movement artifacts in electroencephalographic data. *Frontiers in Human Neuroscience*, **6**:278 (2012). doi:10.3389/fnhum.2012.00278

Conference Contributions

(* talk)

- **Ossandón JP***, Ehinger B, König P. Eye movement-related brain activity in visuospatial information processing. International Conference on Spatial Cognition, Rome, Italy, 7th-11th, September, 2015.
- **Ossandón JP**, Kietzmann T, Timm S, König P. A direct electrophysiological demonstration of object based sensory processing. European Conference on Visual Perception, Liverpool, England, 23th-27th, August, 2015.
- **Ossandón JP**, Heed T, König P. Tactile stimulation biases in free viewing behavior. 18th European Conference on Eye Movements, Vienna, Austria, 16th–21th, August, 2015.
- **Ossandón JP***, Ehinger B, König P. Predictions of visual content across eye movements and their modulation by inferred information. Eye Movements Gordon Research Seminar: Integrating Perception and Action for Optimal Vision, Waltham, USA, 25-26 July, 2015.
- **Ossandón JP**, König P, Heed T. Tactile stimulation biases in free viewing behavior. 16th International Multisensory Research Forum, Pisa, Italy, 13th–17th June, 2015.
- Keyser J, Fischer P, Gulberti A, **Ossandón JP**, Moll CK, Engel AK, König P. The influence of deep brain stimulation on eye movements in Parkinson's Disease: Modulation of visual attention by DBS during visual search. NCM 24th Annual Meeting, Amsterdam, The Netherlands, April, 2014.
- Fischer P, Keyser J, Gulberti A, **Ossandón JP**, Moll CK, König P, Engel AK. Deep brain stimulation in Parkinson's Disease patients modulates visual attention and explorative behaviour during free-viewing. NCM 24th Annual Meeting, Amsterdam, The Netherlands, April, 2014.
- **Ossandón JP**, Keyser J, Fischer P, Gulberti A, König P, Engel AK, Moll CK. Attentional biases in Parkinson's disease are task dependent and respond to ventral subthalamic deep brain stimulation. Rovereto Attention Workshop, Rovereto, Italy, October, 2013.
- Afsari Z, **Ossandón JP**, Krüser M, Hampel M, König P. The effect of language on the horizontal asymmetry in overt attention. Workshop on Eye Tracking Methods and Scan Path Analysis, Bielefeld, March, 2013.
- **Ossandón JP**, König P. Spatial biases in viewing behaviour. Workshop on Eye Tracking Methods and Scan Path Analysis, Bielefeld, March, 2013.
- **Ossandón JP***, Onat S, Cazzoli S, Nyffeler T, Mri R, Knig P. Unmasking the contribution of low-level features to the guidance of attention. Osnabrück Computational Cognition Alliance Meeting OCCAM 2012, Osnabrück, Germany, 4-6 June, 2012.
- **Ossandón JP**, Açık A, König P. Low in the forest, high in the city: Visual selection and natural image statistics. 34th European Conference on Visual Perception, Toulouse, France, August, 2011. Perception 40 ECVP Abstract Supplement, p. 95.
- Porada D, Goeke C, Schledde B, **Ossandón JP**, König P. Top-down but not bottom-up visual attention is mediated by parietal cortical areas during natural viewing. 16th European Conference on Eye Movements, Marseille, France, 21th–25th August, 2011.
- **Ossandón JP***, Onat S, König P. Dynamic spatial asymmetries in overt attention depend on handedness, but not gender, spatial frequency or image type. Symposium - Orienting the base towards prediction. 16th European Conference on Eye Movements, Marseille, France, 21th–25th August, 2011.
- **Ossandón JP***, Onat S, Cazzoli S, Nyffeler T, Müri R, König P. Unmasking the Contribution of Low-level Features to the Guidance of Attention. Program No. 429.4. 2010 Neuroscience Meeting Planner. San Diego, CA: Society for Neuroscience, 2010. Online.
- Helo A, **Ossandón JP**, Sameshima K, Morya E, Maldonado PE. Hemispheric differences in discrimination of facial expressions: The role of spectral components. Program No. 909.16. 2010 Neuroscience Meeting Planner. San Diego, CA: Society for Neuroscience, 2010. Online.

Publication List

- **Ossandón JP***, Onat S, Cazzoli S, Nyffeler T, Müri R, König P. Unmasking the contribution of low-level features to the guidance of attention. Symposium - Adaptivity of Hybrid Cognitive Systems. 10th Biannual Meeting of the German Society for Cognitive Science, KogWis , Potsdam, Germany, October, 2010.
- **Ossandón JP**, Müri R, Cazzoli D, Nyffeler T, Onat S, König P. Increased influence of low-level stimulus features on fixations in neglect patients. 7th FENS forum of european neuroscience, Amsterdam, The Netherlands, 3th–7th July. FENS Abstr. vol 5, 145.18, 2010.
- Plöchl M, **Ossandón JP**, König P. Characterization of eye movement artifacts in EEG data and the implication for artifact-correction algorithms. 15th European Conference on Eye Movements, Southampton, England, 23th–27th August, 2009.

Contents (detailed)

Bibliography

[1] A. Açik, S. Onat, F. Schumann, W. Einhäuser, and P. König. Effects of luminance contrast and its modifications on fixation behavior during free viewing of images from different categories. *Vision research*, 49(12):1541–53, 2009.

[2] S. Aglioti, N. Smania, C. Barbieri, and M. Corbetta. Influence of stimulus salience and attentional demands on visual search patterns in hemispatial neglect. *Brain and cognition*, 34(3):388–403, 1997.

[3] G. Aguirre, E. Zarahn, and M. D'esposito. An area within human ventral cortex sensitive to building stimuli: evidence and implications. *Neuron*, 21:373–383, 1998.

[4] G. K. Aguirre and M. D'Esposito. Topographical disorientation: a synthesis and taxonomy. *Brain*, 122 (Pt 9):1613–28, 1999.

[5] M. Ahissar and S. Hochstein. Attentional control of early perceptual learning. *Proceedings of the National Academy of Sciences*, 90:5718–5722, 1993.

[6] M. Ahissar and S. Hochstein. Task difficulty and the specificity of perceptual learning. *Nature*, 387:401–406, 1997.

[7] A. Alink, C. M. Schwiedrzik, A. Kohler, W. Singer, and L. Muckli. Stimulus predictability reduces responses in primary visual cortex. *Journal of Neuroscience*, 30(8):2960–6, 2010.

[8] J. Allman, F. Miezin, and E. McGuinness. Stimulus specific responses from beyond the classical receptive field: neurophysiological mechanisms for local-global comparisons in visual neurons. *Annual review of neuroscience*, 8:407–430, 1985.

[9] G. A. Alvarez and P. Cavanagh. Independent resources for attentional tracking in the left and right visual hemifields. *Psychological science*, 16(8):637–43, 2005.

[10] A. Amedi, K. Von Kriegstein, N. M. Van Atteveldt, M. S. Beauchamp, and M. J. Naumer. Functional imaging of human crossmodal identification and object recognition. *Experimental Brain Research*, 166:559–571, 2005.

[11] J. L. Amengual, J. Marco-Pallarés, C. Grau, T. F. Münte, and A. Rodríguez-Fornells. Linking motor-related brain potentials and velocity profiles in multi-joint arm reaching movements. *Frontiers in human neuroscience*, 8(April):271, 2014.

[12] R. Amlôt, R. Walker, J. Driver, and C. Spence. Multimodal visualsomatosensory integration in saccade generation. *Neuropsychologia*, 41:1–15, 2003.

[13] R. A. Andersen and C. A. Buneo. Intentional maps in posterior parietal cortex. *Annual review of neuroscience*, 25:189–220, 2002.

[14] S. J. Anderson, K. T. Mullent, and R. F. Hesst. Human peripheral spatial resolution for achromatic retinal factors. *Journal of Physiology*, 442:47–64, 1991.

[15] J. M. Antelis, L. Montesano, A. Ramos-Murguialday, N. Birbaumer, and J. Minguez. On the Usage of Linear Regression Models to Reconstruct Limb Kinematics from Low Frequency EEG Signals. *PLoS ONE*, 8(4), 2013.

[16] A. Antervo, R. Hari, T. Katila, T. Ryhänen, and M. Seppänen. Magnetic fields produced by eye blinking. *Electroencephalography and clinical neurophysiology*, 61(4):247–53, 1985.

[17] C. A. Antoniades, P. Buttery, J. J. FitzGerald, R. A. Barker, R. H. S. Carpenter, and C. Watts. Deep brain stimulation: eye movements reveal anomalous effects of electrode placement and stimulation. *PloS one*, 7(3):e32830, 2012.

[18] C. A. Antoniades, R. H. S. Carpenter, and Y. Temel. Deep brain stimulation of the subthalamic nucleus in Parkinson's disease: similar improvements in saccadic and manual responses. *Neuroreport*, 23(3):179–83, 2012.

[19] G. Arden and P. Constable. The electro-oculogram. *Progress in retinal and eye research*, 25(2):207–48, 2006.

[20] G. Arden and J. Kelsey. Changes produced by light in the standing potential of the human eye. *The Journal of physiology*, 161:189–204, 1962.

[21] J. C. Armington. Visual Psychophysics and Physiology. In J. C. Armington, editor, *Visual Psychophysics and Physiology*, chapter 29, pages 363–372. Elsevier, 1978.

[22] A. Asadollahi, S. P. Mysore, and E. I. Knudsen. Stimulus-driven competition in a cholinergic midbrain nucleus. *Nature neuroscience*, 13(7):889–95, 2010.

[23] J. Ashburner and K. J. Friston. Unified segmentation. *NeuroImage*, 26(3):839–51, 2005.

[24] P. Astikainen, E. Lillstrang, and T. Ruusuvirta. Visual mismatch negativity for changes in orientation–a sensory memory-dependent response. *The European journal of neuroscience*, 28(11): 2319–24, 2008.

[25] G. Aston-Jones and J. D. Cohen. An integrative theory of locus coeruleus-norepinephrine function: adaptive gain and optimal performance. *Annual review of neuroscience*, 28:403–50, 2005.

[26] J. Atick. Could information theory provide an ecological theory of sensory processing? *Network: Computation in Neural Systems*, 3:213–251, 1992.

[27] F. Attneave. Some informational aspects of visual perception. *Psychological review*, 61(3):183–193, 1954.

[28] D. Attwell and S. B. Laughlin. An energy budget for signaling in the grey matter of the brain. *Journal of cerebral blood flow and metabolism*, 21:1133–1145, 2001.

[29] H. Awater, J. Kerlin, K. Evans, and F. Tong. Cortical representation of space around the blind spot. *Journal of Neurophysiology*, 94(5):3314–3324, 2005.

[30] E. Awh, K. M. Armstrong, and T. Moore. Visual and oculomotor selection: links, causes and implications for spatial attention. *Trends in cognitive sciences*, 10(3):124–30, 2006.

[31] E. Azañón and S. Soto-Faraco. Changing reference frames during the encoding of tactile events. *Current biology*, 18(14):1044–9, 2008.

[32] E. Azañón, K. Camacho, and S. Soto-Faraco. Tactile remapping beyond space. *The European journal of neuroscience*, 31(10):1858–67, 2010.

[33] W. F. Bacon and H. E. Egeth. Overriding stimulus-driven attentional capture. *Perception & psychophysics*, 55(5):485–96, 1994.

[34] S. Badde, B. Röder, and T. Heed. Multiple spatial representations determine touch localization on the fingers. *Journal of experimental psychology. Human perception and performance*, 40(2): 784–801, 2014.

[35] S. Badde, B. Röder, and T. Heed. Flexibly weighted integration of tactile reference frames. *Neuropsychologia*, In Press, 2014.

[36] R. Baddeley, L. F. Abbott, M. C. a. Booth, F. Sengpiel, T. Freeman, E. a. Wakeman, and E. T. Rolls. Responses of neurons in primary and inferior temporal visual cortices to natural scenes. *Proceedings of the Royal Society of London. Series B: Biological Sciences*, 264(1389):1775–1783, 1997.

[37] R. J. Baddeley and B. W. Tatler. High frequency edges (but not contrast) predict where we fixate: A Bayesian system identification analysis. *Vision research*, 46(18):2824–33, 2006.

[38] P. F. Balan and J. Gottlieb. Integration of exogenous input into a dynamic salience map revealed by perturbing attention. *Journal of Neuroscience*, 26(36):9239–9249, 2006.

[39] C. A. Bareham, T. Manly, O. V. Pustovaya, S. K. Scott, and T. A. Bekinschtein. Losing the left side of the world: Rightward shift in human spatial attention with sleep onset. *Scientific Reports*, 4:1–5, 2014.

[40] H. Barlow. Possible principles underlying the transformations of sensory messages. In W. Rosenblith, editor, *Sensory Communication*, pages 217–234. MIT Press, Cambridge, MA, 1961.

[41] H. Barlow. Unsupervised Learning, 1989.

[42] H. Barlow. Redundancy reduction revisited. *Network*, 12:241–253, 2001.

[43] W. Barry and G. Jones. Influence of eye lid movement upon electro-oculographic recording of vertical eye movements. *Aerospace medicine*, 36:855–8, 1965.

[44] P. Bartolomeo, M. Thiebaut de Schotten, and F. Doricchi. Left unilateral neglect as a disconnection syndrome. *Cerebral cortex*, 17(11):2479–90, 2007.

[45] P. Bartolomeo, M. Thiebaut de Schotten, and A. Chica. Brain networks of visuospatial attention and their disruption in visual neglect. *Frontiers in Human Neuroscience*, 6:110, 2012.

[46] J. J. S. Barton, N. Radcliffe, M. V. Cherkasova, J. Edelman, and J. M. Intriligator. Information processing during face recognition: The effects of familiarity, inversion, and morphing on scanning fixations. *Perception*, 35(8):1089–1105, 2006.

[47] H. S. Bashinski and V. R. Bacharach. Enhancement of perceptual sensitivity as the result of selectively attending to spatial locations. *Perception & Psychophysics*, 28(3):241–248, 1980.

[48] A. M. Bastos, W. M. Usrey, R. a. Adams, G. R. Mangun, P. Fries, and K. J. Friston. Canonical microcircuits for predictive coding. *Neuron*, 76(4):695–711, 2012.

[49] P. M. Bays, V. Singh-Curry, N. Gorgoraptis, J. Driver, and M. Husain. Integration of goal- and stimulus-related visual signals revealed by damage to human parietal cortex. *The Journal of neuroscience*, 30(17):5968–78, 2010.

[50] J. Beaumont. Lateral organization and aesthetic preference: the importance of peripheral visual asymmetries. *Neuropsychologia*, 23(1):103–113, 1985.

[51] D. Beck, G. Rees, C. Frith, and N. Lavie. Neural correlates of change detection and change blindness. *Nature neuroscience*, 4(6):645–650, 2001.

[52] D. M. Beck, N. Muggleton, V. Walsh, and N. Lavie. Right parietal cortex plays a critical role in change blindness. *Cerebral cortex*, 16(5):712–7, 2006.

[53] W. Becker and A. Fuchs. Lid-Eye Coordination during vertical gaze changes in man and monkey. *J Neurophysiol*, 60(4):1227–1252, 1988.

[54] M. Beckstead, B. Edwards, and A. Frankfurter. A comparison of the intranigral distribution of nigrotectal neurons labeled with horseradish peroxidase in the monkey, cat, and rat. *The Journal of neuroscience*, 1(2):121–125, 1981.

[55] B.-P. Bejjani, I. Arnulf, J.-L. Houeto, D. Milea, S. Demeret, B. Pidoux, P. Damier, P. Cornu, D. Dormont, and Y. Agid. Concurrent excitatory and inhibitory effects of high frequency stimulation: an oculomotor study. *Journal of neurology, neurosurgery, and psychiatry*, 72(4):517–22, 2002.

[56] T. A. Bekinschtein, S. Dehaene, B. Rohaut, F. Tadel, L. Cohen, and L. Naccache. Neural signature of the conscious processing of auditory regularities. *Proceedings of the National Academy of Sciences of the United States of America*, 106(5):1672–7, 2009.

[57] A. Bell and T. Sejnowski. The "independent components" of natural scenes are edge filters. *Vision research*, 37(23):3327–38, 1997.

[58] A. J. Bell and T. J. Sejnowski. An information-maximization approach to blind separation and blind deconvolution. *Neural computation*, 7(6):1129–59, 1995.

[59] M. A. Bellgrove, P. M. Dockree, L. Aimola, and I. H. Robertson. Attenuation of spatial attentional asymmetries with poor sustained attention. *Neuroreport*, 15(6):1065–1069, 2004.

[60] A. V. Belopolsky, L. Zwaan, J. Theeuwes, and A. F. Kramer. The size of an attentional window modulates attentional capture by color singletons. *Psychonomic bulletin & review*, 14(5):934–8, 2007.

[61] C. S. Benwell, G. Thut, G. Learmonth, and M. Harvey. Spatial attention: Differential shifts in pseudoneglect direction with time-on-task and initial bias support the idea of observer subtypes. *Neuropsychologia*, 51(13):2747–2756, 2013.

[62] P. Berg and M. B. Davies. Eyeblink-related potentials. *Electroencephalography and clinical neurophysiology*, 69(1):1–5, 1988.

[63] P. Berg and M. Scherg. Dipole modelling of eye activity and its application to the removal of eye artefacts from the EEG and MEG. *Clinical physics and physiological measurement*, 12 Suppl A: 49–54, 1991.

Bibliography

[64] O. Bergamin, S. Bizzarri, and D. Straumann. Ocular torsion during voluntary blinks in humans. *Investigative ophthalmology & visual science*, 43(11):3438–43, 2002.

[65] J. Bergen and B. Julesz. Rapid discrimination of visual patterns. *IEEE Transactions on systems, man, and cybernetics*, 13(5):857–863, 1983.

[66] C. W. Berridge and B. D. Waterhouse. The locus coeruleus-noradrenergic system: modulation of behavioral state and state-dependent cognitive processes. *Brain research. Brain research reviews*, 42(1):33–84, 2003.

[67] T. Betz, T. Kietzmann, N. Wilming, and P. König. Investigating task-dependent top-down effects on overt visual attention. *Journal of vision*, 10(3):1–14, 2010.

[68] T. Betz, N. Wilming, C. Bogler, J.-D. Haynes, and P. König. Dissociation between saliency signals and activity in early visual cortex. *Journal of vision*, 13(14):1–12, 2013.

[69] J. W. Bisley and M. E. Goldberg. Attention, intention, and priority in the parietal lobe. *Annual review of neuroscience*, 33:1–21, 2010.

[70] O. Bjoertomt, A. Cowey, and V. Walsh. Spatial neglect in near and far space investigated by repetitive transcranial magnetic stimulation. *Brain*, 125(Pt 9):2012–22, 2002.

[71] O. Blanke. Multisensory brain mechanisms of bodily self-consciousness. *Nature Reviews Neuroscience*, 13:556–571, 2012.

[72] O. Blanke and O. J. Grüsser. Saccades guided by somatosensory stimuli. *Vision research*, 41(18):2407–12, 2001.

[73] A. Borji and L. Itti. State-of-the-art in visual attention modeling. *IEEE transactions on pattern analysis and machine intelligence*, 35(1):185–207, 2013.

[74] A. Borji, D. N. Sihite, and L. Itti. Objects do not predict fixations better than early saliency : A re-analysis of Einhäuser et al.'s data. *Journal of vision*, 13(10):18, 1–4, 2013.

[75] M. Botvinick and J. Cohen. Rubber hand feels touch that eyes see. *Nature*, 391:756, 1998.

[76] L. Bour, M. Aramideh, and B. de Visser. Neurophysiological aspects of eye and eyelid movements during blinking in humans. *Journal of neurophysiology*, 83(1):166–76, 2000.

[77] J. Bourassa and M. Deschênes. Corticothalamic projections from the primary visual cortex in rats: A single fiber study using biocytin as an anterograde tracer. *Neuroscience*, 66(2):253–263, 1995.

[78] S. Bouret and S. J. Sara. Network reset: a simplified overarching theory of locus coeruleus noradrenaline function. *Trends in Neurosciences*, 28(11):574–582, 2005.

[79] D. Boussaoud, R. Desimone, and L. G. Ungerleider. Visual topography of area TEO in the macaque. *The Journal of comparative neurology*, 306:554–575, 1991.

[80] A. Bowen, K. McKenna, and R. C. Tallis. Reasons for variability in the reported rate of occurrence of unilateral spatial neglect after stroke. *Stroke*, 30:1196–1202, 1999.

[81] H. S. Bracha, D. J. Seitz, J. Otemaa, and S. D. Glick. Rotational movement (circling) in normal humans: sex difference and relationship to hand, foot and eye preference. *Brain Research*, 411(2): 231–235, 1987.

[82] H. S. Bracha, C. Shults, S. D. Glick, and J. E. Kleinman. Spontaneous asymmetric circling behavior in hemi-parkinsonism; a human equivalent of the lesioned-circling rodent behavior. *Life sciences*, 40(11):1127–1130, 1987.

[83] D. H. Brainard. The psychophysics toolbox. *Spatial vision*, 10(4):433–436, 1997.

[84] D. Braun, H. Weber, T. Mergner, and J. Schulte-Mönting. Saccadic reaction times in patients with frontal and parietal lesions. *Brain*, 115:1359–1386, 1992.

[85] J. B. Brayanov and M. A. Smith. Bayesian and Anti-Bayesian Biases in Sensory Integration for Action and Perception in the Size Weight Illusion. *Journal of neurophysiology*, 103:1518–1531, 2010.

[86] J. Brefczynski and E. DeYoe. A physiological correlate of the 'spotlight' of visual attention. *Nature neuroscience*, 2(4):370–374, 1999.

[87] F. Bremmer, M. Kubischik, K.-P. Hoffmann, and B. Krekelberg. Neural dynamics of saccadic suppression. *The Journal of neuroscience*, 29(40):12374–83, 2009.

[88] K. A. Briand. Feature integration and spatial attention: More evidence of a dissociation between endogenous and exogenous orienting. *Journal of Experimental Psychology: Human Perception and Performance*, 24(4):1243–1256, 1998.

[89] K. A. Briand, D. Strallow, W. Hening, H. Poizner, and A. B. Sereno. Control of voluntary and reflexive saccades in Parkinson's disease. *Experimental Brain Research*, 129(1):38–48, 1999.

[90] B. Bridgeman. Efference copy and its limitations. *Computers in Biology and Medicine*, 37:924–929, 2007.

[91] B. Bridgeman and J. Palca. The role of microsaccades in high acuity observational tasks. *Vision research*, 20(9):813–7, 1980.

[92] F. Brighina, E. Bisiach, M. Oliveri, A. Piazza, V. La Bua, O. Daniele, and B. Fierro. 1 Hz repetitive transcranial magnetic stimulation of the unaffected hemisphere ameliorates contralesional visuospatial neglect in humans. *Neuroscience Letters*, 336(2):131–133, 2003.

[93] D. Bristow, J.-D. Haynes, R. Sylvester, C. D. Frith, and G. Rees. Blinking suppresses the neural response to unchanging retinal stimulation. *Current biology*, 15(14):1296–300, 2005.

[94] D. Broadbent. *Perception and Communication*. Pergamon Press, London, 1958. ISBN 1483225828.

[95] E. Brodie and L. Pettigrew. Note Is left always right? Directional deviations in visual line bisection as a function of hand and initial scanning direction. *Neuropsychologia*, 34(5):467–470, 1996.

[96] A.-M. Brouwer, B. Reuderink, J. Vincent, M. a. J. V. Gerven, and J. B. F. V. Erp. Distinguishing between target and nontarget fixations in a visual search task using fixation-related potentials. *Journal of Vision*, 13(3):17, 2013.

[97] N. Bruce and J. Tsotsos. Saliency, attention, and visual search: An information theoretic approach. *Journal of Vision*, 9(3):5, 1–24, 2009.

[98] M. Bryden. Tachistoscopic recognition, handedness, and cerebral dominance. *Neuropsychologia*, 3(1):1–8, 1965.

[99] V. N. Buchholz, O. Jensen, and W. P. Medendorp. Multiple reference frames in cortical oscillatory activity during tactile remapping for saccades. *The Journal of neuroscience*, 31(46):16864–71, 2011.

[100] C. Buhmann, L. Maintz, J. Hierling, E. Vettorazzi, C. K. E. Moll, A. K. Engel, C. Gerloff, W. Hamel, and W. H. Zangemeister. Effect of subthalamic nucleus deep brain stimulation on driving in Parkinson disease. *Neurology*, 82(1):32–40, 2014.

[101] T. C. Bulea, A. Kilicarslan, R. Ozdemir, W. H. Paloski, and J. L. Contreras-Vidal. Simultaneous scalp electroencephalography (EEG), electromyography (EMG), and whole-body segmental inertial recording for multi-modal neural decoding. *Journal of visualized experiments*, 77:e50602, 2013.

[102] T. C. Bulea, J. Kim, D. L. Damiano, C. J. Stanley, and H.-S. Park. Prefrontal, posterior parietal and sensorimotor network activity underlying speed control during walking. *Frontiers in Human Neuroscience*, 9(May), 2015.

[103] M. W. Burke, R. Kupers, and M. Ptito. Adaptive neuroplastic responses in early and late hemispherectomized monkeys. *Neural Plasticity*, 2012:852423, 2012.

[104] D. Burr and J. Ross. Contrast sensitivity at high velocities. *Vision research*, 22:479–484, 1982.

[105] D. Burr, M. Morrone, and J. Ross. Selective suppression of the magnocelular visual pathway during saccadic eye movemnts. *Nature*, 371:511–513, 1994.

[106] B. E. Burrows and T. Moore. Influence and limitations of popout in the selection of salient visual stimuli by area V4 neurons. *The Journal of neuroscience*, 29(48):15169–77, 2009.

[107] D. Burt and D. Perrett. Perceptual asymmetries in judgements of facial attractiveness, age, gender, speech and expression. *Neuropsychologia*, 35:685–693, 1997.

[108] T. J. Buschman and E. K. Miller. Top-down versus bottom-up control of attention in the prefrontal and posterior parietal cortices. *Science*, 315(5820):1860–2, 2007.

[109] T. J. Buschman, M. Siegel, J. E. Roy, and E. K. Miller. Neural substrates of cognitive capacity limitations. *PNAS*, 108(27):11252–11255, 2011.

[110] M. Bushnell, M. Goldberg, and D. Robinson. Behavioral enhancement of visual responses in monkey cerebral cortex. I. Modulation in posterior parietal cortex related to selective visual attention. *Journal of neurophysiology*, 46(4):755–772, 1981.

[111] G. T. Buswell. *How people look at pictures: A study of the psychology of perception in art*. University of Chicago Press, Chicago, 1935.

[112] S. Butler, I. D. Gilchrist, D. M. Burt, D. I. Perrett, E. Jones, and M. Harvey. Are the perceptual biases found in chimeric face processing reflected in eye-movement patterns? *Neuropsychologia*, 43(1):52–9, 2005.

[113] S. H. Butler and M. Harvey. Perceptual biases in chimeric face processing: eye-movement patterns cannot explain it all. *Brain research*, 1124(1):96–9, 2006.

[114] S. H. Butler and M. Harvey. Effects of aging and exposure duration on perceptual biases in chimeric face processing. *Cortex*, 44(6):665–72, 2008.

[115] C. M. Butter, H. A. Buchtel, and R. Santucci. Spatial attentional shifts: further evidence for the role of polisensory mechanisms using visual and tactile stimuli. *Neuropsychologia*, 27(10): 1231–40, 1989.

[116] R. H. Cai, A. Pouget, M. Schlag-Rey, and J. Schlag. Perceived geometrical relationships affected by eye-movement signals. *Nature*, 386:601–604, 1997.

[117] P. Capotosto, C. Babiloni, G. L. Romani, and M. Corbetta. Differential Contribution of Right and Left Parietal Cortex to the Control of Spatial Attention: A Simultaneous EEG-rTMS Study. *Cerebral Cortex*, 22(2):446–454, 2012.

[118] A. Caramazza and J. R. Shelton. Domain-specific knowledge systems in the brain the animate-inanimate distinction. *Journal of cognitive neuroscience*, 10(1):1–34, 1998.

[119] M. Carandini. Area V1. *Scholarpedia*, 7(7):12105, 2012.

[120] M. Carandini, J. B. Demb, V. Mante, D. J. Tolhurst, Y. Dan, B. a. Olshausen, J. L. Gallant, and N. C. Rust. Do we know what the early visual system does? *The Journal of neuroscience*, 25(46): 10577–97, 2005.

[121] C. Carl, A. Açik, P. König, A. K. Engel, and J. F. Hipp. The saccadic spike artifact in MEG. *NeuroImage*, 59(2):1657–67, 2012.

[122] M. Carli, J. L. Evenden, and T. W. Robbins. Depletion of unilateral striatal dopamine impairs initiation of contralateral actions and not sensory attention. *Nature*, 313:679–682, 1985.

[123] M. Carli, G. Jones, and T. Robbins. Effects of unilateral dorsal and ventral striatal dopamine depletion on visual neglect in the rat: A neural and behavioural analysis. *Neuroscience*, 29(2): 309–327, 1989.

[124] J. Castelhano, J. Rebola, B. Leitão, E. Rodriguez, and M. Castelo-Branco. To Perceive or Not Perceive: The Role of Gamma-band Activity in Signaling Object Percepts. *PLoS ONE*, 8(6):35–37, 2013.

[125] T. Castermans, M. Duvinage, G. Cheron, and T. Dutoit. About the cortical origin of the low-delta and high-gamma rhythms observed in EEG signals during treadmill walking. *Neuroscience Letters*, 561:166–170, 2014.

[126] P. Cavanagh, A. R. Hunt, A. Afraz, and M. Rolfs. Visual stability based on remapping of attention pointers. *Trends in cognitive sciences*, 14(4):147–53, 2010.

[127] K. R. Cave. The FeatureGate model of visual selection. *Psychological Research*, 62(2-3):182–194, 1999.

[128] D. Cazzoli, P. Wurtz, R. M. Müri, C. W. Hess, and T. Nyffeler. Interhemispheric balance of overt attention: a theta burst stimulation study. *The European journal of neuroscience*, 29(6):1271–6, 2009.

[129] C. D. Chambers, J. M. Payne, M. G. Stokes, and J. B. Mattingley. Fast and slow parietal pathways mediate spatial attention. *Nature neuroscience*, 7(3):217–8, 2004.

[130] S. Cheadle, V. Wyart, K. Tsetsos, N. Myers, V. de Gardelle, S. Herce Castañón, and C. Summerfield. Adaptive gain control during human perceptual choice. *Neuron*, 81(6):1429–41, 2014.

[131] M. Cheal and D. R. Lyon. Central and peripheral precuing of forced-choice discrimination. *The Quarterly Journal of Experimental Psychology Section A*, 43(4):859–880, 1991.

[132] C.-M. Chen, P. Lakatos, A. S. Shah, A. D. Mehta, S. J. Givre, D. C. Javitt, and C. E. Schroeder. Functional Anatomy and Interaction of Fast and Slow Visual Pathways in Macaque Monkeys. *Cerebral Cortex*, 17:1561–1569, 2007.

[133] S. Chennu, V. Noreika, D. Gueorguiev, A. Blenkmann, S. Kochen, A. Ibáñez, A. M. Owen, and T. A. Bekinschtein. Expectation and attention in hierarchical auditory prediction. *The Journal of neuroscience*, 33(27):11194–205, 2013.

[134] C. Cherry. Some Experiments on the Recognition of Speech, with One and with Two Ears. *The Journal of he Acoustical Society of America*, 25(5):975–979, 1953.

[135] C. H. Chiang, A. O. Ballantyne, and D. A. Trauner. Development of perceptual asymmetry for free viewing of chimeric stimuli. *Brain and cognition*, 44(3):415–24, 2000.

[136] E. J. Chichilnisky. A simple white noise analysis of neuronal light responses. *Network: Computation in Neural Systems*, 12:199–213, 2001.

[137] G. Chioran and R. Yee. Analysis of electro-oculographic artifact during vertical saccadic eye movements. *Graefe's archive for clinical and experimental ophthalmology*, 229:237–241, 1991.

[138] S. Chokron and M. De Agostini. Reading habits influence aesthetic preference. *Cognitive brain research*, 10(1-2):45–9, 2000.

[139] J. Christie, J. P. Ginsberg, J. Steedman, J. Fridriksson, L. Bonilha, and C. Rorden. Global versus local processing: seeing the left side of the forest and the right side of the trees. *Frontiers in human neuroscience*, 6:28, 2012.

[140] S. Christman. Perceptual characteristics in visual laterality research. *Brain and cognition*, 11(2):238–57, 1989.

[141] S. Christman, F. L. Kitterle, and J. Hellige. Hemispheric asymmetry in the processing of absolute versus relative spatial frequency. *Brain and cognition*, 16(1):62–73, 1991.

[142] M. M. Chun and Y. Jiang. Contextual cueing: implicit learning and memory of visual context guides spatial attention. *Cognitive psychology*, 36(1):28–71, 1998.

[143] M. M. Chun and Y. Jiang. Top-Down Attentional Guidance Based on Implicit Learning of Visual Covariation. *Psychological Science*, 10(4):360–365, 1999.

[144] J.-Y. Chung, H. W. Yoon, M.-S. Song, and H. Park. Event related fMRI studies of voluntary and inhibited eye blinking using a time marker of EOG. *Neuroscience letters*, 395(3):196–200, 2006.

[145] A. Clark. Whatever next? Predictive brains, situated agents, and the future of cognitive science. *The Behavioral and brain sciences*, 36(3):181–204, 2013.

[146] S. Classen, B. Brumback, M. Monahan, I. I. Malaty, R. L. Rodriguez, M. S. Okun, and N. R. Mcfarland. Driving Errors in Parkinsons Disease: Moving Closer to Predicting On-Road Outcomes. *The American Journal of Occupational Therapy*, 68(1):77–85, 2014.

[147] L. Cohen. Attention getting and attention holding processes of infant visual preferences. *Child development*, 43:869–879, 1972.

[148] L. Cohen. Visual Word Recognition in the Left and Right Hemispheres: Anatomical and Functional Correlates of Peripheral Alexias. *Cerebral Cortex*, 13(12):1313–1333, 2003.

[149] L. Cohen, S. Dehaene, L. Naccache, S. Lehericy, G. Dehaene-lambertz, M.-A. Henaff, and F. Michel. The visual word form area: Spatial and temporal characterization of an initial stage of reading in normal subjects and posterior split-brain patients. *Brain*, 123:291–307, 2000.

[150] Y. E. Cohen and R. a. Andersen. A common reference frame for movement plans in the posterior parietal cortex. *Nature Reviews Neuroscience*, 3(7):553–62, 2002.

[151] C. L. Colby and M. E. Goldberg. Space and attention in parietal cortex. *Annual review of neuroscience*, 22:319–349, 1999.

[152] C. L. Colby, J. R. Duhamel, and M. E. Goldberg. Visual, presaccadic, and cognitive activation of single neurons in monkey lateral intraparietal area. *Journal of neurophysiology*, 76(5):2841–2852, 1996.

[153] M. Colombo and P. Seriès. Bayes in the brain - On Bayesian modelling in neuroscience. *British Journal for the Philosophy of Science*, 63(3):697–723, 2012.

[154] J. Coolican, G. a. Eskes, P. a. McMullen, and E. Lecky. Perceptual biases in processing facial identity and emotion. *Brain and cognition*, 66(2):176–87, 2008.

[155] M. Corbetta. Frontoparietal cortical networks for directing attention and the eye to visual locations: Identical, independent, or overlapping neural systems? *Proceedings of the National Academy of Sciences*, 95(3):831–838, 1998.

[156] M. Corbetta and G. L. Shulman. Control of goal-directed and stimulus-driven attention in the brain. *Nature Reviews Neuroscience*, 3(3):201–15, 2002.

[157] M. Corbetta and G. L. Shulman. Spatial neglect and attention networks. *Annual review of neuroscience*, 34:569–99, 2011.

[158] M. Corbetta, J. M. Kincade, J. M. Ollinger, M. P. McAvoy, and G. L. Shulman. Voluntary orienting is dissociated from target detection in human posterior parietal cortex. *Nature neuroscience*, 3 (3):292–7, 2000.

[159] M. Corbetta, M. J. Kincade, C. Lewis, A. Z. Snyder, and A. Sapir. Neural basis and recovery of spatial attention deficits in spatial neglect. *Nature neuroscience*, 8(11):1603–10, 2005.

[160] M. Corbetta, G. Patel, and G. L. Shulman. The reorienting system of the human brain: from environment to theory of mind. *Neuron*, 58(3):306–24, 2008.

[161] J. C. Corby and B. S. Kopell. Differential Contributions of Blinks and Vertical Eye Movements as Artifacts in EEG Recording. *Psychophysiology*, 9(6):640–644, 1972.

[162] F. W. Cornelissen, E. M. Peters, and J. Palmer. The Eyelink Toolbox: eye tracking with MATLAB and the psychophysics toolbox. *Behavior Research Methods, Instruments, & Computers*, 34(4): 613–617, 2002.

[163] L. Craighero, A. Carta, and L. Fadiga. Peripheral oculomotor palsy affects orienting of visuospatial attention. *Neuroreport*, 12(15):3283–3286, 2001.

[164] T. B. Crapse and M. A. Sommer. Corollary discharge across the animal kingdom. *Nature Reviews Neuroscience*, 9(8):587–600, 2008.

[165] R. J. Croft and R. J. Barry. EOG correction: a new aligned-artifact average solution. *Electroencephalography and clinical neurophysiology*, 107(6):395–401, 1998.

[166] R. J. Croft and R. J. Barry. EOG correction: a new perspective. *Electroencephalography and clinical neurophysiology*, 107(6):387–94, 1998.

[167] R. J. Croft and R. J. Barry. Removal of ocular artifact from the EEG: a review. *Clinical neurophysiology*, 30(1):5–19, 2000.

[168] R. J. Croft and R. J. Barry. EOG correction: which regression should we use? *Psychophysiology*, 37(1):123–5, 2000.

[169] R. J. Croft, J. S. Chandler, R. J. Barry, N. R. Cooper, and A. R. Clarke. EOG correction: a comparison of four methods. *Psychophysiology*, 42(1):16–24, 2005.

[170] M. Czerwinski, N. Lightfoot, and R. Shiffrin. Automatization and training in visual search. *The American journal of psychology*, 105(2):271–315, 1992.

[171] S. Dandekar, J. Ding, C. Privitera, T. Carney, and S. A. Klein. The fixation and saccade P3. *PloS one*, 7(11):e48761, 2012.

[172] S. Dandekar, C. Privitera, T. Carney, and S. A. Klein. Neural saccadic response estimation during natural viewing. *Journal of neurophysiology*, 107(6):1776–90, 2012.

[173] P. Daniel and D. Whitteridge. The representation of the visual field on the cerebral cortex in monkeys. *Journal of Physiology*, 159:203–221, 1961.

[174] S. V. David, W. E. Vinje, and J. L. Gallant. Natural stimulus statistics alter the receptive field structure of v1 neurons. *The Journal of neuroscience*, 24(31):6991–7006, 2004.

[175] S. Davidsdottir, A. Cronin-Golomb, and A. Lee. Visual and spatial symptoms in Parkinson's disease. *Vision Research*, 45:1285–1296, 2005.

[176] P. Dayan, G. E. Hinton, R. M. Neal, and R. S. Zemel. The Helmholtz machine. *Neural computation*, 7(5):889–904, 1995.

[177] M. De Agostini, S. Kazandjian, J. Lellouch, and S. Chokron. Visual aesthetic preference: Effects of handedness, sex, and age-related reading/writing directional scanning experience. *Writing Systems Research*, 2(2):77–85, 2010.

[178] J. de Fockert, G. Rees, C. Frith, and N. Lavie. Neural correlates of attentional capture in visual search. *Journal of cognitive neuroscience*, 16(5):751–9, 2004.

[179] R. de la Fuente-Fernández, A. Kishore, D. B. Calne, T. J. Ruth, and A. Stoessl. Nigrostriatal dopamine system and motor lateralization. *Behavioural Brain Research*, 112(1-2):63–68, 2000.

[180] E. De Renzi, D. Perani, G. A. Carlesimo, M. C. Silveri, and F. Fazio. Prosopagnosia can be associated with damage confined to the right hemisphere–an MRI and PET study and a review of the literature. *Neuropsychologia*, 32(8):893–902, 1994.

[181] R. L. De Valois and K. K. De Valois. *Spatial vision*. Oxford University Press, New York, NY, US, 1990.

[182] . Deep-Brain Stimulation for Parkinson's Disease Study Group. Deep-brain stimulation of the subthalamic nucleus or the pars interna of the globus pallidus in Parkinson's disease. *The New England journal of medicine*, 345(13):956–963, 2001.

[183] D. Delis, L. Robertson, and R. Efron. Hemispheric specialization of memory for visual hierarchical stimuli. *Neuropsychologia*, 24(2):205–214, 1986.

[184] S. Della Sala, S. Darling, and R. H. Logie. Items on the left are better remembered. *Quarterly journal of experimental psychology*, 63(5):848–55, 2010.

[185] A. Delorme and S. Makeig. EEGLAB: an open source toolbox for analysis of single-trial EEG dynamics including independent component analysis. *Journal of neuroscience methods*, 134(1): 9–21, 2004.

[186] E. Demandt, C. Mehring, K. Vogt, A. Schulze-Bonhage, A. Aertsen, and T. Ball. Reaching movement onset- and end-related characteristics of EEG spectral power modulations. *Frontiers in Neuroscience*, 6(MAY):1–11, 2012.

[187] A. M. Derrington, J. Krauskopf, and P. Lennie. Chromatic mechanisms in lateral geniculate nucleus of macaque. *The Journal of physiology*, 357:241–65, 1984.

[188] R. Desimone and J. Duncan. Neural mechanisms of selective visual attention. *Annual review of neuroscience*, 18:193–222, 1995.

[189] R. Desimone and C. G. Gross. Visual areas in the temporal cortex of the macaque. *Brain Research*, 178(2-3):363–380, 1979.

[190] H. Deubel. The time course of presaccadic attention shifts. *Psychological research*, 72(6):630–40, 2008.

[191] H. Deubel and W. Schneider. Saccade target selection and object recognition. *Vision research*, 36(12):1827–1837, 1996.

[192] H. Deubel, B. Bridgeman, and W. X. Schneider. Different effects of eyelid blinks and target blanking on saccadic suppression of displacement. *Perception & psychophysics*, 66(5):772–778, 2004.

[193] J. A. Deutsch and D. Deutsch. Attention: Some Theoretical Considerations. *Psychological Review*, 70(1):80–90, 1963.

[194] V. Di Lollo, J. Kawahara, S. Zuvic, and T. Visser. The preattentive emperor has no clothes: a dynamic redressing. *Journal of experimental psychology. General*, 130(3):479–492, 2001.

[195] F. Di Russo, A. Martínez, M. I. Sereno, S. Pitzalis, and S. A. Hillyard. Cortical sources of the early components of the visual evoked potential. *Human Brain Mapping*, 15(2):95–111, 2001.

[196] M. R. Diamond, J. Ross, and M. C. Morrone. Extraretinal control of saccadic suppression. *The Journal of neuroscience*, 20(9):3449–55, 2000.

[197] C. Dickinson and H. Intraub. Spatial asymmetries in viewing and remembering scenes: Consequences of an attentional bias? *Attention, Perception, & Psychophysics*, 71(6):1251–1262, 2009.

[198] A. Diederich and H. Colonius. Bimodal and trimodal multisensory enhancement: Effects of stimulus onset and intensity on reaction time. *Perception & Psychophysics*, 66(8):1388–1404, 2004.

[199] A. Diederich, H. Colonius, D. Bockhorst, and S. Tabeling. Visual-tactile spatial interaction in saccade generation. *Experimental brain research*, 148(3):328–37, 2003.

[200] O. Dimigen, M. Valsecchi, W. Sommer, and R. Kliegl. Human microsaccade-related visual brain responses. *The Journal of neuroscience*, 29(39):12321–31, 2009.

[201] O. Dimigen, W. Sommer, A. Hohlfeld, A. M. Jacobs, and R. Kliegl. Coregistration of eye movements and EEG in natural reading: analyses and review. *Journal of experimental psychology. General*, 140(4):552–72, 2011.

[202] E. Donchin and M. G. H. Coles. Is the P300 component a manifestation of context updating? *Behavioral and Brain Sciences*, 11(03):355–374, 1988.

[203] K. Doré-Mazars, P. Pouget, and C. Beauvillain. Attentional selection during preparation of eye movements. *Psychological research*, 69(1-2):67–76, 2004.

[204] M. C. Dorris and D. P. Munoz. A neural correlate for the gap effect on saccadic reaction times in monkey. *Journal of neurophysiology*, 73(6):2558–62, 1995.

[205] M. C. Dorris, M. Paré, and D. P. Munoz. Neuronal activity in monkey superior colliculus related to the initiation of saccadic eye movements. *The Journal of neuroscience*, 17(21):8566–79, 1997.

[206] J. Downar, A. P. Crawley, D. J. Mikulis, and K. D. Davis. A multimodal cortical network for the detection of changes in the sensory environment. *Nature neuroscience*, 3(3):277–83, 2000.

[207] J. Downar, A. P. Crawley, D. J. Mikulis, and K. D. Davis. The Effect of Task Relevance on the Cortical Response to Changes in Visual and Auditory Stimuli: An Event-Related fMRI Study. *NeuroImage*, 14(6):1256–1267, 2001.

[208] P. E. Downing, Y. Jiang, M. Shuman, and N. Kanwisher. A cortical area selective for visual processing of the human body. *Science*, 293:2470–2473, 2001.

[209] J. Driver and J. B. Mattingley. Parietal neglect and visual awareness. *Nature neuroscience*, 1(1):17–22, 1998.

[210] J. Driver and C. Spence. Cross-modal links in spatial attention. *Philosophical transactions of the Royal Society of London B*, 353(1373):1319–31, 1998.

[211] F. Du and R. A. Abrams. Visual field asymmetry in attentional capture. *Brain and cognition*, 72(2):310–6, 2010.

[212] J.-R. Duhamel, C. Colby, and M. Goldberg. The Updating of the Representation of Visual space in parietal cortex by intended eye movements. *Science*, 255:90–92, 1992.

[213] J. Duncan and G. W. Humphreys. Visual search and stimulus similarity. *Psychological Review*, 96(3):433–458, 1989.

[214] A. F. Eardley and J. van Velzen. Event-related potential evidence for the use of external coordinates in the preparation of tactile attention by the early blind. *The European journal of neuroscience*, 33(10):1897–907, 2011.

[215] G. Ebersbach, T. Trottenberg, H. Hättig, L. Schelosky, A. Schrag, and W. Poewe. Directional bias of initial visual exploration. A symptom of neglect in Parkinson's disease. *Brain*, 119:79–87, 1996.

[216] H. Egeth, R. Virzi, and H. Garbart. Searching for Conjunctively Defined Targets. *Journal of experimental psychology. Human perception and performance*, 10(1):32–39, 1984.

[217] T. Egner, J. M. Monti, and C. Summerfield. Expectation and surprise determine neural population responses in the ventral visual stream. *The Journal of neuroscience*, 30(49):16601–8, 2010.

[218] B. V. Ehinger, P. Fischer, A. L. Gert, L. Kaufhold, F. Weber, G. Pipa, and P. König. Kinesthetic and vestibular information modulate alpha activity during spatial navigation: a mobile EEG study. *Frontiers in human neuroscience*, 8:71, 2014.

[219] H. Ehrsson. The Concept of Body Ownership and Its Relation to Multisensory Integration. In B. Stein, editor, *The New Handbook of Multisensory Processes*, chapter 43, pages 775–792. MIT Press, Cambridge, MA, 2012.

[220] W. Einhäuser and P. Konig. Does luminance-contrast contribute to a saliency map for overt visual attention? *European Journal of Neuroscience*, 17(5):1089–1097, 2003.

[221] W. Einhäuser, U. Rutishauser, E. P. Frady, S. Nadler, P. König, and C. Koch. The relation of phase noise and luminance contrast to overt attention in complex visual stimuli. *Journal of vision*, 6 (11):1148–58, 2006.

[222] W. Einhäuser, U. Rutishauser, and C. Koch. Task-demands can immediately reverse the effects of sensory-driven saliency in complex visual stimuli. *Journal of vision*, 8(2):2.1–19, 2008.

[223] W. Einhäuser, M. Spain, and P. Perona. Objects predict fixations better than early saliency. *Journal of Vision*, 8(14:18):1–26, 2008.

[224] L. Elazary and L. Itti. Interesting objects are visually salient. *Journal of Vision*, 8(3):3: 1–15, 2008.

[225] T. Elbert, W. Lutzenberger, B. Rockstroh, and N. Birbaumer. Removal of ocular artifacts from the EEG - A biophysical approach to the EOG. *Electroencephalography and Clinical Neurophysiology*, 60(5):455–463, 1985.

[226] R. Engbert. Microsaccades uncover the orientation of covert attention. *Vision Research*, 43(9):1035–1045, 2003.

[227] R. Engbert and K. Mergenthaler. Microsaccades are triggered by low retinal image slip. *Proceedings of the National Academy of Sciences of the United States of America*, 103(18):7192–7, 2006.

[228] R. Engbert, H. A. Trukenbrod, S. Barthelmé, and F. A. Wichmann. Spatial statistics and attentional dynamics in scene viewing. *Journal of Vision*, 15(1):14, 2014.

[229] A. K. Engel, A. Maye, M. Kurthen, and P. König. Where's the action? The pragmatic turn in cognitive science. *Trends in cognitive sciences*, 17(5):202–9, 2013.

[230] F. Engel. Visual conspicuity, directed attention and retinal locus. *Vision research*, 11:563–575, 1971.

[231] S. Engmann, B. 'T Hart, T. Sieren, S. Onat, P. König, and W. Einhäuser. Saliency on a natural scene background: effects of color and luminance contrast add linearly. *Attention, perception & psychophysics*, 71(6):1337–1352, 2009.

[232] R. Epstein and N. Kanwisher. A cortical representation of the local visual environment. *Nature*, 392:598–601, 1998.

[233] B. Eriksen and C. Eriksen. Effects of noise letters upon the identification of a target letter in a nonsearch task. *Perception & psychophysics*, 16(1):143–149, 1974.

[234] C. W. Eriksen and J. E. Hoffman. Temporal and spatial characteristics of selective encoding from visual displays. *Perception & Psychophysics*, 12(2):201–204, 1972.

[235] D. Eriksson, T. Wunderle, and K. Schmidt. Visual cortex combines a stimulus and an error-like signal with a proportion that is dependent on time, space, and stimulus contrast. *Frontiers in systems neuroscience*, 6(April):1–19, 2012.

[236] M. O. Ernst and M. S. Banks. Humans integrate visual and haptic information in a statistically optimal fashion. *Nature*, 415(6870):429–33, 2002.

[237] M. Esterman, R. McGlinchey-Berroth, and W. Milberg. Preattentive and attentive visual search in individuals with hemispatial neglect. *Neuropsychology*, 14(4):599–611, 2000.

[238] C. Evans. Spontaneous excitation of the visual cortex and association areas. *Electroencephalography and clinical neurophysiology*, 5:69–74, 1953.

[239] C. Evans, J. Macedonia, and P. Marler. Effects of apparent size and speed on the response of chickens to computer generated simulations of aerial predators. *Animal Behaviour*, 46:1–11, 1993.

[240] C. Evinger, K. A. Manning, and P. A. Sibony. Eyelid movements. Mechanisms and normal data. *Investigative ophthalmology & visual science*, 32(2):387–400, 1991.

[241] M. J. Farah, A. B. Wong, M. A. Monheit, and L. A. Morrow. Parietal lobe mechanisms of spatial attention: Modality-specific or supramodal? *Neuropsychologia*, 27(4):461–470, 1989.

[242] A. P. Fawcett, J. O. Dostrovsky, A. M. Lozano, and W. D. Hutchison. Eye movement-related responses of neurons in human subthalamic nucleus. *Experimental brain research.*, 162(3):357–65, 2005.

[243] A. P. Fawcett, E. G. González, E. Moro, M. J. Steinbach, A. M. Lozano, and W. D. Hutchison. Subthalamic Nucleus Deep Brain Stimulation Improves Saccades in Parkinson's Disease. *Neuromodulation*, 13(1):17–25, 2010.

[244] J. H. Fecteau and D. P. Munoz. Salience, relevance, and firing: a priority map for target selection. *Trends in cognitive sciences*, 10(8):382–90, 2006.

[245] A. Fedorov, R. Beichel, J. Kalphaty-Cramer, J. Finet, J.-C. Fillion-Robbin, S. Pujol, C. Bauer, D. Jennings, F. Fennessy, M. Sonka, J. Buatti, S. Aylward, J. V. Miller, S. Pieper, and R. Kikinis. 3D slicers as an image computing platform for thw quantitative imaging network. *Magnetic resonance imaging*, 30(9):1323–1341, 2012.

[246] H. Feldman and K. J. Friston. Attention, uncertainty, and free-energy. *Frontiers in human neuroscience*, 4:215, 2010.

[247] D. J. Felleman and D. C. Van Essen. Distributed hierarchical processing in the primate cerebral cortex. *Cerebral cortex*, 1:1–47, 1991.

[248] J. Fellrath and R. Ptak. The role of visual saliency for the allocation of attention: Evidence from spatial neglect and hemianopia. *Neuropsychologia*, 73:70–81, 2015.

[249] G. Felsen and Y. Dan. A natural approach to studying vision. *Nature neuroscience*, 8(12):1643–6, 2005.

[250] D. Field. What is the goal of Sensory Coding? *Neural Computation*, 6:559–601, 1994.

[251] D. J. Field. Relations between the statistics of natural images and the response properties of cortical cells. *Journal of the Optical Society of America. A, Optics and image science*, 4(12):2379–94, 1987.

[252] B. Fierro, F. Brighina, M. Oliveri, A. Piazza, V. La Bua, D. Buffa, and E. Bisiach. Contralateral neglect induced by right posterior parietal rTMS in healthy subjects. *Neuroreport*, 11(7):1519–1521, 2000.

[253] B. Fimm, K. Willmes, and W. Spijkers. Differential Effects of Lowered Arousal on Covert and Overt Shifts of Attention. *Journal of the International Neuropsychological Society*, 21:545–557, 2015.

[254] G. Fink, P. Halligan, J. Marshall, C. Frith, R. Frackowiak, and R. Dolan. Where in the brain does visual attention select the forest and the trees? *Nature*, 382:626–628, 1996.

[255] G. R. Fink, P. W. Halligan, J. C. Marshall, C. D. Frith, R. S. Frackowiak, and R. J. Dolan. Neural mechanisms involved in the processing of global and local aspects of hierarchically organized visual stimuli. *Brain*, 120:1779–91, 1997.

[256] G. R. Fink, J. C. Marshall, P. W. Halligan, and R. J. Dolan. Hemispheric asymmetries in global/local processing are modulated by perceptual salience. *Neuropsychologia*, 37(1):31–40, 1999.

[257] M. Fiorani Júnior, M. G. Rosa, R. Gattass, and C. E. Rocha-Miranda. Dynamic surrounds of receptive fields in primate striate cortex: a physiological basis for perceptual completion? *Proceedings of the National Academy of Sciences of the United States of America*, 89(18):8547–51, 1992.

[258] B. Fischer and E. Ramsperger. Human express saccades: extremely short reaction times of goal directed eye movements. *Experimental Brain Research*, 57:191–195, 1984.

[259] B. Fischer and E. Ramsperger. Human express saccades: effects or randomization and daily practice. *Experimental Brain Research*, 64:569–578, 1986.

[260] J. Fiser, P. Berkes, G. Orbán, and M. Lengyel. Statistically optimal perception and learning: from behavior to neural representations. *Trends in cognitive sciences*, 14(3):119–30, 2010.

[261] W. S. Fleet, E. Valenstein, R. T. Watson, and K. M. Heilman. Dopamine agonist therapy for neglect in humans. *Neurology*, 37(11):1765–1765, 1987.

[262] C. Folk, R. Remington, and J. Johnston. Involuntary covert orienting is contingent on attentional controlsettings. *Journal of Experimental Psychology: Human Perception and Performance*, 18 (4):1030–1044, 1992.

[263] S. L. Foote and J. H. Morrison. Extrathalamic modulation of cortical function. *Annual review of neuroscience*, 10:67–95, 1987.

[264] B. Forster, C. Cavina-Pratesi, S. M. Aglioti, and G. Berlucchi. Redundant target effect and intersensory facilitation from visual-tactile interactions in simple reaction time. *Experimental brain research*, 143(4):480–7, 2002.

[265] D. Foster and S. Westland. Orientation contrast vs orientation line target detection. *Vision research*, 35(6):733–738, 1995.

[266] T. Foulsham, J. J. S. Barton, A. Kingstone, R. Dewhurst, and G. Underwood. Fixation and saliency during search of natural scenes: the case of visual agnosia. *Neuropsychologia*, 47(8-9): 1994–2003, 2009.

[267] T. Foulsham, A. Gray, E. Nasiopoulos, and A. Kingstone. Leftward biases in picture scanning and line bisection: a gaze-contingent window study. *Vision research*, 78:14–25, 2013.

[268] A. Fourment, J. Calvet, and J. Bancaud. Electrocorticography of waves associated with eye movements in man during wakefulness. *Electroencephalography and clinical neurophysiology*, 40: 457–469, 1976.

[269] M. D. Fox, A. Z. Snyder, J. L. Vincent, M. Corbetta, D. C. Van Essen, and M. E. Raichle. The human brain is intrinsically organized into dynamic, anticorrelated functional networks. *Proceedings of the National Academy of Sciences of the United States of America*, 102(27):9673–8, 2005.

[270] M. D. Fox, M. Corbetta, A. Z. Snyder, J. L. Vincent, and M. E. Raichle. Spontaneous neuronal activity distinguishes human dorsal and ventral attention systems. *Proceedings of the National Academy of Sciences of the United States of America*, 103(26):10046–51, 2006.

[271] S. L. Franconeri, D. J. Simons, and J. A. Junge. Searching for stimulus-driven shifts of attention. *Psychonomic Bulletin & Review*, 11(5):876–881, 2004.

Bibliography

[272] F. Frassinetti, N. Bolognini, and E. Làdavas. Enhancement of visual perception by crossmodal visuo-auditory interaction. *Experimental brain research*, 147(3):332–43, 2002.

[273] M. E. Frederikse, A. Lu, E. Aylward, P. Barta, and G. Pearlson. Sex differences in the inferior parietal lobule. *Cerebral cortex*, 9(8):896–901, 1999.

[274] M. Frens, A. van Opstal, and R. van der Willigen. Spatial and temporal factors determine auditory-visual interactions in human saccadic eye movements. *Perception & psychophysics*, 57(6): 802–816, 1995.

[275] D. Friedman, Y. M. Cycowicz, and H. Gaeta. The novelty P3: An event-related brain potential (ERP) sign of the brain's evaluation of novelty. *Neuroscience and Biobehavioral Reviews*, 25: 355–373, 2001.

[276] P. Fries, R. Scheeringa, and R. Oostenveld. Finding gamma. *Neuron*, 58(3):303–5, 2008.

[277] W. Fries. Cortical projections to the superior colliculus in the macaque monkey: a retrograde study using horseradish peroxidase. *The Journal of comparative neurology*, 230(1):55–76, 1984.

[278] K. Friston. A theory of cortical responses. *Philosophical Transactions of the Royal Society B: Biological Sciences*, 360:815–836, 2005.

[279] K. Friston and S. Kiebel. Predictive coding under the free-energy principle. *Philosophical transactions of the Royal Society of London. Series B, Biological sciences*, 364(1521):1211–1221, 2009.

[280] K. Friston, R. A. Adams, L. Perrinet, and M. Breakspear. Perceptions as hypotheses: saccades as experiments. *Frontiers in psychology*, 3:151, 2012.

[281] S. Gabay, A. Henik, and L. Gradstein. Ocular motor ability and covert attention in patients with Duane Retraction Syndrome. *Neuropsychologia*, 48(10):3102–9, 2010.

[282] S. Gandhi, D. Heeger, and G. Boynton. Spatial attention affects brain activity in human primary visual cortex. *Proceedings of the National Academy of Sciences*, 96:3314–3319, 1999.

[283] A. Garcia-Diaz, V. Leboran, X. R. Fdez-Vidal, and X. M. Pardo. On the relationship between optical variability, visual saliency, and eye fixations: A computational approach. *Journal of Vision*, 12(6):17–17, 2012.

[284] M. I. Garrido, J. M. Kilner, S. J. Kiebel, and K. J. Friston. Evoked brain responses are generated by feedback loops. *Proceedings of the National Academy of Sciences*, 104(52):20961–6, 2007.

[285] M. I. Garrido, J. M. Kilner, K. E. Stephan, and K. J. Friston. The mismatch negativity: a review of underlying mechanisms. *Clinical neurophysiology*, 120(3):453–63, 2009.

[286] R. Gattass, C. G. Gross, and J. H. Sandell. Visual topography of V2 in the macaque. *The Journal of comparative neurology*, 201(4):519–539, 1981.

[287] L. Gauthier, F. Dehaut, and Y. Joanette. The Bells Test: A quantitative and qualitative test for visual neglect. *International Journal of Clinical Neuropsychology*, 11(2):49–54, 1989.

[288] K. R. Gegenfurtner. Cortical mechanisms of colour vision. *Nature Reviews Neuroscience*, 4(7):563–72, 2003.

[289] K. R. Gegenfurtner, D. C. Kiper, and S. B. Fenstemaker. Processing of color, form, and motion in macaque area V2. *Visual neuroscience*, 13(1):161–172, 1996.

[290] W. S. Geisler and R. L. Diehl. A Bayesian approach to the evolution of perceptual and cognitive systems. *Cognitive Science: A Multidisciplinary Journal*, 27(3):379–402, 2003.

[291] A. Gelman, J. Hill, and M. Yajima. Why we (usually) don't have to worry about multiple comparisons. *Journal of Research on Educational Effectiveness*, 5:189–211, 2012.

[292] G. Geminiani, G. Bottini, and R. Sterzi. Dopaminergic stimulation in unilateral neglect. *Journal of neurology, neurosurgery, and psychiatry*, 65(3):344–7, 1998.

[293] J. Geng, C. Ruff, and J. Driver. Saccades to a remembered location elicit spatially specific activation in human retinotopic visual cortex. *Journal of cognitive neuroscience*, 21(2):230–245, 2009.

[294] A. A. Ghazanfar, J. X. Maier, K. L. Hoffman, and N. K. Logothetis. Multisensory integration of dynamic faces and voices in rhesus monkey auditory cortex. *J. Neurosci.*, 25:5004–5012, 2005.

[295] S. Gielen, R. Schmift, and P. van den Heuvel. On the nature of intersensory facilitation of reaction time. *Perception & Psychophysics*, 34(2):161–168, 1983.

[296] C. Gilbert and P. Bakan. Visual asymmetry in perception of faces. *Neuropsychologia*, 11(3):355–62, 1973.

[297] D. Girton and J. Kamiya. A simple on-line technique for removing eye movement artifacts from the eeg. *Electroencephalography and clinical neurophysiology*, 34:212–216, 1973.

[298] S. D. Glick and D. A. Ross. Lateralization of function in the rat brain. *Trends in Neurosciences*, 4(August):196–199, 1981.

[299] P. W. Glimcher. The neurobiology of visual-saccadic decision making. *Annual review of neuroscience*, 26:133–79, 2003.

[300] J. D. Golomb, Z. E. L'Heureux, and N. Kanwisher. Feature-binding errors after eye movements and shifts of attention. *Psychological Science*, 25(5):1067–1078, 2014.

[301] S. Gong, M. DeCuypere, Y. Zhao, and M. S. LeDoux. Cerebral cortical control of orbicularis oculi motoneurons. *Brain research*, 1047(2):177–93, 2005.

[302] R. Gonzalez and R. Woods. *Digital image processing*. Prentice Hall, Upper Saddle River, New Jersey, 2nd edition, 2002.

[303] C. D. Good, I. Johnsrude, J. Ashburner, R. N. Henson, K. J. Friston, and R. S. Frackowiak. Cerebral asymmetry and the effects of sex and handedness on brain structure: a voxel-based morphometric analysis of 465 normal adult human brains. *NeuroImage*, 14(3):685–700, 2001.

[304] M. Goodale and A. Milner. Separate visual pathways for perception and action. *Trends in neurosciences*, 15(1):20–5, 1992.

[305] M. Goodale, A. Milner, L. Jakobson, and D. Carey. A neurological dissociation between perceiving objects and grasping them. *Nature*, 349:154–156, 1991.

[306] J. Gottlieb. From thought to action: the parietal cortex as a bridge between perception, action, and cognition. *Neuron*, 53(1):9–16, 2007.

[307] J. P. Gottlieb, M. Kusunoki, and M. E. Goldberg. The representation of visual salience in monkey parietal cortex. *Nature*, 391:481–4, 1998.

[308] J. Graham, C. S. Lin, and J. H. Kaas. Subcortical projections of six visual cortical areas in the owl monkey, Aotus trivirgatus. *The Journal of comparative neurology*, 187(3):557–80, 1979.

[309] K. Gramann, J. T. Gwin, N. Bigdely-Shamlo, D. P. Ferris, and S. Makeig. Visual evoked responses during standing and walking. *Frontiers in human neuroscience*, 4:202, 2010.

[310] G. Gratton, M. Coles, and E. Donchin. A new method for off-line removal of ocular artifact. *Electroencephalography and clinical Neurophysiology*, 55(4):468–484, 1983.

[311] S. T. Graupner, S. Pannasch, and B. M. Velichkovsky. Saccadic context indicates information processing within visual fixations: Evidence from event-related potentials and eye-movements analysis of the distractor effect. *International Journal of Psychophysiology*, 80(1):54–62, 2011.

[312] M. S. Graziano. Where is my arm? The relative role of vision and proprioception in the neuronal representation of limb position. *Proceedings of the National Academy of Sciences of the United States of America*, 96(18):10418–21, 1999.

[313] M. S. Graziano, D. F. Cooke, and C. S. Taylor. Coding the location of the arm by sight. *Science*, 290(5497):1782–1786, 2000.

[314] M. S. A. Graziano, C. G. Gross, C. S. R. Taylor, and T. Moore. A system of multimodal areas in the primate brain. In C. Spence and J. Driver, editors, *Crossmodal space and crossmodal attention*, chapter 3, pages 51–67. Oxford University Press, 2004.

[315] J. Green. Somes observations on lambda waves and peripheral stimulation. *EEG Clin Neurophysiol*, 1957.

[316] C. Grefkes, L. E. Wang, S. B. Eickhoff, and G. R. Fink. Noradrenergic Modulation of Cortical Networks Engaged in Visuomotor Processing. *Cerebral Cortex*, 20(4):783–797, 2010.

[317] R. Gregory. Perceptions as hypotheses. *Philosophical Transactions of the Royal Society B: Biological Sciences*, 290:181–197, 1980.

[318] K. Grill-Spector and R. Malach. The human visual cortex. *Annual review of neuroscience*, 27:649–77, 2004.

[319] K. Grill-Spector, R. Henson, and A. Martin. Repetition and the brain: neural models of stimulus-specific effects. *Trends in Cognitive Sciences*, 10(1):14–23, 2006.

[320] J. Grimes. On the failure to detect changes in scenes across saccades. *Perception*, pages 89–110, 1996.

[321] J. M. Groh and D. L. Sparks. Saccades to somatosensory targets. I. behavioral characteristics. *Journal of neurophysiology*, 75(1):412–27, 1996.

[322] M. T. Groner, R. Groner, and A. von Mühlenen. The effect of spatial frequency content on parameters of eye movements. *Psychological research*, 72:601–608, 2008.

[323] R. W. Guillery, S. L. Feig, and D. P. Van Lieshout. Connections of higher order visual relays in the thalamus: A study of corticothalamic pathways in cats. *Journal of Comparative Neurology*, 438(1):66–85, 2001.

[324] D. Guitton, H. Buchtel, and R. M. Douglas. Frontal lobe lesions in man cause difficulties in suppressing reflexive glances and in generating goal-directed saccades. *Experimental Brain Research*, 58:455–472, 1985.

[325] D. Guitton, R. Simard, and F. Codère. Upper eyelid movements measured with a search coil during blinks and vertical saccades. *Investigative ophthalmology & visual science*, 32(13):3298–305, 1991.

[326] O. Güntürkün. Adult persistence of head-truning asymmetry. *Nature*, 421:711, 2003.

[327] K. Guo, K. Meints, C. Hall, S. Hall, and D. Mills. Left gaze bias in humans, rhesus monkeys and domestic dogs. *Animal cognition*, 12(3):409–18, 2009.

[328] K. Guo, D. Tunnicliffe, and H. Roebuck. Human spontaneous gaze patterns in viewing of faces of different species. *Perception*, 39(4):533–542, 2010.

[329] J. T. Gwin, K. Gramann, S. Makeig, and D. P. Ferris. Removal of movement artifact from high-density EEG recorded during walking and running. *Journal of neurophysiology*, 103(6):3526–34, 2010.

[330] J. T. Gwin, K. Gramann, S. Makeig, and D. P. Ferris. Electrocortical activity is coupled to gait cycle phase during treadmill walking. *NeuroImage*, 54(2):1289–1296, 2011.

[331] Z. M. Hafed and J. J. Clark. Microsaccades as an overt measure of covert attention shifts. *Vision Research*, 42(22):2533–2545, 2002.

[332] Z. M. Hafed, L. Goffart, and R. J. Krauzlis. A neural mechanism for microsaccade generation in the primate superior colliculus. *Science*, 323(5916):940–3, 2009.

[333] S. Han, J. a. Weaver, S. O. Murray, X. Kang, E. Yund, and D. L. Woods. Hemispheric Asymmetry in Global/Local Processing: Effects of Stimulus Position and Spatial Frequency. *NeuroImage*, 17(3):1290–1299, 2002.

[334] Hancock, Baddeley, and Smith. The principal components of natural images. *Network*, 3(1):61–70, 1992.

[335] D. P. Hanes and R. H. Carpenter. Countermanding saccades in humans. *Vision research*, 39(16):2777–91, 1999.

[336] V. Harrar and L. R. Harris. Eye position affects the perceived location of touch. *Experimental brain research*, 198(2-3):403–10, 2009.

[337] V. Harrar and L. R. Harris. Touch used to guide action is partially coded in a visual reference frame. *Experimental brain research*, 203(3):615–20, 2010.

[338] L. K. Harrington and C. K. Peck. Spatial disparity affects visual-auditory interactions in human sensorimotor processing. *Experimental Brain Research*, 122(2):247–252, 1998.

[339] M. Hausmann. Hemispheric asymmetry in spatial attention across the menstrual cycle. *Neuropsychologia*, 43(11):1559–67, 2005.

[340] J. Hay, H. Pick, and K. Ikeda. Visual capture produced by prism spectacles. *Psychonomic science*, 2(8):215–216, 1965.

[341] B. J. He, A. Z. Snyder, J. L. Vincent, A. Epstein, G. L. Shulman, and M. Corbetta. Breakdown of functional connectivity in frontoparietal networks underlies behavioral deficits in spatial neglect. *Neuron*, 53(6):905–18, 2007.

[342] R. L. Heath, A. Rouhana, and D. A. Ghanem. Asymmetric bias in perception of facial affect among Roman and Arabic script readers. *Laterality*, 10(1):51–64, 2005.

[343] T. Heed and E. Azañón. Using time to investigate space: a review of tactile temporal order judgments as a window onto spatial processing in touch. *Frontiers in psychology*, 5:76, 2014.

[344] T. Heed and B. Röder. The Body in a Multisensory World. In M. Murray and M. Wallace, editors, *The neural Bases of multisensory processes*, pages 557–580. London: CRC Press (Taylor & Francis), 2012.

Bibliography

[345] T. Heed, J. Backhaus, and B. Röder. Integration of hand and finger location in external spatial coordinates for tactile localization. *Journal of experimental psychology. Human perception and performance*, 38(2):386–401, 2012.

[346] J. Hegdé and D. C. Van Essen. Selectivity for complex shapes in primate visual area V2. *The Journal of neuroscience*, 20(5):RC61, 2000.

[347] L. M. Heiser and C. L. Colby. Spatial updating in area LIP is independent of saccade direction. *Journal of neurophysiology*, 95(5):2751–67, 2006.

[348] W. Heller and J. Levy. Perception and expression of emotions in right-handers and left-handers. *Neuropsychologia*, 19(2):263–272, 1981.

[349] J. B. Hellige. Hemispheric asymmetry for visual information processing. *Acta neurobiologiae experimentalis*, 56(1):485–97, 1996.

[350] C. Helmchen and H. Rambold. The eyelid and its contribution to eye movements. *Developments in ophthalmology*, 40:110–31, 2007.

[351] J. Henderson, J. Brockmole, M. Castelhano, and M. Mack. Visual saliency does not account for eye movements during visual search in real-world scenes. In R. P. G. V. Gompel, M. Fischer, W. Murray, and R. Hill, editors, *Eye movements: a window on mind and brain*, pages 537–562. Elsevier, 2007.

[352] J. M. Henderson and A. Hollingworth. Global transsaccadic change blindness during scene perception. *Psychological science*, 14(5):493–7, 2003.

[353] J. M. Henderson, S. G. Luke, J. Schmidt, and J. E. Richards. Co-registration of eye movements and event-related potentials in connected-text paragraph reading. *Frontiers in systems neuroscience*, 7(July):28, 2013.

[354] W. Heron. Perception as a function of retinal locus and attention. *The American Journal of Psychology*, 70(1):38–48, 1957.

[355] M. Hershenson. Reaction time as a measure of intersensory facilitation. *Journal of experimental psychology*, 63(3):289–293, 1962.

[356] T. Hershey, M. C. Campbell, T. O. Videen, H. M. Lugar, P. M. Weaver, J. Hartlein, M. Karimi, S. D. Tabbal, and J. S. Perlmutter. Mapping Go-No-Go performance within the subthalamic nucleus region. *Brain*, 133(12):3625–3634, 2010.

[357] O. Hershler and S. Hochstein. At first sight: a high-level pop out effect for faces. *Vision research*, 45(13):1707–24, 2005.

[358] O. Hershler and S. Hochstein. With a careful look: still no low-level confound to face pop-out. *Vision research*, 46(18):3028–35, 2006.

[359] O. Hikosaka and R. H. Wurtz. Visual and oculomotor functions of monkey substantia nigra pars reticulata. III. Memory-contingent visual and saccade responses. *Journal of neurophysiology*, 49 (5):1268–1284, 1983.

[360] O. Hikosaka, Y. Takikawa, and R. Kawagoe. Role of the basal ganglia in the control of purposive saccadic eye movements. *Physiological reviews*, 80(3):953–978, 2000.

[361] C. C. Hilgetag, R. Kötter, and M. P. Young. Inter-hemispheric competition of sub-cortical structures is a crucial mechanism in paradoxical lesion effects and spatial neglect., 1999.

[362] C. C. Hilgetag, H. Théoret, and A. Pascual-Leone. Enhanced visual spatial attention ipsilateral to rTMS-induced 'virtual lesions' of human parietal cortex. *Nature neuroscience*, 4(9):953–7, 2001.

[363] S. A. Hillyard and R. Galambos. Eye movement artifact in the CNV. *Electroencephalography and clinical neurophysiology*, 28(2):173–182, 1970.

[364] J. F. Hipp and M. Siegel. Dissociating neuronal gamma-band activity from cranial and ocular muscle activity in EEG. *Frontiers in human neuroscience*, 7(July):338, 2013.

[365] J. Hoffman and B. Subramaniam. The role of visual attention in saccadic eye movements. *Perception & psychophysics*, 57(6):787–795, 1995.

[366] S. Hoffmann and M. Falkenstein. The correction of eye blink artefacts in the EEG: a comparison of two prominent methods. *PloS one*, 3(8):e3004, 2008.

[367] A. Hollingworth and J. M. Henderson. Accurate visual memory for previously attended objects in natural scenes. *Journal of Experimental Psychology: Human Perception and Performance*, 28 (1):113–136, 2002.

[368] N. Hoogenboom, J.-M. Schoffelen, R. Oostenveld, L. M. Parkes, and P. Fries. Localizing human visual gamma-band activity in frequency, time and space. *NeuroImage*, 29(3):764–73, 2006.

[369] J. B. Hopfinger, M. H. Buonocore, and G. R. Mangun. The neural mechanisms of top-down attentional control. *Nature neuroscience*, 3(3):284–91, 2000.

[370] J. Hornak. Ocular exploration in the dark by patients with visual neglect. *Neuropsychologia*, 30(6):547–552, 1992.

[371] T. Hosoya, S. A. Baccus, and M. Meister. Dynamic predictive coding by the retina. *Nature*, 436(7047):71–7, 2005.

[372] Y. Huang and R. P. N. Rao. Predictive coding. *Wiley Interdisciplinary Reviews: Cognitive Science*, 2(5):580–593, 2011.

[373] Y.-Z. Huang, M. J. Edwards, E. Rounis, K. P. Bhatia, and J. C. Rothwell. Theta burst stimulation of the human motor cortex. *Neuron*, 45(2):201–6, 2005.

[374] D. H. Hubel and T. N. Wiesel. Receptive fields, binocular interaction and functional architecture in the cat's visual cortex. *The Journal of Physiology*, 160:106–154, 1962.

[375] D. H. Hubel and T. N. Wiesel. Receptive fields and functional architecture in two nonstriate visual areas (18 and 19) of the cat. *Journal of neurophysiology*, 28:229–289, 1965.

[376] D. H. Hubel and T. N. Wiesel. Uniformity of monkey striate cortex: a parallel relationship between field size, scatter, and magnification factor. *The Journal of comparative neurology*, 158(3): 295–305, 1974.

[377] H. F. Huddleston. Electronystagmographic studies of small vertical fixation movements. *British Journal of Ophthalmology*, 54(1):37–40, 1970.

[378] A. R. Hunt and A. Kingstone. Covert and overt voluntary attention: Linked or independent? *Cognitive Brain Research*, 18(1):102–105, 2003.

[379] J. Hupé, A. James, P. Girard, and J. Bullier. Response modulations by static texture surround in area V1 of the macaque monkey do not depend on feedback connections from V2. *Journal of Neurophysiology*, 85(1):146–163, 2001.

[380] M. Husain and C. Rorden. Non-spatially lateralized mechanisms in hemispatial neglect. *Nature Reviews Neuroscience*, 4(1):26–36, 2003.

[381] M. R. Ibbotson, N. a. Crowder, S. L. Cloherty, N. S. C. Price, and M. J. Mustari. Saccadic modulation of neural responses: possible roles in saccadic suppression, enhancement, and time compression. *The Journal of neuroscience*, 28(43):10952–60, 2008.

[382] A. Ignashchenkova, P. W. Dicke, T. Haarmeier, and P. Thier. Neuron-specific contribution of the superior colliculus to overt and covert shifts of attention. *Nature neuroscience*, 7(1):56–64, 2004.

[383] I. Indovina and E. Macaluso. Dissociation of stimulus relevance and saliency factors during shifts of visuospatial attention. *Cerebral cortex*, 17(7):1701–11, 2007.

[384] R. Inzelberg, M. Plotnik, T. Flash, E. Schechtman, I. Shahar, and a. D. Korczyn. Mental and motor switching in Parkinson's disease. *Journal of motor behavior*, 33(4):377–385, 2001.

[385] J. Iriarte, E. Urrestarazu, M. Valencia, M. Alegre, A. Malanda, C. Viteri, and J. Artieda. Independent component analysis as a tool to eliminate artifacts in EEG: a quantitative study. *Journal of clinical neurophysiology*, 20(4):249–57, 2003.

[386] D. E. Irwin, a. M. Colcombe, a. F. Kramer, and S. Hahn. Attentional and oculomotor capture by onset, luminance and color singletons. *Vision research*, 40(10-12):1443–58, 2000.

[387] S. Ishiai, T. Furukawa, and H. Tsukagoshi. Visuospatial processes of line bisection and the mechanisms underlying unilateral spatial neglect. *Brain*, 112:1485–1502, 1989.

[388] M. Ito and H. Komatsu. Representation of Angles Embedded within Contour Stimuli in Area V2 of Macaque Monkeys. *Attention, Perception, & Psychophysics*, 24(13):3313–3324, 2004.

[389] L. Itti and C. Koch. A saliency-based search mechanism for overt and covert shifts of visual attention. *Vision research*, 40(10-12):1489–506, 2000.

[390] L. Itti and C. Koch. Computational modelling of visual attention. *Nature Reviews Neuroscience*, 2(3):194–203, 2001.

[391] L. Itti, C. Koch, and E. Niebur. A model of saliency-based visual attention for rapid scene analysis. *IEEE Transactions on Pattern Analysis and Machine Intelligence*, 20(11):1254–1259, 1998.

[392] R. B. Ivry and L. C. Robertson. *The Two Sides of Perception*. MIT Press, Cambridge, Mass, USA, 1998. ISBN 0262090341.

[393] M. Jane Riddoch and G. W. Humphreys. Perceptual and action systems in unilateral visual neglect. *Advances in Psychology*, 45:151–181, 1987.

[394] G. Jewell and M. E. McCourt. Pseudoneglect: a review and meta-analysis of performance factors in line bisection tasks. *Neuropsychologia*, 38(1):93–110, 2000.

[395] H. Jiang, B. E. Stein, and J. G. McHaffie. Opposing basal ganglia processes shape midbrain visuomotor activity bilaterally. *Nature*, 423:982–6, 2003.

[396] H. Jiang, B. E. Stein, and J. G. McHaffie. Cortical lesion-induced visual hemineglect is prevented by NMDA antagonist pretreatment. *The Journal of neuroscience*, 29(21):6917–25, 2009.

[397] W. Jiang, M. T. Wallace, H. Jiang, J. W. Vaughan, and B. E. Stein. Two cortical areas mediate multisensory integration in superior colliculus neurons. *Journal of neurophysiology*, 85(2):506–22, 2001.

[398] W. Jiang, H. Jiang, and B. Stein. Two corticotectal areas facilitate multisensory orientation behavior. *Journal of cognitive neuroscience*, 14(8):1240–1255, 2002.

[399] D. Joel and I. Weiner. The organization of the basal ganglia-thalamocortical circuits: open interconnected rather than closed segregated. *Neuroscience*, 63(2):363–379, 1994.

[400] H. E. Jones, K. L. Grieve, W. Wang, and A. M. Sillito. Surround suppression in primate V1. *Journal of neurophysiology*, 86(4):2011–28, 2001.

[401] J. Jonides. Voluntary versus automatic contorl over the mind's eye's movement. In J. Long and A. Baddeley, editors, *Attention and performance IX*, chapter 11, pages 187–203. Erlbaum, Hillsdale, NJ, 1981.

[402] J. Jonides and S. Yantis. Uniqueness of abrupt visual onset in capturing attention. *Perception & psychophysics*, 1988.

[403] J. S. Joseph, M. M. Chun, and K. Nakayama. Attentional requirements in a preattentive feature search task. *Nature*, 387:805–807, 1997.

[404] J. Jovancevic-Misic and M. Hayhoe. Adaptive gaze control in natural environments. *The Journal of neuroscience*, 29(19):6234–6238, 2009.

[405] C. Joyce, I. Gorodnitsky, and M. Kutas. Automatic removal of eye movement and blink artifacts from EEG data using blind component separation. *Psychophysiology*, 41:313–325, 2004.

[406] B. Julesz. Textons, the elements of texture perception, and their interactions. *Nature*, 290:91–97, 1981.

[407] B. Julesz and J. Bergen. Textons, the fundamental elements in preattentive vision and perception of textures. *The Bell system technical journal*, 62(6):1619–1645, 1983.

[408] T. P. Jung, S. Makeig, C. Humphries, T. W. Lee, M. J. McKeown, V. Iragui, and T. J. Sejnowski. Removing electroencephalographic artifacts by blind source separation. *Psychophysiology*, 37(2): 163–78, 2000.

[409] M. Kaiser and M. Lappe. Perisaccadic Mislocalization Orthogonal to Saccade Direction. *Neuron*, 41:293–300, 2004.

[410] J. E. Kamienkowski, M. J. Ison, R. Q. Qiuiroga, and M. Sigman. Fixation-related potentials in visual search: a combined EEG and eye tracking study. *Journal of Vision*, 12:1–20, 2012.

[411] H. Kamps. *The Rules of Photography and When to Break Them*. ILEX, Lewes, 2012.

[412] N. Kanwisher and G. Yovel. The fusiform face area: a cortical region specialized for the perception of faces. *Philosophical Transactions of the Royal Society B: Biological Sciences*, 361: 2109–2128, 2006.

[413] N. Kanwisher, J. McDermott, and M. M. Chun. The fusiform face area: a module in human extrastriate cortex specialized for face perception. *The Journal of neuroscience*, 17(11):4302–11, 1997.

[414] M. K. Kapadia, G. Westheimer, and C. D. Gilbert. Spatial distribution of contextual interactions in primary visual cortex and in visual perception. *Journal of neurophysiology*, 84(4):2048–62, 2000.

[415] N. Kaptein, J. Theeuwes, and A. van der Heijden. Search for an conjunctively defined target can be selectively limited to color defined subset of elements. *Journal of experimental psychology. Human perception and performance*, 21(1053-1069), 1995.

[416] H.-O. Karnath and M. Niemeier. Task-dependent differences in the exploratory behaviour of patients with spatial neglect. *Neuropsychologia*, 40(9):1577–85, 2002.

[417] H. O. Karnath, M. Niemeier, and J. Dichgans. Space exploration in neglect. *Brain*, 121:2357–2367, 1998.

[418] S. Kastner, P. D. Weerd, R. Desimone, and L. Ungerleider. Mechanisms of directed attention in the human extrastriate cortex as revealed by functional MRI. *Science*, 282:108–112, 1998.

[419] S. Kastner, M. A. Pinsk, P. De Weerd, R. Desimone, and L. G. Ungerleider. Increased activity in human visual cortex during directed attention in the absence of visual stimulation. *Neuron*, 22(4): 751–61, 1999.

[420] M. Kato and S. Miyauchi. Functional MRI of brain activation evoked by intentional eye blinking. *NeuroImage*, 18(3):749–59, 2003.

[421] M. Kato, N. Miyashita, O. Hikosaka, M. Matsumura, S. Usui, and A. Kori. Eye movements in monkeys with local dopamine depletion in the caudate nucleus. I. Deficits in spontaneous saccades. *Journal of Neuroscience*, 15(1):912–927, 1995.

[422] L. N. Kaunitz, J. E. Kamienkowski, A. Varatharajah, M. Sigman, R. Q. Quiroga, and M. J. Ison. Looking for a face in the crowd: fixation-related potentials in an eye-movement visual search task. *NeuroImage*, 89:297–305, 2014.

[423] C. Kayser, R. F. Salazar, and P. Konig. Responses to natural scenes in cat V1. *Journal of neurophysiology*, 90(3):1910–20, 2003.

[424] C. Kayser, C. I. Petkov, M. Augath, and N. K. Logothetis. Integration of touch and sound in auditory cortex. *Neuron*, 48(2):373–84, 2005.

[425] C. Kayser, K. J. Nielsen, and N. K. Logothetis. Fixations in natural scenes: interaction of image structure and image content. *Vision research*, 46(16):2535–45, 2006.

[426] E. G. Keating, S. G. Gooley, S. E. Pratt, and J. E. Kelsey. Removing the superior colliculus silences eye movements normally evoked from stimulation of the parietal and occipital eye fields. *Brain research*, 269(1):145–8, 1983.

[427] S. P. Kelly and R. G. O'Connell. Internal and external influences on the rate of sensory evidence accumulation in the human brain. *The Journal of neuroscience*, 33(50):19434–41, 2013.

[428] S. Kennett, M. Eimer, C. Spence, and J. Driver. Tactile-Visual Links in Exogenous Spatial Attention under Different Postures: Convergent Evidence from Psychophysics and ERPs. *Journal of Cognitive Neuroscience*, 13(4):462–478, 2001.

[429] S. Kennett, C. Spence, and J. Driver. Visuo-tactile links in covert exogenous spatial attention remap across changes in unseen hand posture. *Perception & psychophysics*, 64(7):1083–94, 2002.

[430] A. S. Keren, S. Yuval-Greenberg, and L. Y. Deouell. Saccadic spike potentials in gamma-band EEG: characterization, detection and suppression. *NeuroImage*, 49(3):2248–63, 2010.

[431] D. Kersten. Predictability and redundancy of natural images. *Journal of the Optical Society America A*, 4(12):2395–2400, 1987.

[432] D. Kersten and A. Yuille. Bayesian models of object perception. *Current Opinion in Neurobiology*, 13(2):150–158, 2003.

[433] M. C. Keuken, P.-L. Bazin, A. Schäfer, J. Neumann, R. Turner, and B. U. Forstmann. Ultra-high 7T MRI of structural age-related changes of the subthalamic nucleus. *The Journal of neuroscience*, 33(11):4896–900, 2013.

[434] J. Kierkels and J. Riani. Using an eye tracker for accurate eye movement artifact correction. *IEEE Transactions on Biomedical Engineering*, 54(7):1256–1267, 2007.

[435] T. Kietzmann and P. König. Perceptual learning of parametric face categories leads to the integration of high-level class-based information but not to high-level pop-out. *Journal of vision*, 10: 1–14, 2010.

[436] J.-H. Kim, F. Biessmann, and S.-W. Lee. Decoding Three-Dimensional Trajectory of Executed and Imagined Arm Movements From Electroencephalogram Signals. *IEEE Transactions on Neural Systems and Rehabilitation Engineering*, XX(X):1–1, 2015.

[437] D. Kimura. Dual functional asymmetry of the brain in visual perception. *Neuropsychologia*, 4(3):275–285, 1966.

[438] J. M. Kincade, R. A. Abrams, S. V. Astafiev, G. L. Shulman, and M. Corbetta. An event-related functional magnetic resonance imaging study of voluntary and stimulus-driven orienting of attention. *The Journal of neuroscience*, 25(18):4593–604, 2005.

[439] M. Kinsbourne. Mechanisms of unilateral neglect. In M. Jeannerod, editor, *Neurophysiological and Neuropsychological Aspects of Spatial Neglect*, pages 69–86. Elsevier Science, Amsterdam, 1987.

[440] F. L. Kitterle, S. Christman, and J. B. Hellige. Hemispheric differences are found in the identification, but not the detection, of low versus high spatial frequencies. *Perception & psychophysics*, 48(4):297–306, 1990.

[441] F. L. Kitterle, J. B. Hellige, and S. Christman. Visual hemispheric asymmetries depend on which spatial frequencies are task relevant. *Brain and cognition*, 20(2):308–14, 1992.

[442] R. Klein. Does Oculomotor Readiness Mediate Cognitive Control of Visual Attention? In R. Nickerson, editor, *Attention and performance XVIII*, chapter 13, pages 259–276. Erlbaum, Hillsdale, NJ, 1980. ISBN 0898590388.

[443] R. Klein. On the control of attention. *Canadian journal of experimental psychology*, 63(3):240–252, 2009.

[444] R. M. Klein. Inhibition of return. *Trends in Cognitive Sciences*, 4(4):138–147, 2000.

[445] M. Kleiner, D. Brainard, and D. Pelli. What's new in Psychtoolbox-3? *Perception ECVP abstract*, 36, 2007.

[446] T. Knapen, M. Rolfs, and P. Cavanagh. The reference frame of the motion aftereffect is retinotopic. *Journal of Vision*, 9(5):16, 2009.

[447] D. C. Knill and A. Pouget. The Bayesian brain: the role of uncertainty in neural coding and computation. *Trends in neurosciences*, 27(12):712–9, 2004.

[448] E. I. Knudsen. Fundamental components of attention. *Annual review of neuroscience*, 30:57–78, 2007.

[449] E. I. Knudsen. Control from below: the role of a midbrain network in spatial attention. *The European journal of neuroscience*, 33(11):1961–72, 2011.

[450] C. Koch and S. Ullman. Shifts in selective visual attention: towards the underlying neural circuitry. *Human neurobiology*, 4(4):219–27, 1985.

[451] G. Koch, S. Bonni, V. Giacobbe, G. Bucchi, B. Basile, F. Lupo, V. Versace, M. Bozzali, and C. Caltagirone. Theta-burst stimulation of the left hemisphere accelerates recovery of hemispatial neglect. *Neurology*, 78(1):24–30, 2012.

[452] S. P. Koch, P. Werner, J. Steinbrink, P. Fries, and H. Obrig. Stimulus-induced and state-dependent sustained gamma activity is tightly coupled to the hemodynamic response in humans. *The Journal of neuroscience*, 29(44):13962–70, 2009.

[453] A. Koene and L. Zhaoping. Feature-specific interactions in salience from combined feature contrasts: Evidence for a bottom up saliency map in V1. *Journal of Vision*, 7:1–14, 2007.

[454] P. Kok, J. F. M. Jehee, and F. P. de Lange. Less is more: expectation sharpens representations in the primary visual cortex. *Neuron*, 75(2):265–70, 2012.

[455] S. Kollmorgen, N. Nortmann, S. Schröder, and P. König. Influence of low-level stimulus features, task dependent factors, and spatial biases on overt visual attention. *PLoS computational biology*, 6(5):e1000791, 2010.

[456] A. Kolossa, T. Fingscheidt, K. Wessel, and B. Kopp. A model-based approach to trial-by-trial p300 amplitude fluctuations. *Frontiers in human neuroscience*, 6:359, 2013.

[457] H. Komatsu, M. Kinoshita, and I. Murakami. Neural responses in the retinotopic representation of the blind spot in the macaque V1 to stimuli for perceptual filling-in. *The Journal of neuroscience*, 20(24):9310–9, 2000.

[458] K. P. Körding and D. M. Wolpert. Bayesian integration in sensorimotor learning. *Nature*, 427(6971):244–7, 2004.

[459] A. Kori, N. Miyashita, M. Kato, O. Hikosaka, S. Usui, and M. Matsumura. Eye movements in monkeys with local dopamine depletion in the caudate nucleus. II. Deficits in voluntary saccades. *Journal of Neuroscience*, 15(1):928, 1995.

[460] E. Kowler, E. Anderson, B. Dosher, and E. Blaser. The role of attention in the programming of saccades. *Vision research*, 35(13):1897–1916, 1995.

[461] R. J. Krauzlis. The control of voluntary eye movements: new perspectives. *The Neuroscientist*, 11(2):124–37, 2005.

[462] D. J. Kravitz, K. S. Saleem, C. I. Baker, and M. Mishkin. A new neural framework for visuospatial processing. *Nature Reviews Neuroscience*, 12(4):217–30, 2011.

[463] D. J. Kravitz, K. S. Saleem, C. I. Baker, L. G. Ungerleider, and M. Mishkin. The ventral visual pathway: An expanded neural framework for the processing of object quality. *Trends in Cognitive Sciences*, 17(1):26–49, 2013.

[464] G. Krieger, I. Rentschler, G. Hauske, K. Schill, and C. Zetzsche. Object and scene analysis by saccadic eye-movements: an investigation with higher-order statistics. *Spatial vision*, 13(2-3): 201–14, 2000.

[465] J. Kruschke. *Doing Bayesian data analysis: A tutorial introduction with R*. Academic Press, Burlington, MA, 2011.

[466] J. Kruschke. Bayesian Estimation Supersedes the t Test. *Journal of Experimental Psychology: General*, 142(2):573–603, 2013.

[467] J. Kulynych, K. Vladar, D. W. Jones, and D. R. Weinberger. Gender differences in the normal lateralization of the supratemporal cortex: MRI surface-rendering morphometry of Heschl's gyrus and the planum temporale. *Cerebral cortex*, 4:107–118, 1994.

[468] T. Kumada. Limitations in attending to a feature value for overriding stimulus-driven interference. *Perception & Psychophysics*, 61(1):61–79, 1999.

[469] D. Kurtzberg and H. G. Vaughan. Topographic analysis of human cortical potentials preceding self-initiated and visually triggered saccades. *Brain research*, 243(1):1–9, 1982.

[470] A. Kustov and D. Robinson. Shared neural control of attentional shifts and eye movements. *Nature*, 384:74–77, 1996.

[471] M. Kusunoki, J. Gottlieb, and M. E. Goldberg. The lateral intraparietal area as a salience map: the representation of abrupt onset, stimulus motion, and task relevance. *Vision research*, 40(10-12): 1459–68, 2000.

[472] D. LaBerge. *Attentional processing: The brains art of mindfulness.* Harvard University Press, Cambridge, MA, 1995.

[473] D. LaBerge and V. Brown. Theory of attentional operations in shape identification. *Psychological Review*, 96(1):101–124, 1989.

[474] E. Làdavas, M. Carletti, and G. Gori. Automatic and voluntary orienting of attention in patients with visual neglect: horizontal and vertical dimensions. *Neuropsychologia*, 32(10):1195–208, 1994.

[475] P. Lakatos, C.-M. Chen, M. N. O'Connell, A. Mills, and C. E. Schroeder. Neuronal oscillations and multisensory interaction in primary auditory cortex. *Neuron*, 53(2):279–92, 2007.

[476] P. Lakatos, G. Karmos, A. D. Mehta, I. Ulbert, and C. E. Schroeder. Entrainment of neuronal oscillations as a mechanism of attentional selection. *Science*, 320(5872):110–3, 2008.

[477] M. Lamb and E. Yund. The role of spatial frequency in the processing of hierarchically organized stimuli. *Perception & Psychophysics*, 54(6):773–784, 1993.

[478] D. Lamy and H. E. Egeth. Attentional capture in singleton-detection and feature-search modes. *Journal of experimental psychology. Human perception and performance*, 29(5):1003–20, 2003.

[479] D. Lamy and Y. Tsal. A salient distractor does not disrupt conjunction search. *Psychonomic Bulletin & Review*, 6(1):93–98, 1999.

[480] M. Land and M. Hayhoe. In what ways do eye movements contribute to everyday activities? *Vision research*, 41:3559– 3565, 2001.

[481] P. J. Lang, M. M. Bradley, and B. N. Cuthbert. Emotion, attention, and the startle reflex. *Psychological review*, 97(3):377–95, 1990.

[482] S. R. H. Langton, A. S. Law, A. M. Burton, and S. R. Schweinberger. Attention capture by faces. *Cognition*, 107(1):330–42, 2008.

[483] M. Lappe, H. Awater, and B. Krekelberg. Postsaccadic visual references generate presaccadic compression of space. *Nature*, 403:892–895, 2000.

[484] T. M. Laudate, S. Neargarder, and A. Cronin-Golomb. Line bisection in Parkinson's disease: investigation of contributions of visual field, retinal vision, and scanning patterns to visuospatial function. *Behavioral neuroscience*, 127(2):151–63, 2013.

[485] S. B. Laughlin, S. B. Laughlin, R. R. de Ruyter van Steveninck, R. R. de Ruyter van Steveninck, J. C. Anderson, and J. C. Anderson. The metabolic cost of neural information. *Nature neuroscience*, 1(1):36–41, 1998.

[486] A. C. Lee, J. P. Harris, E. A. Atkinson, and M. S. Fowler. Evidence from a line bisection task for visuospatial neglect in Left Hemiparkinsons disease. *Vision Research*, 41:2677– 2686, 2001.

[487] T. S. Lee and D. Mumford. Hierarchical Bayesian inference in the visual cortex. *Journal of the Optical Society America A*, 20(7):1434–1448, 2003.

[488] P. Lennie. The cost of cortical computation. *Current biology*, 13:493–497, 2003.

[489] U. Leonards and N. E. Scott-Samuel. Idiosyncratic initiation of saccadic face exploration in humans. *Vision research*, 45(20):2677–84, 2005.

[490] J. Lettvin, H. Maturana, W. McCulloch, and W. Pitts. What the frog's eye tells the frog's brain. *Proceedings of the IRE*, 47(11):1940–1951, 1959.

[491] A. G. Leventhal, K. G. Thompson, D. Liu, Y. Zhou, and S. J. Ault. Concomitant sensitivity to orientation, direction, and color of cells in layers 2, 3, and 4 of monkey striate cortex. *The Journal of neuroscience*, 15(3):1808–1818, 1995.

[492] I. Levy, U. Hasson, G. Avidan, T. Hendler, and R. Malach. Center-periphery organization of human object areas. *Nature neuroscience*, 4(5):533–539, 2001.

[493] J. Levy. Lateral dominance and aesthetic preference. *Neuropsychologia*, 14(4):431–45, 1976.

[494] J. Levy, W. Heller, M. Banich, and L. Burton. Asymmetry of perception in free viewing of chimeric faces. *Brain and Cognition*, 2:404–419, 1983.

[495] W. B. Levy and R. a. Baxter. Energy efficient neural codes. *Neural computation*, 8:531–543, 1996.

[496] Y. Li, Z. Ma, W. Lu, and Y. Li. Automatic removal of the eye blink artifact from EEG using an ICA-based template matching approach. *Physiological measurement*, 27(4):425–36, 2006.

[497] Z. Li. Visual segmentation by contextual influences via intra-cortical interactions in the primary visual cortex. *Network: Computation in Neural Systems*, 10(2):187–212, 1999.

[498] Z. Li. Contextual influences in V1 as a basis for pop out and asymmetry in visual search. *Proceedings of the National Academy of Sciences*, 96:10530–10535, 1999.

[499] Z. Li. A saliency map in primary visual cortex. *Trends in cognitive sciences*, 6(1):9–16, 2002.

[500] J. Liederman and M. Kinsbourne. The mechanism of neonatal rightward turning bias: A sensory or motor asymmetry? *Infant Behavior and Development*, 3:223–238, 1980.

[501] Y.-P. Lin, Y. Wang, C.-S. Wei, and T.-P. Jung. Assessing the quality of steady-state visual-evoked potentials for moving humans using a mobile electroencephalogram headset. *Frontiers in human neuroscience*, 8(March):182, 2014.

[502] O. G. Lins, T. W. Picton, P. Berg, and M. Scherg. Ocular artifacts in EEG and event-related potentials. I: Scalp topography. *Brain topography*, 6(1):51–63, 1993.

[503] O. G. Lins, T. W. Picton, P. Berg, and M. Scherg. Ocular artifacts in recording EEGs and event-related potentials. II: Source dipoles and source components. *Brain topography*, 6(1):65–78, 1993.

[504] V. Litvak, J. Mattout, S. Kiebel, C. Phillips, R. Henson, J. Kilner, G. Barnes, R. Oostenveld, J. Daunizeau, G. Flandin, W. Penny, and K. Friston. EEG and MEG data analysis in SPM8. *Computational intelligence and neuroscience*, 2011:852961, 2011.

[505] T. Liu, J. Larsson, and M. Carrasco. Feature-Based Attention Modulates Orientation-Selective Responses in Human Visual Cortex. *Neuron*, 55(2):313–323, 2007.

[506] T. Ljungberg and U. Ungerstedt. Sensory Inattention Degeneration Produced by 6-Hydroxydopamine-Induced of Ascending Dopamine Neurons in the Brain. *Experimental Neurology*, 53: 585–600, 1976.

[507] C. Lohnes and G. Earhart. Effect of Subthalamic Deep Brain Stimulation on Turning Kinematics and Related Saccadic Eye Movements in Parkinson Disease. *Experimental neurology*, 236(2): 389–394, 2012.

[508] S. G. Lomber and B. R. Payne. Removal of two halves restores the whole: Reversal of visual hemineglect during bilateral cortical or collicular inactivation in the cat. *Visual Neuroscience*, 13 (06):1143, 1996.

[509] L. P. Lovejoy and R. J. Krauzlis. Inactivation of primate superior colliculus impairs covert selection of signals for perceptual judgments. *Nature neuroscience*, 13(2):261–6, 2010.

[510] R. E. Lubow and O. Kaplan. Visual search as a function of type of prior experience with target and distractor. *Journal of Experimental Psychology: Human Perception and Performance*, 23(1): 14–24, 1997.

[511] S. J. Luck. *An Introduction to the Event-Related Potential Technique*. MIT Press, Cambridge, MA, 2005.

[512] S. J. Luck, L. Chelazzi, S. a. Hillyard, and R. Desimone. Neural mechanisms of spatial selective attention in areas V1, V2, and V4 of macaque visual cortex. *Journal of neurophysiology*, 77(1): 24–42, 1997.

[513] K. Luh, J. Redl, and J. Levy. Left- and right-handers see people differently: free-vision perceptual asymmetries for chimeric stimuli. *Brain and cognition*, 25:141–160, 1994.

[514] K. E. Luh, L. M. Rueckert, and J. Levy. Perceptual asymmetries for free viewing of several types of chimeric stimuli. *Brain and cognition*, 16(1):83–103, 1991.

[515] O. Lyilikci, C. Becker, O. Güntürkün, and S. Amado. Visual processing asymmetries in change detection. *Perception*, 39(6):761–769, 2010.

[516] J. C. Lynch and J. W. McLaren. Deficits of visual attention and saccadic eye movements after lesions of parietooccipital cortex in monkeys. *Journal of neurophysiology*, 61(1):74–90, 1989.

[517] E. Macaluso and J. Driver. Multisensory spatial interactions: a window onto functional integration in the human brain. *Trends in neurosciences*, 28:264–271, 2005.

[518] E. Macaluso, C. Frith, and J. Driver. Modulation of Human Visual Cortex by Crossmodal Spatial Attention. *Science*, 289:1206–1208, 2000.

[519] E. Macaluso, C. D. Frith, and J. Driver. Supramodal effects of covert spatial orienting triggered by visual or tactile events. *Journal of Cognitive Neuroscience*, 14(3):389–401, 2002.

[520] E. Macaluso, C. D. Frith, and J. Driver. Multisensory stimulation with or without saccades: fMRI evidence for crossmodal effects on sensory-specific cortices that reflect multisensory location-congruence rather than task-relevance. *NeuroImage*, 26(2):414–25, 2005.

[521] B. Machner, M. Dorr, A. Sprenger, J. von der Gablentz, W. Heide, E. Barth, and C. Helmchen. Impact of dynamic bottom-up features and top-down control on the visual exploration of moving real-world scenes in hemispatial neglect. *Neuropsychologia*, 50(10):2415–25, 2012.

[522] K. Macko, C. D. Jarvis, C. Kennedy, M. Miyaoka, M. Shinohara, L. Sololoff, and M. Mishkin. Mapping the primate visual system with [2-14C]deoxyglucose. *Science*, 218:394–397, 1982.

[523] B. Z. Mahon and A. Caramazza. Concepts and categories: a cognitive neuropsychological perspective. *Annual review of psychology*, 60:27–51, 2009.

[524] S. Makeig and J. Onton. ERP Features and EEG Dynamics: An ICA Perspective. In S. Luck and E. Kappenman, editors, *Oxford Handbook of Event-Related Potential Components*, pages 51–87. Oxford University Press, New York, NY, US, 2009.

[525] S. Makeig, A. Bell, T.-P. Jung, and T. Sejnowski. Independent Component Analysis of Electroencephalographic Data. In D. Touretzky, M. Mozer, and M. Hasselmo, editors, *Advances in Neural Information Processing Systems 8*, volume 8, pages 145–151. MIT Press, Cambridge, MA, 1996. ISBN 0780374886.

[526] R. Malach, I. Levy, and U. Hasson. The topography of high-order human object areas. *Trends in Cognitive Sciences*, 6(4):176–184, 2002.

[527] V. Maljkovic and K. Nakayama. Priming of pop-out: I. Role of features. *Memory & cognition*, 22(6):657–672, 1994.

[528] V. Maljkovic and K. Nakayama. Priming of pop-out: II. The role of position. *Perception & psychophysics*, 58(7):977–991, 1996.

[529] L. Maloney and P. Mamassian. Bayesian decision theory as a model of human visual perception: Testing Bayesian transfer. *Visual Neuroscience*, 26(01):147, 2009.

[530] G. R. Mangano, M. Oliveri, P. Turriziani, D. Smirni, L. Zhaoping, and L. Cipolotti. Impairments in top down attentional processes in right parietal patients: Paradoxical functional facilitation in visual search. *Vision Research*, 97:74–82, 2014.

[531] S. Mannan, C. Kennard, and M. Hussain. The role of visual salience in directing eye movements in visual object agnosia. *Current biology*, pages 247–248, 2009.

[532] V. Mante, R. a. Frazor, V. Bonin, W. S. Geisler, and M. Carandini. Independence of luminance and contrast in natural scenes and in the early visual system. *Nature neuroscience*, 8(12):1690–1697, 2005.

[533] E. Maris and R. Oostenveld. Nonparametric statistical testing of EEG- and MEG-data. *Journal of neuroscience methods*, 164(1):177–90, 2007.

[534] N. T. Markov, J. Vezoli, P. Chameau, A. Falchier, R. Quilodran, C. Huissoud, C. Lamy, P. Misery, P. Giroud, S. Ullman, P. Barone, C. Dehay, K. Knoblauch, and H. Kennedy. Anatomy of hierarchy: Feedforward and feedback pathways in macaque visual cortex. *Journal of Comparative Neurology*, 522:225–259, 2014.

[535] R. B. Mars, S. Debener, T. E. Gladwin, L. M. Harrison, P. Haggard, J. C. Rothwell, and S. Bestmann. Trial-by-trial fluctuations in the event-related electroencephalogram reflect dynamic changes in the degree of surprise. *The Journal of neuroscience*, 28(47):12539–45, 2008.

[536] J. Marshall and P. W. Halligan. Blindsight and insight in visuo-spatial neglect. *Nature*, 336:766–767, 1988.

[537] M. H. Martikainen, K.-I. Kaneko, and R. Hari. Suppressed responses to self-triggered sounds in the human auditory cortex. *Cerebral cortex*, 15(3):299–302, 2005.

[538] A. Martinez, P. Moses, L. Frank, R. Buxton, E. Wong, and J. Stiles. Hemispheric asymmetries in global and local processing: evidence from fMRI. *Neuroreport*, 8(7):1685–9, 1997.

[539] S. Martinez-Conde, S. L. Macknik, and D. H. Hubel. The role of fixational eye movements in visual perception. *Nature reviews. Neuroscience*, 5(3):229–40, 2004.

[540] J. Martinez-Trujillo and S. Treue. Feature-Based Attention Increases the Selectivity of Population Responses in Primate Visual Cortex. *Current Biology*, 14:744–751, 2004.

[541] Q. Mateenuddin, B. Patil, and C. Rao. Elimination of eye blink and eye movement artifacts from EEG data using ICA. *Institution of Engineers (India) Journal of Interdisciplinary Engg, India*, 89(I):32–36, 2008.

[542] L. Matin and D. Pearce. Visual perception of direction for stimuli flashed during voluntary saccadic eye movements. *Science*, 148:1485–1488, 1965.

[543] L. Matin, E. Picoult, J. Stevens, M. Edwards, D. Young, and R. MacArthur. Oculoparalytic Illusion: Visual-Field Dependent Spatial mislocalizations by humans partially paralyzed with curare. *Science*, 216:198–201, 1982.

[544] H. Matsumoto, Y. Terao, T. Furubayashi, A. Yugeta, H. Fukuda, M. Emoto, R. Hanajima, and Y. Ugawa. Small saccades restrict visual scanning area in Parkinson's disease. *Movement disorders*, 26(9):1619–1626, 2011.

[545] M. Matsumoto and H. Komatsu. Neural responses in the macaque v1 to bar stimuli with various lengths presented on the blind spot. *Journal of neurophysiology*, 93(5):2374–87, 2005.

[546] M. Matsumura, J. Kojima, T. W. Gardiner, and O. Hikosaka. Visual and oculomotor functions of monkey subthalamic nucleus. *Journal of neurophysiology*, 67(6):1615–32, 1992.

[547] F. Matsuo, J. F. Peters, and E. L. Reilly. Electrical phenomena associated with movements of the eyelid. *Electroencephalography and clinical neurophysiology*, 38(5):507–11, 1975.

[548] J. B. Mattingley, J. L. Bradshaw, N. C. Nettleton, and J. a. Bradshaw. Can task specific perceptual bias be distinguished from unilateral neglect? *Neuropsychologia*, 32(7):805–17, 1994.

[549] J. H. Maunsell and W. T. Newsome. Visual Processing in Monkey Extrastriate Cortex. *Annual review of neuroscience*, 10:363–401, 1987.

[550] L. Mayfrank, M. Mobashery, H. Kimmig, and B. Fischer. The role of fixation and visual attention in the occurrence of express saccades in man. *European Archives of Psychiatry and Clinical Neuroscience*, 235(5):269–275, 1986.

[551] J. A. Mazer and J. L. Gallant. Goal-related activity in V4 during free viewing visual search. Evidence for a ventral stream visual salience map. *Neuron*, 40(6):1241–50, 2003.

[552] V. Mazza, M. Turatto, M. Rossi, and C. Umiltà. How automatic are audiovisual links in exogenous spatial attention? *Neuropsychologia*, 45(3):514–22, 2007.

[553] J. J. McDonald, W. A. Teder-Sälejärvi, and S. A. Hillyard. Involuntary orienting to sound improves visual perception. *Nature*, 407(6806):906–8, 2000.

[554] R. McGlinchey-Berroth, W. Milberg, M. Verfaellie, M. Alexander, and P. Kilduff. Semantic processing in the neglected visual field: Evidence from a lexical decision task. *Cognitive Neuropsychology*, 10(1):79–108, 1993.

[555] C. C. McIntyre, M. Savasta, L. Kerkerian-Le Goff, and J. L. Vitek. Uncovering the mechanism(s) of action of deep brain stimulation: activation, inhibition, or both. *Clinical neurophysiology*, 115 (6):1239–48, 2004.

[556] M. McKenna, R. Grueter, U. Sonnewald, H. Waagepetersen, and A. Schousboe. Energy metabolism of the brain. In S. Brady, editor, *Basic Neurochemistry: molecilar, cellular, and medical aspects*, pages 531–557. Academic Press, Waltham, MA, 8th edition, 2011.

[557] R. M. McPeek and E. L. Keller. Deficits in saccade target selection after inactivation of superior colliculus. *Nature neuroscience*, 7(7):757–63, 2004.

[558] A. Megreya and C. Havard. Left face matching bias: Right hemisphere dominance or scanning habits? *Laterality*, 16(1):75–92, 2011.

[559] D. Melcher and C. L. Colby. Trans-saccadic perception. *Trends in Cognitive Sciences*, 12:466–473, 2008.

[560] M. Meredith and B. Stein. Interaction among converging sensory inputs in the superior colliculus. *Science*, 369:389–391, 1983.

[561] M. Meredith and B. Stein. Descending efferents from the superior colliculus relay integrated multisensory information. *Science*, 8:657–659, 1985.

[562] M. Meredith, M. Wallace, and B. Stein. Visual, auditory and somatosensory convergence in outputs neurons of the cat superior colliculus: multisensory properties of the tecto-reticulo-spinal projection. *Experimental Brain Research*, 88:181–186, 1992.

[563] M. A. Meredith and B. E. Stein. Spatial factors determine the activity of muitisensory neurons in cat superior colliculus. *Brain Research*, 5:350–354, 1986.

[564] E. P. Merriam, C. R. Genovese, and C. L. Colby. Remapping in human visual cortex. *Journal of neurophysiology*, 97(2):1738–55, 2007.

[565] I. Mertens, H. Siegmund, and O. J. Grüsser. Gaze motor asymmetries in the perception of faces during a memory task. *Neuropsychologia*, 31(9):989–98, 1993.

[566] M. M. Mesulam. A cortical network for directed attention and unilateral neglect. *Annals of neurology*, 10(4):309–325, 1981.

[567] M. M. Mesulam. From sensation to cognition. *Brain*, 121:1013–52, 1998.

[568] M. M. Mesulam. Spatial attention and neglect: parietal, frontal and cingulate contributions to the mental representation and attentional targeting of salient extrapersonal events. *Philosophical transactions of the Royal Society of London. Series B, Biological sciences*, 354(1387):1325–46, 1999.

[569] C. Mevorach, G. W. Humphreys, and L. Shalev. Attending to local form while ignoring global aspects depends on handedness: evidence from TMS. *Nature neuroscience*, 8(3):276–7, 2005.

[570] C. Mevorach, G. W. Humphreys, and L. Shalev. Opposite biases in salience-based selection for the left and right posterior parietal cortex. *Nature neuroscience*, 9(6):740–2, 2006.

[571] C. Mevorach, L. Shalev, H. a. Allen, and G. W. Humphreys. The left intraparietal sulcus modulates the selection of low salient stimuli. *Journal of cognitive neuroscience*, 21(2):303–15, 2009.

[572] C. Mevorach, J. Hodsoll, H. Allen, L. Shalev, and G. Humphreys. Ignoring the elephant in the room: a neural circuit to downregulate salience. *Journal of Neuroscience*, 30(17):6072–9, 2010.

[573] R. C. Miall and D. M. Wolpert. Forward models for physiological motor control, 1996.

[574] W. Miles. Modification of the human eye potential by dark and light adaptation. *Science*, 91(2367):456, 1940.

[575] W. R. Miles. Ocular dominance demonstrated by unconscious sighting. *Journal of Experimental Psychology*, 12(2):113–126, 1929.

[576] E. K. Miller and T. J. Buschman. Cortical circuits for the control of attention. *Current Opinion in Neurobiology*, 23(2):216–222, 2013.

[577] J. Miller. Divided attention: Evidence for coactivation with redundant signals. *Cognitive psychology*, 14:247–279, 1982.

[578] M. Mishkin, L. G. Ungerleider, and K. A. Macko. Object vision and spatial vision: Two cortical pathways. *Trends in Neurosciences*, 6:414–417, 1983.

[579] N. Miyashita, O. Hikosaka, and M. Kato. Visual hemineglect induced by unilateral striatal dopamine deficiency in monkeys. *Neuroreport*, 6:1257–1260, 1995.

[580] C. Mohr, T. Landis, H. Bracha, and P. Brugger. Opposite Turning Behavior in Right-Handers and Non-Right-Handers Suggests a Link Between Handedness and Cerebral Dopamine Asymmetries. *Behavioral neuroscience*, 117(6):1448–1452, 2003.

[581] C. Mohr, P. Brugger, H. Bracha, T. Landis, and I. Viaud-Delmon. Human side preferences in three different whole-body movement tasks. *Behavioural Brain Research*, 151(1-2):321–326, 2004.

[582] T. a. Mondor and K. J. Amirault. Effect of same- and different-modality spatial cues on auditory and visual target identification. *Journal of Experimental Psychology: Human Perception and Performance*, 24(3):745–755, 1998.

[583] E. B. Montgomery and J. T. Gale. Mechanisms of action of deep brain stimulation (DBS). *Neuroscience and Biobehavioral Reviews*, 32(3):388–407, 2008.

[584] T. Moore. Shape representations and visual guidance of saccadic eye movements. *Science*, 285(5435):1914–7, 1999.

[585] G. Moraglia. Display organization and the detection of horizontal line segments. *Perception & Psychophysics*, 45(3):265–272, 1989.

[586] J. Moran and R. Desimone. Selective attention gates visual processing in the extrastriate cortex. *Science*, 229:782–784, 1985.

[587] N. Moray. Attention in dichotic listening: Affective cues and the influence of instructions. *Quarterly Journal of Experimental Psychology*, 11(1):56–60, 1959.

[588] L. Morrell. Temporal characteristics of sensory interaction in choice reaction times. *Journal of Experimental Psychology*, 77(1):14–18, 1968.

[589] J. H. Morrison and S. L. Foote. Noradrenergic and serotoninergic innervation of cortical, thalamic, and tectal visual structures in Old and New World monkeys. *The Journal of comparative neurology*, 243:117–138, 1986.

[590] C. Morrone and D. Burr. Visual stability during saccadic eye movements. In M. Gazzaniga, editor, *The Cognitive Neurosciences*, pages 511–524. WW Norton & Compay, New York, 3rd edition, 2009.

[591] B. Motter. Focal attention produces spatially selective processing in visual cortical areas V1, V2, and V4 in the presence of competing stimuli. *Journal of neurophysiology*, 70(3):909–919, 1993.

[592] O. H. Mowrer, T. C. Ruch, and N. E. Miller. The corneo-retinal potential difference as the basis of the galvanometric method of recording eye movements. *American Journal Of Physiology*, 114 (2):423–428, 1935.

[593] N. G. Muggleton, P. Postma, K. Moutsopoulou, I. Nimmo-Smith, A. Marcel, and V. Walsh. TMS over right posterior parietal cortex induces neglect in a scene-based frame of reference. *Neuropsychologia*, 44(7):1222–1229, 2006.

[594] H. Müller and J. Findlay. The effect of visual attention on peripheral discrimination thresholds in single and multiple element displays. *Acta psychologica*, 69:129–155, 1988.

[595] H. Müller and G. Humphreys. Luminance-increment detection: Capacity-limited or not? *Journal of Experimental Psychology: Human Perception and Performance*, 17(1):107–124, 1991.

[596] H. J. Müller and P. M. Rabbitt. Reflexive and voluntary orienting of visual attention: time course of activation and resistance to interruption. *Journal of experimental psychology. Human perception and performance*, 15(2):315–30, 1989.

[597] J. R. Müller, M. G. Philiastides, and W. T. Newsome. Microstimulation of the superior colliculus focuses attention without moving the eyes. *Proceedings of the National Academy of Sciences of the United States of America*, 102(3):524–9, 2005.

[598] D. Mumford. On the computational architecture of the neocortex. *Biological cybernetics*, 251:241–251, 1992.

[599] R. Müri, D. Cazzoli, T. Nyffeler, and T. Pflugshaupt. Visual exploration pattern in hemineglect. *Psychological research*, 73(2):147–57, 2009.

[600] R. M. Müri. MRI and fMRI analysis of oculomotor function. *Progress in brain research*, 151(1988):503–26, 2006.

[601] R. M. Müri, R. Bühler, D. Heinemann, U. P. Mosimann, J. Felblinger, T. E. Schlaepfer, and C. W. Hess. Hemispheric asymmetry in visuospatial attention assessed with transcranial magnetic stimulation. *Experimental Brain Research*, 143(4):426–430, 2002.

[602] M. M. Murray, S. Molholm, C. M. Michel, D. J. Heslenfeld, W. Ritter, D. C. Javitt, C. E. Schroeder, and J. J. Foxe. Grabbing your ear: rapid auditory-somatosensory multisensory interactions in low-level sensory cortices are not constrained by stimulus alignment. *Cerebral cortex*, 15(7):963–74, 2005.

[603] S. O. Murray, D. Kersten, B. a. Olshausen, P. Schrater, and D. L. Woods. Shape perception reduces activity in human primary visual cortex. *Proceedings of the National Academy of Sciences of the United States of America*, 99(23):15164–9, 2002.

[604] S. O. Murray, H. Boyaci, and D. Kersten. The representation of perceived angular size in human primary visual cortex. *Nature Neuroscience*, 9(3):429–434, 2006.

[605] S. P. Mysore and E. I. Knudsen. A shared inhibitory circuit for both exogenous and endogenous control of stimulus selection. *Nature neuroscience*, 16(4):473–478, 2013.

[606] S. P. Mysore and E. I. Knudsen. Descending control of neural bias and selectivity in a spatial attention network: rules and mechanisms. *Neuron*, 84(1):214–26, 2014.

[607] S. P. Mysore, A. Asadollahi, and E. I. Knudsen. Global Inhibition and Stimulus Competition in the Owl Optic Tectum. *The Journal of neuroscience*, 30(5):1727–1738, 2010.

[608] S. P. Mysore, A. Asadollahi, and E. I. Knudsen. Signaling of the Strongest Stimulus in the Owl Optic Tectum. *The journal of neuroscience*, 31(14):5186–5196, 2011.

[609] A. L. Nagy, R. R. Sanchez, and T. C. Hughes. Visual search for color differences with foveal and peripheral vision. *Journal of the Optical Society of America A*, 7(10):1995, 1990.

[610] K. Nakamura and C. L. Colby. Updating of the visual representation in monkey striate and extrastriate cortex during saccades. *Proceedings of the National Academy of Sciences of the United States of America*, 99(6):4026–31, 2002.

[611] T. Nakano and S. Kitazawa. Eyeblink entrainment at breakpoints of speech. *Experimental brain research*, 205(4):577–81, 2010.

[612] K. Nakayama and M. Mackeben. Sustained and transient components of focal visual attention. *Vision research*, 29(11):1631–1647, 1989.

[613] K. Nakayama and G. Silverman. Serial and parallel processing of visual feature conjunctions. *Nature*, 320:264–265, 1986.

[614] A. Nativ, J. M. Weinstein, and R. Rosas-Ramos. Human presaccadic spike potentials. Of central or peripheral origin? *Investigative ophthalmology & visual science*, 31(9):1923–8, 1990.

[615] V. Navalpakkam and L. Itti. An integrated model of top-down and bottom-up attention for optimizing detection speed. *Computer Vision and Pattern Recognition, 2006 IEEE Computer Society Conference on*, 2006.

[616] D. Navon. Forest Before Trees: The Precedence of Global Features in Visual Perception. *Cognitive Psychology*, 9:353–383, 1977.

[617] S. Neggers and H. Bekkering. Integration of visual and somatosensory target information in goal-directed eye and arm movements. *Experimental Brain Research*, 125:97–107, 1999.

[618] U. Neisser. *Cognitive Psychology*. Prentice-Hall, Englewood Cliffs, NJ, 1967.

[619] M. E. Nicholls, J. L. Bradshaw, and J. B. Mattingley. Free-viewing perceptual asymmetries for the judgement of brightness, numerosity and size. *Neuropsychologia*, 37(3):307–14, 1999.

[620] M. E. R. Nicholls and G. R. Roberts. Can free-viewing perceptual asymmetries be explained by scanning, pre-motor or attentional biases? *Cortex*, 38(2):113–36, 2002.

[621] M. H. Nilsson, M. Patel, S. Rehncrona, M. Magnusson, and P.-A. Fransson. Subthalamic deep brain stimulation improves smooth pursuit and saccade performance in patients with Parkinson's disease. *Journal of neuroengineering and rehabilitation*, 10(1):33, 2013.

[622] A. C. Nobre, D. R. Gitelman, E. C. Dias, and M. M. Mesulam. Covert visual spatial orienting and saccades: overlapping neural systems. *NeuroImage*, 11(3):210–6, 2000.

[623] D. A. Norman. Toward a theory of memory and attention. *Psychological Review*, 75(6):522–536, 1968.

Bibliography

[624] A. W. North. Accuracy and Precision of Electro-Oculographic Recording. *Investigative ophthalmology*, 4:343–8, 1965.

[625] H. Nothdurft. Texture segmentation and pop-out from orientation contrast. *Vision research*, 31(6):1073–1078, 1991.

[626] H. Nothdurft. The role of features in preattentive vision: comparison of orientation, motion and color cues. *Vision research*, 33(14):1937–1958, 1993.

[627] H. Nothdurft. Salience from feature contrast: additivity across dimensions. *Vision research*, 40(10-12):1183–201, 2000.

[628] H.-C. Nothdurft. Attention shifts to salient targets. *Vision research*, 42(10):1287–306, 2002.

[629] W. Nultsch. Survey of Photomotile Responses in Microorganisms. In F. Lenci, F. Ghetti, G. Colombetti, D.-P. Häder, and P.-S. Song, editors, *Biophysics of Photoreceptors and Photomovements in Microorganisms*, pages 1–5. Springer US, Boston, MA, 1991.

[630] P. L. Nunez and R. Srinivasan. *Electric fields of the brain: the neurophysics of EEG*. Oxford university press, 2006.

[631] A. Nuthmann and J. M. Henderson. Object-based attentional selection in scene viewing. *Journal of vision*, 10(8):20, 2010.

[632] T. Nyffeler, D. Cazzoli, P. Wurtz, M. Lüthi, R. von Wartburg, S. Chaves, A. Déruaz, C. W. Hess, and R. M. Müri. Neglect-like visual exploration behaviour after theta burst transcranial magnetic stimulation of the right posterior parietal cortex. *The European journal of neuroscience*, 27(7):1809–13, 2008.

[633] T. Nyffeler, D. Cazzoli, P. Wurtz, M. Lüthi, R. von Wartburg, S. Chaves, A. Déruaz, C. W. Hess, and R. M. Müri. Neglect-like visual exploration behaviour after theta burst transcranial magnetic stimulation of the right posterior parietal cortex. *The European journal of neuroscience*, 27(7):1809–13, 2008.

[634] T. Nyffeler, D. Cazzoli, C. Hess, and R. Müri. One session of repeated parietal theta burst stimulation trains induces long-lasting improvement of visual neglect. *Stroke*, 40(8):2791–6, 2009.

[635] R. G. O'Connell, P. M. Dockree, and S. P. Kelly. A supramodal accumulation-to-bound signal that determines perceptual decisions in humans. *Nature neuroscience*, 15(12):1729–35, 2012.

[636] A. Ojeda, N. Bigdely-Shamlo, and S. Makeig. MoBILAB: an open source toolbox for analysis and visualization of mobile brain/body imaging data. *Frontiers in human neuroscience*, 8(March): 121, 2014.

[637] A. Oke, R. Keller, I. Mefford, and R. N. Adams. Lateralization of norepinephrine in human thalamus. *Science*, 200(4348):1411–1413, 1978.

[638] A. Oke, R. Lewis, and R. N. Adams. Hemispheric asymmetry of norepinephrine distribution in rat thalamus. *Brain research*, 188:269–272, 1980.

[639] R. Oldfield. The assessment and analysis of handedness: the Edinburgh inventory. *Neuropsychologia*, 9:97–113, 1971.

[640] A. Oliva and P. G. Schyns. Coarse Blobs or Fine Edges? Evidence that information diagnosticity changes the perception of complex visual stimuli. *Cognitive psychology*, 34:72–107, 1997.

[641] A. Oliva, A. Torralba, M. Castelhano, and J. Henderson. Top-down control of visual attention in object detection. *Proc. IEEE Int. Conf. Image Processing*, 1:253–256, 2003.

[642] M. Oliveri, P. M. Rossini, R. Traversa, P. Cicinelli, M. M. Filippi, P. Pasqualetti, F. Tomaiuolo, and C. Caltagirone. Left frontal transcranial magnetic stimulation reduces contralesional extinction in patients with unilateral right brain damage. *Brain*, 122:1731–1739, 1999.

[643] M. Oliveri, E. Bisiach, F. Brighina, A. Piazza, V. La Bua, D. Buffa, and B. Fierro. rTMS of the unaffected hemisphere transiently reduces contralesional visuospatial hemineglect. *Neurology*, 57: 1338–1340, 2001.

[644] M. Oliveri, L. Zhaoping, G. R. Mangano, P. Turriziani, D. Smirni, and L. Cipolotti. Facilitation of bottom-up feature detection following rTMS-interference of the right parietal cortex. *Neuropsychologia*, 48(4):1003–1010, 2010.

[645] C. A. Olman, K. Ugurbil, P. Schrater, and D. Kersten. BOLD fMRI and psychophysical measurements of contrast response to broadband images. *Vision Research*, 44(7):669–683, 2004.

[646] A. Olmos and F. A. A. Kingdom. A biologically inspired algorithm for the recovery of shading and reflectance images. *Perception*, 33(12):1463–73, 2004.

[647] B. Olshausen and D. Field. Emergence of simple-cell receptive field properties by learnign a sparse code for natural images. *Nature*, 381:607–609, 1996.

[648] B. a. Olshausen and D. J. Field. Sparse coding with an overcomplete basis set: A strategy employed by V1 ? *Vision Research*, 37(23):3311–3325, 1997.

[649] B. A. Olshausen and D. J. Field. Sparse coding of sensory inputs. *Current Opinion in Neurobiology*, 2004.

[650] B. A. Olshausen and D. J. Field. How close are we to understanding v1? *Neural computation*, 17(8):1665–99, 2005.

[651] S. Onat, K. Libertus, and P. König. Integrating audiovisual information for the control of overt attention. *Journal of vision*, 7(10):11.1–16, 2007.

[652] S. Onat, A. Açik, F. Schumann, and P. König. The contributions of image content and behavioral relevancy to overt attention. *PloS one*, 9(4):e93254, 2014.

[653] R. Oostenveld, P. Fries, E. Maris, and J.-M. Schoffelen. FieldTrip: Open source software for advanced analysis of MEG, EEG, and invasive electrophysiological data. *Computational intelligence and neuroscience*, 2011:156869, 2011.

[654] L. N. Orchard and J. A. Stern. Blinks as an index of cognitive activity during reading. *Integrative physiological and behavioral science*, 26(2):108–16, 1991.

[655] J. Ossandón, S. Onat, D. Cazzoli, T. Nyffeler, R. Müri, and P. König. Unmasking the contribution of low-level features to the guidance of attention. *Neuropsychologia*, 50:3478–3487, 2012.

[656] J. P. Ossandón, A. V. Helo, R. Montefusco-Siegmund, and P. E. Maldonado. Superposition model predicts EEG occipital activity during free viewing of natural scenes. *The Journal of neuroscience*, 30(13):4787–95, 2010.

[657] J. P. Ossandón, A. Açik, and P. König. Low in the forest, high in the city: Visual selection and natural image statistics. *Perception*, 40(ECVP Abstract Supplement):95, 2011.

[658] J. P. Ossandón, S. Onat, and P. König. Spatial biases in viewing behavior. *Journal of vision*, 14(2):20, 2014.

[659] E. A. B. Over, I. T. C. Hooge, B. N. S. Vlaskamp, and C. J. Erkelens. Coarse-to-fine eye movement strategy in visual search. *Vision research*, 47(17):2272–80, 2007.

[660] K. E. Overvliet, E. Azañón, and S. Soto-Faraco. Somatosensory saccades reveal the timing of tactile spatial remapping. *Neuropsychologia*, 49(11):3046–52, 2011.

[661] E. F. Pace-Schott and J. A. Hobson. The neurobiology of sleep: genetics, cellular physiology and subcortical networks. *Nature reviews neuroscience*, 3(8):591–605, 2002.

[662] J. Palmer, S. Makeig, K. Kreutz-Delgado, and B. Rao. Newton method for the ica mixture model. *Proceedings of the 33rd IEEE International Conference on Acoustics and Signal Processing*, pages 1805–1808, 2008.

[663] A. Parent and L.-N. Hazrati. Functional anatomy of the basal ganglia. I. The cortico-basal ganglia-thalamo-cortical loop. *Brain Research Reviews*, 20:91–127, 1995.

[664] D. Parkhurst and E. Niebur. Texture contrast attracts overt visual attention in natural scenes. *European Journal of Neuroscience*, 19(3):783–789, 2004.

[665] D. Parkhurst, K. Law, and E. Niebur. Modeling the role of salience in the allocation of overt visual attention. *Vision research*, 42(1):107–23, 2002.

[666] D. J. Parkhurst and E. Niebur. Scene content selected by active vision. *Spatial vision*, 16(2):125–54, 2003.

[667] N. a. Parks and P. M. Corballis. Electrophysiological correlates of presaccadic remapping in humans. *Psychophysiology*, 45(5):776–83, 2008.

[668] P. Pasik, T. Pasik, and M. Bender. Recovery of the electro-oculogram after total ablation of the retina in monkeys. *Electroencephalography and clinical neurophysiology*, 19(3):291–297, 1965.

[669] B. R. Payne and R. J. Rushmore. Functional circuitry underlying natural and interventional cancellation of visual neglect. *Experimental brain research*, 154(2):127–53, 2004.

[670] C. R. Pernet, N. Chauveau, C. Gaspar, and G. A. Rousselet. LIMO EEG: a toolbox for hierarchical LInear MOdeling of ElectroEncephaloGraphic data. *Computational intelligence and neuroscience*, 2011:831409, 2011.

[671] C. R. Pernet, M. Latinus, T. E. Nichols, and G. A. Rousselet. Cluster-based computational methods for mass univariate analyses of event-related brain potentials/fields: A simulation study. *Journal of Neuroscience Methods*, 250:85–93, 2015.

[672] D. Perrott, K. Saberi, K. Brown, and T. Strybel. Auditory psychomotor coordination and visual search performance. *Perception & psychophysics*, 48(3):214–226, 1990.

[673] R. J. Perry and S. Zeki. The neurology of saccades and covert shifts in spatial attention: an event-related fMRI study. *Brain*, 123:2273–88, 2000.

[674] R. J. Peters, A. Iyer, L. Itti, and C. Koch. Components of bottom-up gaze allocation in natural images. *Vision research*, 45(18):2397–416, 2005.

[675] S. Petersen and M. Posner. The attention system of the human brain: 20 years after. *Annual review of neuroscience*, 21(35):73–89, 2012.

[676] S. E. Petersen, D. L. Robinson, and J. D. Morris. Contributions of the pulvinar to visual spatial attention. *Neuropsychologia*, 25(1A):97–105, 1987.

[677] S. E. Petersen, P. T. Fox, a. Z. Snyder, and M. E. Raichle. Activation of extrastriate and frontal cortical areas by visual words and word-like stimuli. *Science*, 249(4972):1041–4, 1990.

[678] C. Peyrin, M. Baciu, C. Segebarth, and C. Marendaz. Cerebral regions and hemispheric specialization for processing spatial frequencies during natural scene recognition. An event-related fMRI study. *NeuroImage*, 23(2):698–707, 2004.

[679] C. Peyrin, S. Schwartz, M. Seghier, C. Michel, T. Landis, and P. Vuilleumier. Hemispheric specialization of human inferior temporal cortex during coarse-to-fine and fine-to-coarse analysis of natural visual scenes. *NeuroImage*, 28(2):464–73, 2005.

[680] M. L. Phillips and A. S. David. Viewing strategies for simple and chimeric faces: an investigation of perceptual bias in normals and schizophrenic patients using visual scan paths. *Brain and cognition*, 35(2):225–38, 1997.

[681] T. W. Picton, P. van Roon, M. L. Armilio, P. Berg, N. Ille, and M. Scherg. The correction of ocular artifacts: a topographic perspective. *Clinical neurophysiology*, 111(1):53–65, 2000.

[682] C. Pierrot-Deseilligny, S. Rivaud, B. Gaymard, and Y. Agid. Cortical control of reflexive visually-guided saccades. *Brain*, 114 (Pt 3:1473–85, 1991.

[683] C. Pierrot-Deseilligny, D. Milea, and R. M. Müri. Eye movement control by the cerebral cortex. *Current Opinion in Neurology*, 17:17–25, 2004.

[684] E. H. Pinkhardt and J. Kassubek. Ocular motor abnormalities in Parkinsonian syndromes. *Parkinsonism & related disorders*, 17(4):223–30, 2011.

[685] Y. Pinto, C. N. L. Olivers, and J. Theeuwes. Target uncertainty does not lead to more distraction by singletons: intertrial priming does. *Perception & psychophysics*, 67(8):1354–1361, 2005.

[686] L. N. Piotrowski and F. W. Campbell. A demonstration of the visual importance and flexibility of spatial-frequency amplitude and phase. *Perception*, 11(3):337–46, 1982.

[687] P. Plaha, Y. Ben-Shlomo, N. K. Patel, and S. S. Gill. Stimulation of the caudal zona incerta is superior to stimulation of the subthalamic nucleus in improving contralateral parkinsonism. *Brain*, 129(7):1732–1747, 2006.

[688] M. Plöchl, J. P. Ossandón, and P. König. Combining EEG and eye tracking: identification, characterization, and correction of eye movement artifacts in electroencephalographic data. *Frontiers in Human Neuroscience*, 6:1–23, 2012.

[689] M. Plotnik, T. Flash, R. Inzelberg, E. Schechtman, and A. D. Korczyn. Motor switching abilities in Parkinson's disease and old age: temporal aspects. *Journal of neurology, neurosurgery, and psychiatry*, 65:328–337, 1998.

[690] U. Polat, K. Mizobe, M. Pettet, T. Kasamatsu, and A. Norcia. Collinear stimuli regulate visual responses depending on cell's contrast threshold. *Nature*, 391:580–584, 1998.

[691] J. Polich. Updating P300: An integrative theory of P3a and P3b. *Clinical Neurophysiology*, 118:2128–2148, 2007.

[692] M. Pomplun. Saccadic selectivity in complex visual search displays. *Vision research*, 46(12):1886–900, 2006.

[693] M. Posner. Orienting of attention. *Quarterly journal of experimental psychology*, 32:3–25, 1980.

[694] M. Posner and Y. Cohen. Components of visual orienting. In H. Bouma and D. Bouhuis, editors, *Attention and performance X*, chapter 32, pages 531–556. Erlbaum, Hillsdale, NJ, 1984.

[695] M. Posner, Y. Cohen, and R. Rafal. Neural systems control of spatial orienting. *Philosophical Transactions of the Royal Society B: Biological Sciences*, 298:187–198, 1982.

[696] M. Posner, J. Walker, F. Friedrich, and R. Rafal. Effects of parietal injury on covert orienting of attention. *The Journal of Neuroscience*, 4(7):1863, 1984.

[697] M. Posner, R. Rafal, L. Choate, and J. Vaughan. Inhibition of return: Neural basis and function. *Cognitive Neuropsychology*, 2(3):211–228, 1985.

[698] M. I. Posner and S. E. Petersen. The attention system of the human brain. *Annual review of neuroscience*, 13:25–42, 1990.

[699] M. I. Posner, M. J. Nissen, and W. C. Ogden. Attended and unattended processing modes: The role of set for spatial location. *Modes of perceiving and processing information*, 137:158, 1978.

[700] B. D. Power, C. A. Leamey, and J. Mitrofanis. Evidence for a visual subsector within the zona incerta. *Visual neuroscience*, 18(2):179–186, 2001.

[701] A. Presacco, R. Goodman, L. Forrester, and J. L. Contreras-Vidal. Neural decoding of treadmill walking from noninvasive electroencephalographic signals. *Journal of Neurophysiology*, 106(4): 1875–1887, 2011.

[702] R. Ptak and J. Fellrath. Exploring the world with Bálint syndrome: biased bottom-up guidance of gaze by local saliency differences. *Experimental Brain Research*, 232(4):1233–1240, 2014.

[703] R. Ptak and A. Schnider. The dorsal attention network mediates orienting toward behaviorally relevant stimuli in spatial neglect. *The Journal of neuroscience : the official journal of the Society for Neuroscience*, 30(38):12557–65, 2010.

[704] R. Ptak, L. Golay, R. Müri, and A. Schnider. Looking left with left neglect: the role of spatial attention when active vision selects local image features for fixation. *Cortex*, 45(10):1156–66, 2008.

[705] A. Puce, T. Allison, M. Asgari, J. C. Gore, and G. McCarthy. Differential sensitivity of human visual cortex to faces, letterstrings, and textures: a functional magnetic resonance imaging study. *The Journal of neuroscience*, 16(16):5205–15, 1996.

[706] C. Quigley, S. Onat, S. Harding, M. Cooke, and P. König. Audio-visual integration during overt visual attention. *Journal of Eye Movement Research*, 1(2):1–17, 2008.

[707] D. H. Raab. Division of psychology: statistical facilitation of simple reaction times. *Transactions of the New York Academy of Sciences*, 24(5):574–590, 1962.

[708] R. D. Rafal and M. I. Posner. Deficits in human visual spatial attention following thalamic lesions. *Proceedings of the National*, 84(20):7349–7353, 1987.

[709] R. D. Rafal, M. I. Posner, J. H. Friedman, A. W. Inhoff, and E. Bernstein. Orienting of visual attention in progressive supranuclear palsy. *Brain*, 111:267–80, 1988.

[710] C. Rajkai, P. Lakatos, C.-M. Chen, Z. Pincze, G. Karmos, and C. E. Schroeder. Transient cortical excitation at the onset of visual fixation. *Cerebral cortex*, 18(1):200–9, 2008.

[711] R. P. Rao and D. H. Ballard. Predictive coding in the visual cortex: a functional interpretation of some extra-classical receptive-field effects. *Nature neuroscience*, 2(1):79–87, 1999.

[712] D. Ravden and J. Polich. Habituation of P300 from visual stimuli. *International journal of psychophysiology*, 30(3):359–65, 1998.

[713] D. Ravden and J. Polich. On P300 measurement stability: habituation, intra-trial block variation, and ultradian rhythms. *Biological psychology*, 51(1):59–76, 1999.

[714] P. Reinagel and A. M. Zador. Natural scene statistics at the centre of gaze. *Network*, 10(4):341–50, 1999.

[715] P. M. R. Reis, F. Hebenstreit, F. Gabsteiger, V. von Tscharner, and M. Lochmann. Methodological aspects of EEG and body dynamics measurements during motion. *Frontiers in human neuroscience*, 8:156, 2014.

[716] R. W. Remington. Attention and saccadic eye movements. *Journal of Experimental Psychology: Human Perception and Performance*, 6(4):726–744, 1980.

[717] J. Reppas, W. Usrey, and R. Reid. Saccadic eye movements modulate visual responses in the lateral geniculate nucleus. *Neuron*, 35:961–974, 2002.

[718] F. C. Riemslag, G. L. Van der Heijde, M. M. Van Dongen, and F. Ottenhoff. On the origin of the presaccadic spike potential. *Electroencephalography and clinical neurophysiology*, 70(4):281–7, 1988.

[719] J. Ristic and A. Kingstone. Attention to arrows: pointing to a new direction. *Quarterly journal of experimental psychology*, 59(11):1921–1930, 2006.

[720] S. Rivaud-Péchoux, A. I. Vermersch, B. Gaymard, C. J. Ploner, B. P. Bejjani, P. Damier, S. Demeret, Y. Agid, and C. Pierrot-Deseilligny. Improvement of memory guided saccades in parkinsonian patients by high frequency subthalamic nucleus stimulation. *Journal of neurology, neurosurgery, and psychiatry*, 68(3):381–4, 2000.

[721] G. Rizzolatti, L. Riggio, I. Dascola, and C. Umiltá. Reorienting attention across the horizontal and vertical meridians: Evidence in favor of a premotor theory of attention. *Neuropsychologia*, 25 (1):31–40, 1987.

[722] L. C. Robertson and D. C. Delis. 'Part-whole' processing in unilateral brain-damaged patients: dysfunction of hierarchical organization. *Neuropsychologia*, 24(3):363–70, 1986.

[723] R. Robinson. Differential Behavioral and Biochemical Effects of Right and Left Hemispheric Cerebral Infarction in the Rat. *Science*, 205:707–710, 1979.

[724] K. Rockland and D. Pandya. Laminar origins and terminations of cortical connections of the occipital lobe in the rhesus monkey. *Brain Research*, 179(1):3–20, 1979.

[725] P. R. Roelfsema. Cortical algorithms for perceptual grouping. *Annual review of neuroscience*, 29:203–27, 2006.

[726] M. Rolfs and M. Carrasco. Rapid simultaneous enhancement of visual sensitivity and perceived contrast during saccade preparation. *The Journal of neuroscience*, 32(40):13744–52, 2012.

[727] M. Rolfs, D. Jonikaitis, H. Deubel, and P. Cavanagh. Predictive remapping of attention across eye movements. *Nature neuroscience*, 14(2):252–6, 2011.

[728] C. Rorden, K. Greene, G. Sasine, and G. Baylis. Enhanced tactile performance at the destination of an upcoming saccade. *Current Biology*, 12(02):1429–1434, 2002.

[729] J. Ross, M. Morrone, and D. Burr. Compression of visual space before saccades. *Nature*, 386:598–601, 1997.

[730] J. Ross, M. Morrone, M. E. Goldberg, and D. C. Burr. Changes in visual perception at the time of saccades. *Trends in Neurosciences*, 24(2):113–121, 2001.

[731] G. A. Rousselet, C. M. Gaspar, K. P. Wieczorek, and C. R. Pernet. Modeling single-trial ERP reveals modulation of bottom-up face visual processing by top-down task constraints (in some subjects). *Frontiers in psychology*, 2:137, 2011.

[732] K. Rubia, T. Russell, S. Overmeyer, M. Brammer, E. Bullmore, T. Sharma, A. Simmons, S. Williams, V. Giampietro, C. Andrew, and E. Taylor. Mapping motor inhibition: conjunctive brain activations across different versions of go/no-go and stop tasks. *Neuroimage*, 13:250–261, 2001.

[733] M. Rucci, R. Iovin, M. Poletti, and F. Santini. Miniature eye movements enhance fine spatial detail. *Nature*, 447(7146):851–4, 2007.

[734] R. J. Rushmore, A. Valero-Cabre, S. G. Lomber, C. C. Hilgetag, and B. R. Payne. Functional circuitry underlying visual neglect. *Brain*, 129(Pt 7):1803–21, 2006.

[735] B. C. Russell, A. Torralba, K. P. Murphy, and W. T. Freeman. LabelMe: A Database and Web-Based Tool for Image Annotation. *International Journal of Computer Vision*, 77(1-3):157–173, 2008.

[736] S. J. Sara and S. Bouret. Orienting and Reorienting: The Locus Coeruleus Mediates Cognition through Arousal. *Neuron*, 76(1):130–141, 2012.

[737] M. G. Saslow. Effects of components of displacement-step stimuli upon latency for saccadic eye movement. *Journal of the Optical Society of America*, 57(8):1024–29, 1967.

[738] P. Sauleau, P. Pollak, P. Krack, J. H. Courjon, A. Vighetto, A. L. Benabid, D. Pélisson, and C. Tilikete. Subthalamic stimulation improves orienting gaze movements in Parkinson's disease. *Clinical Neurophysiology*, 119(8):1857–1863, 2008.

[739] E. Schäfer. Experiments on the electrical excitation of the visual area of the cerebral cortex in the monkey. *Brain*, 10:362–380, 1888.

[740] E. W. Schafer and M. M. Marcus. Self-stimulation sensory responses. *Science*, 181(4095):175–177, 1973.

[741] T. Schenkenberg, D. C. Bradford, and E. T. Ajax. Line bisection and unilateral visual neglect in patients with neurologic impairment. *Neurology*, 30(5):509–17, 1980.

[742] P. H. Schiller and I. H. Chou. The effects of frontal eye field and dorsomedial frontal cortex lesions on visually guided eye movements. *Nature neuroscience*, 1(3):248–53, 1998.

[743] P. H. Schiller and K. Lee. The role of the primate extrastriate area V4 in vision. *Science*, 251(4998):1251–3, 1991.

[744] P. H. Schiller and E. J. Tehovnik. Look and see: how the brain moves your eyes about. *Progress in brain research*, 134:127–42, 2001.

[745] P. H. Schiller, S. D. True, and J. L. Conway. Deficits in eye movements following frontal eye-field and superior colliculus ablations. *Journal of neurophysiology*, 44(6):1175–1189, 1980.

[746] P. H. Schiller, J. H. Sandell, and J. H. Maunsell. The effect of frontal eye field and superior colliculus lesions on saccadic latencies in the rhesus monkey. *Journal of neurophysiology*, 57(4): 1033–49, 1987.

[747] P. H. Schiller, W. M. Slocum, C. Carvey, and A. S. Tolias. Are express saccades generated under natural viewing conditions? *The European journal of neuroscience*, 20(9):2467–73, 2004.

[748] A. Schindler and A. Bartels. Parietal cortex codes for egocentric space beyond the field of view. *Current biology*, 23(2):177–82, 2013.

[749] J. Schlag and M. Schlag-Rey. Through the eye, slowly: delays and localization errors in the visual system. *Nature Reviews Neuroscience*, 3:191–215, 2002.

[750] W. Schleidt, M. D. Shalter, and H. Moura-Neto. The hawk/goose story: the classical ethological experiments of Lorenz and Tinbergen, revisited. *Journal of comparative psychology*, 125(2): 121–33, 2011.

[751] A. Schlögl, C. Keinrath, D. Zimmermann, R. Scherer, R. Leeb, and G. Pfurtscheller. A fully automated correction method of EOG artifacts in EEG recordings. *Clinical neurophysiology*, 118(1): 98–104, 2007.

[752] B. Schmalbach, V. Günther, J. Raethlen, S. Wailke, D. Falk, G. Deuschl, and K. Witt. The subthalamic nucleus influences visuospatial attention in humans. *Journal of Cognitive Neuroscience*, 26 (3):543–50, 2014.

[753] W. Schneider. VAM: A neuro-cognitive model for visual attention control of segmentation, object recognition, and space-based motor action. *Visual Cognition*, 2(2/3):331–375, 1995.

[754] W. Schneider and H. Deubel. Visual attention and saccadic eye movements: evidence for obligatory and selective spatial coupling. In J. Findlay, R. Kentridge, and R. Walker, editors, *Eye Movement Research: Mechanisms, Processes, and Applications*, pages 317–324. Elsevier, Amsterdam, 1995.

[755] W. Schneider and R. Shiffrin. Controlled and automatic human information processing: I. Detection, search, and attention. *Psychological review*, 84(1):1–66, 1977.

[756] C. Schroeder, A. Mehta, and S. Givre. A spatiotemporal profile of visual system activation revealed by current source density analysis in the awake macaque. *Cerebral Cortex*, 8:575–592, 1998.

[757] C. E. Schroeder, C. E. Tenke, J. C. Arezzo, and H. G. Vaughan. Timing and distribution of flash-evoked activity in the lateral geniculate nucleus of the alert monkey. *Brain research*, 477(1-2): 183–95, 1989.

[758] F. Schumann, W. Einhäuser, J. Vockeroth, K. Bartl, E. Schneider, and P. König. Salient features in gaze-aligned recordings of human visual input during free exploration of natural environments. *Journal of Vision*, 8:1–17, 2008.

[759] R. K. W. Schwarting and J. P. Huston. The unilateral 6-hydroxydopamine lesion model in behavioral brain research. Analysis of functional deficits, recovery and treatments. *Progress in Neurobiology*, 50:275–331, 1996.

[760] P. G. Schyns and A. Oliva. From blobs to boundary edges: Evidence for time- and spatial-scale-dependent scene recognition. *Psychological Science*, 5(4):195–200, 1994.

[761] M. Seeber, R. Scherer, J. Wagner, T. Solis-Escalante, and G. R. Müller-Putz. High and low gamma EEG oscillations in central sensorimotor areas are conversely modulated during the human gait cycle. *NeuroImage*, 112:318–326, 2015.

[762] J. T. Serences and G. M. Boynton. Feature-Based Attentional Modulations in the Absence of Direct Visual Stimulation. *Neuron*, 55(2):301–312, 2007.

Bibliography

[763] J. T. Serences and S. Yantis. Selective visual attention and perceptual coherence. *Trends in cognitive sciences*, 10(1):38–45, 2006.

[764] J. T. Serences, S. Shomstein, A. B. Leber, X. Golay, H. E. Egeth, and S. Yantis. Coordination of voluntary and stimulus-driven attentional control in human cortex. *Psychological science*, 16(2): 114–22, 2005.

[765] A. B. Sereno, K. a. Briand, S. C. Amador, and S. V. Szapiel. Disruption of reflexive attention and eye movements in an individual with a collicular lesion. *Journal of clinical and experimental neuropsychology*, 28(1):145–66, 2006.

[766] M. I. Sereno and J. M. Allman. Cortical visual areas in mammals. In A. Leventhal, editor, *The Neural Basis of Visual Function*, pages 160–172. Macmillan, London, 1991.

[767] M. I. Sereno, S. Pitzalis, and A. Martinez. Mapping of contralateral space in retinotopic coordinates by a parietal cortical area in humans. *Science*, 294(5545):1350–4, 2001.

[768] J. Sergent. The cerebral balance of power: confrontation or cooperation? *Journal of experimental psychology. Human perception and performance*, 8(2):253–72, 1982.

[769] P. Seriès and A. R. Seitz. Learning what to expect (in visual perception). *Frontiers in human neuroscience*, 7:668, 2013.

[770] T. Serre, a. Oliva, and T. Poggio. A feedforward architecture accounts for rapid categorization. *Proceedings of the National Academy of Sciences*, 104(15):6424–6429, 2007.

[771] M. Severens, B. Nienhuis, P. Desain, and J. Duysens. Feasibility of measuring event Related Desynchronization with electroencephalography during walking. *Proceedings of the Annual International Conference of the IEEE Engineering in Medicine and Biology Society, EMBS*, 8:2764–2767, 2012.

[772] T. Shakespeare, Y. Pertzov, K. Yong, J. Nicholas, and S. Crutch. Reduced Modulation of Scanpaths in Response To Task Demands in Posterior Cortical Atrophy. *Alzheimer's & Dementia*, 10(4): P177, 2014.

[773] C. E. Shannon. A mathematical theory of communication. *The Bell system technical journal*, 27(3):379–423, 1948.

[774] K. Shen and M. Paré. Neuronal activity in superior colliculus signals both stimulus identity and saccade goals during visual conjunction search. *Journal of vision*, 7(5):15.1–13, 2007.

[775] M. Shepherd and H. Müller. Movement versus focusing of visual attention. *Perception & Psychophysics*, 46(2):146–154, 1989.

[776] M. Shepherd, J. Findlay, and R. Hockey. The relationship between eye movements and spatial attention. *The Quarterly Journal of Experimental Psychology A: Human Experimental Psychology*, 38A:475–491, 1986.

[777] S. Sherman and R. Guillery. *Functional Connections of Cortical Areas: A new view from the thalamus*. MIT Press, Cambridge, MA, 2013.

[778] K. Shindo, K. Sugiyama, L. Huabao, K. Nishijima, T. Kondo, and S.-I. Izumi. Long-term effect of low-frequency repetitive transcranial magnetic stimulation over the unaffected posterior parietal cortex in patients with unilateral spatial neglect. *Journal of Rehabilitation Medicine*, 38(1):65–67, 2006.

[779] D. I. Shore, E. Spry, and C. Spence. Confusing the mind by crossing the hands. *Cognitive Brain Research*, 14(1):153–163, 2002.

[780] G. L. Shulman, S. V. Astafiev, M. P. McAvoy, G. D'Avossa, and M. Corbetta. Right TPJ Deactivation during Visual Search: Functional Significance and Support for a Filter Hypothesis. *Cerebral Cortex*, 17(11):2625–2633, 2007.

[781] G. L. Shulman, S. V. Astafiev, D. Franke, D. L. W. Pope, A. Z. Snyder, M. P. McAvoy, and M. Corbetta. Interaction of stimulus-driven reorienting and expectation in ventral and dorsal frontoparietal and basal ganglia-cortical networks. *The Journal of neuroscience*, 29(14):4392–407, 2009.

[782] G. L. Shulman, D. L. W. Pope, S. V. Astafiev, M. P. McAvoy, A. Z. Snyder, and M. Corbetta. Right hemisphere dominance during spatial selective attention and target detection occurs outside the dorsal frontoparietal network. *The Journal of neuroscience*, 30(10):3640–51, 2010.

[783] T. Sieger, C. Bonnet, T. Serranová, J. Wild, D. Novák, F. Ržička, D. Urgošík, E. Ržička, B. Gaymard, and R. Jech. Basal ganglia neuronal activity during scanning eye movements in Parkinson's disease. *PLoS ONE*, 8(11):e78581, 2013.

[784] G. J. Siegle, N. Ichikawa, and S. Steinhauer. Blink before and after you think: blinks occur prior to and following cognitive load indexed by pupillary responses. *Psychophysiology*, 45(5):679–87, 2008.

[785] A. Sillito, K. Grieve, H. Jones, J. Cudeiro, and J. Davls. Visual cortical mechanisms detecting focal orientation discontinuities. *Nature*, 378:492–496, 1995.

[786] M. A. Silver and S. Kastner. Topographic maps in human frontal and parietal cortex. *Trends in cognitive sciences*, 13(11):488–95, 2009.

[787] M. A. Silver, D. Ress, and D. J. Heeger. Topographic maps of visual spatial attention in human parietal cortex. *Journal of neurophysiology*, 94(2):1358–71, 2005.

[788] T. Siman-Tov, A. Mendelsohn, T. Schonberg, G. Avidan, I. Podlipsky, L. Pessoa, N. Gadoth, L. G. Ungerleider, and T. Hendler. Bihemispheric leftward bias in a visuospatial attention-related network. *The Journal of neuroscience*, 27(42):11271–11278, 2007.

[789] E. P. Simoncelli and B. A. Olshausen. Natural image statistics and neural representation. *Annual review of neuroscience*, 2001.

[790] R. Sireteanu and R. Rettenbach. Perceptual learning in visual search generalizes over tasks, locations, and eyes. *Vision Research*, 40(21):2925–2949, 2000.

[791] W. Skrandies and K. Laschke. Topography of visually evoked brain activity during eye movements: lambda waves, saccadic suppression, and discrimination performance. *International journal of psychophysiology*, 27:15–27, 1997.

[792] D. Smilek, J. S. A. Carriere, and J. A. Cheyne. Out of mind, out of sight: eye blinking as indicator and embodiment of mind wandering. *Psychological science*, 21(6):786–9, 2010.

[793] A. Smith and D. Nutt. Noradrenaline and attention lapses. *Nature*, 380:291, 1996.

[794] A. T. Smith, K. D. Singh, A. L. Williams, and M. W. Greenlee. Estimating receptive field size from fMRI data in human striate and extrastriate visual cortex. *Cerebral cortex*, 11(12):1182–1190, 2001.

[795] D. Smith, C. Rorden, and S. Jackson. Exogenous orienting of attention depends upon the ability to execute eye movements. *Current Biology*, 14:792–795, 2004.

[796] D. T. Smith, T. Schenk, and C. Rorden. Saccade preparation is required for exogenous attention but not endogenous attention or IOR. *Journal of experimental psychology. Human perception and performance*, 38(6):1438–47, 2012.

[797] S. M. Smith and T. E. Nichols. Threshold-free cluster enhancement: addressing problems of smoothing, threshold dependence and localisation in cluster inference. *NeuroImage*, 44(1):83–98, 2009.

[798] Y. Smith, L. N. Hazrati, and A. Parent. Efferent projections of the subthalamic nucleus in the squirrel monkey as studied by the PHA-L anterograde tracing method. *The Journal of comparative neurology*, 294(2):306–323, 1990.

[799] J. Snow. Goal-driven selective attention in patients with right hemisphere lesions: how intact is the ipsilesional field? *Brain*, 129:168–181, 2006.

[800] D. Somers, A. Dale, A. Seiffert, and R. Tootell. Functional MRI reveals spatially specific attentional modulation in human primary visual cortex. *Proceedings of the National Academy of Sciences*, 96:1663–1668, 1999.

[801] M. A. Sommer and R. H. Wurtz. A pathway in primate brain for internal monitoring of movements. *Science*, 296(5572):1480–1482, 2002.

[802] M. A. Sommer and R. H. Wurtz. Influence of the thalamus on spatial visual processing in frontal cortex. *Nature*, 444(7117):374–7, 2006.

[803] M. A. Sommer and R. H. Wurtz. Brain circuits for the internal monitoring of movements. *Annual review of neuroscience*, 31:317–38, 2008.

[804] P. Spear, S. Miller, and L. Ohman. Effects of Lateral Suprasylvian Visual Cortex. *Behavioral Brain Reseearch*, 10:339–359, 1983.

[805] C. Spence and J. Driver. Audiovisual links in endogenous covert spatial attention. *Journal of experimental psychology. Human perception and performance*, 22(4):1005–1030, 1996.

[806] C. Spence and J. Driver. Audiovisual links in exogenous covert spatial orienting. *Perception & Psychophysics*, 59(1):1–22, 1997.

[807] C. Spence and C. Ho. Tactile and Multisensory Spatial Warning Signals for Drivers. *IEEE Transactions on Haptics*, 1(2):121–129, 2008.

[808] C. Spence and M. Walton. On the inability to ignore touch when responding to vision in the crossmodal congruency task. *Acta psychologica*, 118(1-2):47–70, 2005.

[809] C. Spence, M. E. Nicholls, N. Gillespie, and J. Driver. Cross-modal links in exogenous covert spatial orienting between touch, audition, and vision. *Perception & psychophysics*, 60(4):544–57, 1998.

[810] C. Spence, F. Pavani, and J. Driver. Crossmodal links between between vision and touch in covert endogenous spatial attention. *Journal of experimental psychology. Human perception and performance*, 26(4):1289–1319, 2000.

[811] C. Spence, F. Pavani, and J. Driver. Spatial constraints on visual-tactile cross-modal distractor congruency effects. *Cognitive, affective & behavioral neuroscience*, 4(2):148–69, 2004.

[812] G. Sperling. The information available in brief visual presentations. *Psychological monographs: General and applied*, 74(11, Whole No. 498):1–29, 1960.

[813] S. Spotorno and S. Faure. Change detection in complex scenes: Hemispheric contribution and the role of perceptual and semantic factors. *Perception*, 40(1):5–22, 2011.

[814] J. M. Sprague. Interaction of cortex and superior colliculus in mediation of visually guided behavior in the cat. *Science*, 153(743):1544–7, 1966.

[815] M. W. Spratling. Predictive coding as a model of response properties in cortical area V1. *The Journal of neuroscience*, 30(9):3531–43, 2010.

[816] M. Srinivasan, S. Laughlin, and A. Dubs. Predictive coding: a fresh view of inhibition in the retina. *Proceedings of the Royal Society of London*, 216(4205):427–459, 1982.

[817] S. Starkstein, R. Leiguarda, O. Gershanik, and M. Berthier. Neuropsychological disturbances in hemiparkinson's disease. *Neurology*, 37(11):1762–1764, 1987.

[818] G. Stefanics, M. Kimura, and I. Czigler. Visual mismatch negativity reveals automatic detection of sequential regularity violation. *Frontiers in human neuroscience*, 5(May):46, 2011.

[819] B. Stein, T. Stanford, M. Wallace, J. Vaughan, and W. Jiang. Crossmodal spatial interactions in subcortical and cortical circuits. In C. Spence and J. Driver, editors, *Crossmodal space and crossmodal attention*, chapter 2, pages 25–50. Oxford University Press, 2004.

[820] B. E. Stein and T. R. Stanford. Multisensory integration: current issues from the perspective of the single neuron. *Nature Reviews Neuroscience*, 9(4):255–66, 2008.

[821] B. E. Stein, B. Magalhães-Castro, and L. Kruger. Relationship between visual and tactile representations in cat superior colliculus. *Journal of neurophysiology*, 39(2):401–419, 1976.

[822] J. K. Stevens, R. C. Emerson, G. L. Gerstein, T. Kallos, G. R. Neufeld, C. W. Nichols, and A. C. Rosenquist. Paralysis of the awake human: visual perceptions. *Vision research*, 1976.

[823] J. Stoll, M. Thrun, A. Nuthmann, and W. Einhäuser. Overt attention in natural scenes: Objects dominate features. *Vision Research*, 107:36–48, 2015.

[824] S. Stuart, L. Alcock, B. Galna, S. Lord, and L. Rochester. The measurement of visual sampling during real-world activity in Parkinson's disease and healthy controls: a structured literature review. *Journal of neuroscience methods*, 222:175–88, 2014.

[825] C. Summerfield, E. H. Trittschuh, J. M. Monti, M. M. Mesulam, and T. Egner. Neural repetition suppression reflects fulfilled perceptual expectations. *Nature neuroscience*, 11(9):1004–6, 2008.

[826] D. Swick, V. Ashley, and U. Turken. Are the neural correlates of stopping and not going identical? Quantitative meta-analysis of two response inhibition tasks. *Neuroimage*, 56(3):1655–1665, 2011.

[827] C. M. Sylvester, G. L. Shulman, a. I. Jack, and M. Corbetta. Asymmetry of Anticipatory Activity in Visual Cortex Predicts the Locus of Attention and Perception. *Journal of Neuroscience*, 27 (52):14424–14433, 2007.

[828] R. Sylvester, J. Haynes, and G. Rees. Saccades differentially modulate human LGN and V1 responses in the presence and absence of visual stimulation. *Current Biology*, 15:37–41, 2005.

[829] S. M. Szczepanski and S. Kastner. Shifting attentional priorities: control of spatial attention through hemispheric competition. *The Journal of neuroscience*, 33(12):5411–21, 2013.

[830] S. M. Szczepanski, C. S. Konen, and S. Kastner. Mechanisms of Spatial Attention Control in Frontal and Parietal Cortex. *Journal of Neuroscience*, 30(1):148–160, 2010.

[831] K. Tanaka. Inferotemporal cortex and object vision. *Annual review of neuroscience*, 19:109–39, 1996.

[832] K.-J. Tark and C. E. Curtis. Persistent neural activity in the human frontal cortex when maintaining space that is off the map. *Nature neuroscience*, 12(11):1463–8, 2009.

[833] B. Tatler. The central fixation bias in scene viewing: Selecting an optimal viewing position independently of motor biases and image feature distributions. *Journal of Vision*, 7:1–17, 2007.

[834] B. Tatler, R. Baddeley, and I. Gilchrist. Visual correlates of fixation selection: effects of scale and time. *Vision research*, 45(5):643–59, 2005.

[835] B. Tatler, R. Baddeley, and B. Vincent. The long and the short of it: spatial statistics at fixation vary with saccade amplitude and task. *Vision research*, 46(12):1857–62, 2006.

[836] B. Tatler, M. Hayhoe, M. Land, and D. Ballard. Eye guidance in natural vision: Reinterpreting salience. *Journal of vision*, 11:1–23, 2011.

[837] E. J. Tehovnik, W. M. Slocum, and P. H. Schiller. Differential effects of laminar stimulation of V1 cortex on target selection by macaque monkeys. *European Journal of Neuroscience*, 16(4): 751–760, 2002.

[838] E. J. Tehovnik, W. M. Slocum, and P. H. Schiller. Saccadic eye movements evoked by microstimulation of striate cortex. *European Journal of Neuroscience*, 17(4):870–878, 2003.

[839] Y. Temel, V. Visser-Vandewalle, and R. Carpenter. Saccadic latency during electrical stimulation of the human subthalamic nucleus. *Current Biology*, 18(10):412–414, 2008.

[840] Y. Temel, V. Visser-Vandewalle, and R. H. S. Carpenter. Saccadometry: a novel clinical tool for quantification of the motor effects of subthalamic nucleus stimulation in Parkinson's disease. *Experimental neurology*, 216(2):481–9, 2009.

[841] C. ten Cate, W. S. Bruins, J. den Ouden, T. Egberts, H. Neevel, M. Spierings, K. van der Burg, and A. W. Brokerhof. Tinbergen revisited: a replication and extension of experiments on the beak colour preferences of herring gull chicks. *Animal Behaviour*, 77(4):795–802, 2009.

[842] J. Theeuwes. Cross-dimensional perceptual selectivity. *Perception & psychophysics*, 50(2):184–93, 1991.

[843] J. Theeuwes. Perceptual selectivity for color and form. *Perception & psychophysics*, 51(6):599–606, 1992.

[844] J. Theeuwes. Abrupt luminance change pops out; abrupt color change does not. *Perception & psychophysics*, 57(5):637–44, 1995.

[845] J. Theeuwes. Top-down and bottom-up control of visual selection. *Acta psychologica*, 135(2):77–99, 2010.

[846] J. Theeuwes and R. Burger. Attentional control during visual search: the effect of irrelevant singletons. *Journal of experimental psychology. Human perception and performance*, 24(5):1342–53, 1998.

[847] J. Theeuwes and F. Kooi. Parallel Search for a Conjunction and of contrast polarity and shape. *Vision Research*, 34(22):3013–3016, 1994.

[848] J. Theeuwes and A. Kramer. Our eyes do not always go where we want them to go: Capture of the eyes by new objects. *Psychological Science*, 9(5):379–385, 1998.

[849] G. Thickbroom and F. Mastaglia. Presaccadic ' Spike ' Potential : Investigation of Topography and Source. *Brain research*, 339:271–280, 1985.

[850] G. W. Thickbroom and F. L. Mastaglia. Presaccadic spike potential. Relation to eye movement direction. *Electroencephalography and clinical neurophysiology*, 64(3):211–4, 1986.

[851] M. Thiebaut de Schotten, F. Dell'Acqua, S. J. Forkel, A. Simmons, F. Vergani, D. G. M. Murphy, and M. Catani. A lateralized brain network for visuospatial attention. *Nature neuroscience*, 14 (10):1245–6, 2011.

[852] K. V. Thilo, L. Santoro, V. Walsh, and C. Blakemore. The site of saccadic suppression. *Nature neuroscience*, 7(1):13–4, 2004.

[853] K. G. Thompson, N. P. Bichot, and T. R. Sato. Frontal Eye Field Activity Before Visual Search Errors Reveals the Integration of Bottom-Up and Top-Down Salience. *Journal of Neurophysiology*, 93:337–351, 2005.

[854] G. Thut, A. Nietzel, and A. Pascual-Leone. Dorsal posterior parietal rTMS affects voluntary orienting of visuospatial attention. *Cerebral cortex*, 15(5):628–38, 2005.

[855] G. Thut, A. Nietzel, S. a. Brandt, and A. Pascual-Leone. Alpha-band electroencephalographic activity over occipital cortex indexes visuospatial attention bias and predicts visual target detection. *The Journal of neuroscience*, 26(37):9494–502, 2006.

[856] J. Todd. Reaction to multiple stimuli. *The American Journal of Psychology*, 24(1):134, 1912.

[857] S. Todd and a. F. Kramer. Attentional misguidance in visual search. *Perception & psychophysics*, 56(2):198–210, 1994.

[858] A. Todorovic, F. van Ede, E. Maris, and F. P. de Lange. Prior expectation mediates neural adaptation to repeated sounds in the auditory cortex: an MEG study. *The Journal of neuroscience*, 31 (25):9118–23, 2011.

[859] A. S. Tolias, T. Moore, S. M. Smirnakis, E. J. Tehovnik, A. G. Siapas, and P. H. Schiller. Eye Movements Modulate Visual Receptive Fields of V4 Neurons. *Neuron*, 29(3):757–767, 2001.

[860] C. L. Tomlinson, R. Stowe, S. Patel, C. Rick, R. Gray, and C. E. Clarke. Systematic review of levodopa dose equivalency reporting in Parkinson's disease. *Movement disorders*, 25(15):2649–53, 2010.

[861] F. Tong and S. Engel. Interocular rivalry revealed in the human cortical blind-spot representation. *Nature*, 411:195–199, 2001.

[862] R. B. Tootell, M. S. Silverman, E. Switkes, and R. L. De Valois. Deoxyglucose analysis of retinotopic organization in primate striate cortex. *Science*, 218(4575):902–904, 1982.

[863] A. Torralba. Modeling global scene factors in attention. *Journal of the Optical Society of America. A, Optics, image science, and vision*, 20(7):1407–18, 2003.

[864] A. Torralba. Contextual Priming for Object Detection. *International Journal of Computer Vision*, 53(2):169–191, 2003.

[865] A. Torralba and A. Oliva. Statistics of natural image categories. *Network*, 14(3):391–412, 2003.

[866] J. Townsend. Serial vs. parallel processing: Sometimes they look like Tweedledum and Tweedledee but they can (and Should) be distinguished. *Psychological Science*, 1(1):46–54, 1990.

[867] A. Treisman. Selective Attention in Man. *British medical bulletin*, 20:12–16, 1964.

[868] A. M. Treisman. The effect of irrelevant material on the efficiency of selective listening. *The American journal of psychology*, 77(4):533–546, 1964.

[869] A. M. Treisman and G. Gelade. A feature-integration theory of attention. *Cognitive psychology*, 12(1):97–136, 1980.

[870] S. Treue and J. C. Martínez Trujillo. Feature-based attention influences motion processing gain in macaque visual cortex. *Nature*, 399(6736):575–9, 1999.

[871] P.-H. Tseng, R. Carmi, I. G. M. Cameron, D. P. Munoz, and L. Itti. Quantifying center bias of observers in free viewing of dynamic natural scenes. *Journal of Vision*, 9:1–16, 2009.

[872] J. Tsotsos. *A computational perspective on visual selection*. MIT Press, Cambridge, MA, 2011.

[873] J. Tsotsos, S. Culhane, W. K. Wai, Y. Lai, N. Davis, and F. Nuflo. Modeling visual attention via selective tuning. *Artificial intelligence*, 78:507–545, 1995.

[874] M. Turatto, G. Galfano, B. Bridgeman, and C. Umiltà. Space-independent modality-driven attentional capture in auditory, tactile and visual systems. *Experimental brain research*, 155(3):301–10, 2004.

[875] E. Y. Uc, M. Rizzo, S. W. Anderson, J. Sparks, R. L. Rodnitzky, and J. D. Dawson. Impaired visual search in drivers with Parkinson's disease. *Annals of neurology*, 60(4):407–13, 2006.

[876] M. Umeno and M. Goldberg. Spatial processing in the monkey frontal eye field. I. Predictive visual responses. *Journal of Neurophysiology*, 78(3):1373–1383, 1997.

[877] G. Underwood and T. Foulsham. Visual saliency and semantic incongruency influence eye movements when inspecting pictures. *Quarterly journal of experimental psychology*, 59(11):1931–49, 2006.

[878] G. Underwood, T. Foulsham, E. van Loon, L. Humphreys, and J. Bloyce. Eye movements during scene inspection: A test of the saliency map hypothesis. *European Journal of Cognitive Psychology*, 18(3):321–343, 2006.

[879] P. Unema, S. Pannasch, M. Joos, and B. Velichkovsky. Time course of information processing during scene perception: The relationship between saccade amplitude and fixation duration. *Visual Cognition*, 12(3):473–494, 2005.

[880] L. Ungerleider and M. Mishkin. Two cortical visual systems. In D. Ingle, M. Goodale, and R. Mansfield, editors, *Analysis of Visual behavior*. MIT Press, Cambridge, Mass, USA, 1982.

[881] U. Ungerstedt. 6-Hydroxy-dopamine induced degeneration of central monoamine neurons. *European journal of pharmacology*, 5:107–110, 1968.

[882] J. Vaid and M. Singh. Asymmetries in the perception of facial affect: Is there an influence of reading habits? *Neuropsychologia*, 27(10):1277–1287, 1989.

[883] R. J. van Beers, A. C. Sittig, and J. J. van der Gon. Integration of Proprioceptive and Visual Position Information: An Experimentally Supported Model. *Journal of neurophysiology*, 81:1355–1364, 1999.

[884] R. H. J. van der Lubbe and A. Postma. Interruption from irrelevant auditory and visual onsets even when attention is in a focused state. *Experimental brain research*, 164(4):464–71, 2005.

[885] D. C. Van Essen. Organization of visual areas in macaque and human cerebral cortex. In L. Chalupa and J. Werner, editors, *The visual neurosciences*, pages 507–521. MIT Press, 2004.

[886] M. H. Van Kleeck. Hemispheric differences in global versus local processing of hierarchical visual stimuli by normal subjects: New data and a meta-analysis of previous studies. *Neuropsychologia*, 27(9):1165–1178, 1989.

[887] W. van Zoest and M. Donk. Bottom - up and top - down control in visual search. *Perception*, 33(8):927–937, 2004.

[888] W. van Zoest and M. Donk. The effects of salience on saccadic target selection. *Visual Cognition*, 12(2):353–375, 2005.

[889] W. van Zoest, M. Donk, and J. Theeuwes. The role of stimulus-driven and goal-driven control in saccadic visual selection. *Journal of experimental psychology. Human perception and performance*, 30(4):746–759, 2004.

[890] F. VanderWerf, P. Brassinga, D. Reits, M. Aramideh, and B. Ongerboer de Visser. Eyelid movements: behavioral studies of blinking in humans under different stimulus conditions. *Journal of neurophysiology*, 89(5):2784–96, 2003.

[891] R. VanRullen. On second glance: still no high-level pop-out effect for faces. *Vision research*, 46(18):3017–27, 2006.

[892] R. Verleger, T. Gasser, and J. Möcks. Correction of EOG artifacts in event-related potentials of the EEG: aspects of reliability and validity. *Psychophysiology*, 19(4):472–80, 1982.

[893] P. Vetter, G. Edwards, and L. Muckli. Transfer of predictive signals across saccades. *Frontiers in psychology*, 3:176, 2012.

[894] M. Vidailhet, S. Rivaud, N. Gouider-Khouja, B. Pillon, a. M. Bonnet, B. Gaymard, Y. Agid, and C. Pierrot-Deseilligny. Eye movements in parkinsonian syndromes. *Annals of neurology*, 35(4): 420–6, 1994.

[895] C. Villardita, P. Smirni, and G. Zappalà. Visual neglect in Parkinson's disease. *Archives of neurology*, 40:737–739, 1983.

[896] W. E. Vinje and J. L. Gallant. Sparse coding and decorrelation in primary visual cortex during natural vision. *Science*, 287(5456):1273–6, 2000.

[897] F. C. Volkmann, L. A. Riggs, and R. K. Moore. Eyeblinks and visual suppression. *Science*, 207(4433):900–2, 1980.

[898] H. von Helmholtz. *Treatise on Physiological Optics Vol III. The perceptions of vision.* The Optical Society of America. Electronic edition (2001): University of Pennsylvania, 1924.

[899] D. Voyer. On the magnitude of laterality effects and sex differences in functional lateralities. *Laterality*, 1(1):51–83, 1996.

[900] J. Vroomen, B. de Gelder, and B. Sound enhances visual perception: cross-modal effects of auditory organization on vision. *Journal of Experimental Psychology: Human Perception and Performance*, 26(5):1583–1590, 2000.

[901] P. Vuilleumier, D. Hester, G. Assal, and F. Regli. Unilateral spatial neglect recovery after sequential strokes. *Neurology*, 46(1):184–9, 1996.

[902] C. Wacongne, E. Labyt, V. van Wassenhove, T. Bekinschtein, L. Naccache, and S. Dehaene. Evidence for a hierarchy of predictions and prediction errors in human cortex. *Proceedings of the National Academy of Sciences*, 108(51):20754–9, 2011.

[903] C. Wacongne, J.-P. Changeux, and S. Dehaene. A Neuronal Model of Predictive Coding Accounting for the Mismatch Negativity. *Journal of Neuroscience*, 32(11):3665–3678, 2012.

[904] I. Wagman, H. Krieger, and M. Bender. Eye movements elicited by surface and depth stimulation of the occipital lobe of the macaque mulatta. *Journal of Comparative Neurology*, 109:169–193, 1958.

[905] J. Wagner, T. Solis-Escalante, R. Scherer, C. Neuper, and G. Müller-Putz. It's how you get there: walking down a virtual alley activates premotor and parietal areas. *Frontiers in human neuroscience*, 8:93, 2014.

[906] E. Walker and T. Weaver. Ocular movements from the occipital lobe in the monkey. *Journal of Neurophysiology*, 3:353–357, 1940.

[907] D. J. Wallace, D. S. Greenberg, J. Sawinski, S. Rulla, G. Notaro, and J. N. D. Kerr. Rats maintain an overhead binocular field at the expense of constant fusion. *Nature*, 498(7452):65–9, 2013.

[908] M. Wallace and B. Stein. Cross-Modal Synthesis in the Midbrain Depends on Input From Cortex. *Journal of Neurophysiology*, 7(1):429–432, 1994.

[909] M. Wallace, M. Meredith, and B. Stein. Converging influences from visual , auditory , and somatosensory cortices onto output neurons of the superior colliculus. *Journal of Neurophysiology*, 69: 1797–1809, 1993.

[910] M. Wallace, L. Wilkinson, and B. Stein. Representation and Integration of Multiple Sensory Inputs in Primate Superior Colliculus. *Journal of Neurophysiology*, 76(2):1246–1266, 1996.

[911] M. T. Wallace and B. E. Stein. Sensory and multisensory responses in the newborn monkey superior colliculus. *The Journal of neuroscience*, 21(22):8886–8894, 2001.

[912] S. F. Wallace, A. C. Rosenquist, and J. M. Sprague. Ibotenic Acid Lesions of the lateral substantua nigra restore visual orientation behavior in the hemianopic cat. *The Journal of comparative neurology*, 296:222–252, 1990.

[913] Q. Wang, P. Cavanagh, and M. Green. Familiarity and pop-out in visual search. *Perception & Psychophysics*, 56(5):495–500, 1994.

[914] L. Ward, J. Mcdonald, and D. Lin. On asymmetries in cross-modal spatial attention orienting. *Perception & Psychophysics*, 62(6):1258–1264, 2000.

[915] S. Watanabe. Pattern recognition as a quest for minimum entropy. *Pattern Recognition*, 13(5):381–387, 1981.

[916] R. B. Weber and R. B. Daroff. The metrics of horizontal saccadic eye movements in normal humans. *Vision Research*, 11(9):921–928, 1971.

[917] R. A. Weddell. Subcortical modulation of spatial attention including evidence that the Sprague effect extends to man. *Brain and cognition*, 55(3):497–506, 2004.

[918] D. Weisenhorn, R. Illing, and W. Spatz. Morphology and connections of neurons in area 17 projecting to the extrastriate areas MT and 19DM and to the superior colliculus in the monkey Callithrix jacchus. *The Journal of comparative neurology*, 255:233–255, 1995.

[919] Y. Weiss, E. P. Simoncelli, and E. H. Adelson. Motion illusions as optimal percepts. *Nature neuroscience*, 5(6):598–604, 2002.

[920] B. L. Welborn, X. Papademetris, D. L. Reis, N. Rajeevan, S. M. Bloise, and J. R. Gray. Variation in orbitofrontal cortex volume: relation to sex, emotion regulation and affect. *Social cognitive and affective neuroscience*, 4(4):328–39, 2009.

[921] E. M. Whitham, S. P. Fitzgibbon, T. W. Lewis, K. J. Pope, D. DeLosAngeles, C. R. Clark, P. Lillie, A. Hardy, S. C. Gandevia, and J. O. Willoughby. Visual Experiences during Paralysis. *Frontiers in Human Neuroscience*, 5:1–7, 2011.

[922] F. A. Wichmann, D. I. Braun, and K. R. Gegenfurtner. Phase noise and the classification of natural images. *Vision research*, 46(8-9):1520–9, 2006.

[923] R. Wilcox. *Introduction to robust estimation and hypothesis testing*. Academic Press, Waltham, MA, 3rd edition, 2012.

[924] L. Wilkinson, M. Meredith, and B. Stein. The role of anterior ectosylvian cortex in cross-modality orientation and approach behavior. *Experimental Brain Research*, 112(1):1–10, 1996.

[925] N. Wilming. *Computational and neural models of oculomotor control*. PhD thesis, University of Osnabrück, 2014.

[926] N. Wilming, T. Betz, T. Kietzmann, and P. König. Measures and Limits of Models of Fixation Selection. *PloS one*, 6(9):e24038, 2011.

[927] D. E. Winkowski and E. I. Knudsen. Top-down gain control of the auditory space map by gaze control circuitry in the barn owl. *Nature*, 439(7074):336–339, 2006.

[928] D. E. Winkowski and E. I. Knudsen. Article Distinct Mechanisms for Top-Down Control of Neural Gain and Sensitivity in the Owl Optic Tectum. *Neuron*, 60(4):698–708, 2008.

[929] B. J. Winterson and H. Collewijn. Microsaccades during finely guided visuomotor tasks. *Vision research*, 16(12):1387–90, 1976.

[930] K. Witt, F. Kopper, G. Deuschl, and P. Krack. Subthalamic nucleus influences spatial orientation in extra-personal space. *Movement disorders*, 21(3):354–61, 2006.

[931] E. Wolf and A. Morandi. Retinal sensitivity in the region of the blind spot. *Journal of the Optical Society of America*, 52(7):806–812, 1962.

[932] J. M. Wolfe. What Can 1 Million Trials Tell Us About Visual Search? *Psychological Science*, 9(1):33–39, 1998.

[933] J. M. Wolfe. Visual Search. In H. Pashler, editor, *Attention*, pages 1–41. University College London Press, London, 1998.

[934] J. M. Wolfe. Asymmetries in visual search: An introduction. *Perception & psychophysics*, 63(3):381–389, 2001.

[935] J. M. Wolfe. Guided Search 4.0 Current Progress With a Model of Visual Search. In W. Gray, editor, *Integrated Models of Cognitive Systems*, pages 99–119. Oxford, New York, 2007.

[936] J. M. Wolfe and T. S. Horowitz. What attributes guide the deployment of visual attention and how do they do it? *Nature Reviews Neuroscience*, 5(6):495–501, 2004.

[937] J. M. Wolfe, K. R. Cave, and S. L. Franzel. Guided search: An alternative to the feature integration model for visual search. *Journal of Experimental Psychology: Human Perception and Performance*, 15(3):419–433, 1989.

[938] D. M. Wolpert, Z. Ghahramani, M. I. Jordan, N. Series, and N. Sep. An Internal Model for Sensorimotor Integration. *Science*, 269(5232):1880–1882, 1995.

[939] R. Wright and C. Richard. Sensory mediation of stimulus-driven attentional capture in multiple-cue displays. *Perception & Psychophysics*, 65(6):925–938, 2003.

[940] R. Wright and L. Ward. *Orienting of attention*. Oxford University Press, New York, NY, US, 2008.

[941] R. H. Wurtz. Neuronal mechanisms of visual stability. *Vision research*, 48(20):2070–89, 2008.

[942] V. Wyart, V. de Gardelle, J. Scholl, and C. Summerfield. Rhythmic fluctuations in evidence accumulation during decision making in the human brain. *Neuron*, 76(4):847–58, 2012.

[943] T. Xie, J. Bernard, and P. Warnke. Post subthalamic area deep brain stimulation for tremors: a mini-review. *Translational neurodegeneration*, 1(1):20, 2012.

[944] S. Yamamoto and S. Kitazawa. Reversal of subjective temporal order due to arm crossing. *Nature neuroscience*, 4(7):759–765, 2001.

[945] S. Yantis and H. E. Egeth. On the distinction between visual salience and stimulus-driven attentional capture. *Journal of experimental psychology. Human perception and performance*, 25(3): 661–76, 1999.

[946] S. Yantis and A. Hillstrom. Stimulus-driven attentional capture: evidence from equiluminant visual objects. *Journal of experimental psychology. Human perception and performance*, 20(1): 95–107, 1994.

[947] S. Yantis and J. Jonides. Abrupt visual onsets and selective attention: evidence from visual search. *Journal of experimental psychology. Human perception and performance*, 10(5):601–621, 1984.

[948] S. Yantis and J. Jonides. Abrupt visual onsets and selective attention: voluntary versus automatic allocation. *Journal of experimental psychology. Human perception and performance*, 16(1): 121–34, 1990.

[949] A. Yarbus. *Eye movements and vision*. Plenum Press, New York, 1967. ISBN 0306302985.

[950] M. Yilmaz and M. Meister. Rapid innate defensive responses of mice to looming visual stimuli. *Current Biology*, 23(20):2011–2015, 2013.

[951] H. W. Yoon, J.-Y. Chung, M.-S. Song, and H. Park. Neural correlates of eye blinking; improved by simultaneous fMRI and EOG measurement. *Neuroscience letters*, 381(1-2):26–30, 2005.

[952] G. Yovel and W. A. Freiwald. Face recognition systems in monkey and human: are they the same thing? *F1000prime reports*, 5:1–10, 2013.

[953] A. Yugeta, Y. Terao, H. Fukuda, O. Hikosaka, F. Yokochi, R. Okiyama, M. Taniguchi, H. Takahashi, I. Hamada, R. Hanajima, and Y. Ugawa. Effects of STN stimulation on the initiation and inhibition of saccade in Parkinson disease. *Neurology*, 74(9):743–8, 2010.

[954] S. Yuval-Greenberg, O. Tomer, A. S. Keren, I. Nelken, and L. Y. Deouell. Transient induced gamma-band response in EEG as a manifestation of miniature saccades. *Neuron*, 58(3):429–41, 2008.

[955] J. Zahn, L. Abel, and L. Dell'Osso. Audio-ocular response characteristics. *Sensory processes*, 37:32–37, 1978.

[956] S. Zeki. Area V5 - a microcosm of the visual brain. *Frontiers in Integrative Neuroscience*, 9(April):1–18, 2015.

[957] S. M. Zeki. Uniformity and diversity of structure and function in rhesus monkey prestriate visual cortex. *Journal of physiology*, 277:273–290, 1978.

[958] S. M. Zeki. Functional specialisation in the visual cortex of the rhesus monkey. *Nature*, 274(5670):423–428, 1978.

[959] G. Zelinsky and D. Sheinberg. Eye movements during parallelserial visual search. *Journal of Experimental Psychology: Human Perception and Performance*, 23(1):244–262, 1997.

[960] A. Zénon and R. J. Krauzlis. Attention deficits without cortical neuronal deficits. *Nature*, 489(7416):434–7, 2012.

[961] L. Zhang, M. H. Tong, T. K. Marks, H. Shan, and G. W. Cottrell. SUN: A Bayesian framework for saliency using natural statistics. *Journal of vision*, 8(7):32, 1–20, 2008.

[962] X. Zhang, L. Zhaoping, T. Zhou, and F. Fang. Neural activities in v1 create a bottom-up saliency map. *Neuron*, 73(1):183–92, 2012.

[963] B. Zimmerberg, S. Glick, and T. Jerussi. Neurochemical correlate of a spatial preference in rats. *Science*, 185(4151):623, 1974.

[964] K. Zipser, V. Lamme, and P. Schiller. Contextual modulation in primary visual cortex. *The Journal of Neuroscience*, 16(22):7376–7389, 1996.